POLITECNICO DI TORINO

III Facoltà di Ingegneria
Corso di Laurea in Ingegneria Elettronica

Tesi di Laurea Specialistica

Analysis and design of high-performance horn antennas

Relatori:

Prof. Renato Orta

Prof. Oscar Antonio Peverini

Dott. Giuseppe Addamo

Prof. Riccardo Tascone

Candidato:

Alberto Tibaldi

Novembre 2011

Durante i cinque anni costituenti il mio percorso formativo presso il Politecnico di Torino ho avuto occasione di conoscere numerose persone, sia studenti sia professori, che hanno contribuito alla mia crescita sia sotto il punto di vista tecnico sia sotto quello umano; ciascuna di queste persone meriterebbe un ringraziamento personale, che in questo contesto mi è difficile fare. Per questo motivo, potrò solo citare le persone che mi sono state più vicine.

Un ringraziamento speciale va fatto ai miei relatori Renato Orta, Oscar Peverini, Giuseppe Addamo e Riccardo Tascone, per tutta la disponibilità (e la pazienza) che hanno avuto con me in questi mesi, aiutandomi a superare le difficoltà emerse durante questo periodo.

Meritano un sincero ringraziamento i miei compagni di avventura Daniele, Francesco, Marco e Salvatore, con i quali ho avuto la fortuna di instaurare uno splendido rapporto di amicizia e collaborazione.

Infine, vorrei ringraziare i miei genitori e i miei nonni, ai quali sono riconoscente per aver sempre avuto fiducia in me, contribuendo in ogni modo possibile ai risultati che ho raggiunto in questi anni.

Contents

CHAPTER 1

High-efficiency horn antennas

1.1 Introduction

This chapter is aimed at introducing a new type of horn antennas, with very good features under several points of view, such as aperture efficiency or low cross-polarization level. The first section describes multi-beam antennas (MBAs), introducing high-efficiency antennas and comparing them with other feeds. The second section is focused on high-efficiency horn antennas, introducing design strategies.

1.2 Multi-beam antennas

1.2.1 Introduction

Multiple-beam antennas (MBAs) are systems that can illuminate a specific geographical region, using high-gain multiple spot beams for both downlink and uplink coverage. These systems are commonly used in satellite communications, for instance for military, direct-broadcast satellites (DBS), or mobile services. Their goal is, given a well-defined geographic region partitioned in cells,

- to cover each cell uniformly;
- to have low cross-polarization levels.

The evolution of communication systems requires to improve coverage, bandwidth and flexibility of services; out of these needs, in order to provide these services to large geographic areas, one of the newest challenges is the realization of multiple-beam antennas able to operate in separated frequency bands.

The design of hardware with either multi-beam or multi-band features is challenging for many reasons; one issue is the frequency behavior of aperture antennas, which produces narrower beams at high frequencies compared to ones at lower frequencies; therefore, if frequency bands are widely separated, it is hard to obtain the same performances of the designed device.

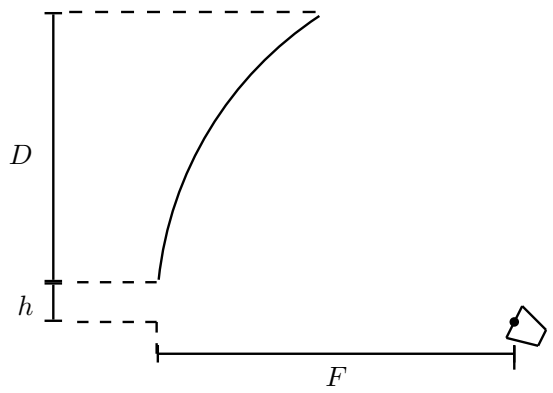

Figure 1.1: Geometry of a parabolic offset reflector.

Focusing firstly on apertures, they can be reflectors or dielectric lenses. Usually, they are realized with offset-parabolic reflectors antennas, because an equivalent lens system would have almost twice the mass compared to the reflector system, and this is not advisable for satellites. The idea for the realization of the aperture for these multi-band MBAs is to synthesize a reflector which produces, for the lower operating frequency range of the required bands, the nominal beam; for signals belonging to the higher band, this reflector have to be oversized. This means that at lower frequencies the design is basically standard, considering a feed in the focus of the reflector system, while at higher frequencies the feed array is de-focused; in other words, there are two different behaviors in different frequency bands, without using frequency-selecting surfaces (FSSs), which are expensive. The de-focusing can be considered by modifying the shape of the reflector.

There are some strategies for the realization of multiple-beam antennas; every design scheme can be characterized by:

- the number of apertures employed;
- the realization scheme of beams starting from feeds.

Most common design strategies are

1. Single-aperture design with a single element per beam (*basic feed concept*); in this case, there is just one aperture, and there is one feed for the realization of each beam. The drawback of this solution is the huge amount of feeds, therefore it is possible to use as radiating elements small horns, in order to obtain high adjacent beam overlap, increasing the value of the minimum gain for each spot. This means that horns need to have either small dimensions or high gain.

2. Single-aperture design with overlapping feed clusters (*enhanced feed concept*); this design strategy is based on using several horns for the formation of each beam; in this case the core of the design is the beam-forming network, which has to provide the correct excitations. So, since power amplifiers have to manage several carriers, their efficiency is reduced, compared to the previous

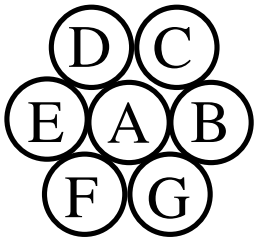

Figure 1.2: Application of the basic feed concept; beam 1 is formed by horn A, beam 2 by horn B, and so on.

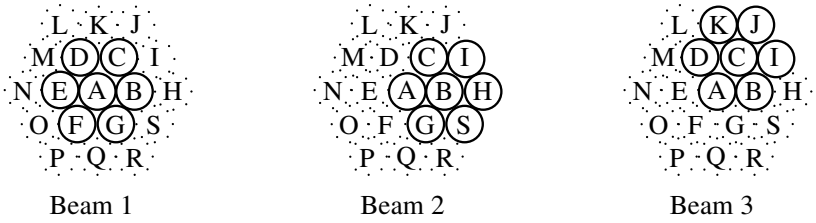

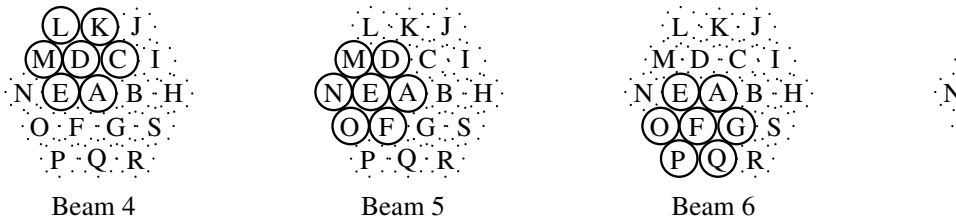

Figure 1.3: Application of the enhanced feed concept; the first beam is formed by horns A,B,C,D,E,F,G; the second beam by horns A,B,C,G,H,I,S, and so on.

strategy; therefore, the drawback of this solution is the design of RF electronics, which results to be more complicated.

3. Multiple-aperture design with a single element per beam; in this case, there are some reflectors, usually three or four, which are independent. Each aperture can be associated to a frequency band, in order to apply a frequency re-use scheme for the realization of the system.

Figures 1.2 and 1.3 show the two ways for the realization of beams, which are the *basic feed concept* and the *enhanced feed concept* ones, respectively. In the former one, each horn is used to generate each beam; this topology is quite easy to realize, since the beam-forming network do not needs to manage composed beams; on the other hand, in order to reduce sidelobes levels it is necessary to taper the field distribution, therefore the antenna efficiency is lowered; this decreases the gain of the structure; to sum up, it is not possible to obtain, by this way, either low sidelobe levels or high gain.

Considering the second concept, there is a cluster of horns instead of a single horn for the generation of each beam. The beam-forming network has to handle

the possibility to compose beams from each cluster of feeds in order to generate the final single beam; in other words, many feeds contribute to the generation of the single beam. This is more difficult to realize in terms of electronics, but it has some advantages; since more feeds contribute to the formation of a single beam, there is a virtual" increase of each equivalent element size. Moreover, it is possible to modify each cluster excitation, in order to address jammers or interferers issues.

1.2.2 Structure of multiple-aperture MBAs

In the following the multiple-aperture strategy is discussed. The first step in order to carry out the design is the partition of the geographic area which has to be covered by the MBA, in a number of contiguous cells; these cells are overlapped with the neighbour cells at their boundary. Then, each cell is related to an aperture, realized with a reflector antenna (i.e. an offset-parabolic antenna). The spatial relationship between ground cells and aperture antennas depends on the number of apertures (typically two, three, four or seven). Since this system is multi-band, there is also a frequency-reuse scheme, where each frequency is related with an aperture. The goal of this system is to generate adjacent beams from different apertures, in order to realize an interleaved spot-beam coverage. In Figure 1.4 two examples of realizations of beams with arbitrary shapes are shown.

Depending on the topology employed, it is possible to relax the feed specifications; an increment of beam spacing relaxes the requirement on the feed size, i.e. it can be bigger, with the consequent higher gain, lower spill-over losses and sidelobe levels.

There are some design parameters which can be shown, in order to understand the operating functions of these systems. Considering a typical hexagonal beam configuration[1], as in Figure 1.5, it is possible to define the most relevant beam angular parameters.

- The angle ϑ_s is the angular spacing between the centers of two adjacent beams.
- The angle $\vartheta_c^{(i)}$ is the minimum angular spacing between the centers of beams re-using the same frequency; i indicates the number of cells for the frequency re-use scheme.
- The angle ϑ_r is the minimum angular spacing between the extremes of two beams re-using the same frequency.

The angle ϑ_0 is the angular beam diameter at the triple beam crossover of three adjacent beams. This last parameter is relevant because, in a hexagonal grid, it indicates the point where the directivity is minimum. From [18] it is possible to find a relationship between ϑ_0 and ϑ_s, which is

$$\vartheta_s = \frac{\sqrt{3}}{2}\vartheta_0$$

[1] like the one proposed in [18]

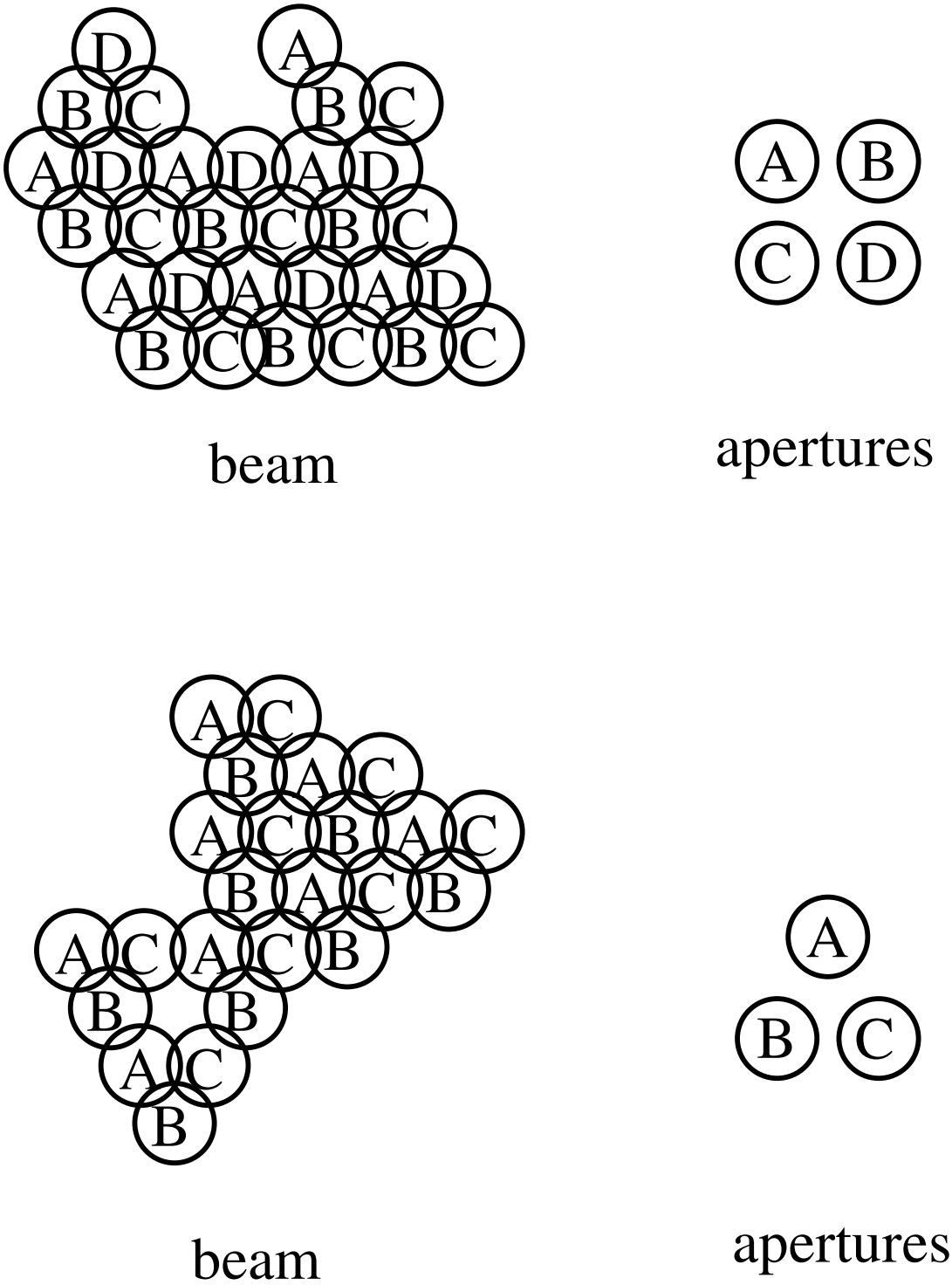

Figure 1.4: Examples of beams with arbitrary shapes, realized with four-apertures design and three-apertures design methods.

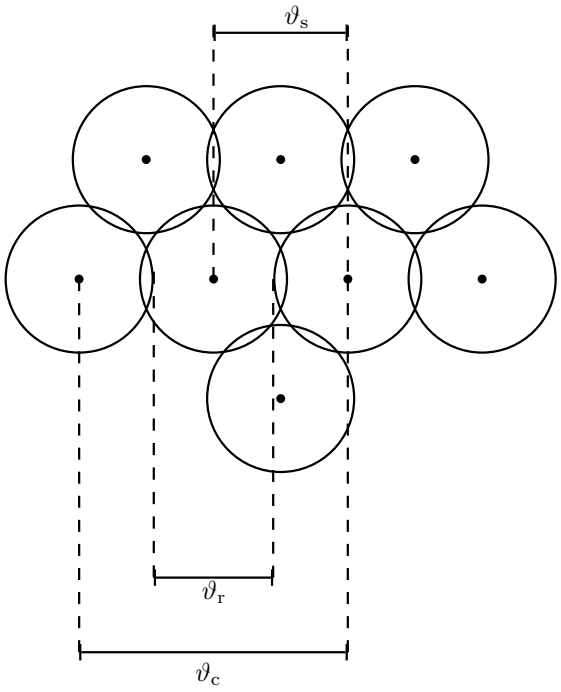

Figure 1.5: Example of beam showing the most significant parameters.

Moreover, depending on the number of frequency re-use cells employed in the system, it is possible to find the $\vartheta_c^{(i)}$ values. Depending on the number of apertures, so on the frequency-reuse scheme, it is possible to find, in literature ([18], [20]), for three-cell, four-cell and seven-cell systems (and relative frequency re-use schemes) respectively, that these parameters are

$$\begin{aligned}\vartheta_c^{(3)} &= 1.732\,\vartheta_s \\ \vartheta_c^{(4)} &= 2.000\,\vartheta_s \\ \vartheta_c^{(7)} &= 2.646\,\vartheta_s\end{aligned}$$

The last parameter introduced in this paragraph is the optimal feed size, d_m (which represents the maximum diameter of circular horns, considering that adjacent feeds are touching each other). For the evaluation of equations which can relate the feed size to other parameters, it is necessary to define from [18] the scan factor S_F as the ratio of the electrical scan angle of the beam to the physical displacement of the feed from the focal point,

$$S_F \triangleq \frac{1 + X\left(\frac{D}{4F}\right)^2}{1 + \left(\frac{D}{4F}\right)^2} \tan^{-1}\left(\frac{1 + \cos\vartheta_2}{2F}\right)$$

where X is a function of tapering ($X = 0.3$ for $t < 6$, $X = 0.36$ for $t \geq 6$, t is the tapering on the edge of the reflector), ϑ_2 is the angle between the lowest point of the offset reflector and its center as function of its geometry parameters D, F and h (diameter, focal point and offset from the axis respectively); it may be found as

$$\vartheta_2 = \frac{1}{2}\left\{\tan^{-1}\left[\frac{D+h}{F-\frac{(D+h)^2}{4F}}\right] + \tan^{-}1\left[\frac{h}{F-\frac{h^2}{4F}}\right]\right\}$$

Given S_{F}, it is possible to evaluate, for each topology, d_{m} as follows

$$d_{\mathrm{m}}^{(3,4,7)} = \frac{\vartheta_{\mathrm{c}}^{(3,4,7)}}{S_{\mathrm{F}}}$$

1.2.3 Feed types

In order to obtain multi-band antennas it is necessary to design multi-band horns as feeds; these structures need to avoid the use of FSS or sub-reflectors. The cluster of feeds forms congruent sets of beams for any considered band. The objective of feed radiators for these systems is to obtain a uniform field distribution and a low cross-polarization level. Excluding the use of dielectrics and dominant-mode conical horns, two common solutions for the realization of feeds are the corrugated horn and the Potter horn. Both choices are not very suitable in this case, for different reasons. The corrugated horn can not be used for many MBA applications because of the spatial occupation caused by corrugations. In fact, since the radial occupation of corrugated horns is larger than the aperture size, efficiency can not be very high. On the other hand, Potter horn radiators have cross-polarization limitations and band issues; as a matter of fact, these structures are based on the use of one step to generate a TM_{11} mode, which is mixed with the TE_{11} mode by designing properly the length of the flared section; this does not work in well-separated bands.

In order to have very high performances under both cross-polarization and gain points of view in several bands, the best choice is the use of high-efficiency radiators based on multimode profiled circular horns; these feeds can be designed in order to assume, just like the reflector, a nominal behavior in lower frequency bands; in addition, they can change their phase center, moving it from the center of the aperture (at lower frequencies), toward the reflector (at higher frequencies). However, since frequency performances of these high-efficiency are generally very good (since they can maintain a very high value of aperture efficiency and a very low cross-polarization level in a large bandwidth), they are the most suitable choice for these new systems. In addition to electrical specifications it is necessary to take into account mechanical requirements too, such as weight and spatial dimensions.

The use of multimode profiled circular horn antennas have a great impact on MBA performances under several points of view. In fact, each high-efficiency horn exploits almost the entire geometric area, since the field distribution is quite uniform. Because of this, the main goal of MBAs, which is the realization of a uniform coverage for each cell, is reached. This implies that these antennas have high gain; therefore, considering feed clusters as arrays, it is possible to reduce the number of feeds in order to obtain the same global gain. Furthermore, it is possible to use these topologies to reduce the cross-polarization. Although it is not possible to obtain either an extremely low cross-polarization or a 100% aperture efficiency, with multimode profiled antennas it is possible to obtain good performances about both the specifications. Figure 1.6 shows the maximum achievable aperture efficiency of

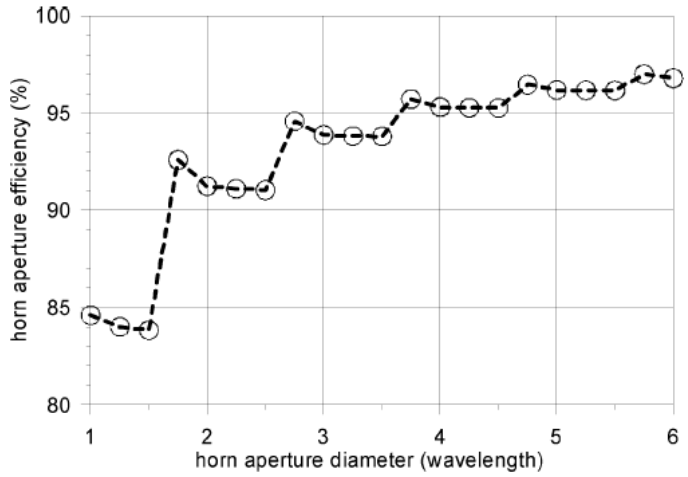

Figure 1.6: Maximum aperture efficiency of a profiled multimode horn.

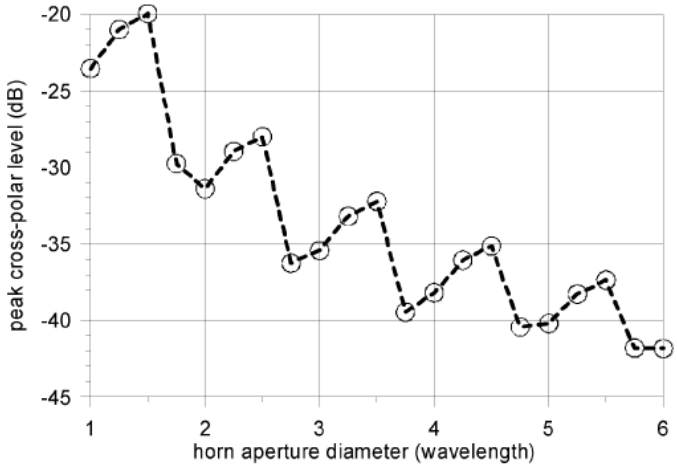

Figure 1.7: Cross-polarization level of maximum aperture efficiency circular horn.

a profiled multimodal circular horn, while Figure 1.7 quantifies the level of cross-polarization; both plots are functions of the aperture diameter, normalized to the free-space wavelength[2].

1.3 High aperture efficiency horn antennas

1.3.1 Introduction

This section is focused on the study of horn antennas, which are one of the most employed types of feed for reflector systems. Basically, a horn antenna is a flared structure which couples the free space to a waveguide. Design goals are the realization of an almost uniform aperture field distribution, and low cross-polarization;

[2]these figures are taken from [19]

moreover, low sidelobe levels are required.

In addition to electrical specifications like gain or polarization, it is necessary to keep into account mechanical specifications, like weight or spatial occupation; these requirements exclude the possibility to use corrugated horns, since corrugations imply the need of a higher spatial occupation in order to obtain the same aperture efficiency, and in many systems, like MBAs, this can not be accepted.

In literature it is possible to find solutions to this problem, based on multimodal profiled circular horn antennas; this means that, designing opportunely the profile of the antenna, it is possible to increase the aperture efficiency of the antenna by providing to the aperture several modes.

To sum up, the goal is to alter the mode content of the transmitted and/or of the received signal by introducing discontinuities in the profile of the antenna, in order to increase the electrical aperture size.

1.3.2 Determination of the modal content at the aperture

The radiation pattern of an aperture antenna equals the spatial Fourier transform of the field distribution at the aperture of the radiator.The aperture field distribution can be represented using the modal expansion, so as a superposition of TE and TM modes. So, it is possible to write

$$\underline{E}_{\mathrm{t}}^{\mathrm{aperture}} = \sum_i V_i' \underline{e}_i'(\rho, \varphi) + \sum_i V_i'' \underline{e}_i''(\rho, \varphi)$$

where the "prime" apex indicates TM modes, while the "second" apex is relative to TE modes.

Modal voltages V_i' and V_i'' represent the weights used for the determination of the electromagnetic field on the aperture as a linear combination of mode functions. Since the aperture field distribution needs to be designed in order to comply with the specifications, it is necessary to find the values of V_i' and V_i'' in order to obtain it.

An example of requirement is the uniform field distribution at the aperture; in order to reach this goal, it is necessary to evaluate, for this case, modal voltages. They can be calculated as projections of the entire field at the aperture on modes;

$$\begin{aligned} V_i' &= \left\langle \underline{E}_{\mathrm{t}}^{\mathrm{aperture}}, \underline{e}_i' \right\rangle \\ V_i'' &= \left\langle \underline{E}_{\mathrm{t}}^{\mathrm{aperture}}, \underline{e}_i'' \right\rangle \end{aligned} \tag{1.1}$$

At this point it is necessary to recall the relationship between geometric area and equivalent area; it is known that

$$A_{\mathrm{eq}} = \frac{\left| \iint_\Sigma \underline{E}_{\mathrm{t}}^{\mathrm{aperture}} \mathrm{d}\Sigma \right|^2}{\iint_\Sigma \left| \underline{E}_{\mathrm{t}}^{\mathrm{aperture}} \right|^2 \mathrm{d}\Sigma}$$

In order to maximize the equivalent area, it may be proved that the electric field must have an expression like

$$\underline{E}_{\mathrm{t}}^{\mathrm{aperture}} = \hat{\mathrm{c}}\, E_0 \tag{1.2}$$

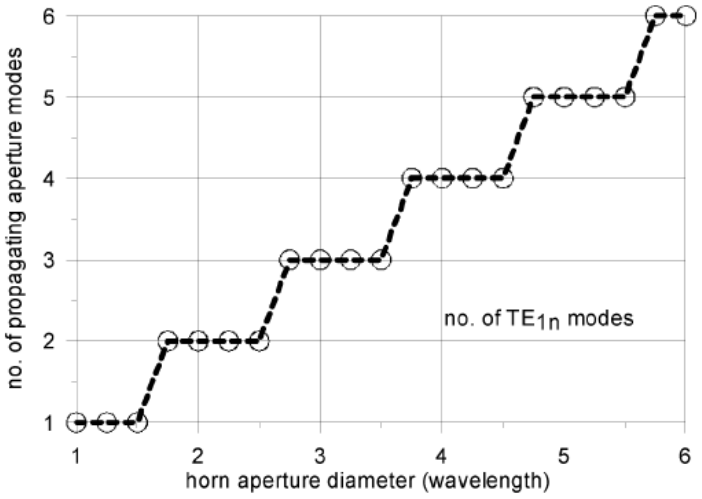

Figure 1.8: Number of propagating TE modes at the aperture of profiled multimode circular horns.

Where ĉ is a constant unit vector. From here, it is possible to prove ([3] or [19]) that in order to obtain the uniform aperture field distribution, TM modes should not be introduced in the final aperture field. On the other hand, it is necessary to provide to the aperture only TE modes. This implies that TM modal voltages V_i' ideally should equal zero. Citing [19], it is possible to quantify, for structures with circular transversal section, the number of TE_{1n} and TM_{1n} modes supported by the aperture; in fact, each aperture can support a limited number of modes. Table 1.1 and Figure 1.8 provide some informations about modes above their cut-off frequency.

Mode	χ_{mn}	guide diameter (in wavelengths λ)
TE_{11}	1.841183	0.5861
TM_{11}	3.831706	1.2197
TE_{12}	5.331443	1.6971
TM_{12}	7.015587	2.2331
TE_{13}	8.536316	2.7172
TM_{13}	10.17346	3.2383
TE_{14}	11.70601	3.7261
TM_{14}	13.32369	4.2411
TE_{15}	14.86359	4.7312
TM_{15}	16.47062	5.2428
TE_{16}	18.01553	5.7345

Table 1.1: Circular waveguide modes, zeros of Bessel functions of first kind and critical guide diameter relative to each mode.

From [19] and from [3] it is possible to find examples of the aperture modal content for the design of profiled multimode horn antennas. Considering the example from [19], it is possible to find the set of modal voltages reported in Table 1.2.

In order to obtain a very uniform field distribution at the aperture, it is necessary

Mode	Ideal $\|V_i\|$ (V)	Ideal $\angle V_i$ (deg)	Actual $\|V_i\|$ (V)	Actual $\angle V_i$ (deg)
TE_{11}	1.0	0.0	1.0	0.0
TM_{11}	0.0	0.0	0.0205	+25.5
TE_{12}	0.3112	0.0	0.2813	-11.4
TM_{12}	0.0	0.0	0.0376	-132.5
TE_{13}	0.2202	0.0	0.0557	+36.3
TM_{13}	0.0	0.0	0.0238	+25.2

Table 1.2: Example of the modal content of the aperture of a high-efficiency profiled multimode circular horn, with diameter of 3.71λ.

to provide a high number of TE modes; obviously, it is necessary to keep into account the theoretical limit of Figure 1.8; this means that a well-defined number of modes can be provided to an aperture, depending on its size.

It may be remarked that these results are valid only in order to produce a uniform distribution; if the specification requires a tapered distribution for the horn aperture, all it is necessary to provide both TE_{1n} and TM_{1n} modes. An antenna with uniform distribution can not have low cross-polarization levels too; therefore, in order to reduce it, it is necessary to have some TM modes contributions in the aperture field distribution. To sum up, there is a trade-off between polarization and uniformity of the field, as previously seen in Figures 1.7 and 1.6.

1.3.3 Synthesis of the profile of the antenna

In this paragraph some ideas for providing the desired modal content to the aperture field are shown. Usually, devices are fed with the fundamental mode. Therefore, it is necessary to consider all modes which are generated from the TE_{11} at each discontinuity.

Considering for example the goal of realizing a uniform field distribution, it is possible to use discontinuities in order to bring several TE modes to the aperture. Qualitatively, with an aperture of about four wavelengths it is possible to support almost three TE modes, which are TE_{11}, TE_{12}, TE_{13}. These modes, starting from the exciting TE_{11}, need to be generated by the structure.

Depending on the amplitude of the horn aperture, it is necessary to introduce a well-defined number of steps; for instance, if the horn aperture size supports three modes as in the previous example, two steps are needed: the first one has to end above the cut-off dimension of the TE_{12} mode, and the second one above the cutoff dimension of the TE_{13} mode. So, amplitudes of these discontinuities depend on the considered mode, but also on the relative amplitudes of higher order modes which need to be introduced.

There are at least three types of discontinuities;

- step discontinuities, which are discontinuities between two waveguides, so two cylindrical regions;
- slope discontinuities, which connect two conical regions with different half-aperture angles;

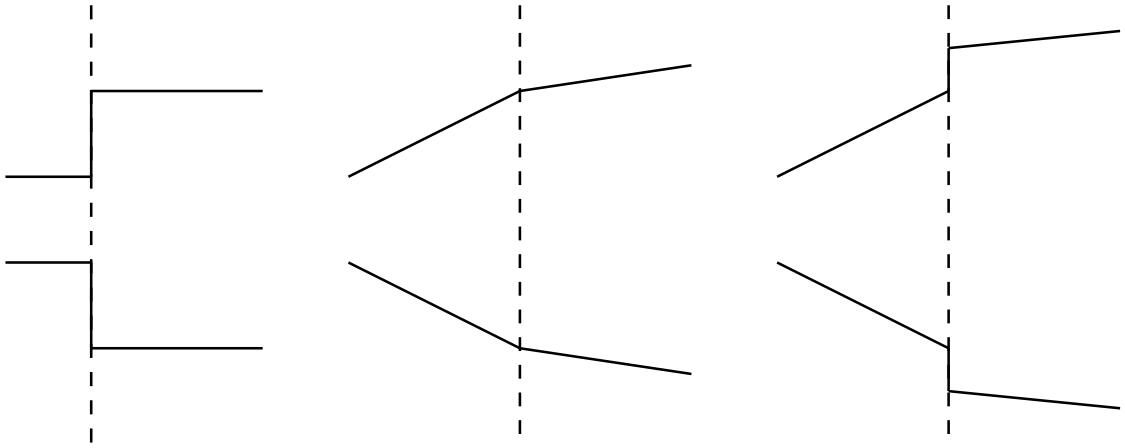

Figure 1.9: Examples of step discontinuity (left), slope discontinuity (center), and step-slope discontinuity (right).

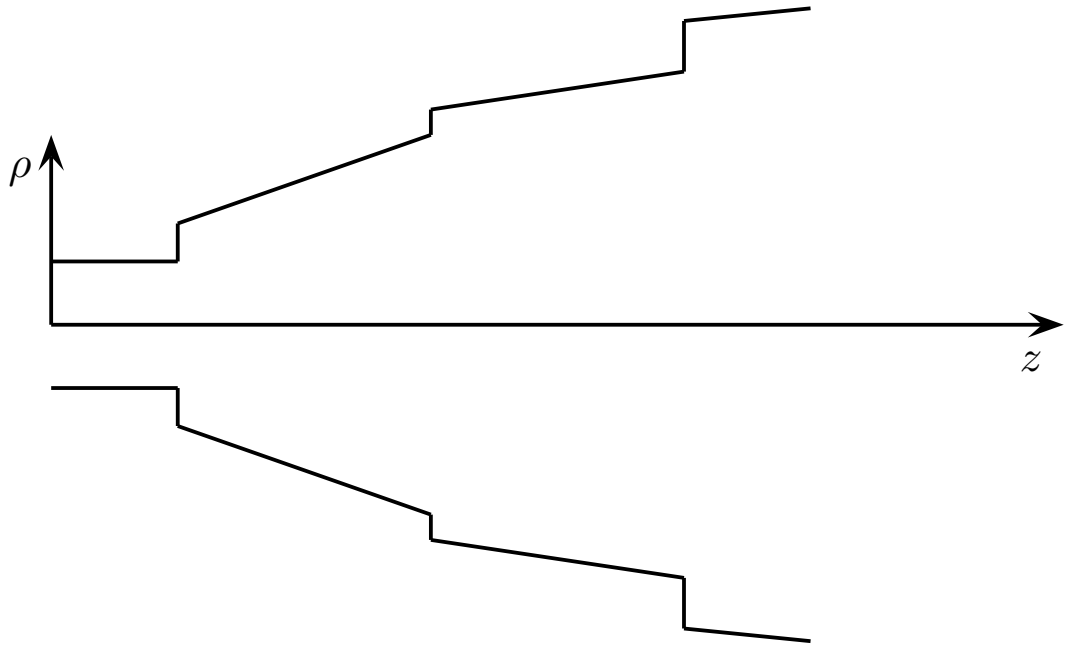

Figure 1.10: Example of horn antenna profile with step-slope discontinuities.

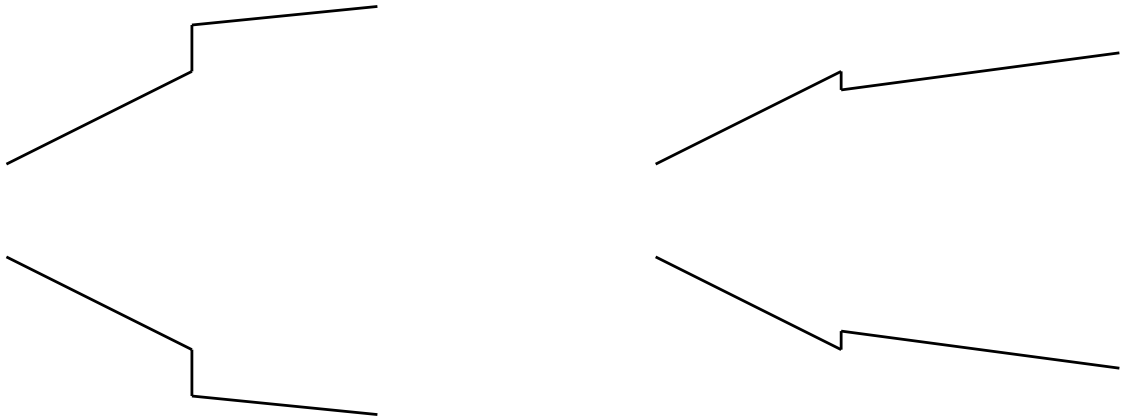

Figure 1.11: Examples of outward (left) and inward (right) step-slope discontinuities.

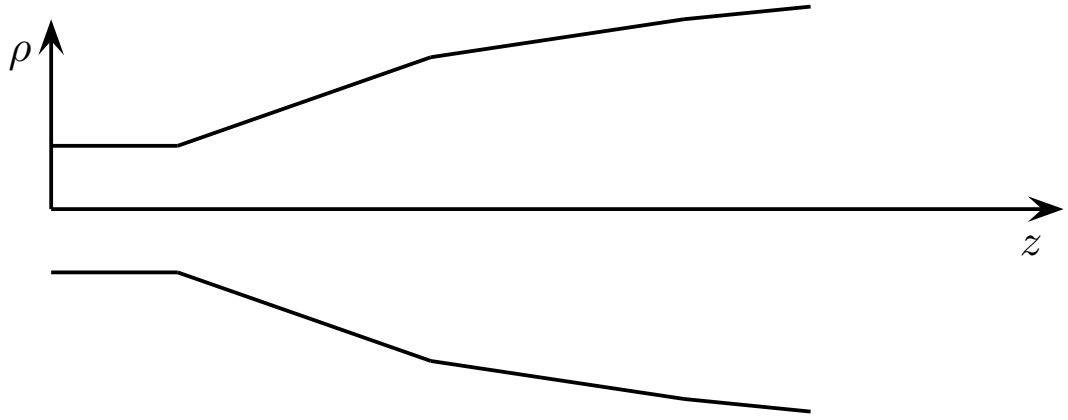

Figure 1.12: Example of horn antenna profile with slope discontinuities.

- step-slope discontinuities, which are step discontinuities between two conical regions with different half-aperture angles.

In all the cases, the discontinuity is just radial; this means that, considering the incident TE_{11}, so with $m = 1$, every excited mode has $m = 1$; therefore, are generated only TE_{1n} and TM_{1n} modes, for both the types of discontinuity.

In literature it is possible to find examples of designs of profiled multimode circular horns based on slope discontinuities, like in [19] or in Figure 1.11, or based on step-slope discontinuities, as in [3], or in Figure 1.12. Both these radiators are high-efficiency horns.

1.3.4 Analysis methods

This thesis is focused on the determination of a design-oriented analysis method for structures with cylindrical invariance, like the fundamental ones of profiled multimode circular horns. The core element of this structure is the discontinuity between a cylindrical region and a conical region, or between two conical regions with different half-aperture angles.

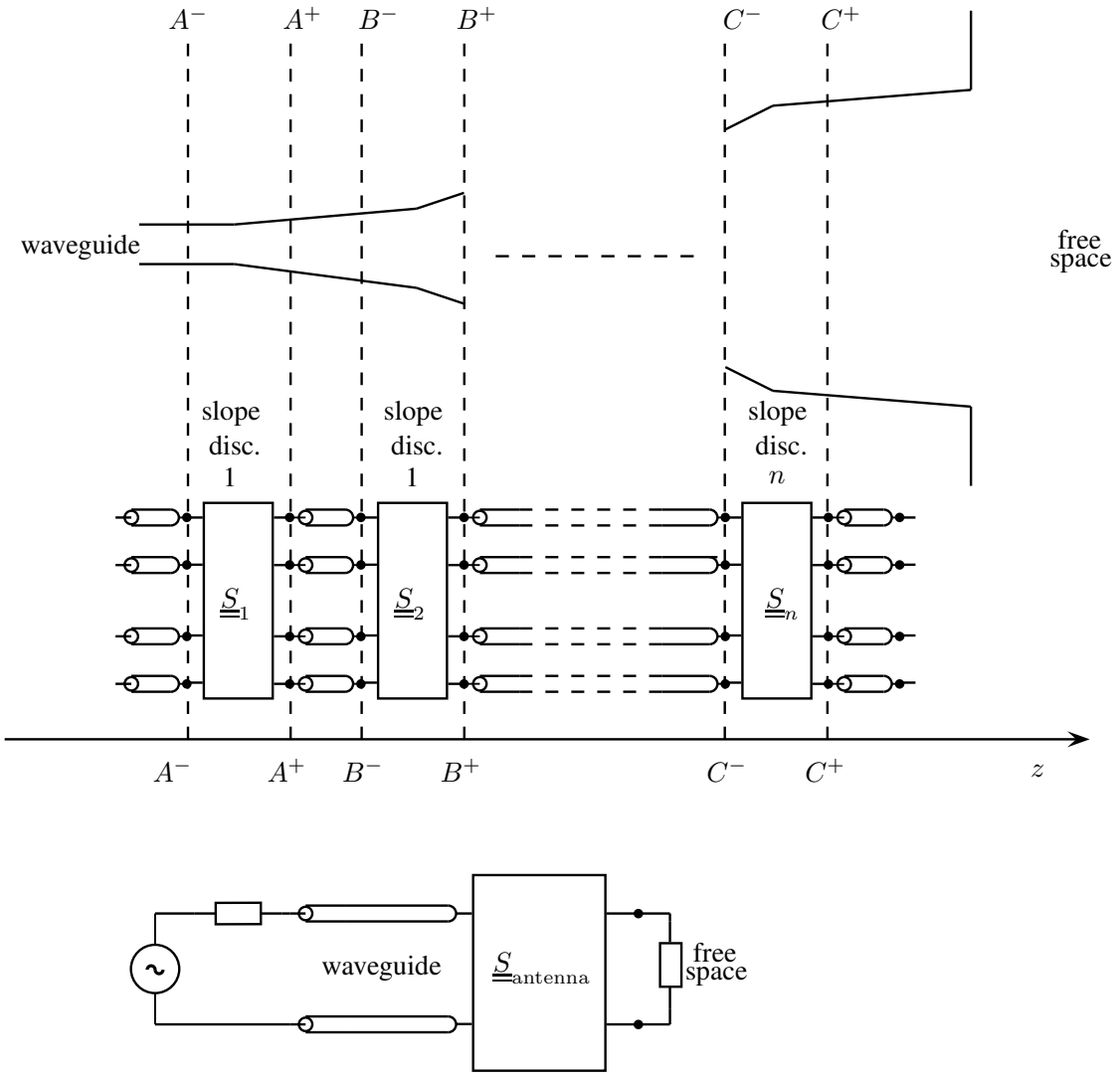

Figure 1.13: Transmission-line analysis approach; each discontinuity is modeled with a scattering matrix, and flared sections are modeled as transmission line sections.

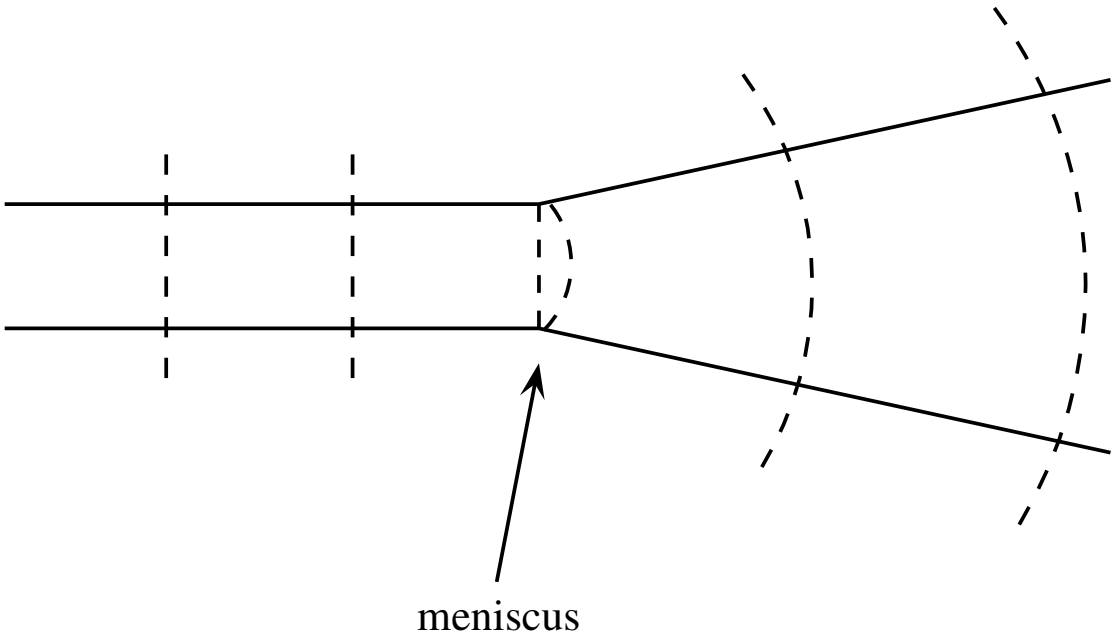

Figure 1.14: Discontinuity between a conical section and a cylindrical one, and phase surfaces in the two sections; the meniscus.

An example of method for the determination of the scattering matrix of a discontinuity is based on the mode-matching technique; this is performed expanding left and right field components with respect to the interface using the set of mode functions, then enforcing the tangential components to be continue at the interface, in weak form. The analysis of the whole structure is based on the study of a distributed parameters network; each discontinuity is modeled with its scattering matrix, then the global scattering parameters of the antenna are computed by the cascade of these matrices. This procedure is graphically summarized in Figure 1.13.

As it is possible to see from Figure 1.14, considering for instance a slope discontinuity between a waveguide and a flared section, in the waveguide phase surfaces are planes, but in the flared section of the antenna phase surfaces are spheres[3]. This means that there is a region where waves have neither plane nor spherical wave surfaces; this region in literature is called "meniscus". The application of the mode-matching technique to this problem is very complicated.

Usually this problem is avoided by discretizing the antenna in terms of waveguide step discontinuities (see Figure 1.15); since waveguide steps can be analyzed easily, it is possible to partition the profile of the antenna with pieces of circular waveguide (since here are considered structures with circular transversal section).

By this way, the profile of the antenna is approximated with a series of waveguide steps. If each step is very short, for instance $\lambda/20$, the approximation is acceptable. Then, for each step is calculated the scattering matrix, and all these matrices are cascaded in order to obtain the matrix of the whole device.

[3]in the case of conical to conical discontinuities, phase surfaces are both spheres, but with different radii

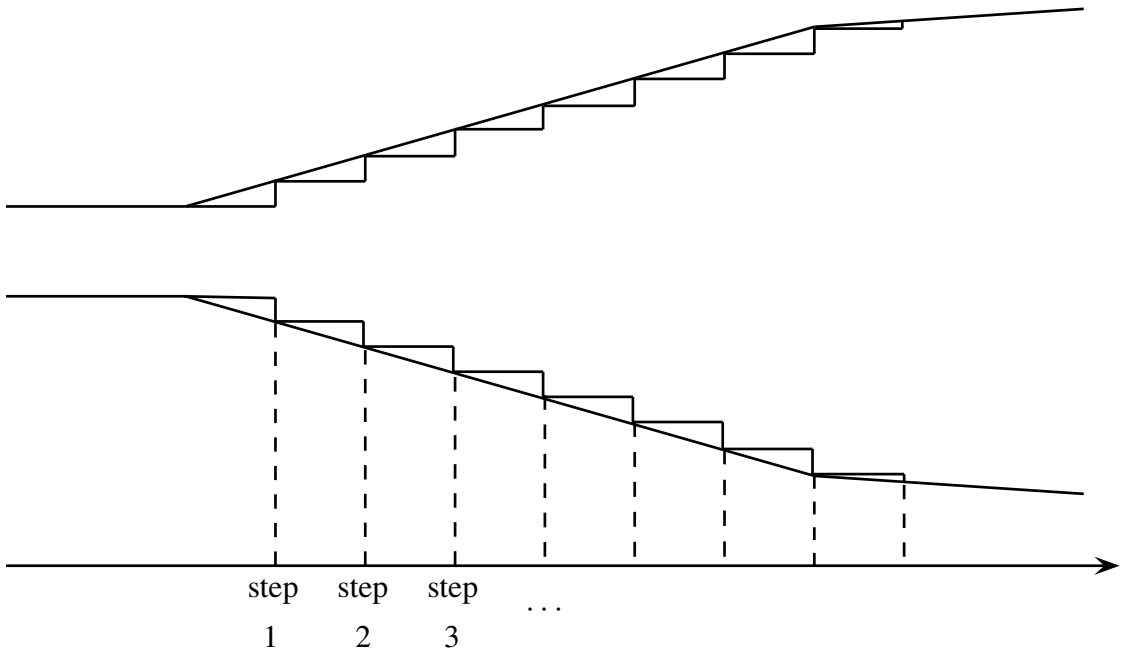

Figure 1.15: Example of approximation of a linear profile as a cascade of waveguide steps

In this work is introduced a method which allows to obtain faster and more reliable simulations, without using the mode-matching approach. The idea is to divide the structure in few subdomains, and then to apply to each subdomain a spectral method. A step or slope discontinuity may imply the presence of an edge, where the electromagnetic field has singular behavior, as known from the theory of Meixner conditions. A singularity is hardly representable with regular functions (like modes), therefore, using a set of regular expansion functions, it would be necessary to use many functions in order to obtain acceptable results, slowing down the simulation. Since these analysis methods are employed to support programs implementing optimizing algorithms, simulations need to be very fast and their results very accurate. So, in order to keep into account the presence of edges, expansion functions have to keep intrinsically into account Meixner conditions. By introducing appropriate singular elements in the set of basis functions, it is not necessary to increase too much the order of the numerical method, therefore it is possible to comply with both speed and accuracy requirements.

CHAPTER 2

Computation of mode functions

Introduction

The objective of this chapter is to explain how the computation of critical constants and of mode functions of a circular waveguide and of a radial waveguide was performed.

2.1 Circular waveguide

2.1.1 Introduction to circular waveguides

The classical approach for the analysis of a waveguide with circular transversal section (see Figure 2.1) can be found on several books, for instance [6]. The most significant results from the classical analysis are resumed here.

The most suitable orthogonal coordinate system for the representation of this structure is the **cylindrical** one: (ρ, φ, z); the transversalization method is applied considering z as longitudinal coordinate. The goal is to find $\Phi_{mn}(\rho, \varphi)$ and $\Psi_{mn}(\rho, \varphi)$, which are respectively the generating function for TM modes eigenfunctions and for TE modes eigenfunctions. It is possible to prove that these functions are representable as the product of a function $R(\rho)$, which contains informations about the radial component of the problem, and $Q(\varphi)$, for the angular component of the problem. Furthermore, it may be proved that $R(\rho)$ is the solution of the Bessel equation, $Q(\varphi)$ of the 1-dimensional Helmholtz equation[1]. The index m is related with the angular geometry parameters of the structure, while n with the radial geometry parameters.

The explicit expressions of the potentials are (see [5])

$$\Phi_{mn} = A_{mn}\, \mathrm{J}_m(k'_{\mathrm{t},i}\rho) \begin{matrix}\cos\\ \sin\end{matrix} m\varphi$$

[1] obviously these equations have to be solved with appropriate boundary conditions, depending on the considered problem and polarization

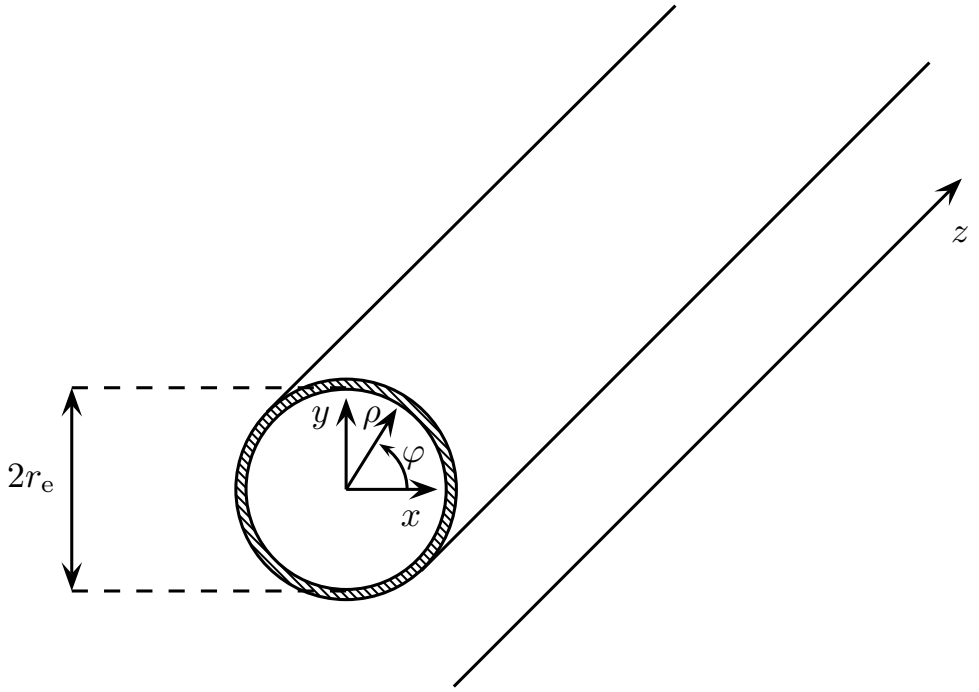

Figure 2.1: Circular waveguide

$$\Psi_{mn} = B_{mn}\,\mathrm{J}_m(k''_{\mathrm{t},i}\rho)\begin{matrix}\cos\\ \sin\end{matrix} m\varphi$$

where

$$k'_{\mathrm{t},i} = \frac{\chi_{mn}}{a} \quad \text{and} \quad k_{\mathrm{t},i}" = \frac{\chi'_{mn}}{a},$$

χ_{mn} is the n-th zero of the Bessel function of first kind and order m, χ'_{mn} is the n-th zero of the first derivative of the Bessel function of first kind, a is the radius of the waveguide, A_{mn} and B_{mn} are the normalization constants for the problem.

2.1.2 Application of the transversal resonance method to circular waveguides

In this section we will use an alternative approach, based on the transversal resonance method, in order to compute the critical constant for the circular waveguide, which may be used in a transmission line model. The most significant advantage of this method is the fact that it does not require a *guess function* for the zeroes of Bessel functions, which are the basic functions for the modal representation of circular waveguides. In fact, since critical frequencies of circular waveguides modes are related with zeroes of Bessel functions, it is necessary to compute them with a numerical method.

The first step in order to perform this process should be guessing the position of the zero, in order to run a numerical method which will find a more precise value

starting from it. Some guess functions may be found for instance on [1], but they are unreliable, especially for the first zeroes and so for the first modes, which are the most significative ones for the purposes of this work.

The problem which must be studied in this section is, for TM modes:

$$\begin{cases} \left(\nabla_{\mathrm{t}}^2 + k_{\mathrm{t}}^2\right) \Phi(\rho, \varphi) = 0 \\ \Phi = 0 \text{ for } \rho = \rho_{\mathrm{e}} \end{cases}$$

where ρ_{e} is the radius of the transversal section of the circular waveguide. Using the variable separation method, it is possible to write $\Phi(\rho, \varphi)$ as:

$$\Phi(\rho, \varphi) = R(\rho)Q(\varphi)$$

Focusing on $R(\rho)$, the problem which must be solved is the analysis of a transversal transmission line, which is a model used in order to determine the modal parameters, where the "propagation direction" is the radial coordinate ρ of the cylindrical coordinate system used in order to represent the transversal section of the waveguide. In this transversal waveguide *natural waves* are not plane waves, but **cylindrical waves**, which are a couple of waves, one expanding from the center (*outgoing wave*), one collapsing toward the center (*ingoing wave*). These waves are mathematically representable with **Hankel functions**. Indeed, the starting equation for this transmission line is a Bessel differential equation, which allows as a solution a combination of Bessel functions, but also of Hankel functions, which are a linear combination of Bessel functions. The latter ones are more interesting, in this case, because they represent traveling waves.

Considering a similar case, in a longitudinal transmission line sine and cosine are solutions of the Helmholtz equation, but they represent standing waves, because their zeroes do not move in time (in other words, considering the inverse phasor transform, there is no term which generates a non-zero phase velocity). The most commonly used solution for this example is the *traveling waves* one, based on complex exponentials. The reason why in this analysis are used Hankel functions instead of Bessel function, is that Bessel functions are *standing solutions*, Hankel functions are *traveling solutions*. In order to fix this idea, it is possible to observe the asymptotic expansions of Hankel and Bessel functions for $x \to \infty$.

$$\begin{aligned} \mathrm{H}_m^{(1)}(x) &\sim \sqrt{\frac{2}{\pi x}} \mathrm{e}^{+\mathrm{j}\left(x - m\frac{\pi}{2} - \frac{\pi}{4}\right)} \\ \mathrm{H}_m^{(2)}(x) &\sim \sqrt{\frac{2}{\pi x}} \mathrm{e}^{-\mathrm{j}\left(x - m\frac{\pi}{2} - \frac{\pi}{4}\right)} \\ \mathrm{J}_m(x) &\sim \sqrt{\frac{2}{\pi x}} \cos\left(x - m\frac{\pi}{2} - \frac{\pi}{4}\right) \\ \mathrm{Y}_m(x) &\sim \sqrt{\frac{2}{\pi x}} \sin\left(x - m\frac{\pi}{2} - \frac{\pi}{4}\right) \end{aligned}$$

Remembering that cylindrical waves, far away from the source, are similar to plane waves, it is evident that Bessel functions are related with standing waves, and Hankel

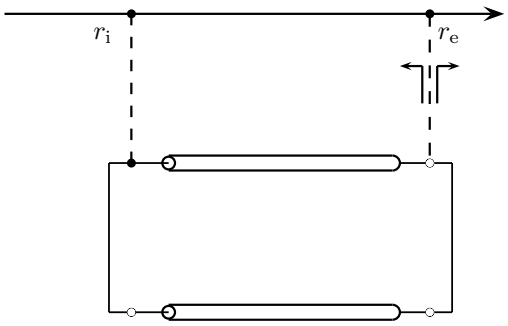

Figure 2.2: Loop Gain calculation model

functions with traveling waves. More in details, outgoing waves (the cylindrical equivalent of progressive waves) are expressed with $\mathrm{H}^{(2)}$; ingoing waves with $\mathrm{H}^{(1)}$. Therefore, it is possible to write $R(\rho)$ as:

$$R(\rho) = A\mathrm{H}_m^{(1)}(k_\mathrm{t}\rho) + B\mathrm{H}_m^{(2)}(k_\mathrm{t}\rho)$$

It is possible to define reflection coefficients for ingoing and outgoing cylindrical waves starting from this last expression; in fact, it can be written as:

$$R(\rho) = B\mathrm{H}_m^{(2)}(k_\mathrm{t}\rho)\left[1 + \frac{A}{B}\frac{\mathrm{H}_m^{(1)}(k_\mathrm{t}\rho)}{\mathrm{H}_m^{(2)}(k_\mathrm{t}\rho)}\right] \triangleq B\mathrm{H}_m^{(2)}(k_\mathrm{t}\rho)\left[1 + \Gamma^\mathrm{o}(\rho)\right] \tag{2.1}$$

where $\Gamma^\mathrm{o}(\rho)$ is the reflection coefficient relative to outgoing waves; $\Gamma^\mathrm{i}(\rho)$ can be defined simply by taking $A\mathrm{H}^{(1)}$ away from the parentheses:

$$R(\rho) = A\mathrm{H}_m^{(1)}(k'_\mathrm{t}\rho)\left[1 + \frac{B}{A}\frac{\mathrm{H}_m^{(2)}(k'_\mathrm{t}\rho)}{\mathrm{H}_m^{(1)}(k'_\mathrm{t}\rho)}\right] \triangleq A\mathrm{H}_m^{(1)}(k'_\mathrm{t}\rho)\left[1 + \Gamma^\mathrm{i}(\rho)\right] \tag{2.2}$$

For $\rho = \rho_\mathrm{e}$, there is the PEC boundary condition, so $\Gamma^\mathrm{o}(r_\mathrm{e}) = -1$; in other words,

$$A\mathrm{H}_m^{(1)}(k'_\mathrm{t}\rho_\mathrm{e}) + B\mathrm{H}_m^{(2)}(k'_\mathrm{t}\rho_\mathrm{e}) = 0 \Longrightarrow B = -A\frac{\mathrm{H}_m^{(1)}(k'_\mathrm{t}\rho_\mathrm{e})}{\mathrm{H}_m^{(2)}(k'_\mathrm{t}\rho_\mathrm{e})}$$

the modulus of the ratio of the Hankel functions equals 1, so $|A| = |B|$. So, by remembering that Hankel functions are defined as

$$\mathrm{H}_m^{(1)}(x) = \mathrm{J}_m(x) + \mathrm{j}\mathrm{Y}_m(x)$$
$$\mathrm{H}_m^{(2)}(x) = \mathrm{J}_m(x) - \mathrm{j}\mathrm{Y}_m(x)$$

if $A = B$ in phase too, Y_m terms are equal with opposite sign, so, because of the fact that $\mathrm{Y}_m(0)$ is the only singular point, the final function is regular. In order to find the critical constants for TM waves, it is necessary to calculate the *loop gain* T for outgoing and ingoing waves. It can be computed as the product of the ingoing and outgoing reflection coefficients in an arbitrary point belonging to the domain; considering the ρ axis, the equivalent line is in Figure 2.2.

Considering $\rho = \rho_\mathrm{e}$ as point for the calculation of the loop gain:

$$\begin{aligned} T &= \Gamma^\mathrm{i}(\rho_\mathrm{e})\Gamma^\mathrm{o}(\rho_\mathrm{e}) \\ &= \frac{\mathrm{H}_m^{(2)}(k'_\mathrm{t}\rho_\mathrm{e})}{\mathrm{H}_m^{(1)}(k'_\mathrm{t}\rho_\mathrm{e})}(-1) \end{aligned} \tag{2.3}$$

The mode functions must satisfy $|T| = 1$, and $\angle T = n2\pi$ conditions, where n is the modal index. $|T| = 1$ is automatically satisfied by (2.3), because the absolute value of the ratio of the two Hankel functions evaluated in the same point equals 1. Actually, this is true only if the argument of Hankel functions is real, therefore k_t have to be real; therefore, the $|T| = 1$ condition gives informations about the domain of the eigenvalue of the problem.

About the phase condition, one Hankel function is the complex conjugate of the other one. About the phase, steps are slightly harder; first of all, from the fact that $\mathrm{H}_m^{(1)} = \mathrm{H}_m^{(2)*}$, it follows that:

$$\angle\mathrm{H}_m^{(1)} = -\angle\mathrm{H}_m^{(2)}$$

so:

$$\angle T = \pi + \angle\frac{\mathrm{H}_m^{(2)}(k'_\mathrm{t}\rho_\mathrm{e})}{\mathrm{H}_m^{(1)}(k'_\mathrm{t}\rho_\mathrm{e})} = \pi - 2\angle\mathrm{H}_m^{(1)}(k'_\mathrm{t}\rho_\mathrm{e}) \tag{2.4}$$

In order to evaluate the critical constant, the $\angle T$ expression will be modified, in order to obtain an **unwrapped** expression. This can be useful because, without unwrapping, the behavior of the phase *jumps* from $-\pi$ to π.

The basic element for the unwrapping process is a $\vartheta(k'_\mathrm{t}\rho)$ function, which estimates the phase of $\mathrm{H}_m^{(1,2)}$. The required quality for the estimated phase is not high; in fact, the only purpose for $\vartheta(k'_\mathrm{t}\rho)$ function is to count correctly the number of turns of the phase (every turn is 2π), in order to have:

$$\left|\angle\mathrm{H}_m^{(1)}(k_\mathrm{t}\rho)\mathrm{e}^{-\mathrm{j}\vartheta(k_\mathrm{t}\rho)}\right| < 2\pi$$

in other words, the phase of the Hankel function multiplied by the unwrap function has to shift less than 2π. This method is called **analytical unwrap**. From (2.4),

$$\angle T = \pi - 2\angle\mathrm{H}_m^{(1)}(k'_\mathrm{t}\rho_\mathrm{e})\mathrm{e}^{-\mathrm{j}\vartheta(k'_\mathrm{t}\rho_\mathrm{e})} - 2\vartheta(k'_\mathrm{t}\rho_\mathrm{e}) = n2\pi$$

The modes of the circular waveguide are those solutions of the Bessel equation with $|T| = 1$, and $\angle T = n2\pi$; n is the modal index, which is also the index of the considered zero of the Bessel function (for instance, $n = 2$ identifies the second zero of the Bessel function, so the second critical constant for a fixed m, order of Bessel function). The unwrap function ϑ can be found in [1], (9.2.29) for TM modes.

TE modes

For TE modes the procedure is almost the same, considering the fact that the problem is:

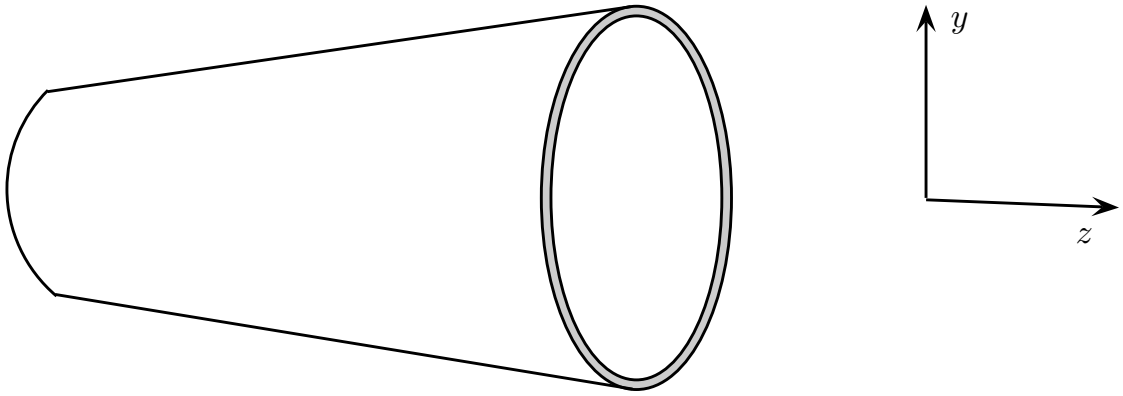

Figure 2.3: Example of conical section (of a horn antenna)

$$\begin{cases} \left(\nabla_{\mathrm{t}}^2 + k_{\mathrm{t}}^2\right) \Psi(\rho, \varphi) = 0 \\ \dfrac{\mathrm{d}\Psi}{\mathrm{d}\nu} = 0 \text{ for } \rho = \rho_{\mathrm{e}} \end{cases}$$

Therefore, there are some basic differences; in fact:

$$\Psi(\rho, \varphi) = A\mathrm{H}_m^{(1)}(k_{\mathrm{t}}\rho) + B\mathrm{H}_m^{(2)}(k_{\mathrm{t}}\rho)$$

just like in the previous case, this time the boundary condition is about the derivative normal with respect to the contour of the waveguide, which is $\hat{\rho}$; so:

$$\frac{\mathrm{d}\Psi}{\mathrm{d}\rho} = A\mathrm{H}_m^{\prime(1)}(k_{\mathrm{t}}\rho) + B\mathrm{H}_m^{\prime(2)}(k_{\mathrm{t}}\rho)$$

In conclusion, the procedure is basically identical, compared to the previous one, using the derivatives of the Hankel functions instead of the Hankel functions. For the unwrap it is possible to do almost the same considerations, using as approximating expression for the phase, ϑ, formula (9.2.31) from [1].

2.2 Conical waveguide modes

This section focuses on a different problem, which is the computation of modal critical constants for a conical waveguide.

The geometry of the structure is in Figure 2.3. ϑ_0 is the flare angle and φ is the azimuthal angular coordinate.

It is possible to apply to the this structure the Marcuvitz and Schwinger transversalization method, using as *longitudinal* coordinate the radial one, r; this means that modal eigenfunctions will be functions of φ and ϑ.

The application of this method and the main results are slightly different compared to the rectangular or circular waveguide cases. In fact, the most significant difference between this case and the previous ones is that, for waveguides analyzed with *radial Marcuvitz and Schwinger equations*, propagation of modes toward the

radial direction is mathematically representable using spherical Bessel functions, instead of exponential functions. These functions are related with Bessel functions, and so their asymptotic behaviors are similar to Bessel functions ones; this means that all previous considerations about the representation of traveling or standing cylindrical waves respectively for Hankel and Bessel functions, are still correct about spherical waves and spherical Hankel or spherical Bessel functions.

Another difference with respect to the previous method may be found by observing the generating functions for modal eigenfunctions. Once again it is possible to use the variable separation method in order to obtain

$$\Phi(\vartheta,\varphi) = \Phi_m(\varphi)\Phi_p^m(\vartheta)$$

$$\Psi(\vartheta,\varphi) = \Psi_m(\varphi)\Psi_p^m(\vartheta)$$

where Φ is the generating function for TM mode eigenfunctions, Ψ for TE mode eigenfunctions. These functions come from the solution of differential equations with Dirichlet or Neumann boundary conditions respectively for TM and TE modes.

About φ coordinate, the component of the generating function, $\Phi_m(\varphi)$ or $\Psi_m(\varphi)$ is $\mathrm{e}^{\pm \mathrm{j}m\varphi}$. In ϑ, the problem is much more complicated, because $\Phi_p^m(\vartheta)$ and $\Psi_p^m(\vartheta)$ are solutions of the following equation;

$$\left\{\frac{\mathrm{d}}{\mathrm{d}\vartheta}\sin\vartheta\frac{\mathrm{d}}{\mathrm{d}\vartheta} - \frac{m^2}{\sin\vartheta} + k_\mathrm{t}^2\sin\vartheta\right\}\Phi_p^m(\vartheta) \tag{2.5}$$

considering a change of variable, $x = \cos\vartheta$, it is possible to see that

$$\vartheta = \arccos x \Longrightarrow \mathrm{d}\vartheta = -\frac{1}{\sqrt{1-x^2}}\mathrm{d}x$$

so

$$\frac{\mathrm{d}x}{\mathrm{d}\vartheta} = -\sqrt{1-x^2}$$

Moreover,

$$\frac{\mathrm{d}}{\mathrm{d}\vartheta} = \frac{\mathrm{d}x}{\mathrm{d}\vartheta}\frac{\mathrm{d}}{\mathrm{d}x}$$

and

$$\sin\vartheta = \sqrt{1-\cos^2\vartheta} = \sqrt{1-x^2}$$

Finally, substituting all these steps in (2.5), it is possible to find

$$\begin{aligned}&\left\{-\sqrt{1-x^2}\frac{\mathrm{d}}{\mathrm{d}x}\left[-\sqrt{1-x^2}\sqrt{1-x^2}\frac{\mathrm{d}}{\mathrm{d}x}\right] + \sqrt{1-x^2}\,k_\mathrm{t}^2 - \frac{m^2}{\sqrt{1-x^2}}\right\}\Phi_p^m(x)\\ =&\left\{(1-x^2)\frac{\mathrm{d}}{\mathrm{d}x}\left[(1-x^2)\frac{\mathrm{d}}{\mathrm{d}x}\right] + (1-x^2)k_\mathrm{t}^2 - m^2\right\}\Phi_p^m(x)\end{aligned}$$

The last equation, writing $k_t^2 = p(p+1)$ with p real in general, is known as associated Legendre equation. Its solutions are associated Legendre functions of order m and degree p, $\mathrm{P}_p^m(x)$. Considering TM case, instead of p it is smarter to use a p' degree, where the single apex recalls the fact that the parameter is referred to TM polarization.

For TM modes, the differential problem which has to be solved is

$$\begin{cases} \left\{(1-x^2)\dfrac{\mathrm{d}}{\mathrm{d}x}\left[(1-x^2)\dfrac{\mathrm{d}}{\mathrm{d}x}\right] + (1-x^2)p'(p'+1) - m^2\right\}\Phi_{p'}^m(x) \\ \Phi_{p'}^m(x) = 0 \text{ for } x = x_0 = \cos\vartheta_0 \end{cases} \tag{2.6}$$

where ϑ_0 is the flare angle. The solution of this problem is

$$\Phi_{p'}^m(x) = \mathrm{P}_{p'}^m(x)$$

The objective is to find the p' value such that the boundary condition is satisfied.

For TE modes, the only difference is in the boundary condition, which is a Neumann condition instead of a Dirichlet one.

$$\begin{cases} \left\{(1-x^2)\dfrac{\mathrm{d}}{\mathrm{d}x}\left[(1-x^2)\dfrac{\mathrm{d}}{\mathrm{d}x}\right] + (1-x^2)p''(p''+1) - m^2\right\}\Psi_{p''}^m(x) \\ \left.\dfrac{\mathrm{d}\Phi_{p''}^m(\vartheta)}{\mathrm{d}\vartheta}\right|_{\vartheta=\vartheta_0} = 0 \end{cases} \tag{2.7}$$

where

$$\Psi_{p''}^m(x) = \mathrm{P}_{p''}^m(x)$$

In this case the goal is to find the p'' degree.

Boundary conditions

Both systems (2.6) and (2.7) introduce conditions only on the $x = x_0$ point, without specifying any boundary condition for the other integral end, which is, for the case study, $x = +1$.

There are two kinds of boundary conditions which can be enforced, defining a differential problem: **numerical** boundary conditions and **behavioral** boundary conditions.

- Numerical boundary conditions are those conditions which specify the numerical value of the solution in a specific point. These conditions have the following form:

$$af(x_0) + b\left.\frac{\mathrm{d}}{\mathrm{d}x}f(x)\right|_{x=x_0} = 0 \tag{2.8}$$

  if $b = 0$, (2.8) is a Dirichlet boundary condition, because it enforces the value of the solution of the problem in a specific point x_0 to equal zero. By contrast,

if $a = 0$, (2.8) is a Neumann condition, because it enforces the value of the derivative in $x = x_0$ to equal zero. Finally, the most general case is for $a, b \neq 0$, which is the Robin condition case (also known as **impedance conditions**, when applied on transmission lines, because it sets the value of the ratio of a quantity and its derivative, so of the voltage in a point and its derivative, which is the current).

- Behavioural boundary conditions are those conditions which does not specify a specific value for the solution of the differential problem, but just enforce a property for the solution. Examples of behavioral boundary conditions are periodicity, regularity (N continuous derivatives) or symmetries. Many times behavioral boundary conditions are implicitly satisfied simply by choosing basis functions for the representation of solutions which satisfy them.

This introduction is necessary because in the case study of this work there are one numerical boundary condition for $x = x_0$ (Dirichlet or Neumann/Robin, depending on the analyzed equation), and one behavioral condition for $x = 1$.

2.3 Numerical methods for the solution of the associated Legendre equation

2.3.1 Introduction

Generating functions $\Phi_{p'}^{m}(\vartheta)$ and $\Psi_{p''}^{m}(\vartheta)$ unfortunately are not evaluable easily with non-integer p. However, the non-integer p case is very significative, because it occurs almost every time that $x \notin [-1, 1]$, so when $x_0 \neq -1$.

Therefore, the purpose of this section is to introduce numerical methods aimed at solving (2.6) and (2.7), so to find p', p'', and the related generating functions. The numerical methods used in this study belong to two main families, which are

- pseudospectral methods;
- spectral methods.

These methods were applied directly to the associated Legendre equation, in a slightly modified form compared to (2.6) or (2.7), or to Gegenbauer equation, which is a differential equation related with the associated Legendre one.

2.3.2 Associated Legendre equation

Starting from (2.6) or (2.7), it is possible to write the differential equation in a slightly different way. Using the Leibnitz derivative formula and considering a generic solution $L(x)$ of the following equation,

$$\frac{\mathrm{d}}{\mathrm{d}x}\left[(1-x^2)\frac{\mathrm{d}}{\mathrm{d}x}\right]L(x) = (1-x^2)\frac{\mathrm{d}^2}{\mathrm{d}x^2}L(x) - 2x\frac{\mathrm{d}}{\mathrm{d}x}L(x)$$

by substituting this expression in the equation and dividing all the members by $(1-x^2)$, it is possible to find the following equation:

$$(1-x^2)\frac{\mathrm{d}^2}{\mathrm{d}x^2}L(x) - 2x\frac{\mathrm{d}}{\mathrm{d}x}L(x) + \left(p(p+1) - \frac{m^2}{1-x^2}\right)L(x) = 0 \tag{2.9}$$

Solutions of the associated Legendre equation, regular in ± 1, are **associated Legendre polynomials** $\mathrm{P}_n^m(x)$, if m and n are integer numbers. More in general, if $m \to \mu$, $n \to p$ where $p, \mu \in \mathbb{R}$, solutions for the equation are **associated Legendre functions**. m is the **order** of the function, and p is its **degree**. In all the considered cases for this study, the order is always an integer number, so it will be represented simply as m. By contrast, the degree is almost every time a non-integer number, so it will be represented as p.

2.3.3 Gegenbauer equation

$$\frac{\mathrm{d}^2}{\mathrm{d}x^2}L(x) - \frac{2x}{1-x^2}\frac{\mathrm{d}}{\mathrm{d}x}L(x) + \left(\frac{c}{1-x^2} - \frac{m^2}{(1-x^2)^2}\right)L(x) = 0 \tag{2.10}$$

This equation has two **regular singular points**, so it is possible to apply to it the Fuchs-Frobenius method, which permits to find an analytical solution, so expansible as Taylor series. The equation now is written in the following form:

$$\frac{\mathrm{d}^2}{\mathrm{d}x^2}L(x) + p(x)\frac{\mathrm{d}}{\mathrm{d}x}L(x) + q(x)L(x) = 0$$

where

$$p(x) = -\frac{2x}{1-x^2} \quad q(x) = \frac{c}{1-x^2} - \frac{m^2}{(1-x^2)^2}$$

Now this equation must be modified, exploiting the fact that coefficients have particular singularities. So, it is possible to define two coefficients $A(x)$ and $B(x)$, for the $x = +1$ discontinuity:

$$A(x) = (x-1)p(x) = -(x-1)\frac{2x}{(1-x)(1+x)} = \frac{2x}{x+1}$$

$$B(x) = (x-1)^2 q(x) = (x-1)^2\frac{c}{(1-x)(1+x)} - (x-1)^2\frac{m^2}{(1-x)^2(1+x)^2} = \\ = c\frac{1-x}{1+x} - \frac{m^2}{(1+x^2)^2}$$

$A(x)$ and $B(x)$ are analytical functions for $x = +1$; in fact, it is possible to expand them with Taylor series, because they are not singular anymore in this point. So,

$$A(x) = \sum_{n=0}^{\infty} a_n (x-x_0)^n = a_0 + a_1 (x-1)^1 + a_2 (x-1)^2 + ...$$

the coefficient a_0 equals the function $A(x)$, evaluated for $x = 1$:

$$a_0 = A(1) = \frac{2}{1+1} = 1$$

the same idea must be applied on $B(x)$:

$$B(x) = \sum_{n=0}^{\infty} b_n (x - x_0)^n = b_0 + b_1 (x-1)^1 + b_2 (x-1)^2 + ...$$

where:

$$b_0 = B(1) = c\frac{1-1}{1+1} - \frac{m^2}{(1+1)^2} = \frac{m^2}{4}$$

It may be proved[2] the following **indicial equation** is satisfied:

$$\lambda_0(r) = r^2 + (a_0 - 1)\, r + b_0 = 0$$

in this equation, $a_0 = 1$, $b_0 = \frac{m^2}{4}$. Therefore, by substituting:

$$r^2 - \frac{m^2}{4} = 0 \Longrightarrow r = \pm\frac{m}{2}$$

so, for the $x = 1$ case:

$$L(x) = (x-1)^{\frac{m}{2}} \sum_{n=0}^{\infty} c_n (x-1)^{\frac{m}{2}}$$

It is possible to repeat the same procedure in order to solve the $x = -1$ case and take away the other discontinuity from the Legendre equation. This means that:

$$L(x) = \left(1 - x^2\right)^{\frac{m}{2}} G(x) = f(x)G(x) \tag{2.11}$$

where $G(x)$ is an analytical function in the closed interval $[-1, 1]$. The last equation suggests that it is better to perform a change of variable, substituting $L(x)$ written in (2.11) form, in order to obtain a differential equation with more regular solution. Therefore, it is necessary to calculate some terms, as follows;

$$\frac{\mathrm{d}}{\mathrm{d}x}L(x) = G(x)\frac{\mathrm{d}}{\mathrm{d}x}f(x) + f(x)\frac{\mathrm{d}}{\mathrm{d}x}G(x)$$

$$\frac{\mathrm{d}^2}{\mathrm{d}x^2}L(x) = G(x)\frac{\mathrm{d}^2}{\mathrm{d}x^2}f(x) + 2\frac{\mathrm{d}}{\mathrm{d}x}f(x)\frac{\mathrm{d}}{\mathrm{d}x}G(x) + f(x)\frac{\mathrm{d}^2}{\mathrm{d}x^2}G(x)$$

where

$$\frac{\mathrm{d}}{\mathrm{d}x}f(x) = -mx\left(1 - x^2\right)^{\frac{m}{2}-1}$$

$$\frac{\mathrm{d}^2}{\mathrm{d}x^2}f(x) = -m\left(1 - x^2\right)^{\frac{m}{2}-1} + 2m\left(\frac{m}{2} - 1\right)x^2\left(1 - x^2\right)^{\frac{m}{2}-2}$$

[2] [7], section 14.4 (Solution of a Differential Equation in a Neighborhood of a Regular Singuar Point)

These results have to be substituted in (2.10):

$$\begin{aligned}
&\left(1-x^2\right)\left\{2mx^2\left(\frac{m}{2}-1\right)\left(1-x^2\right)^{\frac{m}{2}-2}-mx\left(1-x^2\right)^{\frac{m}{2}-1}\right\}G(x)+\\
&+\left(1-x^2\right)\left\{2\left(1-x^2\right)^{\frac{m}{2}}-2mx\left(1-x^2\right)^{\frac{m}{2}-1}\right\}\frac{\mathrm{d}}{\mathrm{d}x}G(x)+\\
&+\left(1-x^2\right)\left\{\left(1-x^2\right)^{\frac{m}{2}}\right\}\frac{\mathrm{d}^2}{\mathrm{d}x^2}G(x)-\\
&+2x\left\{-mx\left(1-x^2\right)^{\frac{m}{2}-1}G(x)+\left(1-x^2\right)^{\frac{m}{2}}\frac{\mathrm{d}}{\mathrm{d}x}G(x)\right\}+\\
&+\left(c-\frac{m^2}{1-x^2}\right)\left(1-x^2\right)^{\frac{m}{2}}G(x)=0
\end{aligned}$$

With simple algebra it may be shown that:

- the second derivative coefficient is

$$\left(1-x^2\right)^{\frac{m}{2}+1}$$

- the first derivative coefficient is

$$-2x\left(m+1\right)\left(1-x^2\right)^{\frac{m}{2}}$$

- the function coefficient is

$$\begin{aligned}
&\left(1-x^2\right)^{\frac{m}{2}}\left\{-m+2m\left(\frac{m}{2}-1\right)\frac{x^2}{1-x^2}+2m\frac{x^2}{1-x^2}+c-\frac{m^2}{1-x^2}\right\}=\\
&=\left(1-x^2\right)^{\frac{m}{2}}\left\{-m+m^2\frac{x^2}{1-x^2}+c-\frac{m^2}{1-x^2}\right\}=\\
&=\left(1-x^2\right)^{\frac{m}{2}}\left\{-m-m^2+c\right\}
\end{aligned}$$

Finally, it is possible to write the alternative form of (2.10) using these coefficients:

$$\left(1-x^2\right)\frac{\mathrm{d}^2}{\mathrm{d}x^2}G(x)-2x\left(m+1\right)\frac{\mathrm{d}}{\mathrm{d}x}G(x)+\left(c-m(m+1)\right)G(x)=0 \qquad (2.12)$$

The most important advantage of working on (2.12) instead of (2.10) is the fact that its solution is regular in the closed interval. Moreover, equation (2.11) emphasizes an interesting aspect of the behavior of associated Legendre functions. In fact, if $m \neq 0$, even without applying Dirichlet conditions, $L(x)$ function will be zero in $x = \pm 1$. Furthermore, this zero is generally not of first order, unless $m = 2$.

At this point it is possible to apply two different approaches; the first one, based on the direct solution of associated Legendre equation, and the second one, based on the solution of the modified equation. Equation (2.12) is the "Gegenbauer equation".

2.3.4 Boundary conditions for Gegenbauer equation

Gegenbauer equation has to be solved in order to satisfy (2.6) or (2.7). About the former's one boundary conditions, there are no major problems; indeed, since Dirichlet boundary conditions are homogeneous, the value of a or b of (2.8) is not relevant. This is no longer true for Robin conditions, because in this case it is mandatory to enforce the correct ratio a/b.

However, in order to find TE modes eigenvalues, Gegenbauer equation must not be solved with Neumann conditions, because the equation which has to be solved with a Neumann condition is the associated Legendre equation.

The following algebra leads to an expression of boundary conditions for Gegenbauer equations equivalent to the Neumann condition for associated Legendre equation.

From (2.7),

$$\frac{\mathrm{d}}{\mathrm{d}\vartheta}L(\cos\vartheta) = \frac{\mathrm{d}L(\cos\vartheta)}{\mathrm{d}\cos\vartheta}\frac{\mathrm{d}(\cos\vartheta)}{\mathrm{d}\vartheta} = -\sin\vartheta\frac{\mathrm{d}L(\cos\vartheta)}{\mathrm{d}\cos\vartheta} = \\ = -\sin\vartheta\frac{\mathrm{d}L(x)}{\mathrm{d}x}$$

where $x = \cos\vartheta$. By differentiating (2.11), it is possible to see that

$$\frac{\mathrm{d}L(x)}{\mathrm{d}x} = \frac{\mathrm{d}}{\mathrm{d}x}\left[\left(1-x^2\right)^{\frac{m}{2}}G(x)\right] = \\ = -2x\frac{m}{2}\left(1-x^2\right)^{\frac{m}{2}-1}G(x) + \left(1-x^2\right)^{\frac{m}{2}}\frac{\mathrm{d}G(x)}{\mathrm{d}x}$$

This equation has to be evaluated in $x = x_0 = \cos\vartheta_0$. This means that

$$\left.\frac{\mathrm{d}G(x)}{\mathrm{d}x}\right|_{x=x_0} = -x_0\left(1-x_0\right)^{\frac{m}{2}-1}G(x_0) + \left(1-x_0^2\right)^{\frac{m}{2}}\left.\frac{\mathrm{d}G(x)}{\mathrm{d}x}\right|_{x=x_0} \tag{2.13}$$

This condition has to be applied to Gegenbauer equation solved in the canonical interval ξ (see A.6); taking into account this, (2.13) becomes

$$\left.\frac{\mathrm{d}G(x)}{\mathrm{d}x}\right|_{x=x_0} = -x_0\left(1-x_0^2\right)^{\frac{m}{2}-1}G(x_0) + \left(1-x_0^2\right)^{\frac{m}{2}}\frac{1}{J_1}\left.\frac{\mathrm{d}G(x)}{\mathrm{d}x}\right|_{x=x_0} \tag{2.14}$$

where J_1 comes from (A.30)

2.3.5 Pseudospectral methods

Pseudospectral methods are based on **interpolation**; the basic idea is to interpolate a function evaluated on a set of points which are commonly called **nodes**. This means that, given a function $f(x)$ which is for instance the solution of a differential equation, it has to be represented with an approximated $f_N(x)$. The representation

of a generic function $f(x)$ as a sum of a finite number of other functions $\varphi_n(x)$ implies an approximation of the solution of the differential equation, because the generic $f(x)$ belonging to an infinite-dimensional space of functions is represented with functions belonging to a finite subset of the former space of functions. So, $f_N(x)$ may be written as follows;

$$f_N(x) = \sum_{n=0}^{N} f_n \varphi_n(x) \tag{2.15}$$

$\varphi_n(x)$ can be almost every function at this step; depending on the type of differential equation which has to be solved and on boundary conditions which define the domain of the solution of the equation, there are different suitable choices. For instance, if the solution of the differential equation has to be periodic, $\varphi_n(x)$ can be a sine or cosine function. Generally, it is a good criterium to choose functions similar to the expected solution; for instance, if the expected unknown function is a polynomial, it is better to use polynomials for the representation.

The criterium for building the system is to find functions which satisfy exactly the equation in chosen nodes. In other words,

$$f_N(x_n) = f(x_n) = f_n$$

This is the philosophy of pseudospectral and collocation methods. As a matter of fact, the name *collocation* comes from the fact that the equation is *collocated*, so it is exactly satisfied in the nodes. This method is applied to a differential equation in order to build a finite-dimensional eigenvalue problem. An eigenvalue problem has two outputs: eigenvalues and eigenvectors. Eigenvalues λ are strictly related with p, because

$$\lambda = p(p+1)$$

for both p' and p'' values. On the other hand, eigenvectors contain the interpolating values of the function, evaluated in the nodes. These values are used by an interpolating function in order to evaluate the plot points for the function.

Equation (2.15) may be misleading; f_n are **not** weights, because they are the values of the function $f(x)$ in nodes $\{x_n\}$. The meaning of $\{f_n\}$ is the most important difference between pseudospectral methods and spectral methods.

The unknown of the system for these methods is the set of values $\{f_n\}$; in fact, the set of interpolating functions $\{\varphi_n(x)\}$ is chosen, just like the set of nodes $\{x_n\}$.

These methods are called "pseudospectral" because (2.15) recalls a spectral representation, but it is not exactly spectral. Once upon a time the Galerkin method was called *spectral* and, since pseudospectral methods are **identical** to the Galerkin method if inner product integrals are evaluated using Gaussian integration formulae, the label "pseudospectral" is reasonable. Moreover, Gaussian integration formulae are the most efficient scheme for numerical quadrature for Galerkin method, using the roots of functions of the same kind of the basis functions. For instance, if basis functions are Chebyshev polynomials, the best choice for quadrature nodes (which are also the pseudospectral grid nodes) are the zeroes of Chebyshev polynomials.

Implementation notes for the case study

Pseudospectral methods were implemented in this work using [24]. This consists of a suite of functions which evaluates differentiation matrices with different kinds of interpolating nodes and functions.

There are some types of functions, for each kind of interpolating functions:

- functions which evaluate interpolation nodes (for instance Chebyshev nodes, even-spaced nodes, Laguerre nodes);
- functions which evaluate differentiation matrices for chosen nodes and interpolating functions in given nodes;
- functions which exploit previous functions to implement boundary conditions on differentiation matrices.

The best choice for problems in bounded intervals, such as $\xi \in [-1, 1]$ are Chebyshev nodes and interpolating functions. This is also the choice performed in this case study.

Boundary conditions deserve some extra explanations; in the case study it is necessary to enforce one numerical boundary condition, for $x = x_0$, and one behavioral boundary condition for the other interval end.

Most of functions necessary for the implementation of these methods were already inside of the suite, and they are described in [24]. Unfortunately, the case of one numerical condition and one behavioral condition was not considered by the authors of the suite, therefore it was necessary to edit a function in order to introduce it.

First of all, [24] explains that the implementation of Dirichlet functions is based on the elimination of a row from every differentiation matrix. Then, if the boundary condition is homogeneous, the work is done; otherwise, if the boundary condition is not homogeneous (case not interesting for this study), it is necessary to add other terms to the matrix equation. Anyway, in order to introduce a behavioral condition, an idea may simply be to remove a Dirichlet condition, so to maintain the row which should be deleted. For instance, if it is necessary to have a numerical Robin condition on $\xi = -1$ and a behavioral condition on $\xi = +1$, the idea is to take the case from the original code where there is a Dirichlet condition in the right bound and a Robin condition in the left bound, and then take away from it the Dirichlet condition simply by maintaining the erased row in the original code.

2.3.6 Spectral methods

The second family of methods implemented in order to evaluate the modal functions was the *spectral* one. In spectral methods a function $f(x)$, solution of a differential equation, is expanded as a series of functions.

$$f(x) = \sum_{n=0}^{n_{\max}} a_n u_n(x) \tag{2.16}$$

In this case a_n are not the values of the $f(x)$ function evaluated in some points, but they are **weights** of the linear combination. In other words, now each a_n

quantifies the importance of the $u_n(x)$ function contribution in the representation of $f(x)$ (like Fourier coefficients in Fourier series quantify how significative is a frequency contribution compared with others).

Generalities about spectral methods

Spectral methods involve three elements:

- expansion functions $u_n(x)$; $\{u_n\}$ is the set of functions used for the representation of the solution of the differential equation, $f(x)$;
- test functions; these are functions used to project a function on the expansion functions.
- the inner product; it is characterized by the weight used in order to perform projection.

In order to fix these ideas, it is possible to consider a symbolic example. Given $f(x)$ represented as

$$f(x) = \sum_{n=0}^{n_{\max}} a_n u_n(x)$$

and given for example $g(x) = f'(x)$ (instead of the derivative operation it is possible to apply almost any linear operator, such as multiplication by a constant, by a variable, by the cosine of a variable and so on), represented in the same basis $\{u_n(x)\}$, but with different weight coefficients b_n

$$g(x) = \sum_{n=0}^{n_{\max}} b_n u_n(x)$$

It is interesting to relate a_n coefficients with b_n coefficients, in order to approximate the differential equation with a matrix equation. This last expression can be written as

$$\sum_{n=0}^{n_{\max}} b_n u_n(x) = \sum_{n=0}^{n_{\max}} a_n \frac{\mathrm{d}}{\mathrm{d}x} u_n(x)$$

Generally, in order to find a relationship between $\{a_n\}$ and $\{b_n\}$, the method is based on the study of the projection of the left-hand side and of the right-hand side on test functions, which are for instance (just in this example) functions of the same type, u_m.

$$\langle \sum_{n=0}^{n_{\max}} b_n u_n(x), u_m(x) \rangle = \langle \sum_{n=0}^{n_{\max}} a_n \frac{\mathrm{d}}{\mathrm{d}x} u_n(x), u_m(x) \rangle, \quad m = 0 \text{ to } n_{\max}$$

Now, considering for example an inner product with weight 1, the result is

$$\int \sum_{n=0}^{n_{\max}} b_n u_n(x) u_m(x) \mathrm{d}x = \int \sum_{n=0}^{n_{\max}} a_n \frac{\mathrm{d}}{\mathrm{d}x} u_n(x) u_m(x) \mathrm{d}x, \quad m = 0 \text{ to } n_{\max}$$

so

$$\sum_{n=0}^{n_{\max}} b_n \int u_n(x) u_m(x) \mathrm{d}x = \sum_{n=0}^{n_{\max}} a_n \int \frac{\mathrm{d}}{\mathrm{d}x} u_n(x) u_m(x) \mathrm{d}x, \quad m = 0 \text{ to } n_{\max} \tag{2.17}$$

This equation can be represented with a matrix equation. Given

$$\underline{a} \triangleq \begin{bmatrix} a_0 \\ a_1 \\ \vdots \\ a_{n_{\max}} \end{bmatrix} \quad \underline{b} \triangleq \begin{bmatrix} b_0 \\ b_1 \\ \vdots \\ b_{n_{\max}} \end{bmatrix}$$

and a $\underline{\underline{M}}$ matrix defined as

$$\underline{\underline{M}} \triangleq \langle \frac{\mathrm{d}}{\mathrm{d}x} u_n(x), u_m(x) \rangle, \quad m = 0 \text{ to } n_{\max}$$

and finally the Gram matrix $\underline{\underline{G}}$ defined as

$$\underline{\underline{G}} \triangleq \langle u_n(x), u_m(x) \rangle, \quad m = 0 \text{ to } n_{\max}$$

it is possible to write (2.17) as follows

$$\underline{\underline{G}}\, \underline{b} = \underline{\underline{M}}\, \underline{a} \tag{2.18}$$

the relationship which relates $\underline{b}$ with $\underline{a}$ is simply

$$\begin{aligned} \underline{b} &= \left(\underline{\underline{G}}^{-1}\, \underline{\underline{M}} \right) \underline{b} \\ &= \underline{\underline{D}}^{-1}\, \underline{b} \end{aligned} \tag{2.19}$$

This is the general procedure for the computation of b_n coefficients starting from a_n ones.

Some remarks:

- the choice of the inner product weight depends on chosen functions $u_n(x)$; in fact, it is better to use the weight which guarantees orthonormality between u_n (for instance, for Chebyshev polynomials, it is $w_n = (1 - x^2)^{-\frac{1}{2}}$); if there is orthonormality, the projection of u_n on u_m is non-zero only when $n = m$; moreover, it equals 1, in this case. This means that if the inner product is well-chosen, the Gram matrix equals the identity matrix. $\underline{\underline{M}}$, in this case, is the matrix which represents the discretization of the operator (in this example, the derivative operator). The inner product choice may be fundamental because the inversion of a matrix is very expensive, and it introduces numerical errors in the final results;

- it is possible to use Gaussian quadrature formulae with a polynomial basis, because they produce **exact** results with an appropriate number of nodes ($2N + 1$ nodes, where N is the order of polynomials).

The method which will be described is equivalent to a "general" spectral method, with a difference. Relationships between a_n and b_n will not be found with **analytical** calculations (calculating inner products), but with **algebraic** calculations, by exploiting some properties of basis functions. The result of this approach are **exact** matrices (except for the last term) even without using Gaussian quadrature formulae.

This procedure equals the general spectral method using the same set of functions as test and expansion functions, and as inner product the one which ensures the orthonormality of the function (and so that $\underline{\underline{G}} = \underline{\underline{I}}$).

Moreover, all basis functions which will be used as expansion functions are polynomials. This is interesting, because the operators of interest here are applied on these polynomials are multiplication for x or x^2, or differentiation. These operators are applied on polynomials, but they return polynomials.Just like pseudospectral methods, this method is used to build an eigenvalue problem.Eigenvectors coefficients are weights which have to be multiplied by the single basis functions.

For spectral methods, it may be interesting to plot (in logarithmic scale) the n-th component of the eigenvector versus n. In fact, if the method is well-constructed, the first components will be high, but then they will decrease sharply; this because if the method suits well the differential equation it is possible to use few components to represent well the solution.

Eigenvectors can provide useful informations about the quality of a method. However, it is better to implement a convergence study, in order to quantify the actual performances of the numerical method. Obviously, for general problems, increasing the number of expansion functions used N, the quality of results improves.

Enforcing boundary conditions

Given the representation (2.16), it may be necessary to enforce a numerical boundary condition at $x = x_0$. Considering for instance a Dirichlet boundary condition (Neumann/Robin conditions are almost identical to implement), it is necessary to require that

$$f(x_0) = 0 \Longrightarrow \sum_{n=0}^{n_{\max}} a_n u_n(x_0) = 0$$

renaming $c_n = u_n(x_0)$, this condition is translated in the following one

$$\sum_{n=0}^{n_{\max}} a_n c_n = 0 \tag{2.20}$$

where c_n are values of the basis function in $x = x_0$. (2.20) may be written in matrix form as follows:

$$\left[\begin{array}{ccc|c} c_0 & c_1 & \dots & \underline{c}_{\mathrm{BC}} \end{array}\right] \left[\begin{array}{c} a_0 \\ a_1 \\ \vdots \\ \hline a_{n_{\max}} \\ \hline \underline{a}_{\mathrm{BC}} \end{array}\right]$$

or

$$\left[\begin{array}{c|c} \underline{c}_0 & \underline{c}_{\mathrm{BC}} \end{array}\right] \left[\begin{array}{c} \underline{a} \\ \hline \underline{a}_{\mathrm{BC}} \end{array}\right]$$

this last equation may be written as

$$\underline{c}_0\, \underline{a} + \underline{c}_{\mathrm{BC}}\, \underline{a}_{\mathrm{BC}} = 0$$

In this equation, $\underline{c}_0$ and $\underline{c}_{\mathrm{BC}}$ are known, while $\underline{a}$ and $\underline{a}_{\mathrm{BC}}$ are unknown. However, by modifying this equation it is possible to obtain an equation which can be added in the matrix which discretizes the operator; this equation enforces boundary condition(s). In fact, by inverting it, it is possible to find:

$$\underline{a}_{\mathrm{BC}} = -\left(\underline{c}_{\mathrm{BC}}\right)^{-1} \underline{c}_0 \underline{a} \tag{2.21}$$

Considering (2.19),

$$\underline{b} = \underline{\underline{D}}\, \underline{a}$$

In order to enforce boundary conditions on this matrix $\underline{\underline{D}}$, the idea is to introduce a partition in it.

$$\left[\begin{array}{c} b_0 \\ b_1 \\ \vdots \\ \hline b_{n_{\max}} \\ \hline \underline{b}_{\mathrm{BC}} \end{array}\right] = \left[\begin{array}{c|c} \multirow{2}{*}{$\underline{\underline{D}}^{\mathrm{NBC}}$} & \\ & \\ \hline \underline{\underline{D}}^{\mathrm{BC}} & \end{array}\right] \left[\begin{array}{c} a_0 \\ a_1 \\ \vdots \\ \hline a_{n_{\max}} \\ \hline \underline{a}_{\mathrm{BC}} \end{array}\right]$$

The last matrix equation can be written as follows:

$$\underline{b} + \underline{b}_{\mathrm{BC}} = \left[\underline{\underline{D}}^{\mathrm{NBC}}\, \underline{a} + \underline{\underline{D}}^{\mathrm{BC}} \underline{a}_{\mathrm{BC}}\right]$$

where $\underline{\underline{D}}^{\mathrm{NBC}}$ is $\underline{\underline{D}}$ without the last column and row. By applying to this equation the (2.21), it is possible to find the matrix formula for the implementation of boundary conditions to the discretized operator:

$$\begin{aligned} \underline{b} + \underline{b}_{\mathrm{BC}} &= \left[\underline{\underline{D}}^{\mathrm{NBC}} \underline{a} - \underline{\underline{D}}^{\mathrm{BC}} \left(\underline{c}_{\mathrm{BC}}\right)^{-1} \underline{c}_0 \underline{a}\right] = \\ &= \left[\underline{\underline{D}}^{\mathrm{NBC}} \underline{a} - \underline{\underline{D}}^{\mathrm{BC}} \left(\underline{c}_{\mathrm{BC}}\right)^{-1} \underline{c}_0\right] \underline{a} \end{aligned} \tag{2.22}$$

$\underline{\underline{D}}$ may be the discretization matrix of every operator: single, double or higher order differentiation, multiplication for polynomials and so on.

The procedure for the application of Neumann/Robin conditions is almost the same; the only difference is in $\underline{c}_0$ and $\underline{c}_{\mathrm{BC}}$, which contains $\frac{\mathrm{d}}{\mathrm{d}x}f(x)\big|_{x=x_0}$ coefficients, or more in general (2.8) coefficients. It is necessary to know values of basis functions in $x = x_0$; for this reason, it is advisable to use the canonical interval ξ instead of the natural one, x, for the implementation, and then use a handbook (for example [1]) in order to find the values of function in $\xi = \pm 1$.

A remark on boundary conditions

The previous subsection explained how to enforce a boundary condition with the spectral method implemented in this study. However, it is very important to be careful every time that this procedure is applied; these conditions have to be applied only being sure that it is necessary.

In order to fix the idea, it is now proposed an example. Given the multipication-by-ξ matix $\underline{\underline{D}}_{\xi}$ and the differentiation matrix $\underline{\underline{D}}_{\frac{\mathrm{d}}{\mathrm{d}\xi}}$, it may be necessary to represent the discretized operator

$$\xi \frac{\mathrm{d}}{\mathrm{d}\xi}\left[f(\xi)\right]$$

where $f(\xi)$ must satisfy boundary conditions. In this case, the method explained in the previous subsection must be applied to $\underline{\underline{D}}_{\frac{\mathrm{d}}{\mathrm{d}\xi}}$ matrix, but **not** to $\underline{\underline{D}}_{\xi}$ matrix; in fact, the equivalent discretized operator is given by the matrix product $M_{\xi}\,\underline{\underline{D}}_{\frac{\mathrm{d}}{\mathrm{d}\xi}}$. The first operator applied to $f(\xi)$ is the discretized differentiation, which returns a function which is applied to the discretized multiplication operator. Differentiation returns a function which does not have to satisfy Dirichlet boundary conditions; in fact, it is $f(\xi)$ the one which does, not $\frac{\mathrm{d}}{\mathrm{d}\xi}f(\xi)$. So, the discretized multiplication operator must be unedited, in order to obtain the correct representation of the equivalent operator.

2.3.7 Legendre spectral method

For each spectral method it is necessary to find $\underline{\underline{D}}$ matrices which relate the a_n coefficients of the $f(x)$ representation (2.16), with the b_n ones. In this case study, differential equations are the associated Legendre equation or the Gegenbauer equation, which have, as operators, $xf(x)$, $x^2 f(x)$, $\frac{\mathrm{d}}{\mathrm{d}x}f(x)$, $\frac{\mathrm{d}^2}{\mathrm{d}x^2}f(x)$. In this subsection and in the following ones are shown some proofs to find some of these discretization matrices. Some of final results can be compared with [9].

Legendre spectral method is a numerical method which involves Legendre polynomials as expansion and test functions; this means that (2.16) becomes

$$f(x) = \sum_{n=0}^{n_{\max}} a_n \mathrm{P}_n(x)$$

In addition, it is better to do calculations for associated Legendre polynomials as basis functions; these degenerate in Legendre polynomials for $m = 0$, but results are more general. So

$$f(x) = \sum_{n=0}^{n_{\max}} a_n \mathrm{P}_n^m(x) \tag{2.23}$$

$xf(x)$ matrix

Now, the objective is to represent $xf(x)$ using $\mathrm{P}_n^m(x)$ as expansion functions.

$$xf(x) = \sum_{n=0}^{n_{\max}} a_n x \mathrm{P}_n^m(x) = \sum_{n=0}^{n_{\max}} b_n \mathrm{P}_n^m(x)$$

now, by inverting (A.3), which is here recalled,

$$\left(1 - x^2\right) \frac{\mathrm{d}}{\mathrm{d}x} \mathrm{P}_n^m(x) = (n+m)\mathrm{P}_{n-1}^m(x) - nx\mathrm{P}_n^m(x)$$

it is possible to find $x\mathrm{P}_n^m(x)$

$$x\mathrm{P}_n^m(x) = \frac{n-m+1}{2n+1}\mathrm{P}_{n+1}^m(x) - \frac{n+m}{2n+1}\mathrm{P}_{n-1}^m(x) \tag{2.24}$$

so, by substituting

$$xf(x) = \sum_{n=m}^{n_{\max}} a_n \left[\frac{n-m+1}{2n+1}\mathrm{P}_{n+1}^m + \frac{n+m}{2n+1}\mathrm{P}_{n-1}^m(x)\right] = \mathrm{T}_1 + \mathrm{T}_2$$

Now it is necessary to change indexes of the associated Legendre polynomials in order to obtain all the times a $\mathrm{P}_n^m(x)$ function; this is necessary in order to write the last equation in (2.23) form.

- T_1 case

$$\sum_{n=m}^{n_{\max}} a_n \frac{n-m+1}{2n+1}\mathrm{P}_{n+1}^m(x)$$

so

$$n + 1 = n' \Longrightarrow n = n' - 1$$

the equation may be re-written as

$$\sum_{n'=m+1}^{n_{\max}} a_{n'-1} \frac{n'-m}{2n'-1}\mathrm{P}_{n'}^m(x)$$

- T_2 case

$$\sum_{n=m}^{n_{\max}} a_n \frac{n+m}{2n+1}\mathrm{P}_{n-1}^m(x)$$

so

$$n-1=n'' \Longrightarrow n=n''+1$$

the equation may be re-written as

$$\sum_{n''=m-1}^{n_{\max}} a_{n''+1}\frac{n''+1+m}{2n''+3}\mathrm{P}_{n''}^{m}(x)$$

To sum up, by substituting n'' and n' with n, it is possible to find b_n as function of a_n as

$$b_n=\frac{n-m}{2n-1}a_{n-1}+\frac{n+1+m}{2n+3}a_{n+1}=c_{n-1}a_{n-1}+c_{n+1}a_{n+1} \tag{2.25}$$

This system can be written as a matrix; in fact, it is possible to write this equation as follows

$$\begin{bmatrix} b_0 \\ b_1 \\ b_2 \\ \vdots \end{bmatrix} = \begin{bmatrix} 0 & c_2 & 0 & \cdots & \\ c_0 & 0 & c_3 & \cdots & \\ 0 & c_1 & 0 & c_4 & \cdots \\ \vdots & & \ddots & \ddots & \ddots \end{bmatrix} \begin{bmatrix} a_0 \\ a_1 \\ a_2 \\ \vdots \end{bmatrix} \tag{2.26}$$

$x^2 f(x)$ matrix

In this case the procedure is quite similar to the previous one;

$$x^2 f(x)=\sum_{n=m}^{n_{\max}} a_n x^2 \mathrm{P}_n^m(x)=\sum_{n=m}^{n_{\max}} a_n x^2 \mathrm{P}_n^m(x)$$

It is possible to use again (2.24) relationship, but it has to be used twice. In fact

$$x^2\mathrm{P}_n^m(x)=\frac{n-m+1}{2n+1}x\mathrm{P}_{n+1}^m(x)+\frac{n+m}{2n+1}x\mathrm{P}_{n-1}^m(x)$$

so, by using again it, being careful with the indexes,

$$x\mathrm{P}_{n+1}^m(x)=\frac{n-m+2}{2n+3}\mathrm{P}_{n+2}^m(x)+\frac{n+m+1}{2n+3}\mathrm{P}_n^m(x)$$

$$x\mathrm{P}_{n-1}^m(x)=\frac{n-m}{2n-1}\mathrm{P}_n^m(x)+\frac{n-1+m}{2n-1}\mathrm{P}_{n-2}^m(x)$$

by substituting

$$\frac{n-m+1}{2n+1}\left[\frac{n-m+2}{2n+3}\mathrm{P}_{n+2}^m(x)+\frac{n+m+1}{2n+3}\mathrm{P}_n^m(x)\right]+$$
$$+\frac{n+m}{2n+1}\left[\frac{n-m}{2n-1}\mathrm{P}_n^m(x)+\frac{n-1+m}{2n-1}\mathrm{P}_{n-2}^m(x)\right]$$

so, considering T_1, T_2 and T_3 cases

- T_1:

$$\mathrm{T}_1 = \sum_{n=m}^{n_{\max}} a_n \frac{n-m+1}{2n+1}\frac{n-m+2}{2n+3}\mathrm{P}^m_{n+2}(x)$$

with the change of indexes, same procedure of $xf(x)$ case,

$$\begin{aligned} &= \sum_{n'=m+2}^{n_{\max}} a_{n'-2}\frac{n'-2-m+1}{2(n'-2)+1}\frac{n'-2-m+2}{2(n'-2)+3}\mathrm{P}^m_{n'}(x) \\ &= \sum_{n'=m+2}^{n_{\max}} a_{n'-2}\frac{n'-m-1}{2n'-3}\frac{n'-m}{2n'-1}\mathrm{P}^m_{n'}(x) \end{aligned}$$

- T_2,

$$\mathrm{T}_2 = \sum_{n=m}^{n_{\max}} a_n \left[\frac{n-m+1}{2n+1}\frac{n+m+1}{2n+3} + \frac{n+m}{2n+1}\frac{n-m}{2n-1}\right]\mathrm{P}^m_n$$

- T_3,

$$\begin{aligned} \mathrm{T}_3 &= \sum_{n=m}^{n_{\max}} a_n \frac{n+m}{2n+1}\frac{n-1+m}{2n-1}\mathrm{P}_{n-2}(x) = \\ &= \sum_{n''=m}^{n_{\max}} a_{n''+2}\frac{n''+2+m}{2n''+5}\frac{n''+1+m}{2n''+3}\mathrm{P}^m_{n''}(x) \end{aligned}$$

By substituting all these expressions, it is possible to find

$$\begin{aligned} b_n &= \frac{n-m-1}{2n-3}\frac{n-m}{2n-1}a_{n-2} + \left(\frac{n-m+1}{2n+1}\frac{n+m+1}{2n+3} + \frac{n+m}{2n+1}\frac{n-m}{2n-1}\right)a_n + \\ &+ \frac{n+2+m}{2n+5}\frac{n+1+m}{2n+3}a_{n+2} \\ &= c_{n-2}a_{n-2} + c_n a_n + c_{n+2}a_{n+2} \end{aligned} \tag{2.27}$$

$$\begin{bmatrix} b_0 \\ b_1 \\ b_2 \\ \vdots \end{bmatrix} = \begin{bmatrix} c_0 & 0 & c_2 & \cdots & \\ 0 & c_1 & 0 & c_3 & \cdots \\ c_0 & 0 & c_2 & 0 & c_4 \\ \vdots & \ddots & \ddots & \ddots & \ddots \end{bmatrix} \begin{bmatrix} a_0 \\ a_1 \\ a_2 \\ \vdots \end{bmatrix} \tag{2.28}$$

Expressions of Legendre matrices

Starting from previous calculations it is possible to find coefficients for Legendre polynomials expansion. In fact, considering (2.25) and (2.27) with $m = 0$, it is trivial to find

- $\mathcal{L}f(x) = xf(x)$

$$b_n = \frac{n}{2n-1}a_{n-1} + \frac{n+1}{2n+3}a_{n+1} = c_{n-1}a_{n-1} + c_{n+1}a_{n+1}$$

- $\mathcal{L}f(x) = x^2 f(x)$

$$b_n = \frac{n-1}{2n-3}\frac{n}{2n-1}a_{n-2} + \left(\frac{n+1}{2n+1}\frac{n+1}{2n+3} + \frac{n}{2n+1}\frac{n}{2n-1}\right)a_n + \\ + \frac{n+2}{2n+5}\frac{n+1}{2n+3}a_{n+2}$$

Moreover, for derivatives cases, from [9],it is possible to find

- $\mathcal{L}f(x) = \frac{\mathrm{d}}{\mathrm{d}x}f(x)$

$$b_n = (2n+1)\sum_{\substack{p=n+1 \\ p+n \text{ odd}}}^{n_{\max}} a_p \tag{2.29}$$

- $\mathcal{L}f(x) = \frac{\mathrm{d}^2}{\mathrm{d}x^2}f(x)$

$$b_n = \left(n+\frac{1}{2}\right)\sum_{\substack{p=n+2 \\ p+n \text{ even}}}^{n_{\max}} \left[p(p+1) - n(n+1)\right]a_p \tag{2.30}$$

2.3.8 Gegenbauer spectral method

The goal of this subsection is to find discretization matrices, using as basis functions Gegenbauer polynomials $\mathrm{C}_n^{(\lambda)}(x)$.

As written in Appendix A.4, (A.14) here recalled

$$\left(1-x^2\right)\frac{\mathrm{d}^2}{\mathrm{d}x^2}\mathrm{C}_\kappa^{(\lambda)}(x) - (2\lambda+1)\frac{\mathrm{d}}{\mathrm{d}x}\mathrm{C}_\kappa^{(\lambda)}(x) + \kappa(\kappa+2\lambda)\mathrm{C}_\kappa^{(\lambda)}(x)$$

is strictly related with the equation (2.12); considering the latter one, written as

$$\left(1-x^2\right)\frac{\mathrm{d}^2}{\mathrm{d}x^2}G(x) - 2\,(m+1)\,x\frac{\mathrm{d}}{\mathrm{d}x}G(x) + \\ + \left[(l+m)\,(l+m+1) - m\,(m+1)\right]G(x) = 0$$

with $\lambda = m + \frac{1}{2}$, it is possible to see that

$$\begin{cases} 2\lambda + 1 = 2m + 2 = 2(m+1) \\ \kappa\,(\kappa + 2\lambda) = \kappa\,(\kappa + 2m + 1) \end{cases}$$

On the other hand, from (2.12), it is possible to see that

$$\begin{aligned} &(l+m)\,(l+m+1) - m\,(m+1) = \\ =&l^2 + l(m+1) + ml + m(m+1) - m(m+1) = \\ =&l^2 + 2ml + l = l\,(l + 2m + 1) \end{aligned}$$

with $\kappa = l$, those two equations are the same. This means that calling (2.12) the "Gegenbauer equation" is absolutely correct.

The idea of choosing Gegenbauer polynomials was born from the fact that, being Gegenbauer polynomials the solution of Gegenbauer equation, it may be a good idea to use them as expansion functions.

$xf(x)$ matrix

Considering (A.15) here recalled,

$$\kappa \mathrm{C}_{\kappa}^{(\lambda)}(x) = 2(\kappa + \lambda - 1)x\mathrm{C}_{\kappa-1}^{(\lambda)}(x) - (\kappa + 2\lambda - 2)\mathrm{C}_{\kappa-2}^{(\lambda)}(x), \quad \kappa \geq 2$$

with $\kappa = n$, it is possible to use the following representation:

$$f(x) = \sum_{n=0}^{n_{\max}} a_n \mathrm{C}_n^{(\lambda)}(x) \tag{2.31}$$

so, for the $xf(x)$ operator,

$$xf(x) = \sum_{n=0}^{n_{\max}} a_n x\mathrm{C}_n^{(\lambda)}(x) = \sum_{n=0}^{n_{\max}} b_n \mathrm{C}_n^{(\lambda)}(x)$$

by applying the recurrence relationship,

$$x\mathrm{C}_n^{(\lambda)}(x) = \frac{1}{2(n+\lambda)}\left[(n+1)\mathrm{C}_{n+1}^{(\lambda)}(x) + (n + 2\lambda - 1)\mathrm{C}_{n-1}^{(\lambda)}(x)\right]$$

it is possible to identify T_1 and T_2 terms

- T_1:

$$\mathrm{T}_1 = \sum_{n=0}^{n_{\max}} a_n \frac{n+1}{2(n+\lambda)}\mathrm{C}_{n+1}^{(\lambda)}(x) = \sum_{n'=1}^{n_{\max}} a_{n'-1}\frac{n'}{2(n'-1+\lambda)}\mathrm{C}_{n'}^{(\lambda)}(x)$$

- T_2:

$$\mathrm{T}_2 = \sum_{n=0}^{n_{\max}} a_n \frac{n+2\lambda-1}{2(n+\lambda)}\mathrm{C}_{n-1}^{(\lambda)}(x) = \sum_{n''=0}^{n_{\max}-1} a_{n''+1}\frac{n''+2\lambda}{2(n''+\lambda+1)}\mathrm{C}_{n''}^{(\lambda)}(x)$$

In conclusion,

$$b_n = a_{n-1}\frac{n}{2(n-1+\lambda)} + a_{n+1}\frac{n+2\lambda}{2(n+\lambda+1)} \tag{2.32}$$

The structure is the same of (2.26).

$x^2 f(x)$ matrix

The purpose of this subsection is to evaluate the $x^2 f(x)$ discretized matrix. Once again,

$$x^2 f(x) = \sum_{n=0}^{n_{\max}} a_n x^2 \mathrm{C}_n^{(\lambda)}(x) = \sum_{n=0}^{n_{\max}} b_n \mathrm{C}_n^{(\lambda)}(x)$$

but

$$x^2 \mathrm{C}_n^{(\lambda)}(x) = x\frac{1}{2(n+\lambda)}\left[(n+1)\mathrm{C}_{n+1}^{(\lambda)}(x) + (n-1+2\lambda)\mathrm{C}_{n-1}^{(\lambda)}(x)\right]$$

this can be re-written as follows

$$\begin{aligned} &= \frac{1}{2(n+\lambda)}\left\{\frac{n+1}{2(n+1+\lambda)}\left[(n+2)\mathrm{C}_{n+2}^{(\lambda)}(x) + (n+2\lambda)\mathrm{C}_n^{(\lambda)}(x)\right] + \right. \\ &\left. + \frac{n-1+2\lambda}{2(n+\lambda-1)}\left[n\mathrm{C}_n^{(\lambda)}(x) + (n-2+2\lambda)\mathrm{C}_{n-2}^{(\lambda)}(x)\right]\right\} \end{aligned}$$

This permits to re-write the sum as follows

$$\begin{aligned} \sum \Bigg\{ & a_n \mathrm{C}_{n+2}^{(\lambda)}(x)\frac{n+2}{2(n+\lambda)}\frac{n+1}{2(n+1+\lambda)} + a_n \mathrm{C}_{n-2}^{(\lambda)}(x)\frac{n-2+2\lambda}{2(n+\lambda)}\frac{n-1+2\lambda}{2(n+\lambda-1)} \\ & + a_n \mathrm{C}_n^{(\lambda)}(x)\left[\frac{n+2\lambda}{2(n+\lambda)}\frac{n+1}{2(n+1+\lambda)} + \frac{n}{2(n+\lambda)}\frac{n-1+2\lambda}{2(n+\lambda-1)}\right]\Bigg\} \end{aligned}$$

so, there are three cases.

- T_1:

$$\begin{aligned} \mathrm{T}_1 &= \sum_{n=0}^{n_{\max}} a_n \mathrm{C}_{n+2}^{(\lambda)}(x)\frac{n+2}{2(n+\lambda)}\frac{n+1}{2(n+1+\lambda)} = \\ &= \sum_{n'=2}^{n_{\max}} a_{n'-2}\mathrm{C}_{n'}^{(\lambda)}(x)\frac{n'}{2(n'-2+\lambda)}\frac{n'-1}{2(n'-1+\lambda)} \end{aligned}$$

- T_2:

$$\mathrm{T}_2 = a_n \mathrm{C}_n^{(\lambda)}(x)\left[\frac{n+2\lambda}{2(n+\lambda)}\frac{n+1}{2(n+1+\lambda)} + \frac{n}{2(n+\lambda)}\frac{n-1+2\lambda}{2(n+\lambda-1)}\right]$$

- T_3:

$$\begin{aligned}\mathrm{T}_3 &= a_n \mathrm{C}_{n-2}^{(\lambda)}(x)\frac{n-2+2\lambda}{2(n+\lambda)}\frac{n-1+2\lambda}{2(n+\lambda-1)} \\ &= a_{n''+2}\mathrm{C}_{n''}^{(\lambda)}(x)\frac{n''+2\lambda}{2(n''+2+\lambda)}\frac{n''+1+2\lambda}{2(n''+1+\lambda)}\end{aligned}$$

finally,

$$\begin{aligned}b_n = a_{n-2}\frac{n}{2(n-2+\lambda)}\frac{n-1}{2(n-1+\lambda)} + a_{n+2}\frac{n+2\lambda}{2(n+2+\lambda)}\frac{n+1+2\lambda}{2(n+1+\lambda)} + \\ + a_n\left[\frac{n+2\lambda}{2(n+\lambda)}\frac{n+1}{2(n+1+\lambda)} + \frac{n}{2(n+\lambda)}\frac{n-1+2\lambda}{2(n+\lambda-1)}\right]\end{aligned} \tag{2.33}$$

In this case, the matrix structure is the same of (2.28).

Differentiation matrices

Starting from (A.13) here recalled,

$$\begin{aligned}\frac{\mathrm{d}}{\mathrm{d}x}\left[\mathrm{C}_{\kappa+1}^{(\lambda)}(x) - \mathrm{C}_{\kappa-1}^{(\lambda)}(x)\right] &= 2(\kappa+\lambda)\mathrm{C}_{\kappa}^{(\lambda)}(x) \\ &= 2\lambda\left[\mathrm{C}_{\kappa}^{(\lambda+1)}(x) - \mathrm{C}_{\kappa-2}^{(\lambda+1)}(x)\right] \\ &\kappa \geq 1, \mathrm{C}_{-1}^{(\lambda)}(x) = 0\end{aligned}$$

it is possible to prove the relationship between a_n and b_n, where b_n are coefficients of the derivative of the function. In other words, given

$$\frac{\mathrm{d}}{\mathrm{d}x}f(x) = \sum_{n=0}^{n_{\max}} a_n \frac{\mathrm{d}}{\mathrm{d}x}\mathrm{C}_n^{(\lambda)}(x) = \sum_{n=0}^{n_{\max}} b_n \mathrm{C}_n^{(\lambda)}(x)$$

In order to find the relationship between b_n and a_n an idea may be to write coefficients of left hand side and right left side members, using for the right hand side the relationship (A.13).

- For the left hand side member, first coefficients are

$$a_0\frac{\mathrm{d}}{\mathrm{d}x}\mathrm{C}_0^{(\lambda)} + a_1\frac{\mathrm{d}}{\mathrm{d}x}\mathrm{C}_1^{(\lambda)} + a_2\frac{\mathrm{d}}{\mathrm{d}x}\mathrm{C}_2^{(\lambda)} + a_3\frac{\mathrm{d}}{\mathrm{d}x}\mathrm{C}_3^{(\lambda)} + \ldots$$

- For the right hand side member,

$$
\begin{aligned}
&b_0\left(\frac{1}{2\lambda}\frac{\mathrm{d}}{\mathrm{d}x}\mathrm{C}_1^{(\lambda)}-\frac{\mathrm{d}}{\mathrm{d}x}\mathrm{C}_{-1}^{(\lambda)}\right)+\\
&+b_1\left(\frac{1}{2(1+\lambda)}\frac{\mathrm{d}}{\mathrm{d}x}\mathrm{C}_2^{(\lambda)}-\frac{1}{2(1+\lambda)}\frac{\mathrm{d}}{\mathrm{d}x}\mathrm{C}_0^{(\lambda)}\right)+\\
&+b_2\left(\frac{1}{2(2+\lambda)}\frac{\mathrm{d}}{\mathrm{d}x}\mathrm{C}_3^{(\lambda)}-\frac{1}{2(2+\lambda)}\frac{\mathrm{d}}{\mathrm{d}x}\mathrm{C}_1^{(\lambda)}\right)+\\
&+b_3\left(\frac{1}{2(3+\lambda)}\frac{\mathrm{d}}{\mathrm{d}x}\mathrm{C}_4^{(\lambda)}-\frac{1}{2(3+\lambda)}\frac{\mathrm{d}}{\mathrm{d}x}\mathrm{C}_2^{(\lambda)}\right)
\end{aligned}
$$

At this point, remembering that $\mathrm{C}_n^{(\lambda)}=0$ for $n<1$, it is necessary to identify a_n coefficients by grouping all terms with same $\mathrm{C}_n^{(\lambda)}$ functions; in other words

$$
\begin{aligned}
a_1&=\frac{b_0}{2\lambda}-\frac{b_2}{2(2+\lambda)}\\
a_2&=\frac{b_1}{2(1+\lambda)}-\frac{b_3}{2(3+\lambda)}\\
a_3&=\frac{b_2}{2(2+\lambda)}-\frac{b_4}{2(4+\lambda)}
\end{aligned}
$$

By watching these terms it is possible to identify a pattern, a recursive relationship between coefficients, which is

$$
a_n=\frac{b_{n-1}}{2(n-1+\lambda)}-\frac{b_{n+1}}{2(n+1+\lambda)} \tag{2.34}
$$

It is possible to prove that the solution of this recurrence relationship is

$$
b_n=2\,(n+\lambda)\sum_{k=1}^{\infty}a_{n+2k-1} \tag{2.35}
$$

In fact, by substituting (2.35) in (2.34), it is possible to find:

$$
\begin{aligned}
b_{n+1}&=2(n+1+\lambda)\sum_{k=1}^{\infty}a_{n+2k}\\
b_{n-1}&=2(n-1+\lambda)\sum_{k=1}^{\infty}a_{n+2k-2}
\end{aligned}
$$

so

$$
\begin{aligned}
a_n&=\sum_{k=1}^{\infty}\left[a_{n+2k-2}-a_{n+2k}\right]=\\
&=a_n-a_{n+1}+a_{n+2}-a_{n+4}+a_{n+4}+\ldots=a_n
\end{aligned}
$$

From (2.35), instead of $2(n+1)$ as expected from Legendre polynomial expansion, there is $2(n+\lambda)$. This final result is remarkable; in fact, Legendre spectral differentiation matrices and Gegenbauer spectral differentiation matrices are very related. Furthermore, it is possible to find that they satisfy the following relationships;

- $\mathcal{L}f(x) = \frac{\mathrm{d}}{\mathrm{d}x}f(x)$

$$b_n = (2n + 2\lambda) \sum_{\substack{p=n+1 \\ p+n \text{ odd}}}^{n_{\max}} a_p \tag{2.36}$$

- $\mathcal{L}f(x) = \frac{\mathrm{d}^2}{\mathrm{d}x^2}f(x)$

$$b_n = (n + \lambda) \sum_{\substack{p=n+2 \\ p+n \text{ even}}}^{n_{\max}} \left[p(p + 2\lambda) - n(n + 2\lambda)\right] a_p \tag{2.37}$$

which are basically the same of Legendre method, substituting $1 \leftrightarrow \lambda$.

As a final observation, it may be useful to say that all Gegenbauer matrices degenerate in Legendre matrices, for $\lambda = \frac{1}{2}$. This is obvious, because in this case $m = 0$, so, as already known from (A.8), the two polynomial families are equal.

2.3.9 Normalized Gegenbauer spectral method

Due to the fact that Gegenbauer polynomials near to the boundaries ± 1 have high value compared to central zone ones, an idea may to normalize those polynomials, used as expansion functions, in order to try to reduce this problem.

From [1], it is possible to find that

$$h_n = \int_{-1}^{1} \left[\mathrm{C}_n^{(\lambda)}(x)\right]^2 \mathrm{d}x = \frac{\pi\, 2^{1-2\lambda}\Gamma(n2\lambda)}{n!(n + \lambda)\left[\Gamma(\lambda)\right]^2}, \quad \lambda \neq 0, \lambda > -\frac{1}{2} \tag{2.38}$$

$\Gamma(x)$ is the Euler's Gamma function; it is related with the factorial function, because, for $x = n$, $n \in \mathbb{N}$,

$$\Gamma(n + 1) = n! \tag{2.39}$$

In this case study, Gegenbauer polynomials are used as expansion functions for particular cases. Since m is an integer number, $m \geq 0$, and $\lambda = m + \frac{1}{2}$, it is possible to simplify (2.38); this is useful because it is better to avoid the computation of $\Gamma()$, which may return huge numbers. More in details, λ can assume only very specific values;

$$\lambda = m + \frac{1}{2}, m = 0, 1, 2....$$

so, the Gamma function at the numerator may be re-written as

$$\Gamma(n + 2\lambda) = (n + 2\lambda - 1)!$$

because $(n + 2\lambda - 1)$ is always an integer. Furthermore, it is possible to write this expression as follows:

$$(n + 2\lambda - 1)! = \prod_{i=1}^{2\lambda-1} (n + i)n! \tag{2.40}$$

This means that (2.38) may be re-written as

$$h_n = \frac{\pi\, 2^{1-2\lambda}}{(n + \lambda)\left[\Gamma(\lambda)\right]^2} \prod_{i=1}^{2\lambda-1} (n + i) \tag{2.41}$$

Using (2.38) it is possible to re-write the spectral representation for Gegenbauer polynomials (2.31) as follows

$$f(x) = \sum_{n=0}^{n_{\max}} a_n \mathrm{C}_n^{(\lambda)}(x) = \sum_{n=0}^{n_{\max}} A_n C_{n,\text{normalized}}^{(\lambda)}(x) = \sum_{n=0}^{n_{\max}} A_n h_n^{-\frac{1}{2}} \mathrm{C}_n^{(\lambda)}(x) \tag{2.42}$$

where A_n are weights for normalized Gegenbauer polynomials.

These coefficients $\{A_n\}$ are related with $\{a_n\}$. First of all it is fundamental to recognize that a representation similar to (2.42) is satisfied also for b_n and B_n coefficients, about the representation of the discretization matrix of $\mathcal{L}f(x)$.

$$\mathcal{L}f(x) = \sum_{n=0}^{n_{\max}} a_n \mathcal{L}\mathrm{C}_n^{(\lambda)}(x) = \sum_{n=0}^{n_{\max}} b_n \mathrm{C}_n^{(\lambda)}(x)$$

where

$$\sum_{n=0}^{n_{\max}} b_n \mathrm{C}_n^{(\lambda)}(x) = \sum_{n=0}^{n_{\max}} B_n C_{n,\text{normalized}}^{(\lambda)}(x) = \sum_{n=0}^{n_{\max}} B_n h_n^{-\frac{1}{2}} \mathrm{C}_n^{(\lambda)}(x)$$

so

$$\begin{aligned} a_n &= A_n h_n^{-\frac{1}{2}} \\ b_n &= B_n h_n^{-\frac{1}{2}} \end{aligned} \tag{2.43}$$

This is true for every $\mathcal{L}f(x)$. Furthermore, considering for instance (2.32), it is possible to write

$$B_n h_n^{-\frac{1}{2}} = A_{n-1} h_{n-1}^{-\frac{1}{2}} \frac{n}{2(n - 1 + \lambda)} + A_{n+1} h_{n+1}^{-\frac{1}{2}} \frac{n + 2\lambda}{2(n + \lambda + 1)}$$

so, for this case,

$$B_n = A_{n-1} \sqrt{\frac{h_n}{h_{n-1}}} \frac{n}{2(n - 1 + \lambda)} + A_{n+1} \sqrt{\frac{h_n}{h_{n+1}}} \frac{n + 2\lambda}{2(n + \lambda + 1)}$$

This means that, in this case,

$$\mathrm{C}_{n-1} = c_n \sqrt{\frac{h_n}{h_{n-1}}} \qquad \mathrm{C}_{n+1} = c_n \sqrt{\frac{h_n}{h_{n+1}}}$$

These observations are interesting not just for this case, but also for other cases: x^2, first derivative, second derivative.

An interesting observation is that most of the time the direct computation of h_n is redundant, because expressions contain the ratio of two $h_{i,j}$, $i \neq j$. Starting from (2.41), it is possible to evaluate

$$\frac{h_n}{h_p} = \frac{\frac{\pi\, 2^{1-2\lambda}}{(n+\lambda)[\Gamma(\lambda)]^2} \prod_{i=1}^{2\lambda-1}(n+i)}{\frac{\pi\, 2^{1-2\lambda}}{(p+\lambda)[\Gamma(\lambda)]^2} \prod_{i=1}^{2\lambda-1}(p+i)}$$

Since λ is the same in both numerator and denominator, this equation may be re-written as

$$\frac{h_n}{h_p} = \frac{p+\lambda}{n+\lambda} \frac{\prod_{i=1}^{2\lambda-1}(n+i)}{\prod_{i=1}^{2\lambda-1}(p+i)} \tag{2.44}$$

This expression is much more useful compared to the previous one, because it does not contain $\Gamma()$ functions or exponentials, so it is cheaper to calculate.

2.3.10 Associated Legendre spectral method

The last spectral method that could be used in order to find the modal critical constants is the solution of the associated Legendre differential equation using of associated Legendre functions as expansion functions. Unfortunately, the use of these polynomials is very tricky; as a matter of fact, the procedure used up to this subsection was based on the interval mapping of the differential equation in ξ and on the solution of the differential equation in that interval. It is impossible to apply this procedure to associated Legendre polynomials, because they equal zero in $\xi = \pm 1$ boundaries, so, considering (2.22), there is a divide-by-zero operation.

An alternative at this point might be the solution of the differential problem on $x \in [-1, 1]$ interval, without performing the interval mapping in ξ; then, instead of enforcing the value of the function on the boundary, it is possible to work on x_0, considering that $\underline{c}_0$ and $\underline{c}_{\mathrm{BC}}$ are known, being $\mathrm{P}_n^m(x)$ known for integer n, m. However, this method is impossible to apply too. In fact, $\mathrm{P}_m^n(x)$ are orthogonal polynomials just if considered on $[-1, 1]$ interval. So, considering boundary conditions which limit the domain on $[x_0, 1]$, associated Legendre polynomials are not independent anymore. In fact, the boundary condition must enforce a first order zero in $x = x_0$, which is different from the zero of order dependent on m. So, by using numerical integration and by evaluating the Gram matrix of these polynomials, it may be observed that it has many singular values, which reveal the presence of linear dependence.

To sum up, due to these considerations, the idea of using associated Legendre polynomials as expansion functions was abandoned.

2.3.11 Associated Legendre functions implementation

On [25][3], it is possible to find a series expansion of associated Legendre functions of real degree.This expression is:

$$\begin{aligned} \mathrm{P}_p^m(x) =& (-1)^m \frac{1}{2^m m!} \left(1-x^2\right)^{\frac{m}{2}} \frac{\Gamma(p+m+1)}{\Gamma(p-m+1)} \\ & \sum_{k=0}^{\infty} \frac{(-p+m)_k \, (p+1+m)_k}{k!(m+1)_k} \left(\frac{1-x}{2}\right)^k \end{aligned} \tag{2.45}$$

where $(x)_k$ is the Pockhammer symbol, defined as

$$(x)_k \triangleq \frac{\Gamma(x+k)}{\Gamma(x)} \tag{2.46}$$

Unfortunately, a routine implementing this formula can not be very accurate, because most significant terms of the series may have the order or magnitude of 10^6 for some values of p. Moreover, these terms have alternate sign. This means that the final result of the series can not be as precise as the ones calculated by the previously shown numerical methods, where there are less numerical cancellation phenomena.

2.3.12 Visualization of some eigenvectors

With these implemented methods it is possible to obtain both eigenvalues and eigenvectors. The most significant case is for $m = 1$, since the structure is usually excited by a circular waveguide with its fundamental mode (which is the TE_{11}). Some examples of curves are drawn here.

[3] (4.6.14), (4.6.15), (4.6.16), (4.6.17), (4.6.18)

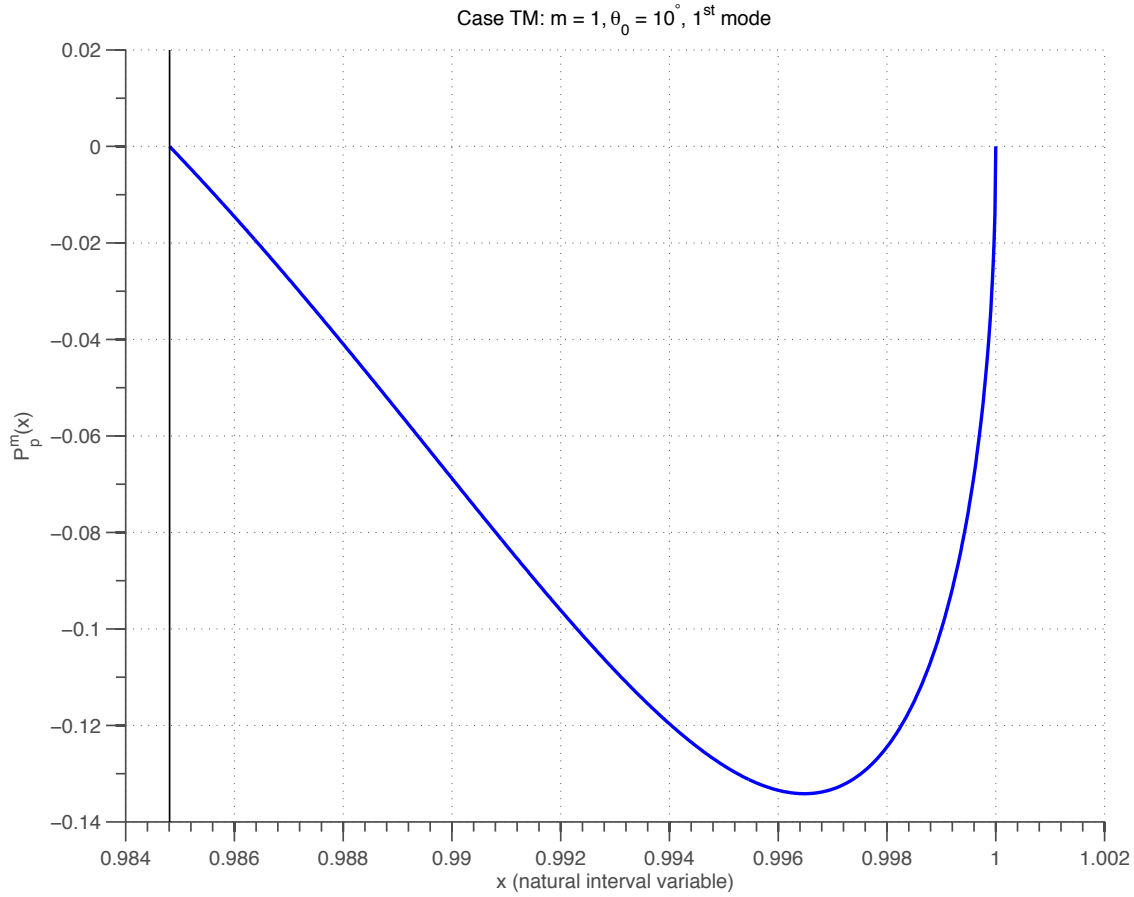

Figure 2.4: TM mode function relative to the first eigenvalue, $m = 1$, $\vartheta_0 = 10°$

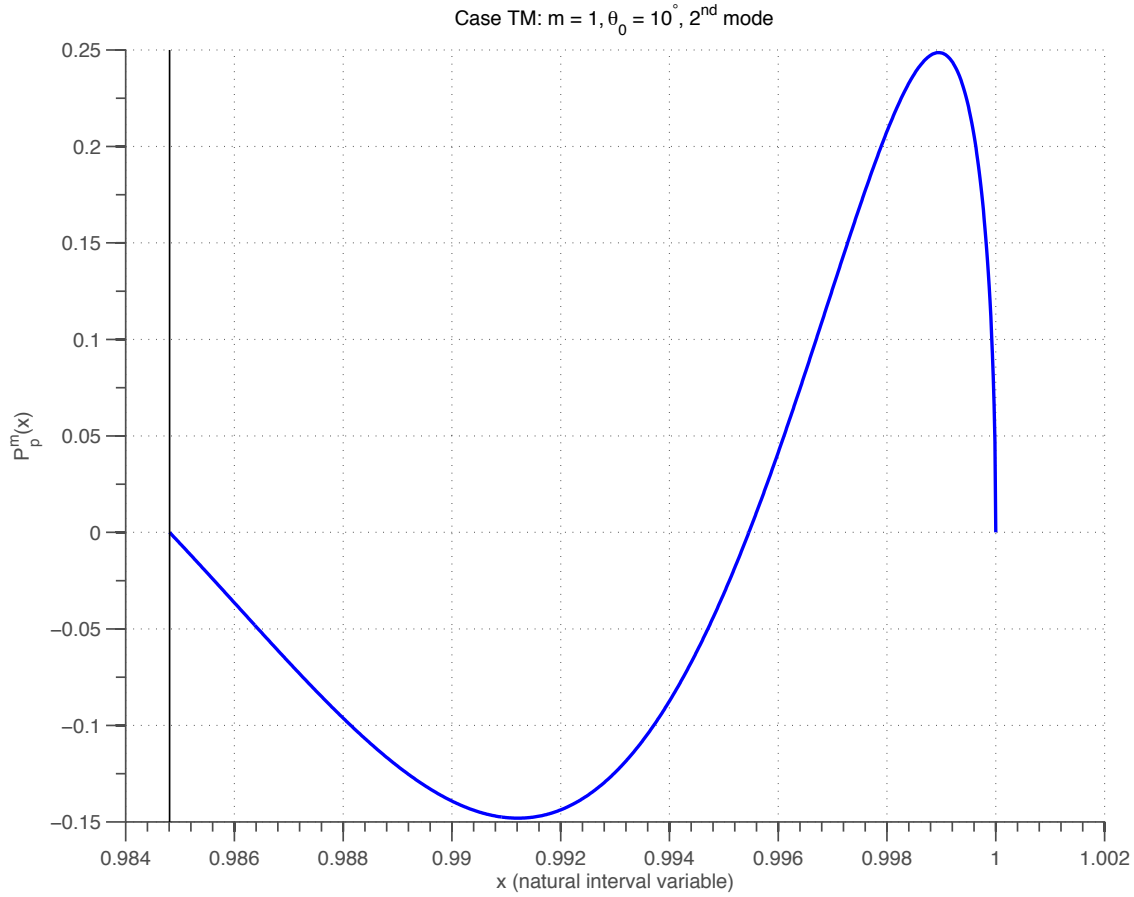

Figure 2.5: TM mode function relative to the second eigenvalue, $m = 1$, $\vartheta_0 = 10°$

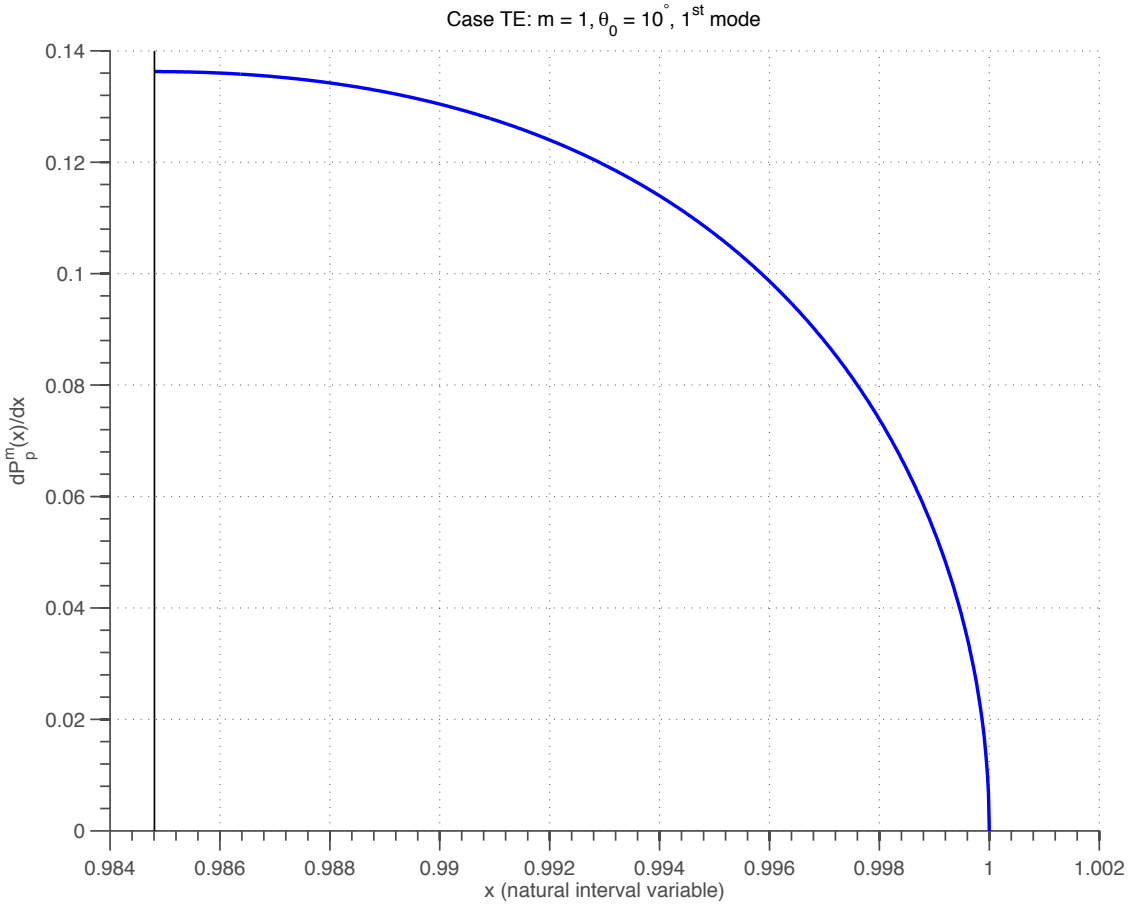

Figure 2.6: TE mode function relative to the first eigenvalue, $m = 1$, $\vartheta_0 = 10°$

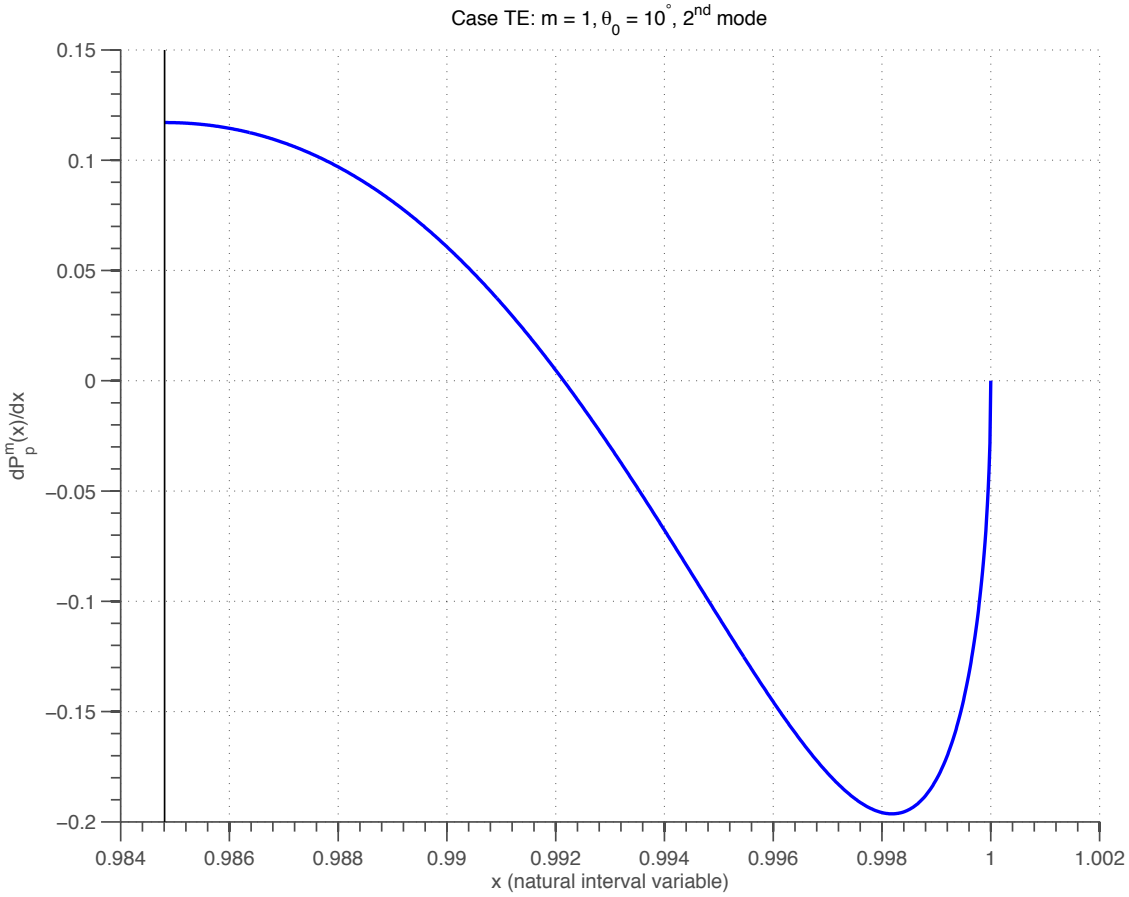

Figure 2.7: TE mode function relative to the second eigenvalue, $m = 1$, $\vartheta_0 = 10°$

2.4 Comparison between numerical methods and final results

This section contains a comparison between many numerical methods described in the previous section. All these methods were used in order to build a finite eigenvalue problem starting from a differential equation, so the output of those methods are an eigenvalue and an eigenvector. The quality of a numerical method applied on an equation may be evaluated by studying the trend of the error between the eigenvalue evaluated with the numerical method by using a well-defined set of parameters, and a reference value.

The main parameters of the two methods are:

- for pseudospectral methods, the number of collocating nodes;
- for spectral methods, the number of expansion functions used.

A problem for the implementation of convergence studies is the evaluation the reference value used to calculate the error. There are two possible approaches:

- using as a reference value the value evaluated with the same numerical method, applied with the best set of parameters (maximum number of nodes for pseudospectral methods or maximum number of used functions for spectral methods) of the convergence study;
- evaluate with a robust numerical algorithm the position of the zero of a $\mathrm{P}_p^m(x)$ function, where p is a value chosen by the user; then, use this value as x_0, and see how precise is the corresponding eigenvalue.

For both pseudospectral and spectral methods, convergence studies were performed using the latter approach; in fact, the former approach is not convenient, since the "numerical noise" can affect eigenvalues found solving higher order systems, therefore these results may be less reliable; therefore, in order to perform the convergence study, it is better to use the latter approach.

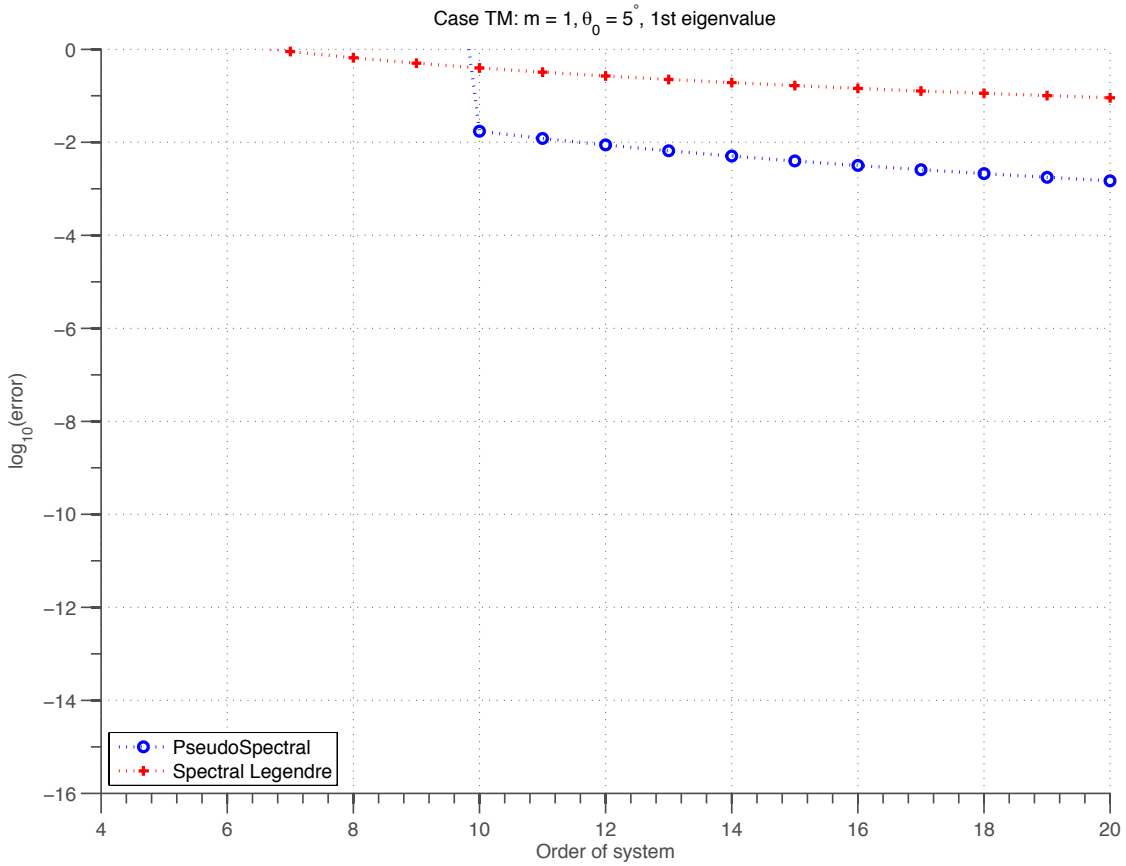

Figure 2.8: Pseudospectral and Legendre spectral methods applied to the associated Legendre equation

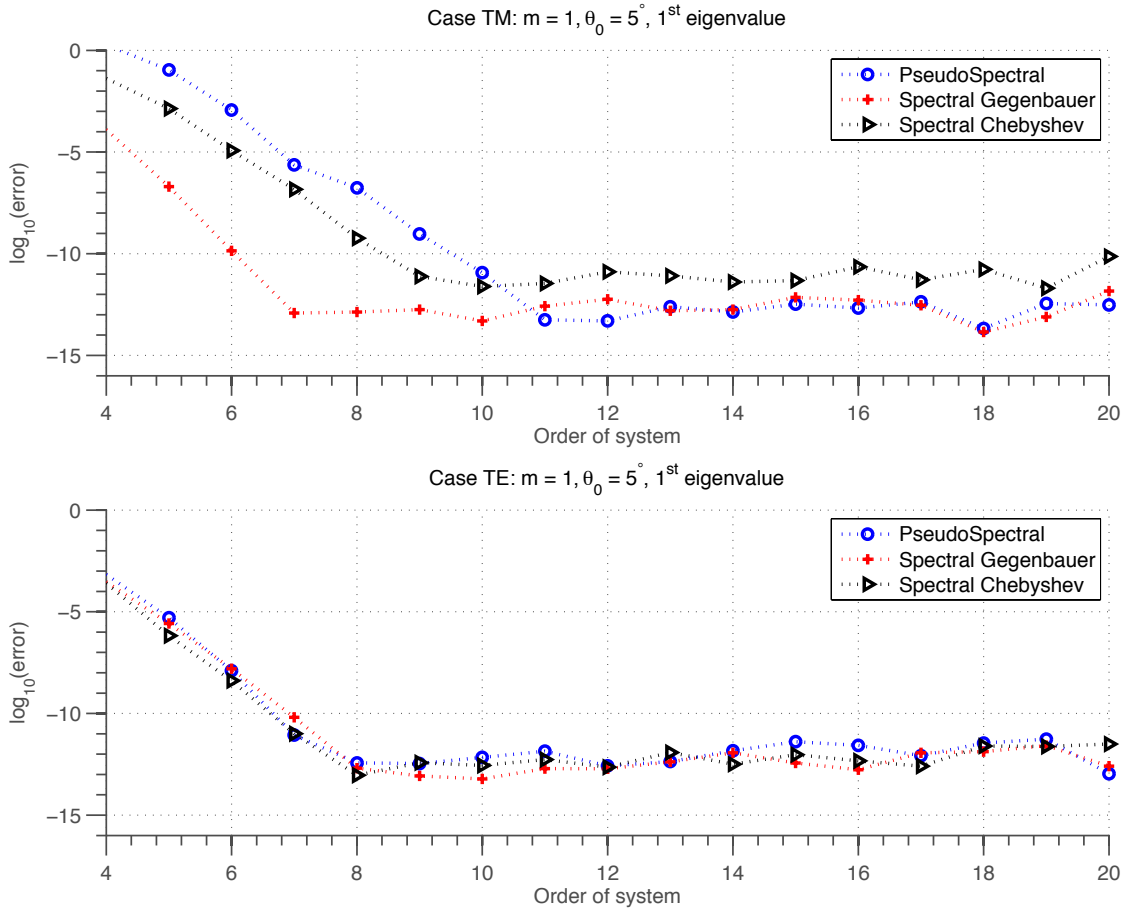

Figure 2.9: Gegenbauer equation: convergence curves for TM and TE eigenvalues.

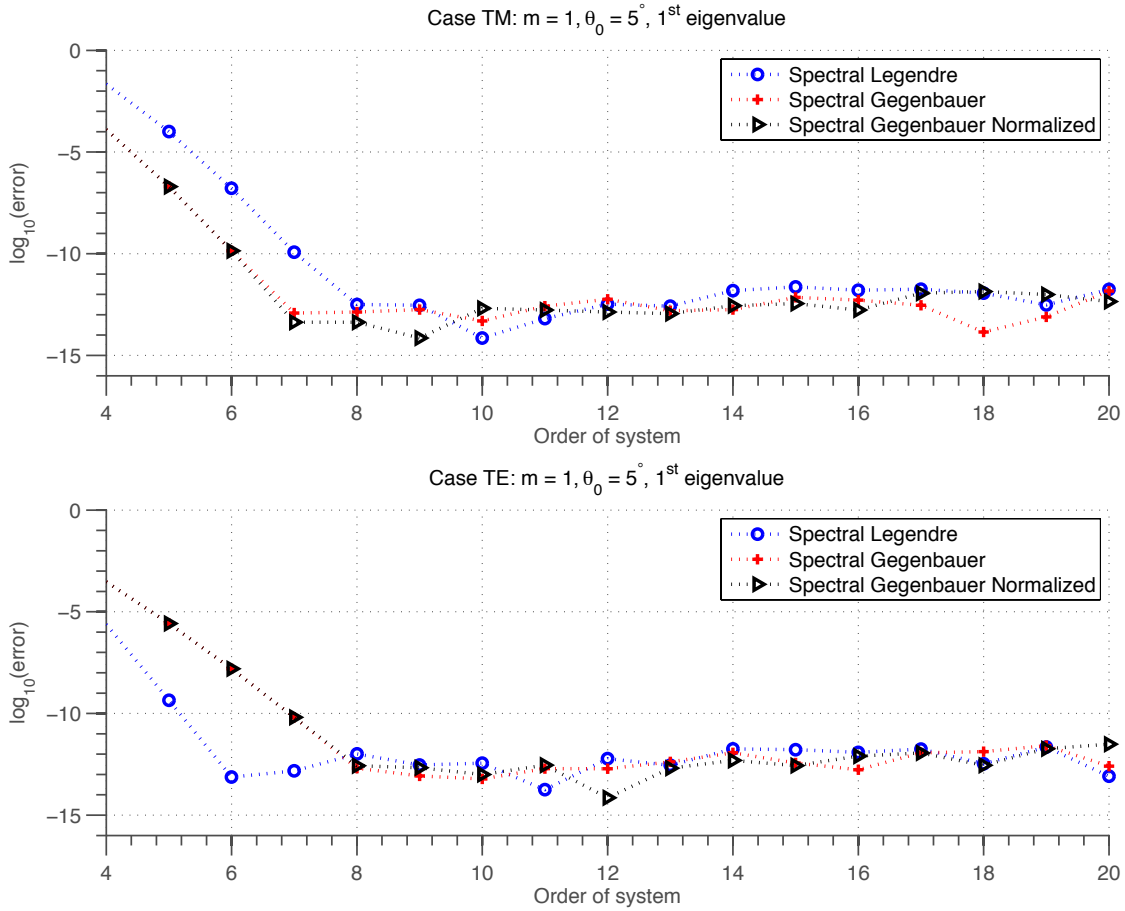

Figure 2.10: Gegenbauer equation: convergence curves for TM and TE eigenvalues.

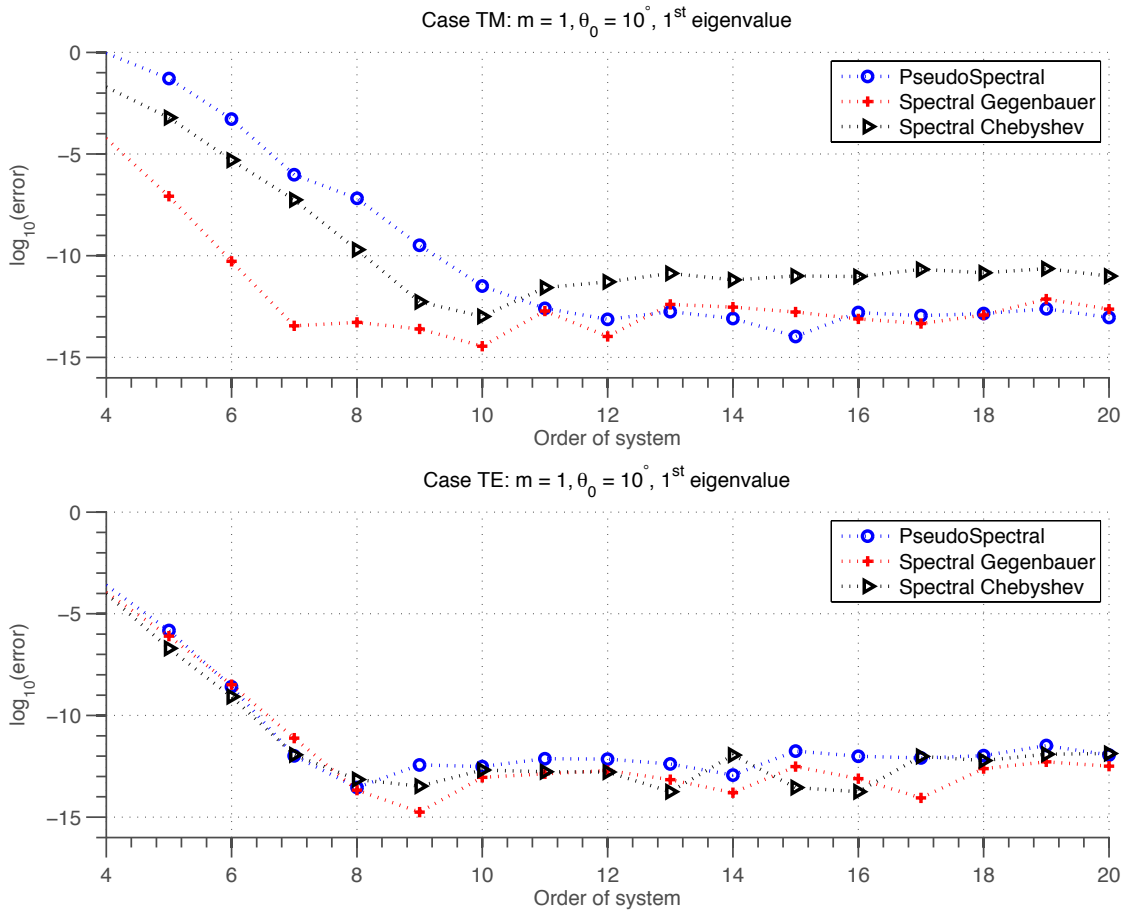

Figure 2.11: Gegenbauer equation: convergence curves for TM and TE eigenvalues.

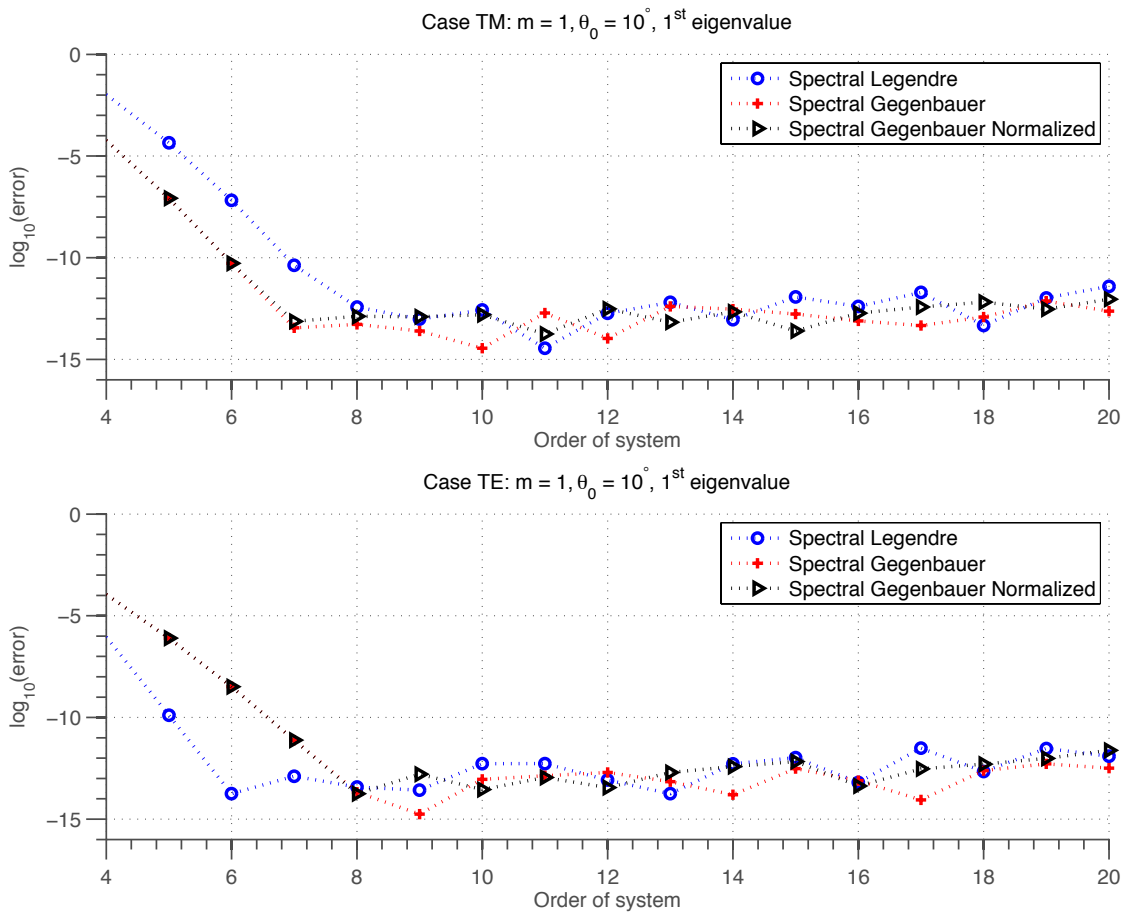

Figure 2.12: Gegenbauer equation: convergence curves for TM and TE eigenvalues.

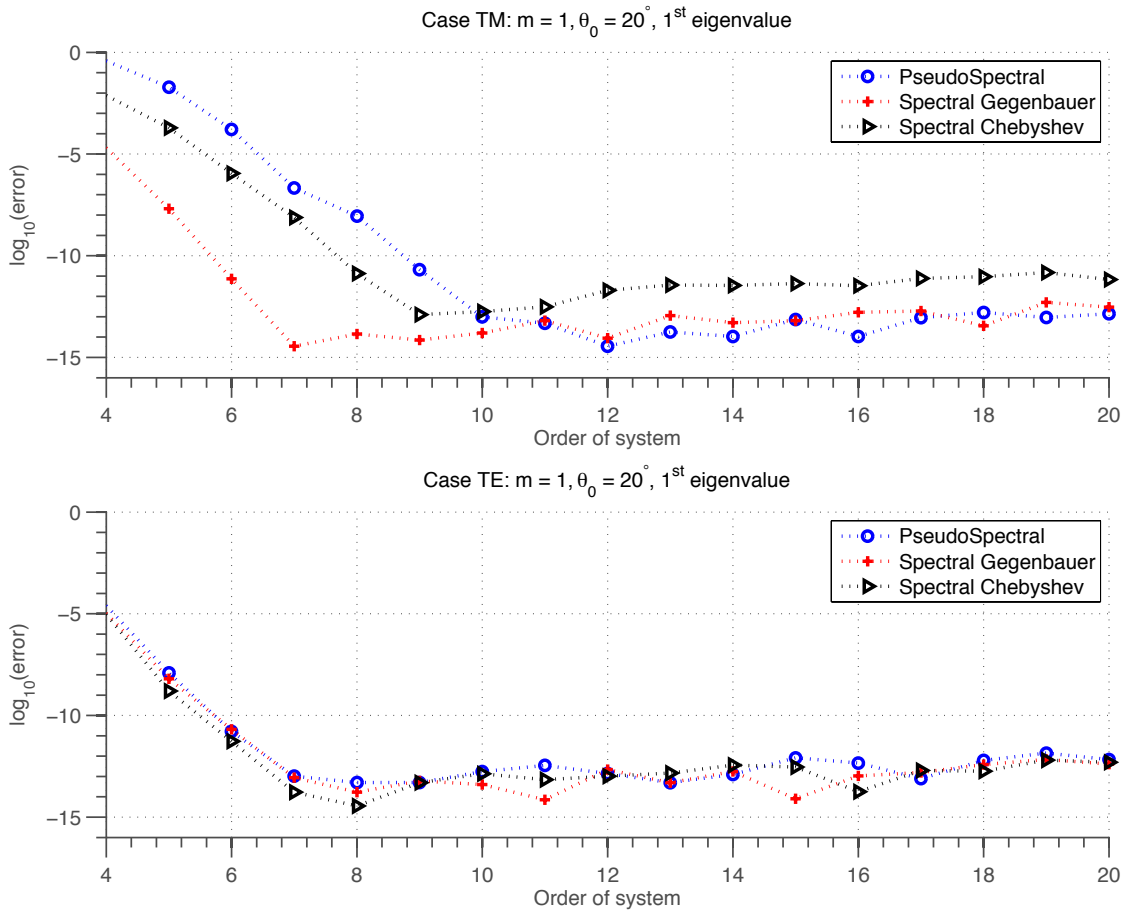

Figure 2.13: Gegenbauer equation: convergence curves for TM and TE eigenvalues.

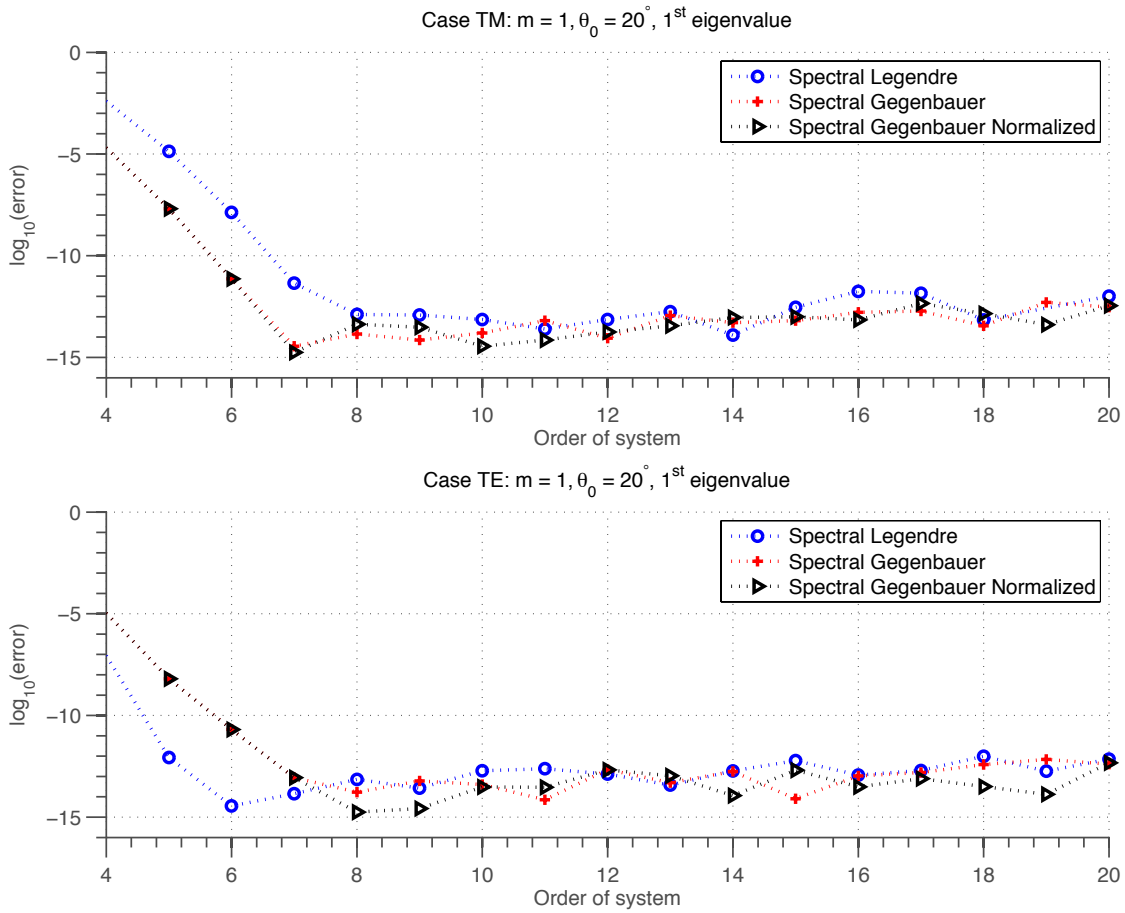

Figure 2.14: Gegenbauer equation: convergence curves for TM and TE eigenvalues.

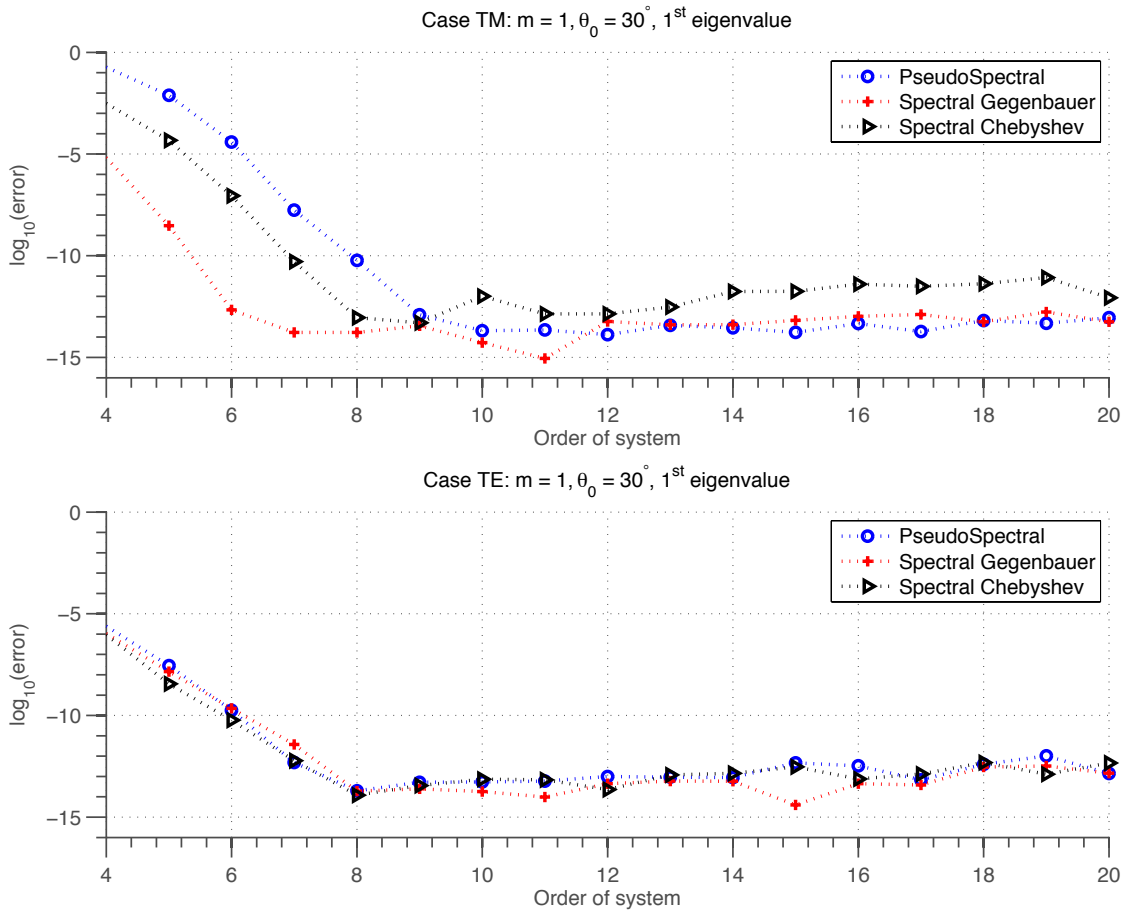

Figure 2.15: Gegenbauer equation: convergence curves for TM and TE eigenvalues.

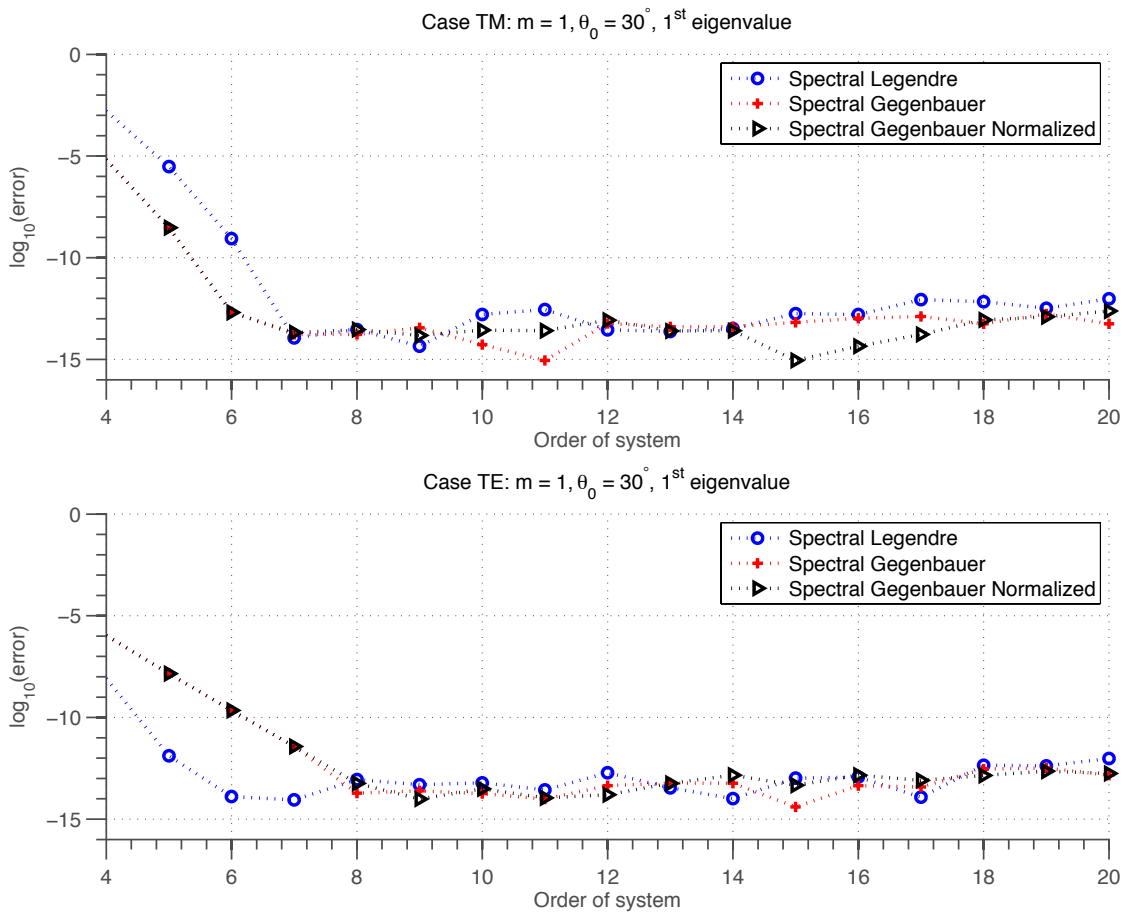

Figure 2.16: Gegenbauer equation: convergence curves for TM and TE eigenvalues.

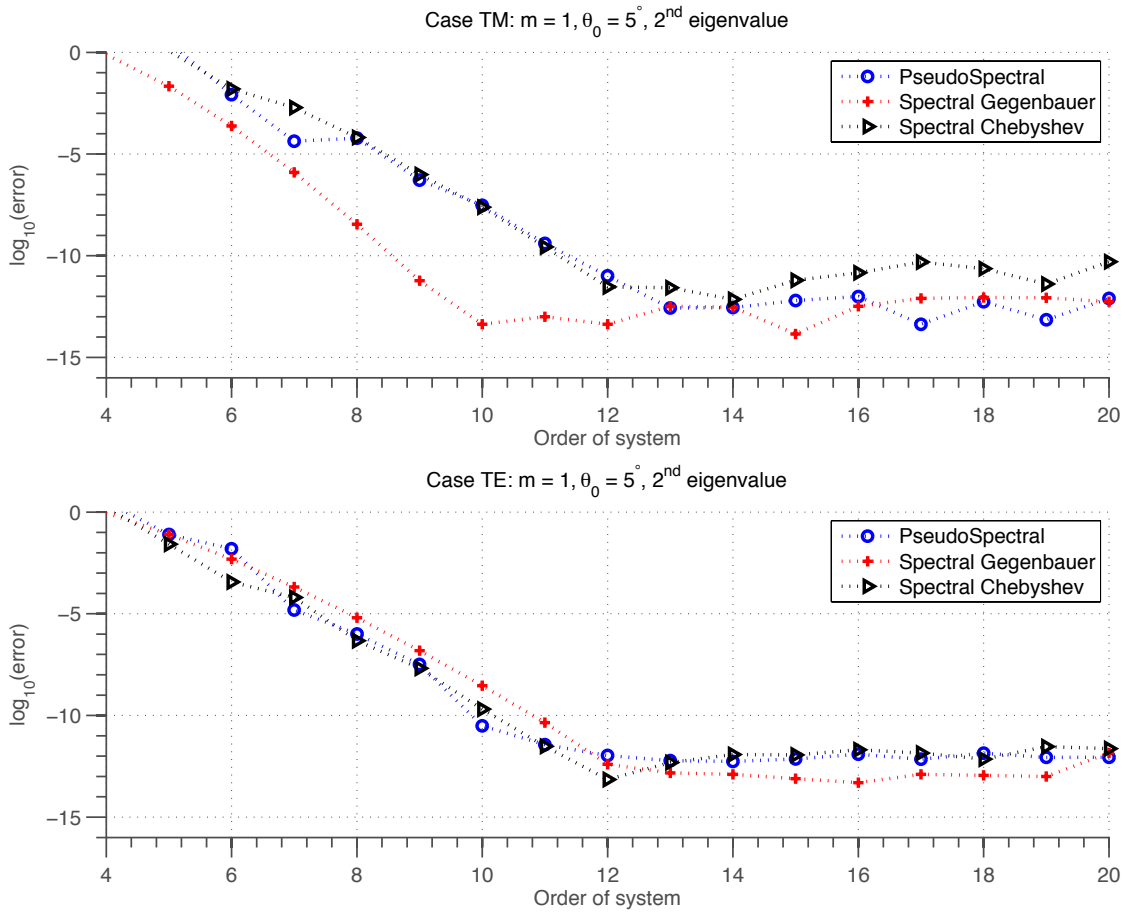

Figure 2.17: Gegenbauer equation: convergence curves for TM and TE eigenvalues.

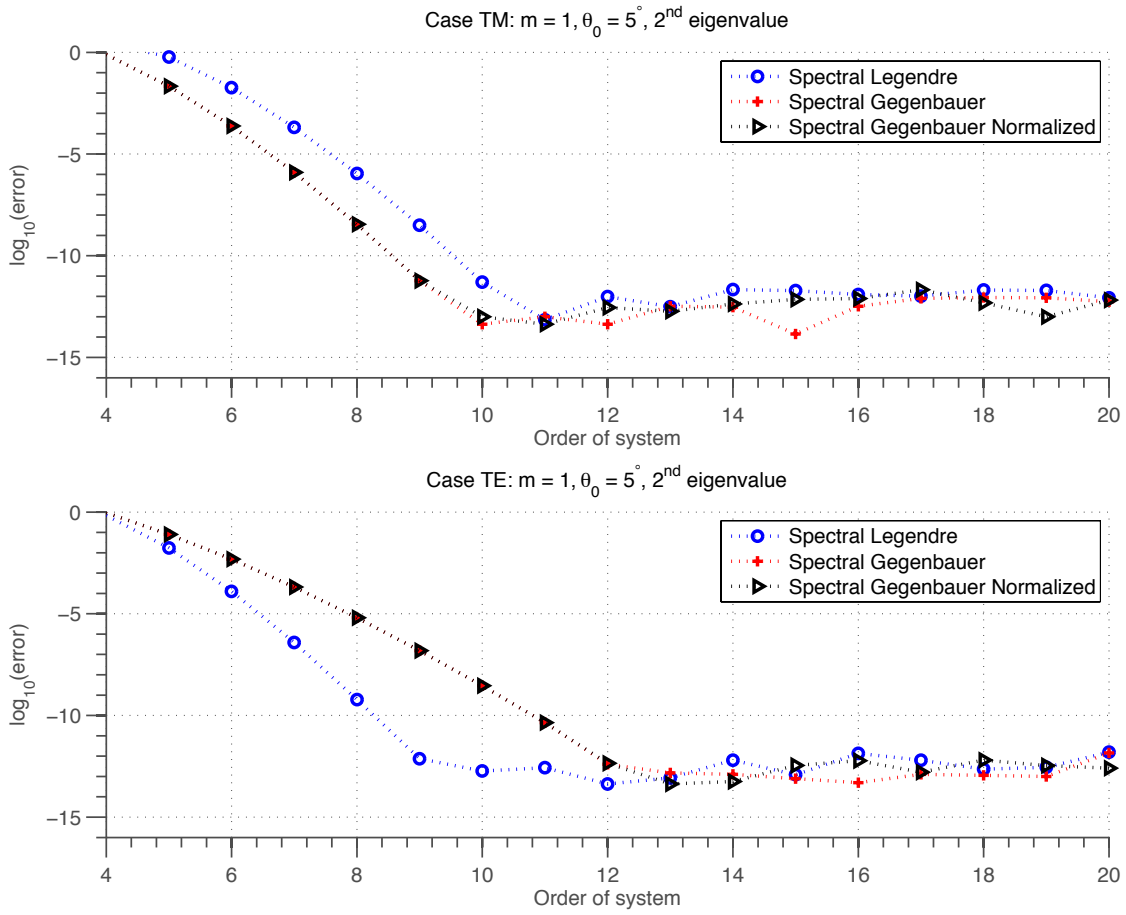

Figure 2.18: Gegenbauer equation: convergence curves for TM and TE eigenvalues.

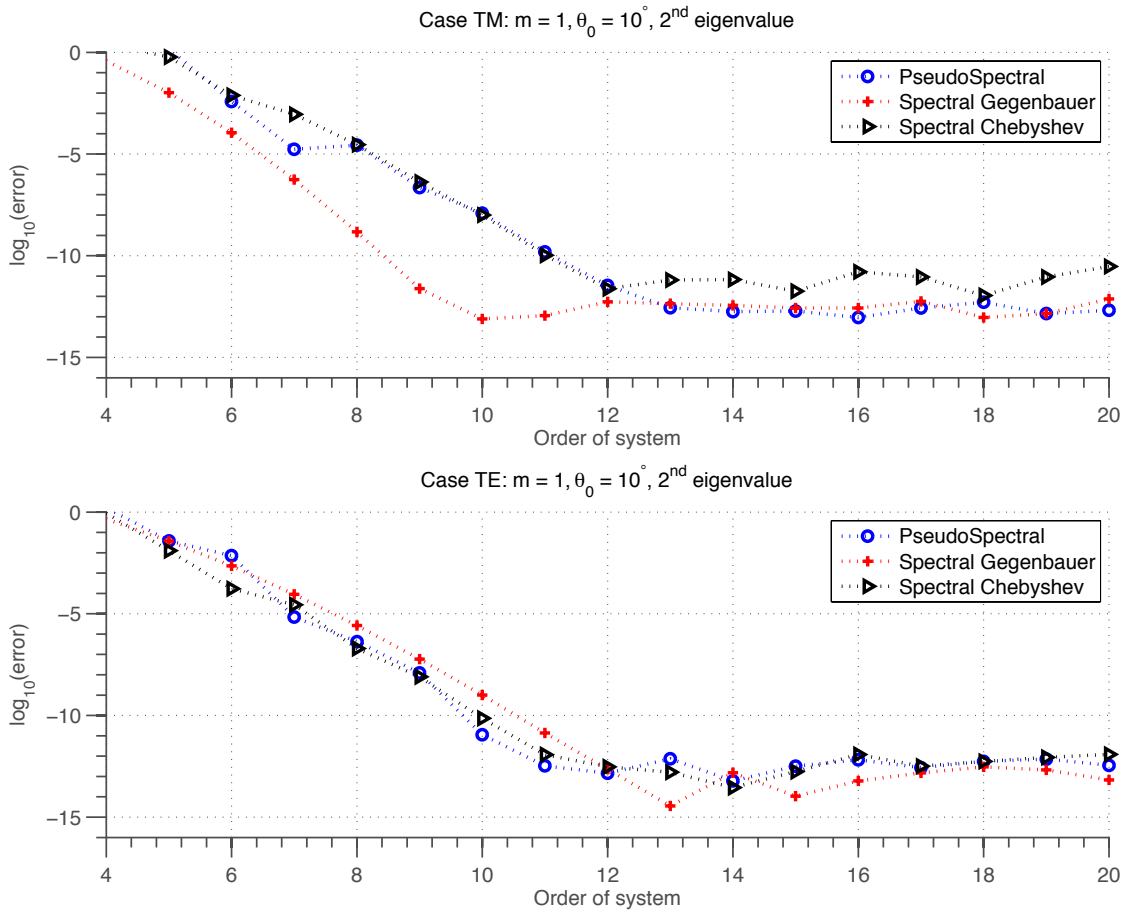

Figure 2.19: Gegenbauer equation: convergence curves for TM and TE eigenvalues.

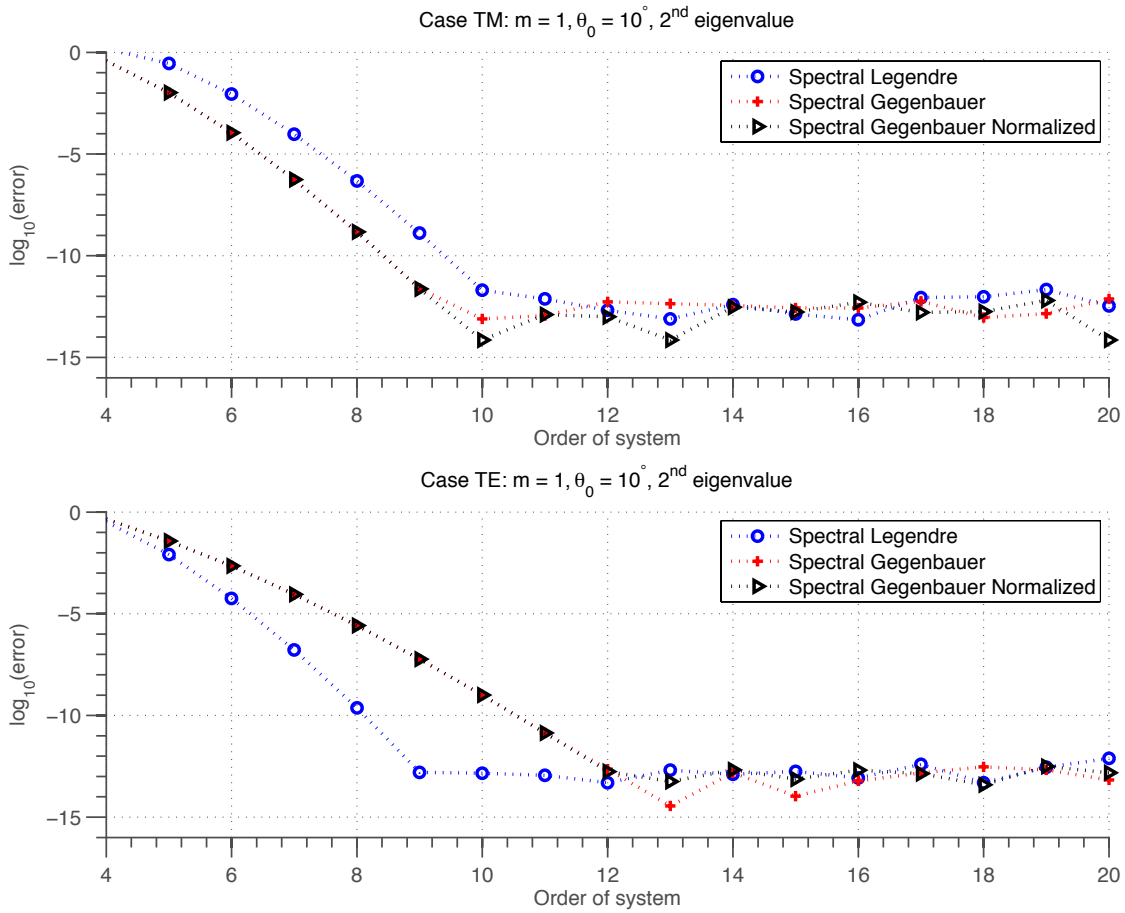

Figure 2.20: Gegenbauer equation: convergence curves for TM and TE eigenvalues.

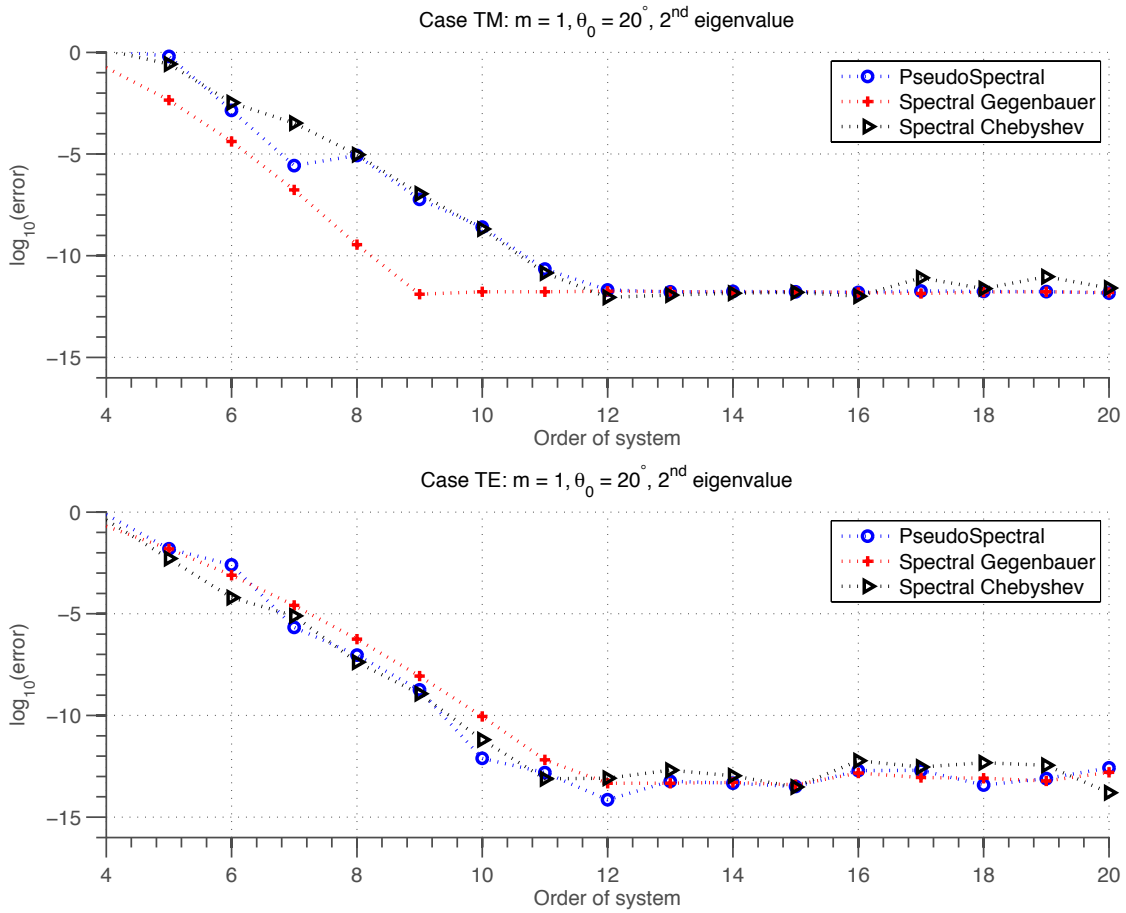

Figure 2.21: Gegenbauer equation: convergence curves for TM and TE eigenvalues.

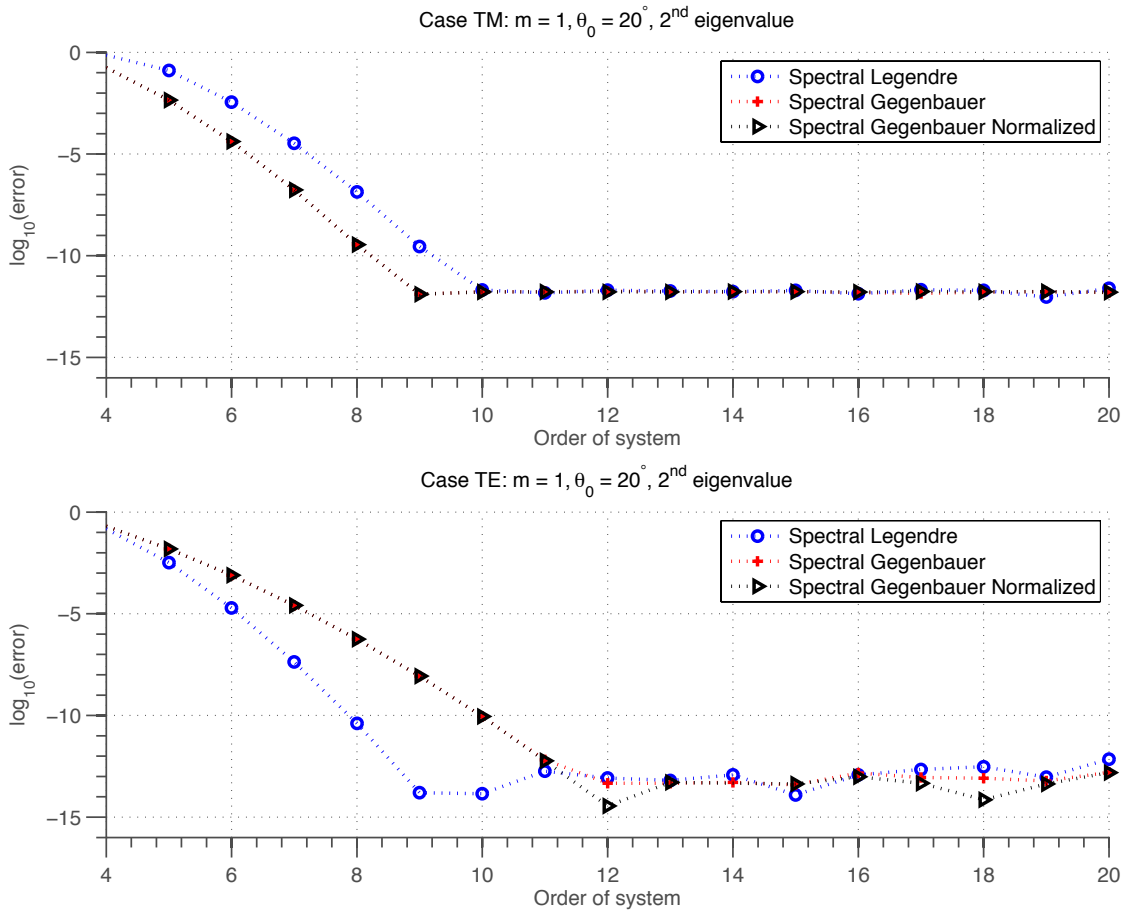

Figure 2.22: Gegenbauer equation: convergence curves for TM and TE eigenvalues.

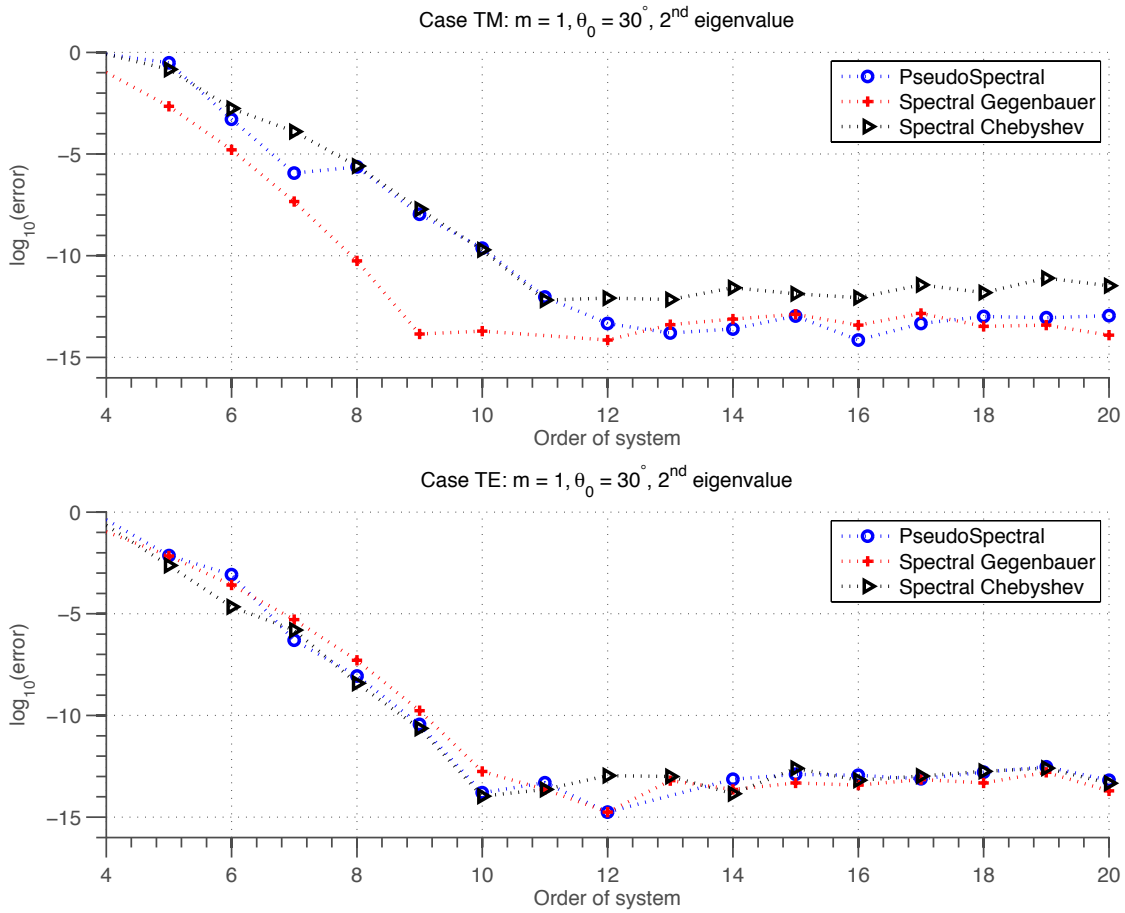

Figure 2.23: Gegenbauer equation: convergence curves for TM and TE eigenvalues.

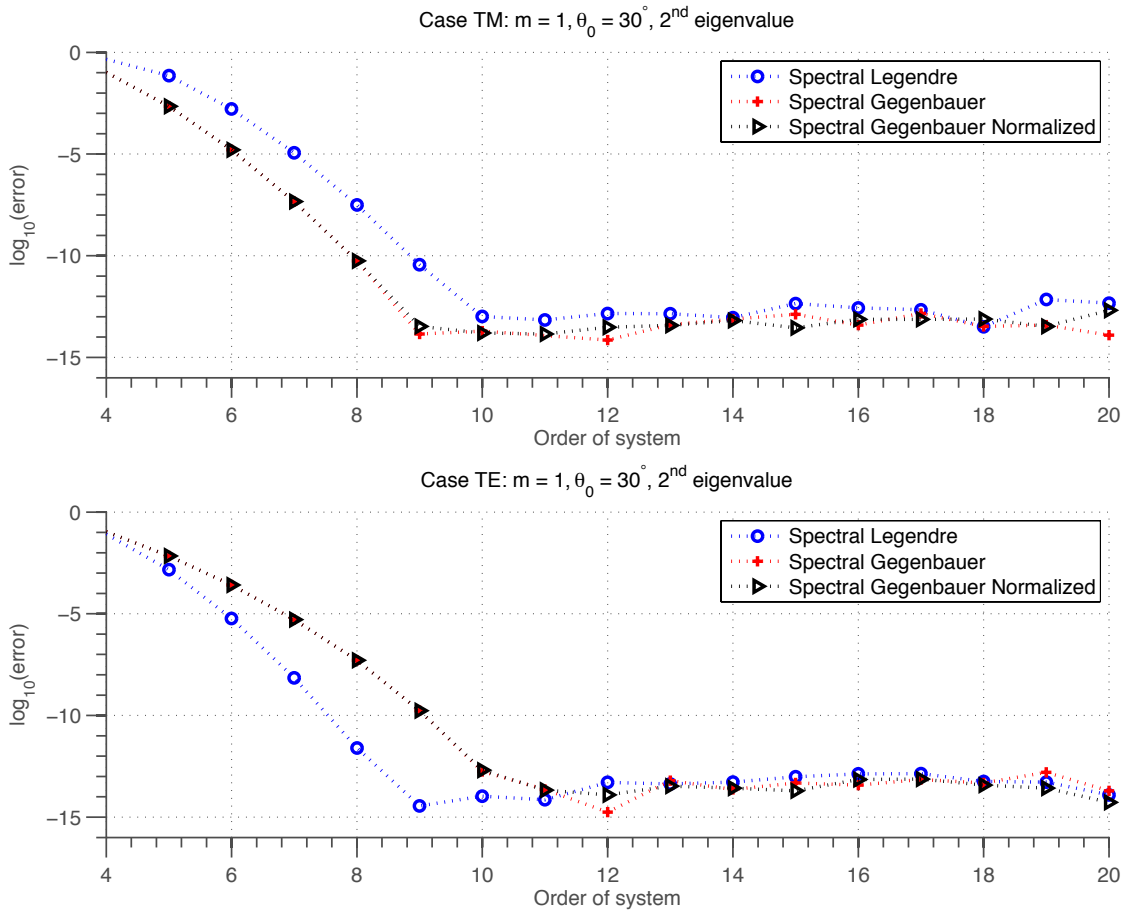

Figure 2.24: Gegenbauer equation: convergence curves for TM and TE eigenvalues.

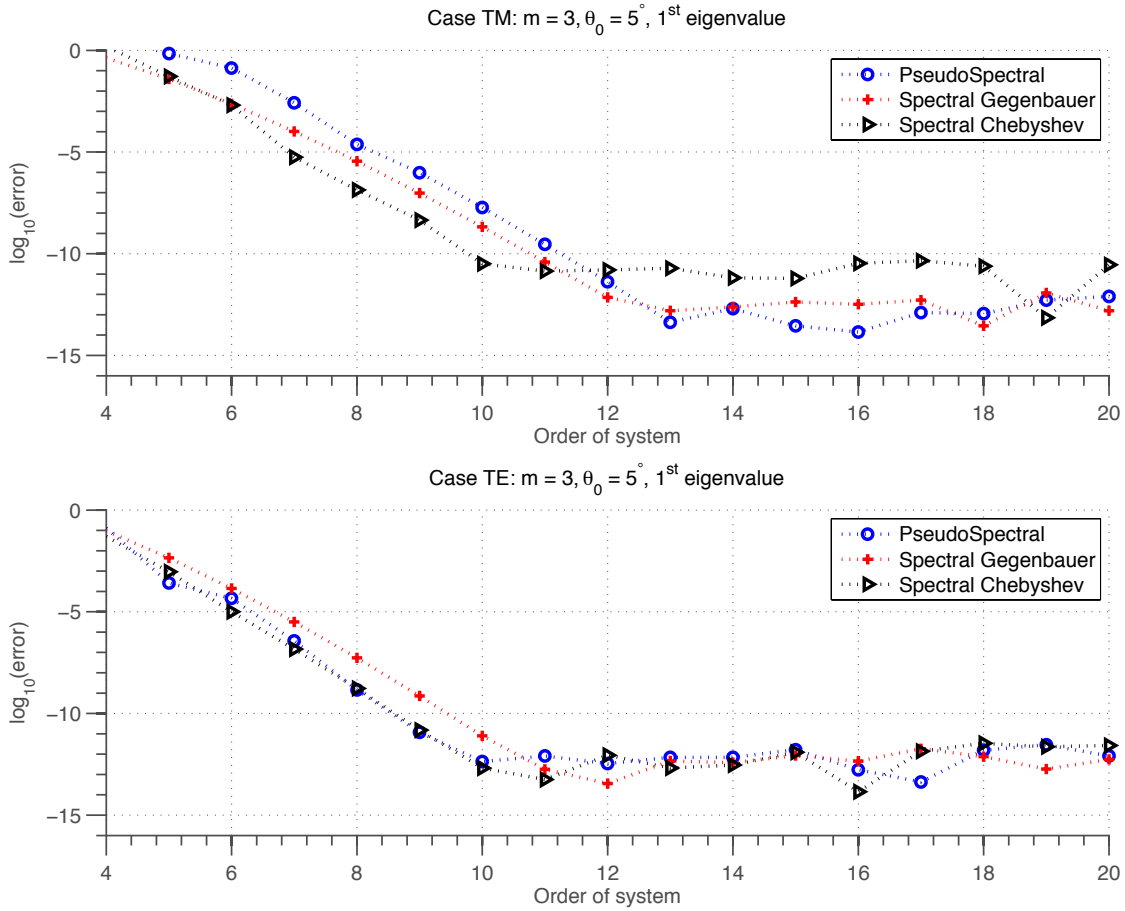

Figure 2.25: Gegenbauer equation: convergence curves for TM and TE eigenvalues.

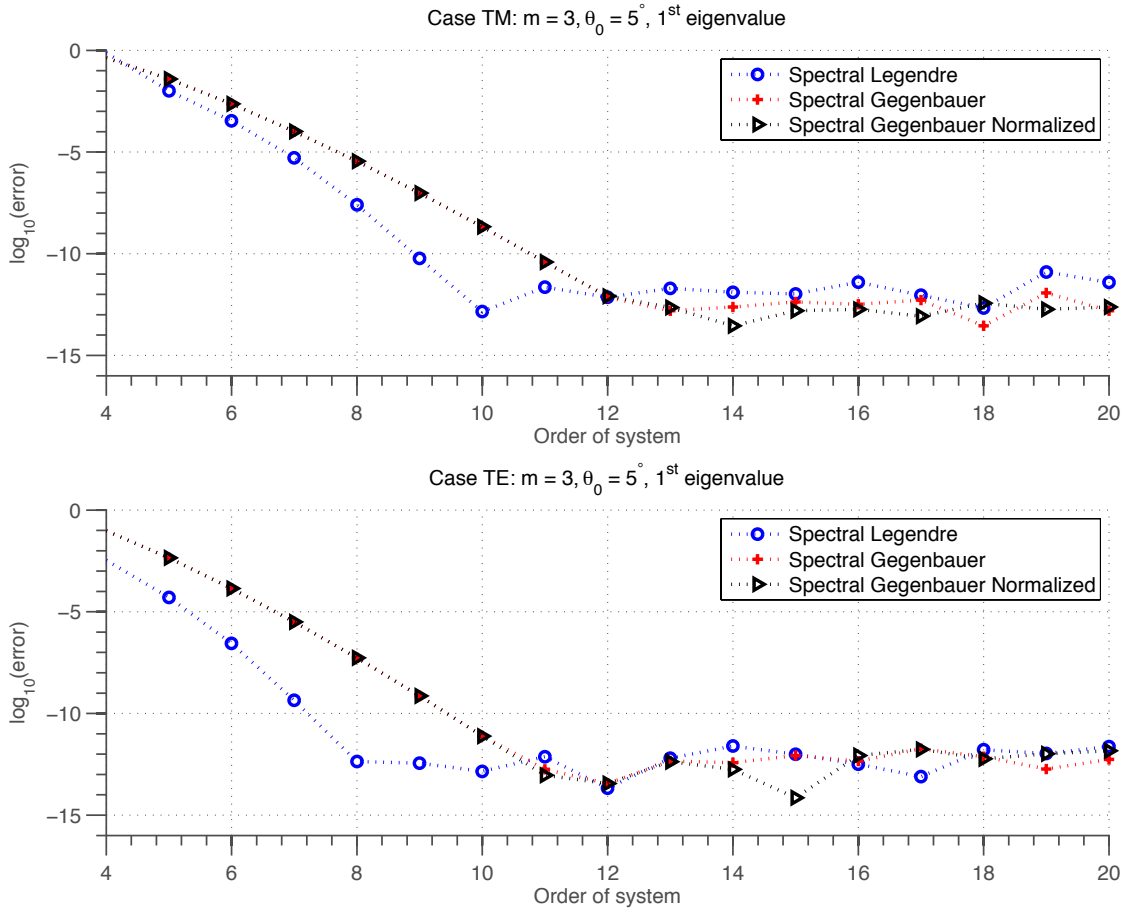

Figure 2.26: Gegenbauer equation: convergence curves for TM and TE eigenvalues.

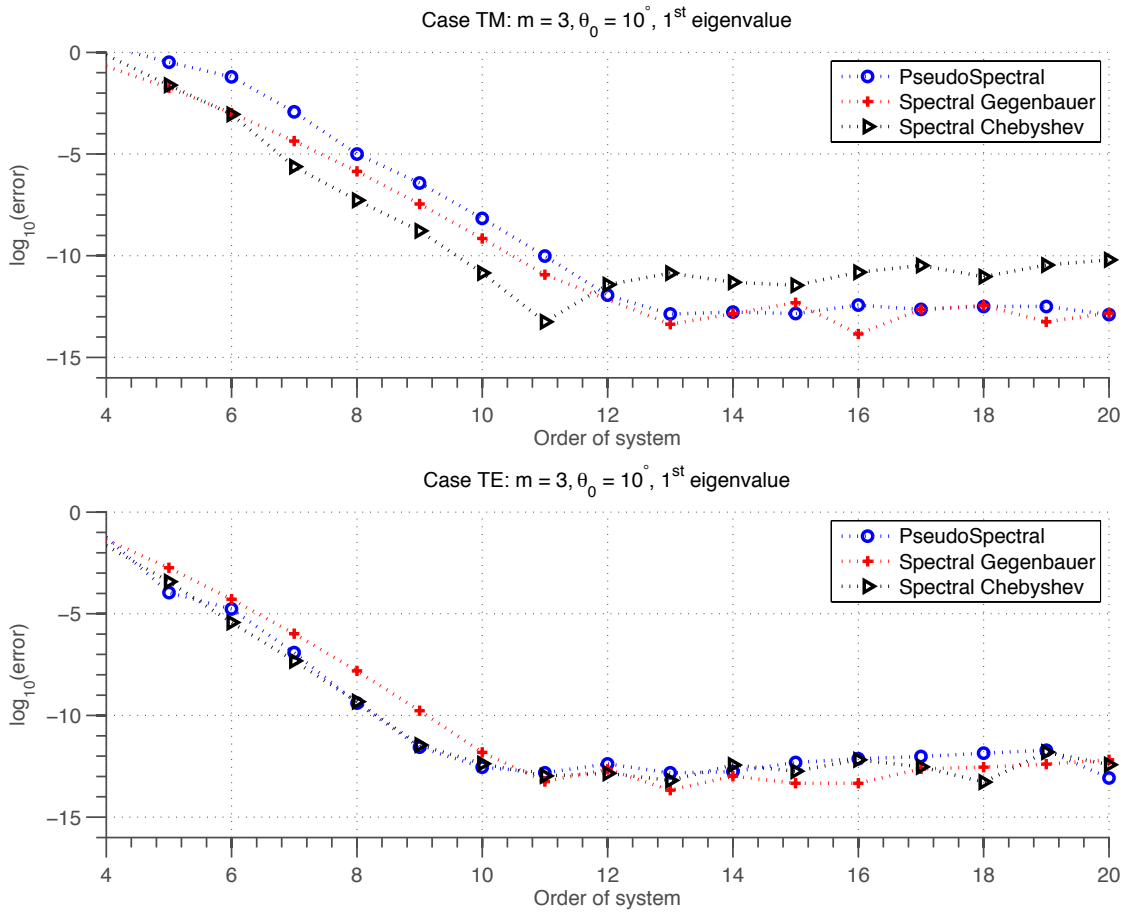

Figure 2.27: Gegenbauer equation: convergence curves for TM and TE eigenvalues.

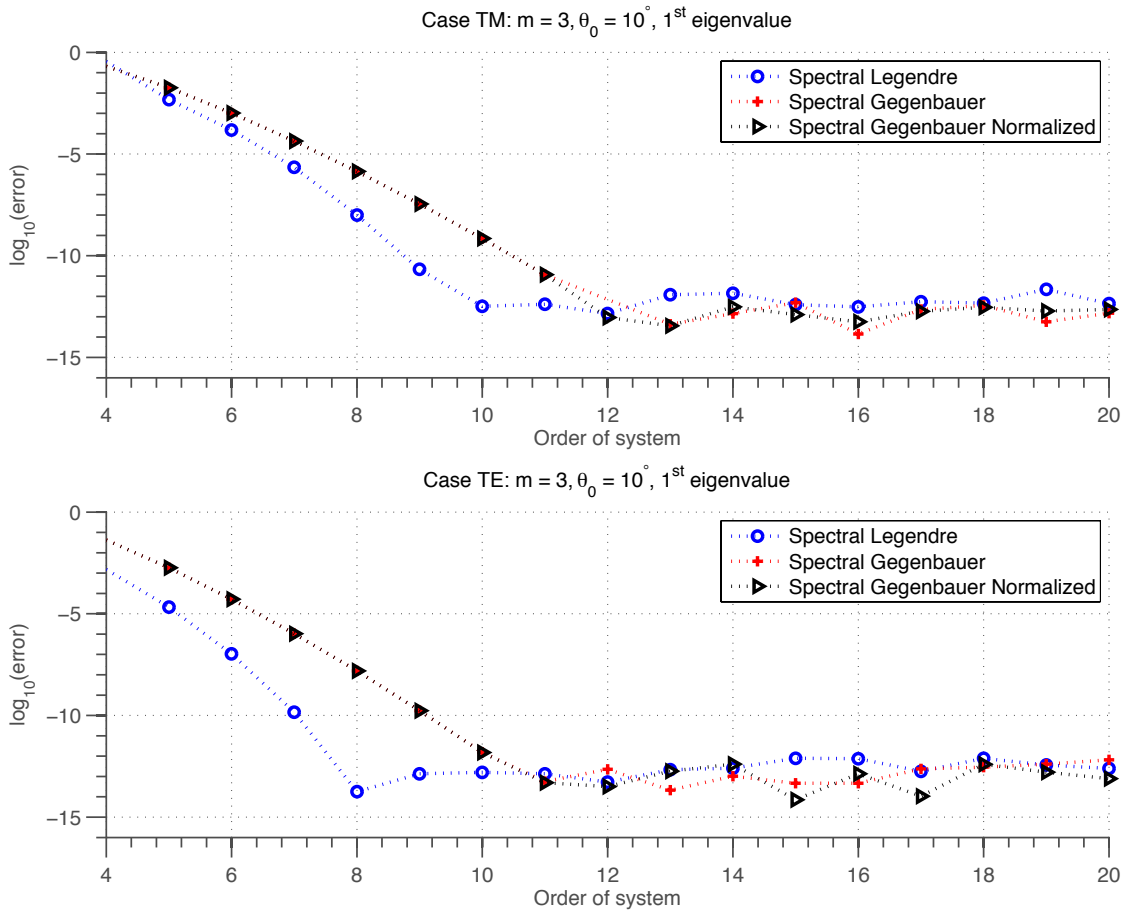

Figure 2.28: Gegenbauer equation: convergence curves for TM and TE eigenvalues.

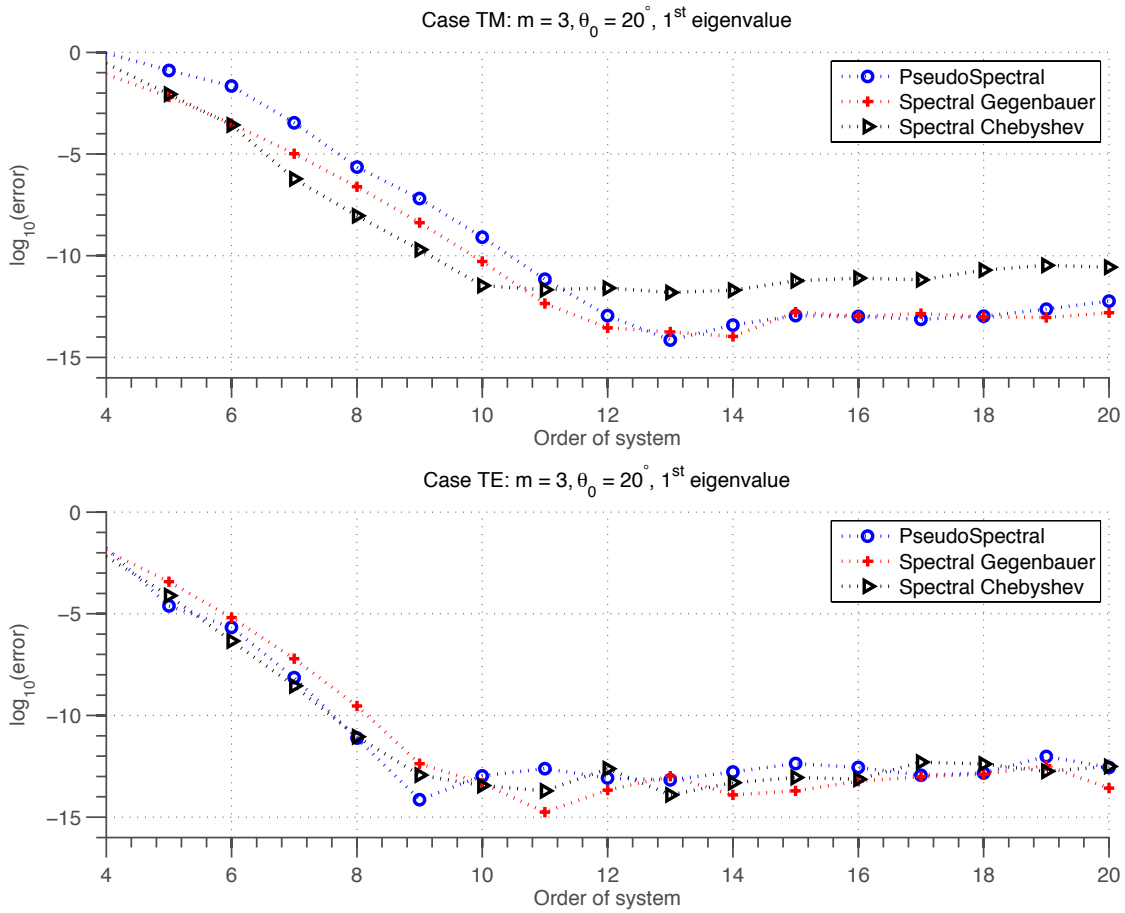

Figure 2.29: Gegenbauer equation: convergence curves for TM and TE eigenvalues.

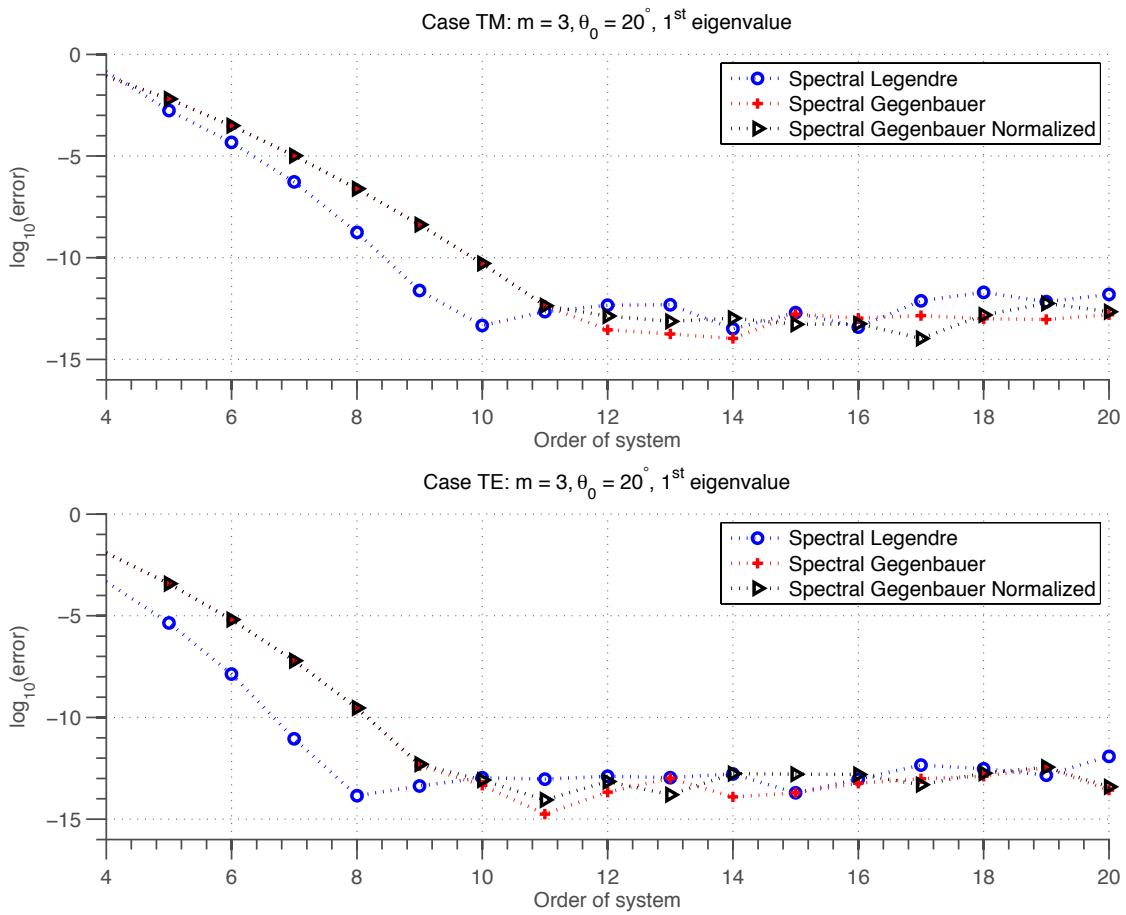

Figure 2.30: Gegenbauer equation: convergence curves for TM and TE eigenvalues.

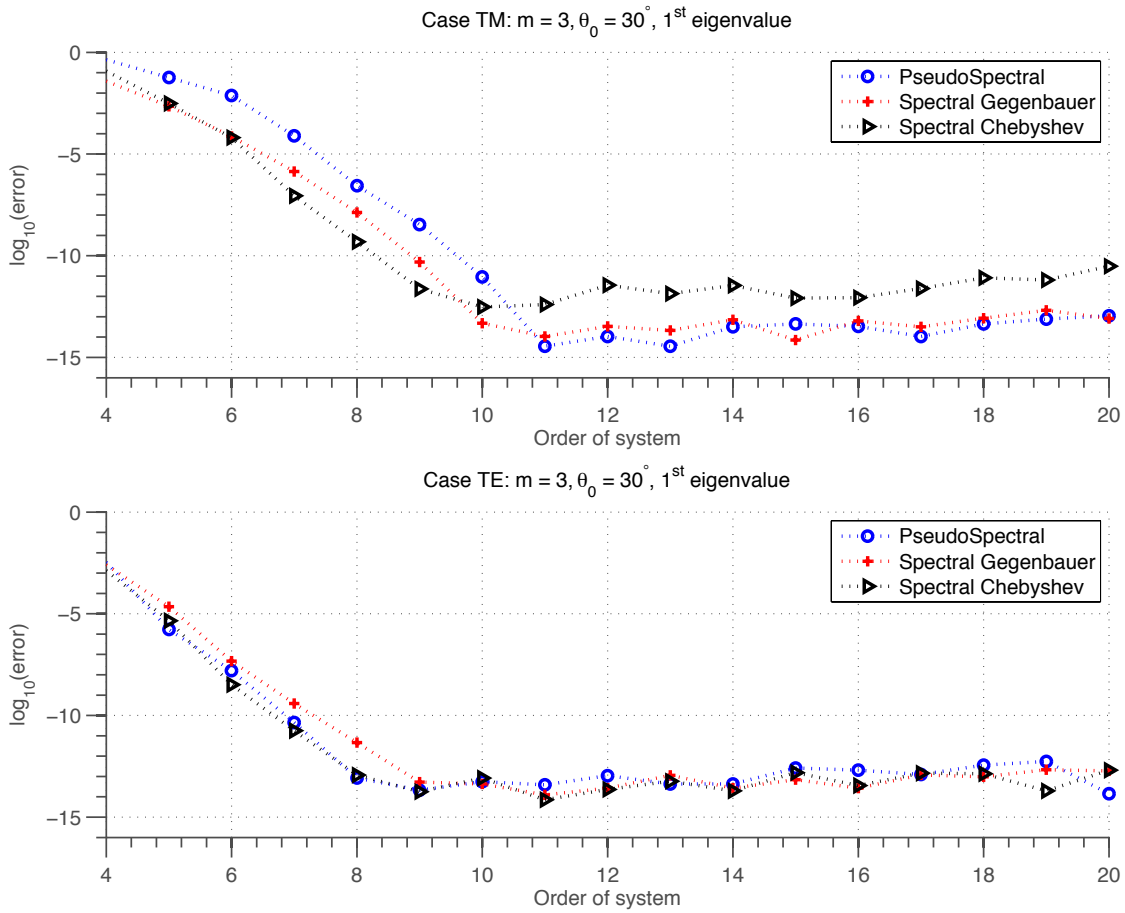

Figure 2.31: Gegenbauer equation: convergence curves for TM and TE eigenvalues.

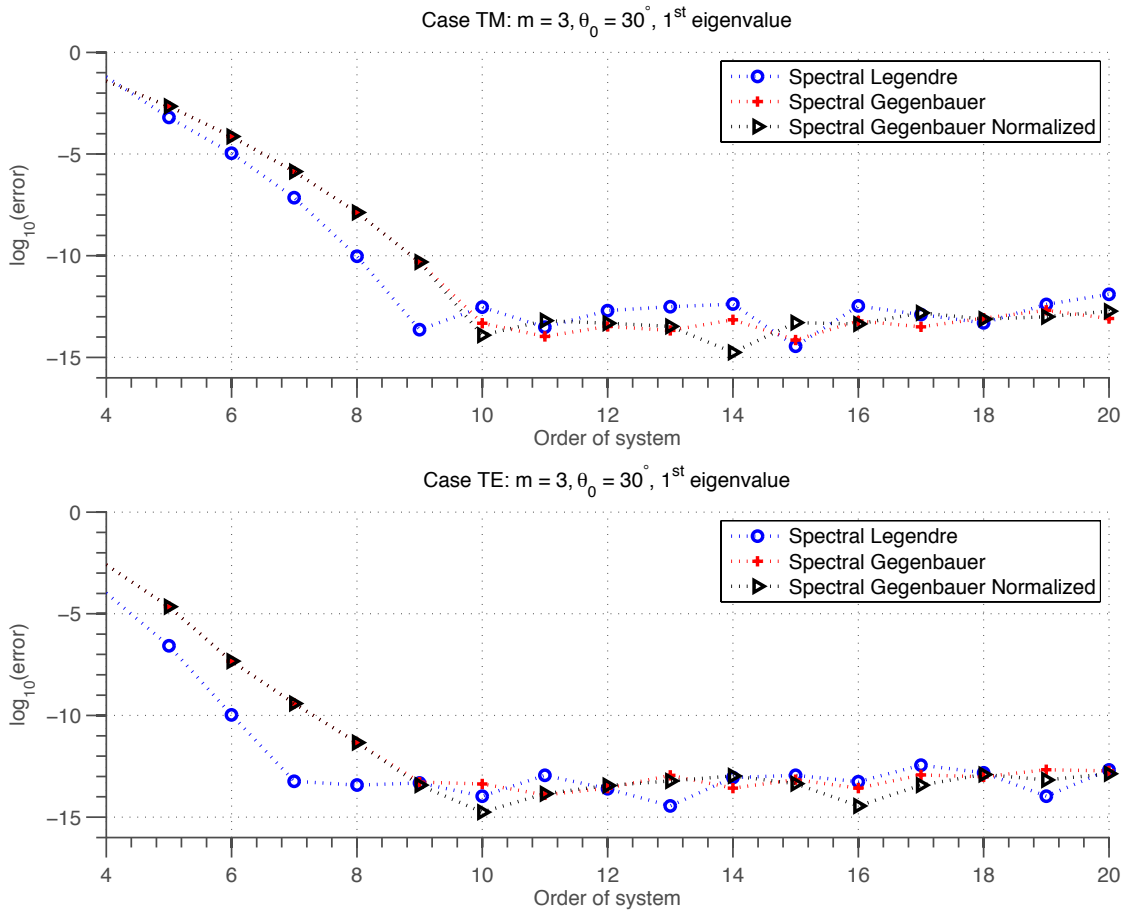

Figure 2.32: Gegenbauer equation: convergence curves for TM and TE eigenvalues.

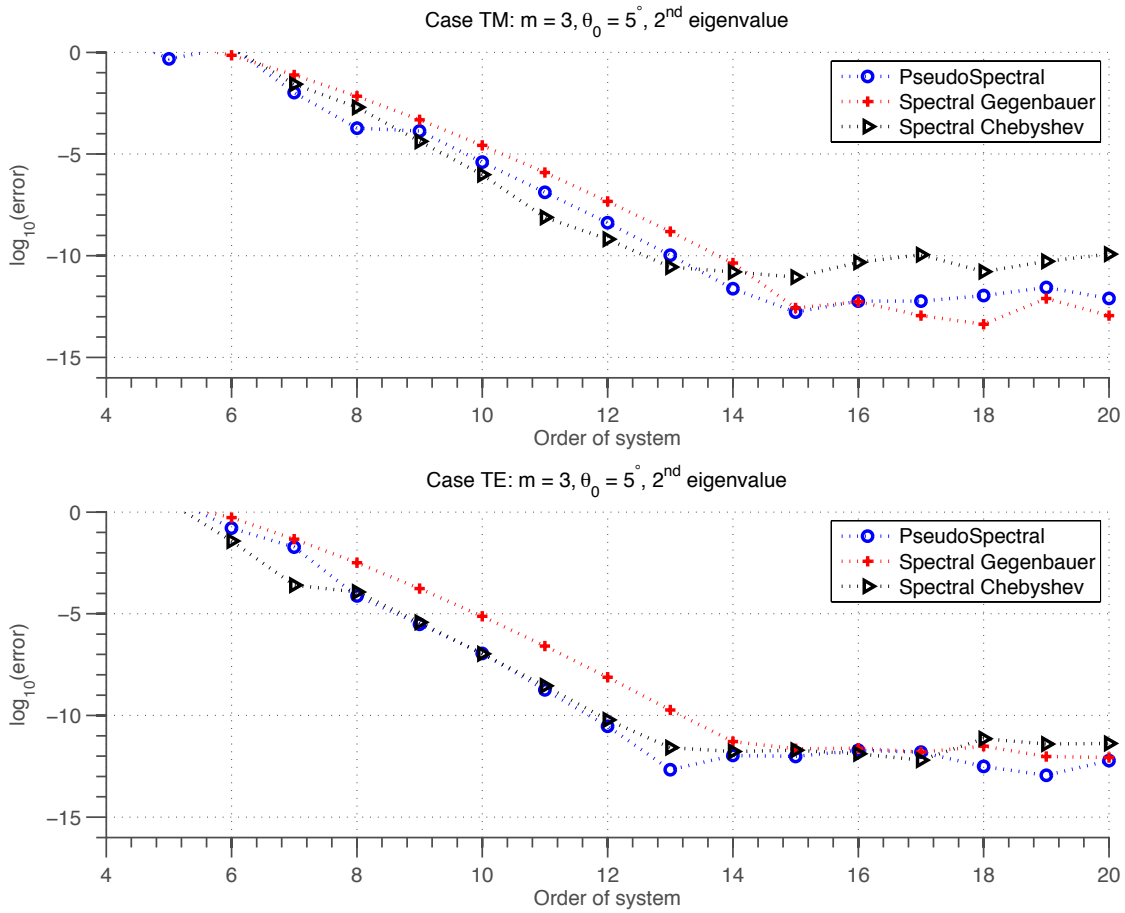

Figure 2.33: Gegenbauer equation: convergence curves for TM and TE eigenvalues.

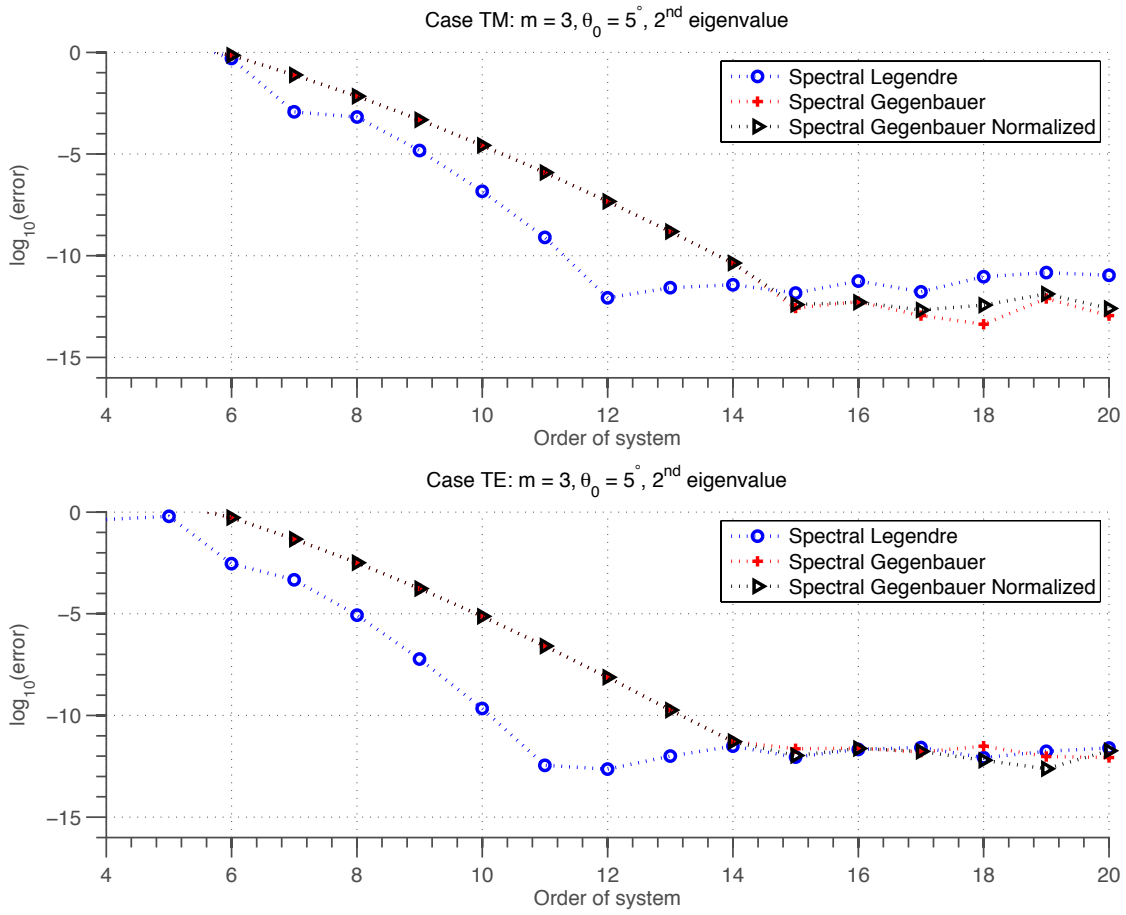

Figure 2.34: Gegenbauer equation: convergence curves for TM and TE eigenvalues.

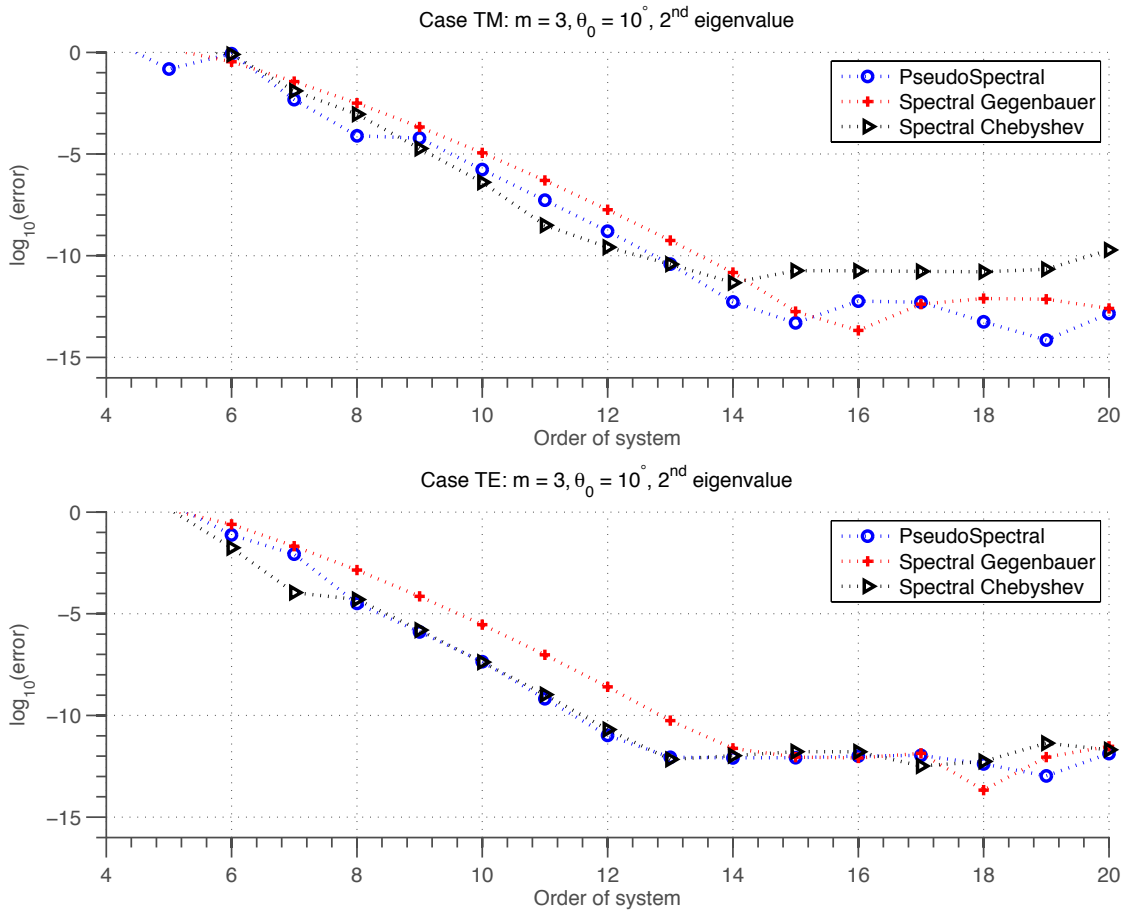

Figure 2.35: Gegenbauer equation: convergence curves for TM and TE eigenvalues.

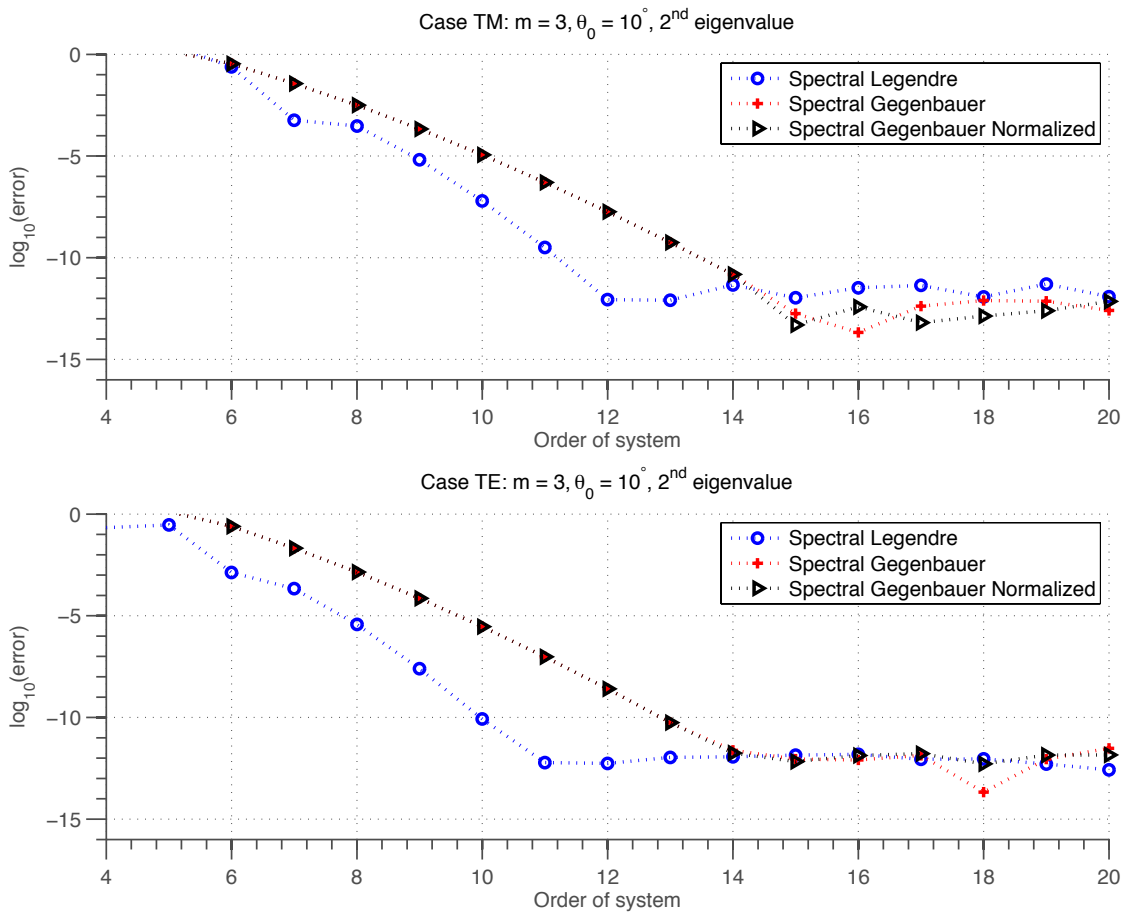

Figure 2.36: Gegenbauer equation: convergence curves for TM and TE eigenvalues.

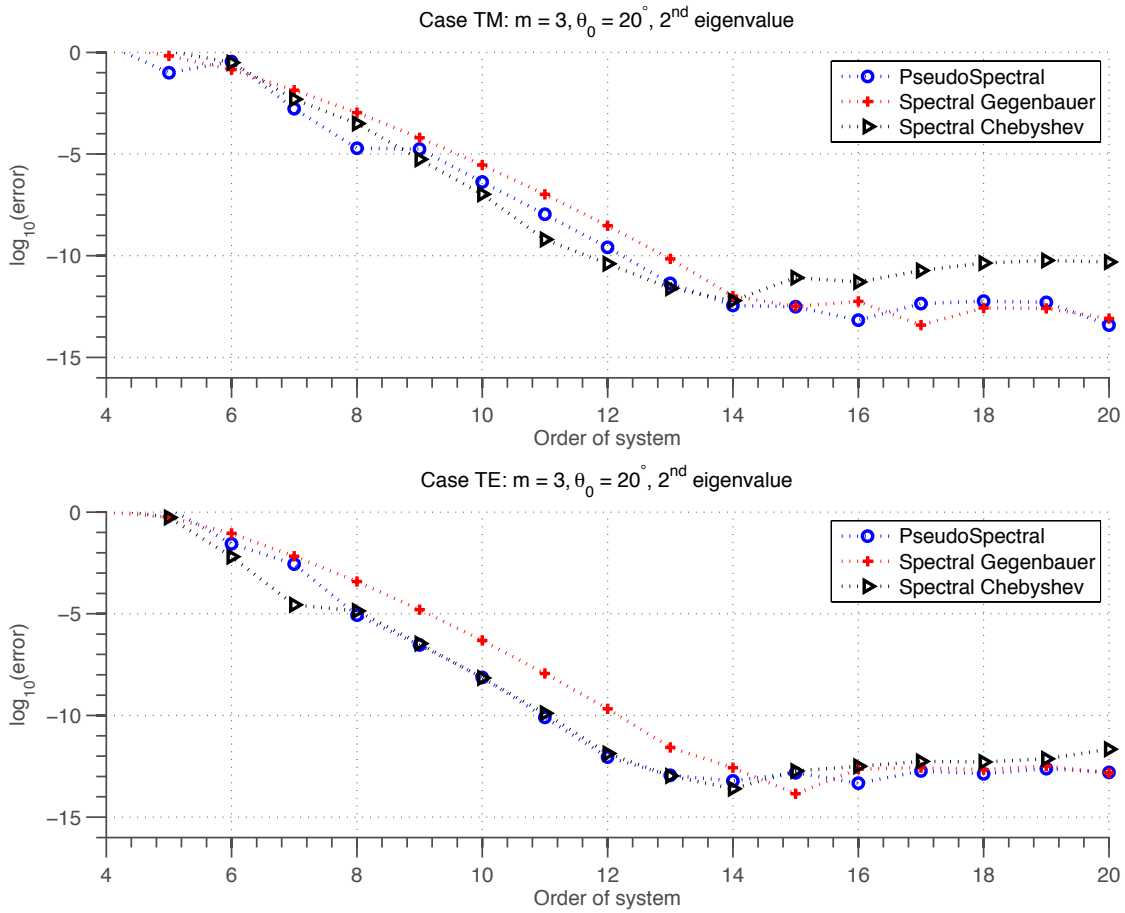

Figure 2.37: Gegenbauer equation: convergence curves for TM and TE eigenvalues.

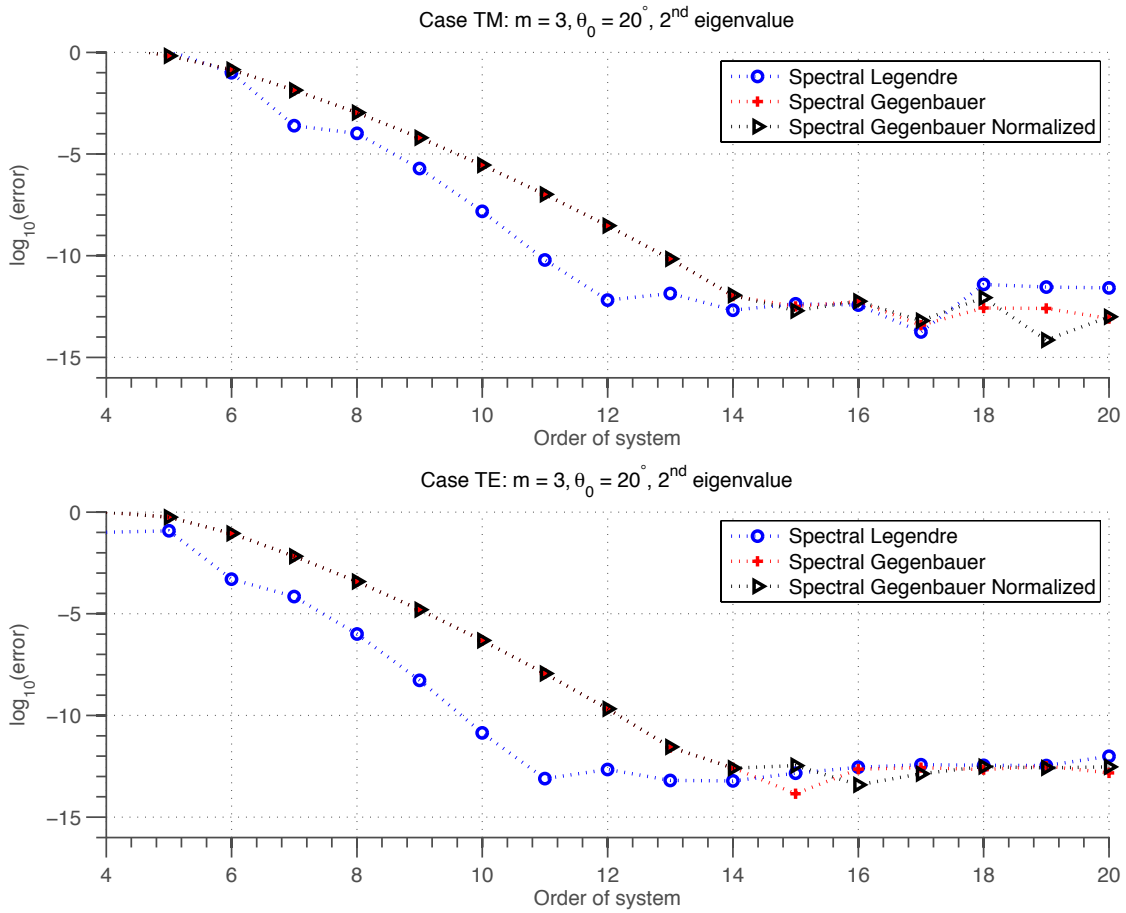

Figure 2.38: Gegenbauer equation: convergence curves for TM and TE eigenvalues.

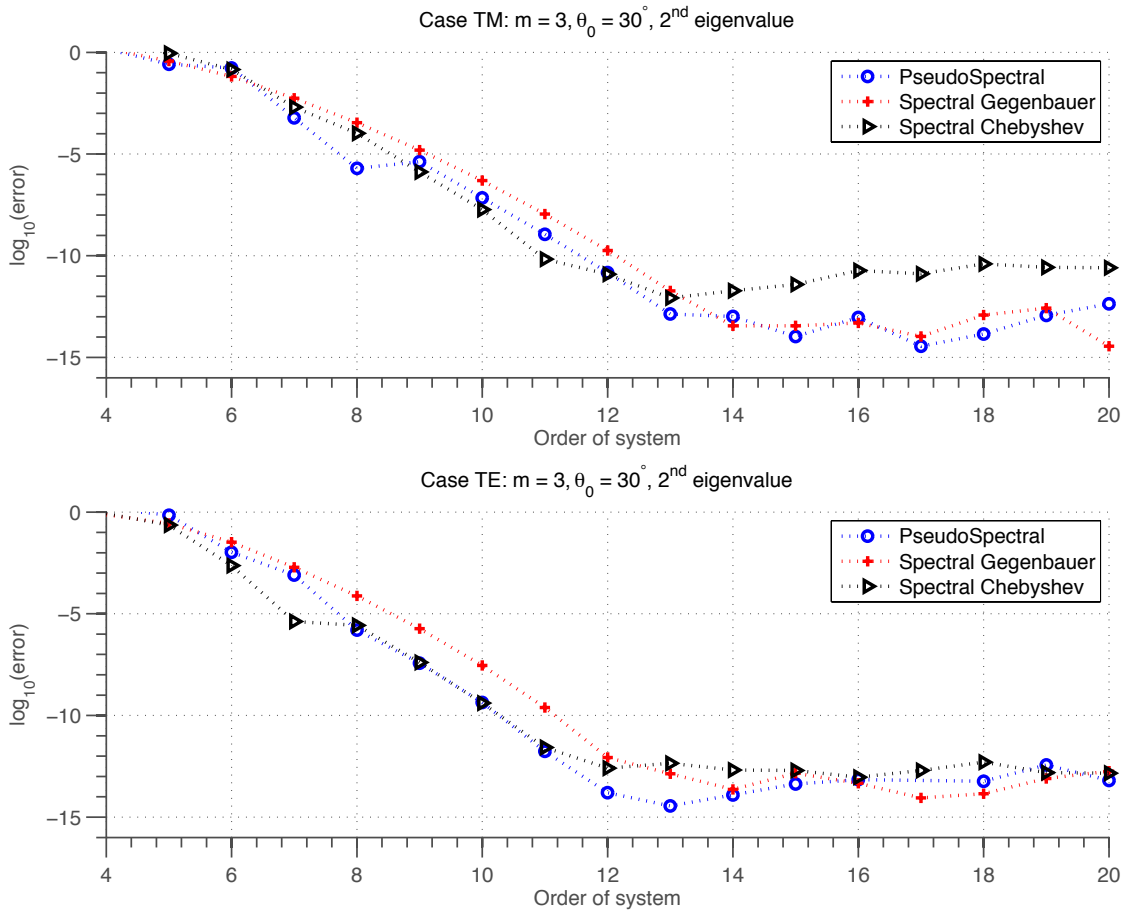

Figure 2.39: Gegenbauer equation: convergence curves for TM and TE eigenvalues.

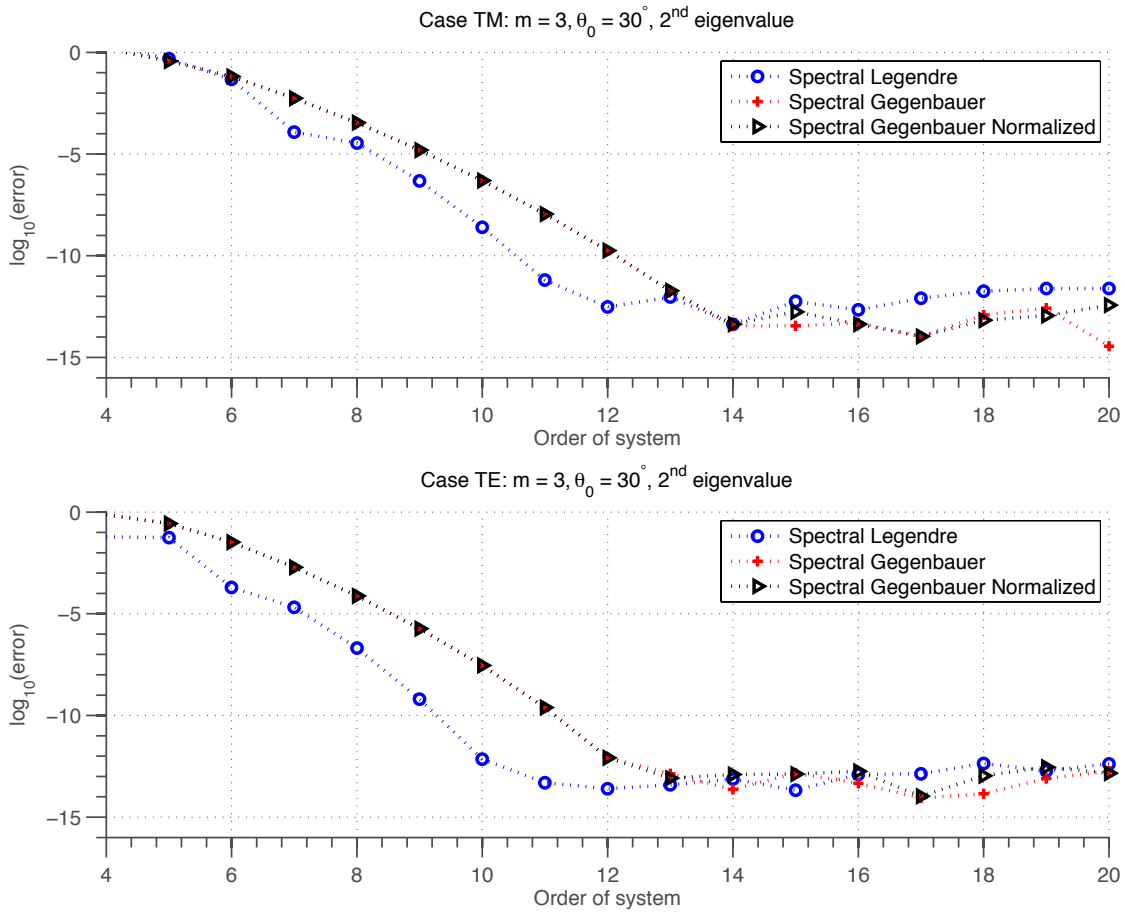

Figure 2.40: Gegenbauer equation: convergence curves for TM and TE eigenvalues.

2.4.1 Final results

From the comparison of the plots it is possible to draw some conclusions.

The first observation is about the direct solution of associated Legendre equation. This approach has to be avoided, because convergence is very slow; therefore, all considerations are based on the solution of Gegenbauer equation, found starting from the associated Legendre equation, taking away its singularity.

Considering the order of the linear system which has to be solved as comparison parameter, pseudospectral methods are generally worse than spectral methods.

About spectral methods, it is necessary to distinguish TE and TM cases, which produce different results. About TM cases, the best method is the Gegenbauer one, which is, on the other hand, the worst one, about TE modes. However, differences are little, therefore all methods work quite well. Chebyshev methods are slightly better, compared to Gegenbauer methods, for TE cases, therefore it is possible to say that, for the evaluation of TM modes, the best method is the Gegenbauer method, while for the evaluation of TE modes the best method is the Legendre method.

Normalized Gegenbauer have a very similar behavior, compared to Gegenbauer standard methods; this means that normalization does not play a major role in convergence.

An interesting observation is about pseudospectral methods and Chebyshev spectral methods; in the convergence study relative to the second eigenvalue, it is possible to see that curves are very close, except for a few points; this relationship may be explained remembering that pseudospectral methods actually are Chebyshev methods, so methods where both collocation nodes and interpolation functions are Chebyshev polynomials.

CHAPTER 3

Analysis of rectangular E-plane and H-plane devices

3.1 Introduction

In this chapter we introduce a numerical method for the analysis of 2-D rectangular devices based on Spectral-Element Methods (SEMs). These devices are two-dimensional because their geometry is invariant with respect to one cartesian direction, therefore it is possible to study them in a plane.

SEMs are a hybrid of FEMs and spectral methods; in FEMs, the domain is partitioned in several sub-domains, then the differential equation is solved in each of them. In SEMs, there is still a partition step, but the number of sub-domains is small. Then, each sub-domain is mapped in a canonical domain, so a set of basis functions is defined in order to expand the electromagnetic field in it; this is why this method is "spectral".

In addition to this procedure, it is possible to define the basis functions in order to take into account the presence of edges, obtaining results with good accuracy even with few basis functions. Unfortunately, this procedure introduces linear dependance between basis functions, therefore it is necessary to orthonormalize this set. The final model should approximate the electromagnetic field in the structure in the best possible way over a wide range of frequencies. By applying this model to a few frequency points and then processing the result, it is possible to obtain a reduced-order model for a bandwidth instead of for a single frequency.

To summarize, this method may be explained by dividing it in the following steps:

1. formulation of the problem in integral (weak) form;
2. determination of the orthonormal set of basis functions, keeping into account the edge effect and boundary conditions;
3. determination and solution of the linear system, applying the Galerkin version of the weighted residual method;

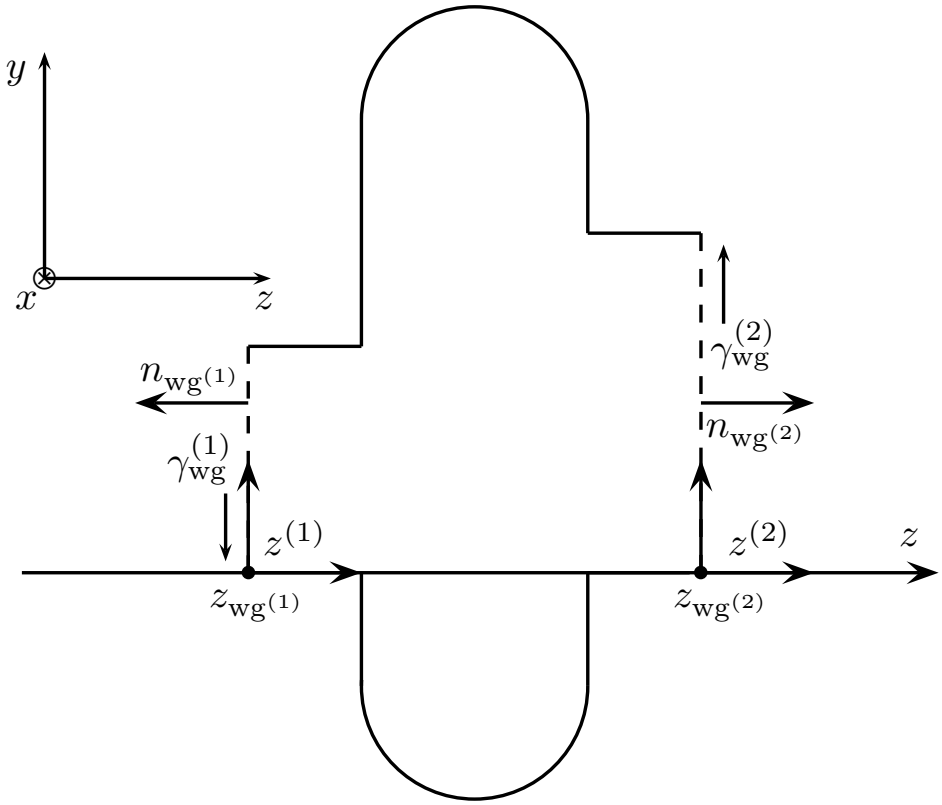

Figure 3.1: Geometry of a x-invariant structure

3.2 Formulation of the problem

In this section we formulate the study of a generic device invariant with respect to a cartesian coordinate.

Considering the coordinate reference system defined in Figure 3.1, the structure is invariant along the x-axis; therefore, the 2-D geometry of the device must be described on the zy plane.

In practical applications, the mode of interest in the feeding of this structure is the TE_{10}, which is the dominant mode of a rectangular waveguide. The only non-vanishing x component for this mode is h_x''; this is interesting because since this geometry is invariant along the x direction, in each section of the zy plane the electromagnetic field has the same variation as that of the exciting field.

Depending on the type of incident modes, it is possible to excite just H_x or E_x for this structure. This suggests that, instead of classifying modes in the structure as TE or TM like in waveguides, it is better to characterize them as $\mathrm{LSE}_{mn}^{(x)}$ or $\mathrm{LSM}_{mn}^{(x)}$. $\mathrm{LSE}_{mn}^{(x)}$ and $\mathrm{LSM}_{mn}^{(x)}$ are acronyms for Longitudinal Section Electric or Longitudinal Section Magnetic modes, respectively, with respect to the x direction. Therefore, $\mathrm{LSE}_{mn}^{(x)}$ have $E_x = 0$, while $\mathrm{LSM}_{mn}^{(x)}$ have $H_x = 0$. These fields are built as a linear combination of TE_{mn} and TM_{mn}; in LSE or LSM modes, the transversalization procedure is still applied with respect to the z direction; this means that these modes represent linear combinations of TE or TM modes which satisfy respectively $E_x = 0$ or $H_x = 0$. Because of the fact that in these structures is excited just one of

the x components (electric or magnetic), if $E_x = 0$ it is necessary to use a $\mathrm{LSE}^{(x)}_{mn}$ representation, while if $H_x = 0$ it is necessary to use the $\mathrm{LSM}^{(x)}_{mn}$ one.

Depending on the type of modes in the structure, the zy plane will be the E-plane or the H-plane. In next subsections we prove that, if $E_x = 0$, E lays only on the zy plane; therefore, in this case, zy is the E-plane. By contrast, if $H_x = 0$, the magnetic field H lays only on the zy plane, which is, in this case, the H-plane.

To summarize,

- for $\mathrm{LSE}^{(x)}_{mn}$ modes, $E_x = 0$, so zy is the E-plane of the structure, since the electric field lays on it;
- for $\mathrm{LSM}^{(x)}_{mn}$ modes, $H_x = 0$, so zy is the H-plane of the structure, since the magnetic field lays on it;

Considering the μ-th waveguide of the whole system, tangential to the μ-th port of the junction, if the k-th port of the junction is fed with a field containing only the dominant TE_{10} component, the index m of the excited $\mathrm{LSE}^{(x)}_{mn}$ or $\mathrm{LSM}^{(x)}_{mn}$ is constant, due to the translational symmetry along the x-axis; this means that, given the exciting TE_{10}, in the structure are excited $\mathrm{LSE}^{(x)}_{1n}$ or $\mathrm{LSM}^{(x)}_{1n}$ modes only. Because of this reason, it is convenient to transversalize the electromagnetic field with respect to x direction, obtaining

$$\begin{cases} \underline{H}(x,y,z) = \underline{H}_{\mathrm{t}}(x,y,z) + \hat{\mathrm{x}} H_x(x,y,z) \\ \underline{E}(x,y,z) = \underline{E}_{\mathrm{t}}(x,y,z) + \hat{\mathrm{x}} E_x(x,y,z) \end{cases} \tag{3.1}$$

Since the electromagnetic field in the structure, thanks to the geometrical invariance, has the same variation along the x-axis of the exciting field, it is possible to re-write (3.1), taking away the dependance on x; therefore, recalling the expressions of rectangular waveguide modes with $m = 1$ (since we are considering a TE_{10} exciting mode),

$$\begin{cases} \underline{H}(x,y,z) = \underline{H}_{\mathrm{t}}(x,y,z) + H_x(x,y,z) = \\ \qquad\qquad = \underline{H}^{(x)}_{\mathrm{t}}(y,z)\cos\left(\dfrac{\pi}{a}x\right) + \hat{\mathrm{x}}\, H^{(x)}_x(y,z)\sin\left(\dfrac{\pi}{a}x\right) \\ \underline{E}(x,y,z) = \underline{E}_{\mathrm{t}}(x,y,z) + E_x(x,y,z) = \\ \qquad\qquad = \underline{E}^{(x)}_{\mathrm{t}}(y,z)\sin\left(\dfrac{\pi}{a}x\right) + \hat{\mathrm{x}}\, E^{(x)}_x(y,z)\cos\left(\dfrac{\pi}{a}x\right) \end{cases} \tag{3.2}$$

where $\underline{H}^{(x)}_{\mathrm{t}}$, $\underline{E}^{(x)}_{\mathrm{t}}$, $E^{(x)}_x$, $H^{(x)}_x$ are field components of the structure without their dependance on x, which equals the one of waveguide modes.

At this point it is necessary to find the differential equations satisfied by $E^{(x)}_x$ and $H^{(x)}_x$, considering two separated cases. This means that it is necessary to start from Maxwell equations, considering two hypotheses.

- All the derivatives evaluated along x direction equal zero. This hypothesis may be found by solving these equations considering $H_x = 0$ or $E_x = 0$, and exciting the non-vanishing variable with the same dependance of the TE_{10} exciting mode, which is $\cos\left(\frac{\pi}{a}x\right)$ or $\sin\left(\frac{\pi}{a}x\right)$. By doing these calculations, it is

possible to see that two systems with decoupled variables are generated. The same result can be found by enforcing $\frac{\partial}{\partial x} = 0$.

- For E-plane devices, $E_x = 0$, $H_x \neq 0$; for H-plane devices, $E_x \neq 0$, $H_x = 0$.

3.2.1 E-plane devices

The first step is to write Maxwell equations, which are

$$\begin{cases} \nabla \times \underline{E} = -\mathrm{j}\omega\mu\underline{H} \\ \nabla \times \underline{H} = \mathrm{j}\omega\varepsilon\underline{E} \end{cases} \tag{3.3}$$

Now, these expression must be written by components, keeping into account previous hypotheses. For E-plane devices, $\frac{\partial}{\partial x} = 0$ and $E_x = 0$. So,

$$\begin{aligned} \nabla \times \underline{E} = \det \begin{bmatrix} \hat{\mathrm{x}} & \hat{\mathrm{y}} & \hat{\mathrm{z}} \\ 0 & \dfrac{\partial}{\partial y} & \dfrac{\partial}{\partial z} \\ 0 & E_y & E_z \end{bmatrix} = \\ = \hat{\mathrm{x}} \left(\frac{\partial E_z}{\partial y} - \frac{\partial E_y}{\partial z} \right) - \hat{\mathrm{y}} \, (0) + \hat{\mathrm{z}} \, (0) \end{aligned}$$

where the second term is proportional to H_y, and the third term to H_z. Therefore, it is immediately possible to write

$$H_y = 0 \quad H_z = 0$$

So, there is no magnetic field component on the zy plane; therefore, it is the E-plane of the structure. About the second Maxwell equation,

$$\begin{aligned} \nabla \times \underline{H} = \det \begin{bmatrix} \hat{\mathrm{x}} & \hat{\mathrm{y}} & \hat{\mathrm{z}} \\ 0 & \dfrac{\partial}{\partial y} & \dfrac{\partial}{\partial z} \\ H_x & H_y & H_z \end{bmatrix} = \\ = \hat{\mathrm{x}} \left(\frac{\partial H_z}{\partial y} - \frac{\partial H_y}{\partial z} \right) - \hat{\mathrm{y}} \left(-\frac{\partial H_x}{\partial z} \right) + \hat{\mathrm{z}} \left(-\frac{\partial H_x}{\partial y} \right) \end{aligned}$$

The first term is proportional to E_x, which equals zero for hypothesis. The three non-vanishing components which can be written are

$$\begin{cases} \dfrac{\partial E_z}{\partial y} - \dfrac{\partial E_y}{\partial z} = -\mathrm{j}\omega\mu H_x \\ \dfrac{\partial H_x}{\partial z} = \mathrm{j}\omega\varepsilon E_y \\ -\dfrac{\partial H_x}{\partial y} = \mathrm{j}\omega\varepsilon E_z \end{cases}$$

From here,

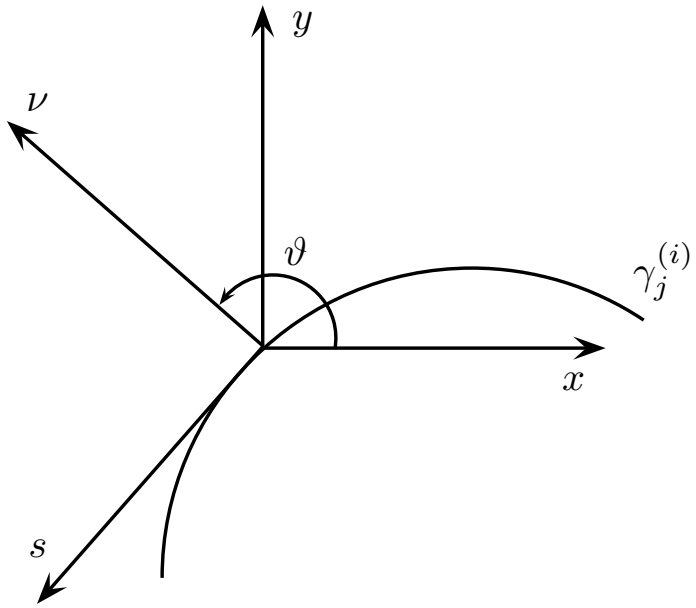

Figure 3.2: Reference system for PEC boundary condition

$$\begin{cases} E_y = \dfrac{1}{\mathrm{j}\omega\varepsilon}\dfrac{\partial H_x}{\partial z} \\ E_z = -\dfrac{1}{\mathrm{j}\omega\varepsilon}\dfrac{\partial H_x}{\partial y} \end{cases} \tag{3.4}$$

so, by substituting these expressions in the first equation of the system,

$$\frac{\partial}{\partial y}\left(-\frac{1}{\mathrm{j}\omega\varepsilon}\frac{\partial H_x}{\partial y}\right) - \frac{\partial}{\partial z}\left(\frac{1}{\mathrm{j}\omega\varepsilon}\frac{\partial H_x}{\partial z}\right) = -\mathrm{j}\omega\mu H_x$$

which becomes

$$\frac{\partial^2 H_x}{\partial y^2} + \frac{\partial^2 H_x}{\partial z^2} = -\omega^2\varepsilon\mu H_x$$

And, finally,

$$\nabla_{\mathrm{t}}^2 H_x + k^2 H_x = 0 \tag{3.5}$$

where ∇_{t} is transversal with respect to the x direction.

This equation must be coupled with PEC boundary conditions and with the continuity condition with each waveguide.

The PEC boundary condition requires that

$$\underline{E}_{\mathrm{t}} \cdot \hat{s} = 0 \tag{3.6}$$

At this point it is necessary to define correctly each variable of (3.6); considering for instance Figure 3.2, given ϑ the angle evaluated with respect to the zy system,

$$\hat{\nu} = \hat{\mathrm{z}}\cos\vartheta + \hat{\mathrm{y}}\sin\vartheta$$

Since $\hat{s}$ is rotated of 90° with respect to $\hat{\nu}$, it is possible to write the expression of $\hat{s}$ as follows

$$\begin{aligned}\hat{s} &= \hat{\mathrm{z}}\cos\left(\vartheta+\frac{\pi}{2}\right)+\hat{\mathrm{y}}\sin\left(\vartheta+\frac{\pi}{2}\right)= \\ &= -\hat{\mathrm{z}}\sin\vartheta+\hat{\mathrm{y}}\cos\vartheta\end{aligned}$$

so, considering the transversal field with respect to the x direction, $\underline{E}_{\mathrm{t}}$, as

$$\underline{E}_{\mathrm{t}} = E_z\hat{\mathrm{z}}+E_y\hat{\mathrm{y}}$$

it is possible to evaluate the dot product as follows

$$\begin{aligned}\underline{E}_{\mathrm{t}}\cdot\hat{s} &= (E_z\hat{\mathrm{z}}+E_y\hat{\mathrm{y}})\cdot\hat{s}= \\ &= \left(-\hat{\mathrm{z}}\frac{1}{\mathrm{j}\omega\varepsilon}\frac{\partial H_x}{\partial y}+\hat{\mathrm{y}}\frac{1}{\mathrm{j}\omega\varepsilon}\frac{\partial H_x}{\partial z}\right)\cdot(-\hat{\mathrm{z}}\sin\vartheta+\hat{\mathrm{y}}\cos\vartheta)= \\ &= \frac{1}{\mathrm{j}\omega\varepsilon}\left(\sin\vartheta\frac{\partial H_x}{\partial y}+\cos\vartheta\frac{\partial H_x}{\partial z}\right)= \\ &= \frac{1}{\mathrm{j}\omega\varepsilon}\frac{\partial H_x}{\partial\nu}\end{aligned} \tag{3.7}$$

in fact,

$$\begin{aligned}(\nabla_{\mathrm{t}}H_x)\cdot\hat{\nu} &= \left(\frac{\partial H_x}{\partial z}\hat{\mathrm{z}}+\frac{\partial H_x}{\partial y}\hat{\mathrm{y}}\right)\cdot(\hat{\mathrm{z}}\cos\vartheta+\hat{\mathrm{y}}\sin\vartheta)= \\ &= \frac{\partial H_x}{\partial y}\sin\vartheta+\frac{\partial H_x}{\partial z}\cos\vartheta\end{aligned}$$

Finally, it is necessary to find the continuity condition at each port, which must be enforced for each component of the electromagnetic field which lays on the discontinuity section. In this case, the discontinuity is on the plane normal to $\hat{\mathrm{z}}$, therefore the components of interest are E_x, H_x, E_y, H_y. Of these components, the non-vanishing ones are H_x and E_y. Furthermore, it is possible to see, from the first equation of (3.4), that

$$E_y = \frac{1}{\mathrm{j}\omega\varepsilon}\frac{\partial H_x}{\partial z}$$

so, the two conditions which must be enforced in order to guarantee the continuity of the electromagnetic field at each port are

$$\begin{cases} H_x = H_{x,\mathrm{wg}^{(k)}} \\ \dfrac{\partial H_x}{\partial z} = \dfrac{\partial H_{x,\mathrm{wg}^{(k)}}}{\partial z} \end{cases} \tag{3.8}$$

3.2.2 H-plane devices

Now are performed the same calculations of E-plane devices, considering the presence of $\mathrm{LSM}_{mn}^{(x)}$ modes. So, in this case, the zy plane is the H-plane of the structure. Considering all the derivatives evaluated with respect to x equal to zero, and $H_x = 0$, it is possible to write Maxwell equations by components as follows:

$$\nabla \times \underline{E} = \det \begin{bmatrix} \hat{\mathrm{x}} & \hat{\mathrm{y}} & \hat{\mathrm{z}} \\ 0 & \dfrac{\partial}{\partial y} & \dfrac{\partial}{\partial z} \\ E_x & E_y & E_z \end{bmatrix} = \\ = \hat{\mathrm{x}} \left(\frac{\partial E_z}{\partial y} - \frac{\partial E_y}{\partial z} \right) - \hat{\mathrm{y}} \left(-\frac{\partial E_x}{\partial z} \right) + \hat{\mathrm{z}} \left(-\frac{\partial E_x}{\partial y} \right)$$

where the first term equals zero, since it is proportional to H_x which equals zero for hypothesis. About the second Maxwell equation,

$$\nabla \times \underline{H} = \det \begin{bmatrix} \hat{\mathrm{x}} & \hat{\mathrm{y}} & \hat{\mathrm{z}} \\ 0 & \dfrac{\partial}{\partial y} & \dfrac{\partial}{\partial z} \\ 0 & H_y & H_z \end{bmatrix} = \\ = \hat{\mathrm{x}} \left(\frac{\partial H_z}{\partial y} - \frac{\partial H_y}{\partial z} \right) - \hat{\mathrm{y}} \left(0 \right) + \hat{\mathrm{z}} \left(0 \right)$$

where the second term is proportional to E_y, and the third term to E_z. Therefore, it is immediately possible to write

$$E_y = 0 \quad E_z = 0$$

So, there is no electric field component on the zy plane, which is the H-plane of the structure. The three non-vanishing components for these equations are:

$$\begin{cases} \dfrac{\partial H_z}{\partial y} - \dfrac{\partial H_y}{\partial z} = \mathrm{j}\omega\varepsilon E_x \\ \dfrac{\partial E_x}{\partial z} = -\mathrm{j}\omega\mu H_y \\ -\dfrac{\partial E_x}{\partial y} = -\mathrm{j}\omega\mu H_z \end{cases}$$

so

$$\begin{cases} H_y = -\dfrac{1}{\mathrm{j}\omega\mu} \dfrac{\partial E_x}{\partial z} \\ H_z = \dfrac{1}{\mathrm{j}\omega\mu} \dfrac{\partial E_x}{\partial y} \end{cases} \tag{3.9}$$

so, by substituting these expressions in the first equation of the system,

$$\frac{\partial}{\partial y}\left(\frac{1}{\mathrm{j}\omega\mu}\frac{\partial E_x}{\partial y}\right) - \frac{\partial}{\partial z}\left(-\frac{1}{\mathrm{j}\omega\mu}\frac{\partial E_x}{\partial z}\right) = \mathrm{j}\omega\varepsilon E_x$$

which becomes

$$\frac{\partial^2 E_x}{\partial y^2} + \frac{\partial^2 E_x}{\partial z^2} = -\omega^2\varepsilon\mu E_x$$

And, finally,

$$\nabla_{\mathrm{t}}^2 E_x + k^2 E_x = 0 \tag{3.10}$$

About the PEC boundary condition, in this case it is just

$$E_x = 0$$

In fact, $E_z = E_y = 0$, therefore it is necessary to enforce only E_x to equal zero, on the PEC surface.

Finally, it is necessary to work on continuity conditions at each port. In this case, the only two non-vanishing components are H_y and E_x. First of all, it is necessary to enforce the continuity of E_x at each port. In addition, from the first equation of (3.9), it is possible to find

$$H_y = -\frac{1}{\mathrm{j}\omega\mu}\frac{\partial E_x}{\partial z}$$

therefore, it is necessary to enforce the continuity of the derivative of E_x with respect to z, which is the axis normal to the discontinuity plane.

Resume of previous results

In the rectangular case, it is necessary to study two decoupled problems. Exception made for PEC boundary conditions, results of previous cases are very similar. In fact,

- for $\mathrm{LSE}_{mn}^{(x)}$ modes, if H_x is renamed ϕ,
- for $\mathrm{LSM}_{mn}^{(x)}$ modes, if E_x is renamed ϕ,

the differential equation satisfied by ϕ is, for both cases, the Helmholtz equation, with ∇_{t} transversal to the invariance direction x;

$$\nabla_{\mathrm{t}}^2 \phi + k^2 \phi = 0 \tag{3.11}$$

Continuity boundary conditions are the same for both cases; as a matter of fact, for both cases it is necessary to enforce either ϕ or its derivative to be continue on each access line. So

$$\begin{cases} \phi = \phi_{\mathrm{wg}} \\ \dfrac{\partial \phi}{\partial n_{\mathrm{wg}^{(k)}}} = \dfrac{\partial \phi_{\mathrm{wg}}}{\partial n_{\mathrm{wg}^{(k)}}} \end{cases} \tag{3.12}$$

since the discontinuity plane in both cases is normal to the access line plane, $n_{\mathrm{wg}^{(k)}}$. By contrast, it is necessary to distinguish $\mathrm{LSE}^{(x)}_{mn}$ and $\mathrm{LSM}^{(x)}_{mn}$ cases during the formulation of PEC boundary conditions; in fact,

- for $\mathrm{LSE}^{(x)}_{mn}$, it is necessary to enforce the value of the normal derivative of ϕ;

$$\left.\frac{\partial\phi}{\partial\nu}\right|_{\gamma_{\mathrm{PEC}}} = 0 \tag{3.13}$$

- for $\mathrm{LSM}^{(x)}_{mn}$ cases, the same procedure must be applied on the value of ϕ;

$$\left.\phi\right|_{\gamma_{\mathrm{PEC}}} = 0 \tag{3.14}$$

3.2.3 Modal expansion of waveguide electromagnetic field components

In order to enforce continuity conditions for each access port, it is necessary to represent opportunely the electromagnetic field on it. In this work, basis functions used for the expansion of the electromagnetic field are the LSE and LSM modes. The whole procedure for the determination of following expressions is carried out in Subsection 4.2.3; here, the result is

$$E^{(k)}_{x,\mathrm{wg}} = \sum_{\mu=0}^{\infty} \sqrt{Z^{(k)}_{\infty,\mu}} \left[a^{(k)}_{\mu} \mathrm{e}^{-\mathrm{j}\beta^{(k)}_{\mu} z^{(k)}} + b^{(k)}_{\mu} \mathrm{e}^{+\mathrm{j}\beta^{(k)}_{\mu} z^{(k)}} \right] e^{(k)}_{x,\mu}(\underline{\rho}) \tag{3.15}$$

$$H^{(k)}_{x,\mathrm{wg}} = \sum_{\mu=0}^{\infty} \sqrt{Y^{(k)}_{\infty,\mu}} \left[a^{(k)}_{\mu} \mathrm{e}^{-\mathrm{j}\beta^{(k)}_{\mu} z^{(k)}} - b^{(k)}_{\mu} \mathrm{e}^{+\mathrm{j}\beta^{(k)}_{\mu} z^{(k)}} \right] h^{(k)}_{x,\mu}(\underline{\rho}) \tag{3.16}$$

Where $Y^{(k)}_{\infty,\mu}$ and $Z^{(k)}_{\infty,\mu}$ are respectively the modal admittance and the modal impedance relative to mode μ at port k, and $\beta^{(k)}_{\mu}$ is the modal wavenumber (propagation constant) relative to mode μ. $z^{(k)}$ is the propagation coordinate relative to the origin of each local coordinate system at each k-th port. Finally, $a^{(k)}_{\mu}$ and $b^{(k)}_{\mu}$ are the incident and scattered waves, for each k-th port.

In order to satisfy boundary conditions, it is necessary to evaluate also the derivatives of these expressions; therefore, since the normal to the discontinuity plane is z,

$$\frac{\partial E^{(k)}_{x,\mathrm{wg}}}{\partial z} = \sum_{\mu=0}^{\infty} \sqrt{Z^{(k)}_{\infty,\mu}}\, \mathrm{j}\beta^{(k)}_{\mu} \left[-a^{(k)}_{\mu} \mathrm{e}^{-\mathrm{j}\beta^{(k)}_{\mu} z^{(k)}} + b^{(k)}_{\mu} \mathrm{e}^{+\mathrm{j}\beta^{(k)}_{\mu} z^{(k)}} \right] e^{(k)}_{x,\mu}(\underline{\rho})$$

$$\frac{\partial H^{(k)}_{x,\mathrm{wg}}}{\partial z} = \sum_{\mu=0}^{\infty} \sqrt{Y^{(k)}_{\infty,\mu}}\, \mathrm{j}\beta^{(k)}_{\mu} \left[-a^{(k)}_{\mu} \mathrm{e}^{-\mathrm{j}\beta^{(k)}_{\mu} z^{(k)}} - b^{(k)}_{\mu} \mathrm{e}^{+\mathrm{j}\beta^{(k)}_{\mu} z^{(k)}} \right] h^{(k)}_{x,\mu}(\underline{\rho})$$

In conclusion, all these expressions are usually evaluated for $z^{(k)} = z_{\mathrm{wg}^{(k)}}$, so at each port. Since all local reference systems have their origin at their respective device

port, all the exponentials equal 1, because $z^{(k)} = 0\ \forall k$. So, previous expressions are simplified, as follows

$$\frac{\partial E^{(k)}_{x,\mathrm{wg}}}{\partial z} = \sum_{\mu=0}^{\infty} \sqrt{Z^{(k)}_{\infty,\mu}}\, \mathrm{j}\beta^{(k)}_{\mu} \left[-a^{(k)}_{\mu} + b^{(k)}_{\mu}\right] e^{(k)}_{x,\mu}(\underline{\rho}) \tag{3.17}$$

$$\frac{\partial H^{(k)}_{x,\mathrm{wg}}}{\partial z} = \sum_{\mu=0}^{\infty} \sqrt{Y^{(k)}_{\infty,\mu}}\, \mathrm{j}\beta^{(k)}_{\mu} \left[-a^{(k)}_{\mu} - b^{(k)}_{\mu}\right] h^{(k)}_{x,\mu}(\underline{\rho}) \tag{3.18}$$

3.2.4 Weak-form formulation of the problem

If the domain where the differential equation solution is defined may not be represented as the cartesian product of 1-dimensional domains, it is not possible to use the variable separation method for the determination of the solution of the problem. In this case, the approach used is based on casting the differential problem (3.11) and its boundary conditions (3.12), (3.13) or (3.14) in weak form. Given a space of test functions X_v, the projection of (3.11) on these functions is

$$\iint_{\Sigma} \nabla^2_{\mathrm{t}}\phi\, v_\beta \,\mathrm{d}\Sigma - k^2 \iint_{\Sigma} \phi\, v_\beta \,\mathrm{d}\Sigma = 0 \quad \forall v_\beta \in X_v \tag{3.19}$$

It is important to remark that the numerical scheme which will be applied is Galerkin-based, because ϕ, which is the unknown of the problem, will be expanded as a sum of functions which equal v_β. This means that v_β has the same properties of ϕ, because they have to satisfy PEC boundary conditions just like ϕ.

Expression (3.19) can be modified by applying the first Green scalar theorem, recalled here;

$$\iiint_{V} \left(\nabla\phi \cdot \nabla\psi + \psi\nabla^2\phi\right) \mathrm{d}V = \iint_{\Sigma} \psi \frac{\partial\phi}{\partial n} \mathrm{d}\underline{s}$$

this can be applied (in the 2-D case) to discharge one ∇_{t} operator to test functions v_β, obtaining

$$\iint_{\Sigma} \nabla^2_{\mathrm{t}}\phi\, v_\beta \,\mathrm{d}\Sigma = -\iint_{\Sigma} (\nabla_{\mathrm{t}}\phi) \cdot (\nabla_{\mathrm{t}} v_\beta) \,\mathrm{d}\Sigma + \int_{\gamma} v_\beta \frac{\partial\phi}{\partial n} \mathrm{d}\underline{s}$$

By substituting this last expression in the weak form Helmholtz equation it is possible to obtain

$$\iint_{\Sigma} (\nabla_{\mathrm{t}}\phi) \cdot (\nabla_{\mathrm{t}} v_\beta) \,\mathrm{d}\Sigma - k^2 \iint_{\Sigma} \phi\, v_\beta \,\mathrm{d}\Sigma = \int_{\gamma} v_\beta \frac{\partial\phi}{\partial n} \mathrm{d}\underline{s}$$

The right-hand side term has a line integral, which can be divided in two kinds of contributions: integrals on PEC surfaces and integrals on access lines. First of all, it is possible to write the line integral as follows

$$\int_{\gamma} v_\beta \frac{\partial\phi}{\partial n} \mathrm{d}\underline{s} = \int_{t_a}^{t_b} \left(v_\beta(x(t), y(t)) \left.\frac{\partial\phi}{\partial n}\right|_{(x(t),y(t))} \right) \cdot \underline{s}'(t) \mathrm{d}t$$

The PEC integral contributions equal zero, because one of v or the derivative of ϕ satisfy PEC boundary conditions (which involve the dot product of the electric field and the unit vector tangent to the PEC surface), so the only non-vanishing contributions are the ones from the ports. Therefore,

$$\int_{\gamma} v_\beta \frac{\partial \phi}{\partial n} \mathrm{d}\underline{s} = \sum_{k=1}^{N_{\text{ports}}} \int_{\gamma_{\text{wg}}^{(k)}} \frac{\partial \phi}{\partial n} v_\beta \, \mathrm{d}\underline{s}$$

Now, recalling the second equation from (3.12), it is possible to substitute it in the integral, obtaining

$$\iint_{\Sigma} (\nabla_{\text{t}} \phi) \cdot (\nabla_{\text{t}} v_\beta) \, \mathrm{d}\Sigma - k^2 \iint_{\Sigma} \phi \, v_\beta \, \mathrm{d}\Sigma = \sum_{k=1}^{N_{\text{ports}}} \int_{\gamma_{\text{wg}}^{(k)}} \frac{\partial \phi_{\text{wg}}^{(k)}}{\partial n} v_\beta \, \mathrm{d}\underline{s} \tag{3.20}$$

This equation satisfies implicitly the second condition of (3.12), in strong form; as a matter of fact, this condition is enforced by performing a substitution in the equation, instead of by projection.

In order to complete the weak-form formulation it is still necessary to project on a chosen basis the first equation of (3.12). This time, in order to simplify some integrals, it is possible to use, as expansion functions, mode functions $h_{x,\beta}^{(k)}$ for E-plane devices, or $e_{x,\mu}$ for H-plane devices. Since the method is Galerkin, h_x or e_x act either as test functions or as expansion functions for the waveguide fields. Therefore, in weak form, it is possible to write, for each access line, considering E-plane devices,

$$\left\langle \phi, h_{x,\nu}^{(k)} \right\rangle \Big|_{\gamma^{(k)}} = \left\langle \phi_{\text{wg}}, h_{x,\nu}^{(k)} \right\rangle \Big|_{\gamma^{(k)}} \tag{3.21}$$

or, in integral form,

$$\int_{\gamma^{(k)}} \phi \, h_{x,\nu}^{(k)} \mathrm{d}\underline{s} = \int_{\gamma^{(k)}} \phi_{\text{wg}} \, h_{x,\nu}^{(k)} \mathrm{d}\underline{s} \tag{3.22}$$

While, for H-plane devices,

$$\left\langle \phi, e_{x,\nu}^{(k)} \right\rangle \Big|_{\gamma^{(k)}} = \left\langle \phi_{\text{wg}}, e_{x,\nu}^{(k)} \right\rangle \Big|_{\gamma^{(k)}} \tag{3.23}$$

or, in integral form,

$$\int_{\gamma^{(k)}} \phi \, e_{x,\nu}^{(k)} \mathrm{d}\underline{s} = \int_{\gamma^{(k)}} \phi_{\text{wg}} \, e_{x,\nu}^{(k)} \mathrm{d}\underline{s} \tag{3.24}$$

3.3 Application of the Spectral-Element Method

Up to this point, no hypotheses about domain properties were introduced, so every equation introduced is valid for arbitrary geometries.

The numerical scheme which must be applied to this problem is a Spectral-Element Method. This name describes its philosophy; in fact, it mixes Finite-Element Methods and Spectral methods to solve a PDE (Partial Differential Equation).

The Finite-Element Methods concept is based on the idea of partitioning a domain in a big number of points or sub-domains; then, the solution of the PDE can be approximated by integrating numerically, using standard techniques such as Euler's method or Runge-Kutta methods. Then, the PDE is transformed in a linear system. Spectral methods, like the Galerkin method, are based on the expansion of the solution of the differential problem on a set of known expansion functions. By obtaining a linear system, for instance by testing the expanded differential equation on a set of test functions, it is possible to find a solution of the problem.

Spectral-Element Methods are a hybrid of these two methods; there is a partition of the domain in few subdomains, then for each of them a set of basis functions is chosen, defining N-dimensional domains as tensor products; each differential equation can be solved using numerical integration techniques, such as Gaussian integration formulae. Finally, solutions belonging to each "patch" (subdomain) is joined, by enforcing continuity boundary conditions between each patch.

Given M the number of subdomains, the problem (3.20) is divide in M subproblems like

$$\iint_{\Sigma} \nabla_{\mathrm{t}}\phi^{(j)} \cdot \nabla_{\mathrm{t}} v_{\beta}^{(j)} \,\mathrm{d}\Sigma - k^2 \iint_{\Sigma} \phi^{(j)}\, v_{\beta}^{(j)} \,\mathrm{d}\Sigma = \sum_{k=1}^{N_{\mathrm{ports}}} \int_{\gamma_{\mathrm{wg}}^{(k)}} \frac{\partial \phi_{\mathrm{wg^{(i)}}}^{(j)}}{\partial n}\, v_{\beta}^{(j)} \,\mathrm{d}\underline{s} \tag{3.25}$$

where j denotes each patch.

Between each couple of patches it is necessary to enforce continuity boundary conditions; since this is similar to the problem of enforcing continuity to between waveguides and device ports, it is possible to define the following continuity conditions

$$\begin{cases} \phi^{(a)} = \phi^{(b)} \\ \dfrac{\partial \phi^{(a)}}{\partial n^{(a)}} = \dfrac{\partial \phi_{\mathrm{wg}}^{(b)}}{\partial n^{(b)}} \end{cases} \tag{3.26}$$

and these conditions must be enforced on common boundaries $\partial\Sigma^{(a,b)}$, where $j = a$ and $j = b$ are the indexes of two patches. The boundary between a and b is defined as

$$\partial\Sigma^{(a,b)} = \partial\Sigma^{(a)} \cap \Sigma^{(b)}, \quad a \neq b$$

It is important to remark that supports of sub-domains are disjoined; this means that they have no intersection, exception made for the boundary.

3.3.1 Definition of non-specialized basis functions

The unknown of each problem, related with each j-th patch, is $\phi^{(j)}$; therefore, it will be expanded in a linear combination of functions. Basis functions which will be used for both expansion and test tasks are "specialized" functions, because they generate a very particular range of functions. As a matter of fact, out of the need to choose functions which show special features, such as assuming particular values in some

points, boundary conditions must be enforced, since they "select", of all possible functions able to generate a range of behaviors, only the ones which present these special features. However, the procedure for the determination of these specialized functions starts from "raw" functions, which does not comply with any particular specification; in a second moment, these functions will be specialized finding, starting from them, a set of functions which satisfy Dirichlet, Neumann or Robin boundary conditions, which are continue in particular points, orthonormal, and so on. So, the first step is the definition of non-specialized basis functions, in order to find a set of functions defined on a canonical domain, which does not satisfy any boundary condition.

Raw functions must be defined on a canonical domain, also known as "parent domain" $\underline{\sigma} = (\xi, \eta)$, because the geometry of the problem described in the natural domain may be complex, so it would be hard to describe functions directly on it. In order to propose a general case, the E- or H-plane of the structure is described on an xy plane, just to ease the reader; this means that, in this case,

$$z \longrightarrow x \quad y \longrightarrow y$$

Then, it is necessary to find a correspondence between the natural domain xy and the parent domain $\xi\eta$, which is

$$\underline{\rho} = F_{\rho\sigma}(\underline{\sigma})$$

It is possible to prove that $F_{\rho\sigma}$, which maps a generic point of the parent domain $\underline{\sigma}$ to a point in the natural $\underline{\rho}$ domain, assumes a form like

$$\begin{aligned} F_{\rho\sigma}^{(j)}(\underline{\sigma}) = {} & \frac{1-\eta}{2}\pi_1^{(j)}(\xi) + \frac{1+\eta}{2}\pi_3^{(j)}(\xi) + \\ & + \frac{1-\xi}{2}\left[\pi_4^{(j)}(\eta) - \frac{1+\eta}{2}\pi_4^{(j)}(1) - \frac{1-\eta}{2}\pi_4^{(j)}(-1)\right] + \\ & + \frac{1+\xi}{2}\left[\pi_2^{(j)}(\eta) - \frac{1+\eta}{2}\pi_2^{(j)}(1) - \frac{1-\eta}{2}\pi_2^{(j)}(-1)\right] \end{aligned} \tag{3.27}$$

Where (ξ, η) are the abscissa and the ordinate of the parent domain coordinate system, $\pi_n^{(j)}$ are the parametric transformations for mapping each n-th side of the arbitrary quadrilateral to each n-th side of the parent domain, which is the square defined by the cartesian product

$$[-1, +1] \times [-1, +1]$$

and j indexes each j-th patch where this procedure is applied. Usually, even the hardest geometries of practical interest may be described analytically, as parametric curves, therefore it is possible to find an analytical mapping function $F_{\rho\sigma}(\underline{\sigma})$ able to map a function, starting from the parent domain $\underline{\sigma}$, to the $\underline{\rho}$ natural domain. The convention chosen is to use as $n = 1$ side the lower one, while the others are sorted following the counterclockwise order.

So, the procedure used to build basis functions starts from their definition in the parent domain, as tensor product[1] of known functions, like Chebyshev polynomials. So, an example of basis for the parent domain is

$$P_{mn}(\underline{\sigma}) = P_{mn}(\xi, \eta) = T_m(\xi)\, T_n(\eta)$$

These functions must be mapped in the parent domain $\underline{\rho}$; so, given $\left\{P_{mn}^{(j)}(\underline{\sigma})\right\}$ the set of functions for the parent design, it is possible to define non-specialized functions by this way:

$$s_{\delta}^{(j)}(\underline{\rho}) = P_{mn}^{(j)}(\underline{\sigma}), \quad \underline{\rho} = F_{\rho\sigma}^{(j)}(\underline{\sigma}),\ \underline{\rho} \in \Sigma_i$$

where δ is a multiple index, since it retains informations about m and n; in other words, $\delta = (m, n)$. This means that, given $P_{mn}^{(j)}(\underline{\sigma})$ in the parent domain, its mapped version is basically made by evaluating each $\underline{\rho}$ from the transformation, obtaining a relationship between each point of $\underline{\rho}$ and each point of $\underline{\sigma}$; so, by relating these correspondence with $P_{mn}^{(j)}(\underline{\sigma})$, it is possible to obtain non-specialized functions $s_{mn}^{(j)}(\underline{\rho})$.

3.3.2 Meixner conditions

The electromagnetic field nearby the edges is singular, therefore a standard SEM can not describe it maintaining its exponential convergence. Commercial codes, such as Ansoft HFSS, in order to describe properly these elements refine the mesh nearby each edge, obtaining a better accuracy but increasing computational time.

An alternative idea should be the synthesis of basis functions which take into account the presence of edges intrinsically, in order to use them in a Spectral-Element Method. The synthesis procedure can be carried out using the asymptotic behavior formulae of the electromagnetic field near to the edges as weights for non-specialized basis functions; considering $s_{mn}(\underline{\rho}) = s_{\delta}(\underline{\rho})$ the set of basis functions in the natural domain, the idea is, given weight functions $\psi_e^{(p)}$, to build a set of functions like

$$\{F_{\delta}(\underline{\sigma})\} \bigcup \{F_{\delta}(\underline{\sigma})\psi_e^{(p_1)}\} \bigcup ... \bigcup \{F_{\delta}(\underline{\sigma})\psi_e^{(p_n)}\}$$

This means joining the same set of non-specialized basis functions $s_{\delta}(\underline{\sigma})$ with many different $\psi_e^{(p_i)}$ weight functions, where the order of each weight function depends on p_i.

Weight functions $\psi_e^{(p)}$ are defined in a third domain, called "companion domain" $\underline{\chi}$, which is related to the natural domain $\underline{\rho}$. In fact, the companion domain definition is based on the concept of "companion structure", which is obtained transforming each curved side in a straight side, tangent at the edge. This structure allows the user to define easily the angle of the edge δ_e.

The singular behavior of the electromagnetic field (ϕ) can be modeled as follows

- for the $\mathrm{LSE}_{mn}^{(x)}$ case, so for E-plane structures,

[1] which is the product of functions of different variables

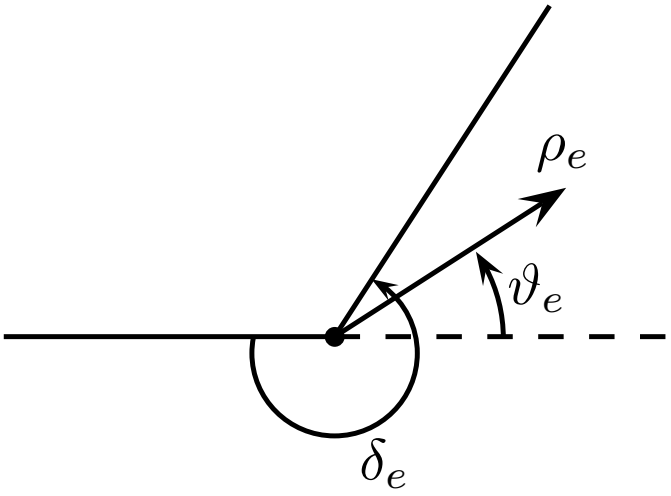

Figure 3.3: Detail of the geometry of an edge

$$\psi_e^{(p)}(\underline{\chi}) = \rho_e^{\frac{p\pi}{\delta_e}} \cos\left(\frac{p\pi}{\delta_e}\vartheta_e\right)$$

- for the $\mathrm{LSM}_{mn}^{(x)}$ case, so for H-plane structures,

$$\psi_e^{(p)}(\underline{\chi}) = \rho_e^{\frac{p\pi}{\delta_e}} \sin\left(\frac{p\pi}{\delta_e}\vartheta_e\right)$$

Where δ_e is the angle of the metallic edge. (ρ_e, ϑ_e) are coordinates for the local coordinate system on the edge e. Since the companion domain is basically identical to the natural one, less than the approximation of curved lines with straight lines, ρ_e and ϑ_e may be used for the representation of the behavior of the electromagnetic field also in the natural domain.

Considering the multidimensional index $\alpha = (m, n, p)$, where m and n are indexes for non-specialized basis functions, while p is related to the weight function, basis functions which take into account only the Meixner condition may be found as

$$f_\alpha^{(j)}(\underline{\rho}) = \left[\prod_{e=1}^{N_e^{(j)}} \psi_e^{(p)}\left(F_{\chi\sigma}^{(j)}(\underline{\sigma})\right)\right] P_{mn}^{(j)}(\underline{\sigma}), \quad \underline{\rho} = F_{\rho\sigma}^{(j)}(\underline{\sigma}) \in \Sigma_i \tag{3.28}$$

Considering an example, given $P_{mn}^{(j)}(\underline{\sigma})$, if $p = \{0, 1, 2\}$, the result of this operation is this set of basis functions

$$\begin{aligned} &\left\{P_{mn}^{(j)}\psi_e^{(0)}\right\} \bigcup \left\{P_{mn}^{(j)}\psi_e^{(1)}\right\} \bigcup \left\{P_{mn}^{(j)}\psi_e^{(2)}\right\} = \\ &= \left\{P_{mn}^{(j)}\right\} \bigcup \left\{P_{mn}^{(j)}\psi_e^{(1)}\right\} \bigcup \left\{P_{mn}^{(j)}\psi_e^{(2)}\right\} \end{aligned}$$

Near to the edges, each set of functions will act in a different way, because of the fact that weights have significative values in these situations. On the other hand,

far away from the edges, the contribution of weights decays, therefore the final set of basis functions has many replicas of the same set of basis functions, joined together. This means that this is not actually a basis, since it does not comply with the "independence" property. This property has to be re-established, in a second time.

3.3.3 Specialization of basis functions

The $f_\alpha^{(j)}$ functions satisfy only Meixner conditions. In order to use them for the representation of $\phi^{(j)}$, they must satisfy every boundary condition satisfied by it, so PEC boundary conditions and continuity conditions between each patch.

Starting from PEC conditions, it is possible to use a basis-recombination approach for the determination of a set of functions $\left\{g_l^{(j)}\right\}$, defined as linear combinations of functions belonging to $\left\{f_\alpha^{(j)}\right\}$, which satisfy PEC boundary conditions.

The idea of basis recombination is to recombine the functions $f_\alpha^{(j)}$ in order linear combinations of them which satisfy homogeneous boundary conditions and, hence, to obtain a more specialized set of functions, compared to $f_\alpha^{(j)}$. The formulation of the basis recombination strategy is based on the solution of the following equation

$$g_l^{(j)}(\underline{\rho}) = \sum_\alpha y_\alpha^{(l)} f_\alpha^{(j)}(\underline{\rho}) \tag{3.29}$$

where l is the index for the identification of each single new function $g_l^{(j)}$, relative to each j-th patch. For each l-th function of the more specialized basis $\left\{g_l^{(j)}(\underline{\rho})\right\}$ there is a set of coefficients $y_\alpha^{(l)}$ which represent the change of basis from $f^{(j)}$ to $g^{(j)}$, by building an appropriated linear combination of $f^{(j)}$ functions. So, in order to build each l-th function $g_l^{(j)}$, it is necessary to solve an homogeneous system of type

$$\underline{\underline{L}}^{(j)}\ \underline{y}^{(l)} = 0 \tag{3.30}$$

in fact, for both E-plane and H-plane devices, boundary conditions are homogeneous. The difference between the two cases is in $\underline{\underline{L}}$. In fact,

- in E-plane devices, it is necessary to enforce, as PEC boundary condition,

$$\frac{\partial \phi^{(j)}}{\partial n^{(j)}} = 0$$

which implies

$$\frac{\partial g_l^{(j)}}{\partial n^{(j)}} = 0$$

therefore, substituting it in (3.29), remembering that $y_\alpha^{(l)}$ are just recombination coefficients, so constants,

$$\frac{\partial g_l^{(j)}}{\partial n^{(j)}} = 0 \Longrightarrow \frac{\partial}{\partial n^{(j)}} \sum_\alpha y_\alpha^{(l)} f_\alpha^{(j)}(\underline{\rho}) = \\ = \sum_\alpha y_\alpha^{(l)} \frac{\partial f_\alpha^{(j)}}{\partial n^{(j)}} \tag{3.31}$$

- in H-plane devices, it is necessary to enforce

$$\phi^{(j)} = 0$$

which implies

$$g_l^{(j)} = 0$$

therefore, substituting it in (3.29),

$$g_l^{(j)} = 0 \Longrightarrow \sum_\alpha y_\alpha^{(l)} f_\alpha^{(j)}(\underline{\rho}) = 0 \tag{3.32}$$

These expressions must be satisfied only on PEC surface. In order to write coefficients for (3.30), the following step is the projection, on a set of test functions v_β, of expressions (3.31) or (3.32), depending on the type of structure. Results are

- for E-plane structures,

$$L_{q\alpha}^{(j)} \left\langle \frac{\partial f_\alpha^{(j)}}{\partial n^{(j)}}, v_q \right\rangle_{\gamma_{\mathrm{PEC}}^{(j)}} = \int_{\gamma_{\mathrm{PEC}}^{(j)}} \frac{\partial f_\alpha^{(j)}}{\partial n^{(j)}} \, v_q \, \mathrm{d}\underline{s} \tag{3.33}$$

- for H-plane structures,

$$L_{q\alpha}^{(j)} \left\langle f_\alpha^{(j)}, v_q \right\rangle_{\gamma_{\mathrm{PEC}}^{(j)}} = \int_{\gamma_{\mathrm{PEC}}^{(j)}} f_\alpha^{(j)} \, v_q \, \mathrm{d}\underline{s} \tag{3.34}$$

Now, every coefficient of system (3.30) is found. Recalling its expression,

$$\underline{\underline{L}}^{(j)} \; \underline{y}^{(l)} = 0$$

The unknown of this system is $\underline{y}^{(l)}$; since this system is homogeneous, its solution is the set of vectors belonging to the kernel space of $\underline{\underline{L}}^{(j)}$ matrix. Therefore, in order to carry out the basis recombination strategy and determine recombination coefficients $y_\alpha^{(l)}$, it is necessary to determine a basis for the representation of the kernel space of $\underline{\underline{L}}^{(j)}$.

In order to compute a basis for the kernel of $\underline{\underline{L}}^{(j)}$, it is possible to use the economic size singular value decomposition on it;

$$L^{(j)} = \underline{\underline{U}}\,\underline{\underline{S}}\,\underline{\underline{V}}^{\mathrm{H}}$$

The columns of $\underline{\underline{V}}$ which are related to a null singular value are a basis for the kernel space of $\underline{\underline{L}}^{(j)}$; therefore, by establishing a threshold, considering all singular values below this threshold and columns of $\underline{\underline{V}}$ corresponding to them, it is possible to find $y_\alpha^{(l)}$ values, which will be called $G_{l\alpha}^{(j)}$. $G_{l\alpha}^{(j)}$ represents a projection coefficient from the basis $f_\alpha^{(j)}$ to the $g_l^{(j)}$ one. This means that there is a linear application, represented with the matrix $\underline{\underline{G}}$ of chosen columns of $\underline{\underline{V}}$, which transforms $f_\alpha^{(j)}$ in $g_l^{(j)}$.

$g_l^{(j)}$ functions are just a recombination of $f_\alpha^{(j)}$ functions, which were non-specialized functions, keeping into account only the presence of Meixner conditions; these functions, because of the method used for their constructions, are linearly dependent.

In order to solve the final system for the determination of scattering matrix, it is necessary to build the mass matrix[2], ${}^{(\underline{f})}\underline{\underline{M}}^{(j)}$, as follows

$${}^{(\underline{f})}M_{\beta\alpha}^{(j)} = \left\langle f_\alpha^{(j)}, f_\beta^{(j)} \right\rangle = \iint_{\Sigma_j} f_\alpha^{(j)} f_\beta^{(j)} \mathrm{d}\Sigma_j$$

This matrix can be represented in the $\left\{\underline{g}^{(j)}\right\}$ basis by considering the change of basis

$${}^{(\underline{g})}\underline{\underline{M}}^{(j)} = \underline{\underline{G}}^{\mathrm{H},(j)}\,{}^{(\underline{f})}\underline{\underline{M}}^{(j)}\,\underline{\underline{G}}^{(j)}$$

Because of the fact that $g_l^{(j)}$ functions are not linearly independent, ${}^{(\underline{g})}\underline{\underline{M}}^{(j)}$ mass matrix is ill-conditioned, therefore it is not possible to use it in a linear system, because its solution would be unreliable. So, it is necessary to remove these dependences by building an orthonormal basis $\left\{h_r^{(j)}\right\}$, which can represent the same image of the mass matrix ${}^{(\underline{g})}\underline{\underline{M}}^{(j)}$, enforcing orthonormality. It is possible to apply again the SVD decomposition, this time focusing on matrix $\underline{\underline{U}}$; considering

$${}^{(\underline{g})}\underline{\underline{M}}^{(j)} = \underline{\underline{U}}\,\underline{\underline{S}}\,\underline{\underline{V}}^{\mathrm{H}}$$

It is necessary to define a basis for the range of ${}^{(\underline{g})}\underline{\underline{M}}^{(j)}$; this can be done by considering all singular vectors belonging to $\underline{\underline{U}}$ corresponding to non-vanishing singular values. So, it is defined a threshold, and then are chosen all singular vectors corresponding to singular values above it. Retaining all these singular values in $\underline{\underline{H}}^{(j)}$, it is possible to build functions $\left\{h_r^{(j)}\right\}$, which satisfy PEC and Meixner boundary conditions, and which are orthonormal.

3.3.4 Patching

In order to "glue" all patches, it is necessary to perform a final change of basis to a set of global basis functions, $\left\{u_s(\underline{\rho})\right\}$.

[2] mass matrix is a FEM term, which represents a generalization of the idea of "mass" to generalized coordinate systems

The first step for joining all basis functions is to enforce (3.26) conditions, which guarantee the continuity of the electromagnetic field between confining sub-domains; like previously done, this is done in weak form.

First of all, it is necessary to define this final change of basis. Since all sub-domains are disjoined (because their intersection is the empty set), it is possible to evaluate each s-th function $u_s(\underline{\rho})$ as follows

$$u_s(\underline{\rho}) = \bigcup_j \left\{ \sum_r c_r^{(s,j)} h_r^{(j)}(\underline{\rho}) \right\}$$

It is necessary to enforce continuity between expressions inside the parentheses; therefore, in weak form, it is necessary to test both the conditions on a set of 1-dimensional functions, obtaining, for each confining couple of edges (a, b),

$$\sum_r c_r^{(s,a)} \left\langle h_r^{(a)}, v_q \right\rangle \Big|_{\partial^{(a,b)}} = \sum_r c_r^{(s,b)} \left\langle h_r^{(b)}, v_q \right\rangle \Big|_{\partial^{(a,b)}} \tag{3.35}$$

$$\sum_r c_r^{(s,a)} \left\langle \frac{\partial h_r^{(a)}}{\partial n^{(a)}}, v_q \right\rangle \Bigg|_{\partial^{(a,b)}} = \sum_r c_r^{(s,b)} \left\langle \frac{\partial h_r^{(b)}}{\partial n^{(b)}}, v_q \right\rangle \Bigg|_{\partial^{(a,b)}} \tag{3.36}$$

By building a matrix $\underline{\underline{N}}$ starting from these conditions, it is possible to find another homogeneous system, of type

$$\underline{\underline{N}}\, \underline{c}^{(s)} = 0$$

This system can be solved once again by evaluating the SVD decomposition of $\underline{\underline{N}}$ and using the singular vectors $\underline{\underline{V}}$ corresponding to vanishing singular values. This corresponds to find a basis for the kernel space of $\underline{\underline{N}}$, therefore the vector $\underline{c}^{(s)}$ of coefficients for performing the change of basis. $\left\{u_s(\underline{\rho})\right\}$ is the set of functions which is actually used for the expansion of ϕ, since it is global (it represents a basis for the whole domain, not just for a subdomain), orthonormal, and satisfies PEC and Meixner boundary conditions.

3.4 Application of the Galerkin method

Considering $\left\{u_s(\underline{\rho})\right\}$ as known functions from previous steps, it is possible to apply them to equation (3.20) and to the boundary condition (3.22) or (3.24), recalled here

$$\iint_{\Sigma} (\nabla_{\mathrm{t}}\phi)\cdot(\nabla_{\mathrm{t}} v_\beta)\,\mathrm{d}\Sigma - k^2 \iint_{\Sigma} \phi\, v_\beta\,\mathrm{d}\Sigma = \sum_{k=1}^{N_{\mathrm{ports}}} \int_{\gamma_{\mathrm{wg}}^{(k)}} \frac{\partial \phi_{\mathrm{wg}}^{(k)}}{\partial n}\, v_\beta\,\mathrm{d}\underline{s}$$

$$\int_{\gamma^{(k)}} \phi\, e_{x,\nu}^{(k)}\mathrm{d}\underline{s} = \int_{\gamma^{(k)}} \phi_{\mathrm{wg}}\, e_{x,\nu}^{(k)}\mathrm{d}\underline{s} \quad H\text{-plane}$$

$$\int_{\gamma^{(k)}} \phi\, h_{x,\nu}^{(k)}\mathrm{d}\underline{s} = \int_{\gamma^{(k)}} \phi_{\mathrm{wg}}\, h_{x,\nu}^{(k)}\mathrm{d}\underline{s} \quad E\text{-plane}$$

First of all, it is necessary to recall some basic informations; ϕ function can be expanded using $u_s(\underline{\rho})$ basis function, which take into account (at this step) the fact that the device is E-plane or H-plane. Therefore,

$$\phi = \sum_{s=0}^{N_{\mathrm{fun}}} x_s u_s(\underline{\rho}) \tag{3.37}$$

It is important to recall (3.15) and (3.16) too, so

$$E_{x,\mathrm{wg}}^{(k)} = \sum_{\mu=0}^{\infty} \sqrt{Z_{\infty,\mu}^{(k)}}\left[a_\mu^{(k)} + b_\mu^{(k)}\right] e_{x,\mu}^{(k)}(\underline{\rho})$$

$$H_{x,\mathrm{wg}}^{(k)} = \sum_{\mu=0}^{\infty} \sqrt{Y_{\infty,\mu}^{(k)}}\left[a_\mu^{(k)} - b_\mu^{(k)}\right] h_{x,\mu}^{(k)}(\underline{\rho})$$

3.4.1 Continuity conditions equations

The first equation which can be modified is, considering for instance E-plane devices,

$$\int_{\gamma^{(k)}} \phi\, h_{x,\nu}^{(k)}\,\mathrm{d}\underline{s} = \int_{\gamma^{(k)}} \phi_{\mathrm{wg}}\, h_{x,\nu}^{(k)}\,\mathrm{d}\underline{s} \quad \forall\beta$$

This expression must be modified, by substituting field expansions for both ϕ and ϕ_{wg}, from (3.37) and (3.15) respectively, obtaining

$$\sum_{s=1}^{N_{\mathrm{fun}}} x_s \int_{\gamma^{(k)}} u_s(\underline{\rho})\, h_{x,\nu}^{(k)}(\underline{\rho})\,\mathrm{d}\underline{s} = \sum_{k=1}^{N_{\mathrm{modes}}} \left[a_\mu^{(k)} - b_\mu^{(k)}\right] \sqrt{Y_{\infty,\mu}^{(k)}} \int_{\gamma^{(k)}} h_{x,k}^{(k)}(\underline{\rho})\, h_{x,\nu}^{(k)}(\underline{\rho})\,\mathrm{d}\underline{s}$$

This equation must be satisfied $\forall\nu$, where $\nu \in [0, N_{\mathrm{modes}}]$. It is part of the final system; as a matter of fact, it permits to define two Galerkin coefficients, which must be evaluated by numerical integration. In fact, this equation may be written as follows

$$\underline{\underline{C}}^{(k)} = \underline{\underline{D}}^{(k)} \sqrt{Y_{\infty,\mu}^{(k)}} \left(\underline{a}^{(k)} - \underline{b}^{(k)}\right) \tag{3.38}$$

where each element of $\underline{\underline{C}}$ matrix can be written as

$$C_{\nu s}^{(k)} = \int_{\gamma^{(k)}} u_s(\underline{\rho})\, h_{x,\nu}^{(k)}(\underline{\rho})\, \mathrm{d}\underline{s} = \int_0^{b^{(k)}} u_s(y, z_{\mathrm{wg}^{(k)}}) h_{x,\nu}^{(k)}(y)\, \mathrm{d}y \tag{3.39}$$

where $z = z_{\mathrm{wg}^{(k)}}$ represents the z-section of the k-th port of the device, in the global reference system.

A similar procedure can be carried out about the $\underline{\underline{D}}$ matrix; in fact,

$$D_{\nu k}^{(k)} = \int_{\gamma^{(k)}} h_{x,k}^{(k)}\, h_{x,\nu}^{(k)}\, \mathrm{d}\underline{s} \tag{3.40}$$

$$= \int_0^{b^{(k)}} h_{x,k}^{(k)}(y) h_{x,\nu}^{(k)}(y)\, \mathrm{d}y \tag{3.41}$$

These equations must be enforced in the system $\forall k = 1$ to N_{ports}.

3.4.2 Helmholtz equation

The second equation which must be represented as a linear system is the Helmholtz equation, written in weak form and modifying by applying the Green's theorem. So, it is necessary to start from

$$\iint_{\Sigma} (\nabla_{\mathrm{t}}\phi) \cdot (\nabla_{\mathrm{t}} v_\beta)\, \mathrm{d}\Sigma - k^2 \iint_{\Sigma} \phi\, v_\beta\, \mathrm{d}\Sigma = \sum_{k=1}^{N_{\mathrm{ports}}} \int_{\gamma_{\mathrm{wg}}^{(k)}} \frac{\partial \phi_{\mathrm{wg}}^{(k)}}{\partial n}\, v_\beta\, \mathrm{d}\underline{s}$$

It is possible to identify three contributions:

- the stiffness matrix integral;
- the mass matrix integral;
- line integrals.

About the stiffness matrix, it is possible to expand the integral

$$\iint_{\Sigma} (\nabla_{\mathrm{t}}\phi) \cdot (\nabla_{\mathrm{t}} v_\beta)\, \mathrm{d}\Sigma = \sum_{s=1}^{N_{\mathrm{fun}}} x_s \iint_{\Sigma} (\nabla_{\mathrm{t}} u_s(y,z)) \cdot (\nabla_{\mathrm{t}} v_\beta(y,z)) \mathrm{d}\Sigma$$

but, since this is a Galerkin method,

$$u_s(y,z) = v_\beta(y,z)$$

expansion and test functions are equal; therefore, the elements of the stiffness matrix in the global basis $\{u_s\}$ can be written as

$$ {}^{(\underline{u})}K_{\beta s} = \iint_{\Sigma} (\nabla_{\mathrm{t}} u_s(y,z)) \cdot (\nabla_{\mathrm{t}} u_\beta(y,z)) \mathrm{d}\Sigma $$

about the generic mass matrix element, it is possible to obtain, with the same procedure,

$$ {}^{(\underline{u})}M_{\beta s} = \iint_{\Sigma} u_s(y,z) u_\beta(y,z) \mathrm{d}\Sigma $$

Finally, it is necessary to write the line integral contribution as an integral on an interval. So,

$$ \int_{\gamma_{\mathrm{wg}}^{(k)}} \frac{\partial \phi_{\mathrm{wg}}^{(k)}}{\partial n} v_\beta \, \mathrm{d}\underline{s} = - \int_{\gamma_{\mathrm{wg}}^{(k)}} \frac{\partial \phi_{\mathrm{wg}}^{(k)}}{\partial z} v_\beta \, \mathrm{d}\underline{s} $$

From (3.17) and (3.18)

$$ \begin{aligned} \frac{\partial E_{x,\mathrm{wg}}^{(k)}}{\partial z} &= \sum_{\mu=0}^{\infty} \sqrt{Z_{\infty,\mu}^{(k)}} \, \mathrm{j}\beta_\mu^{(k)} \left[-a_\mu^{(k)} + b_\mu^{(k)} \right] e_{x,\mu}^{(k)}(\underline{\rho}) \\ \frac{\partial H_{x,\mathrm{wg}}^{(k)}}{\partial z} &= \sum_{\mu=0}^{\infty} \sqrt{Y_{\infty,\mu}^{(k)}} \, \mathrm{j}\beta_\mu^{(k)} \left[-a_\mu^{(k)} - b_\mu^{(k)} \right] h_{x,\mu}^{(k)}(\underline{\rho}) \end{aligned} $$

so, by substituting in the line integral,

$$ \int_{\gamma_{\mathrm{wg}}^{(k)}} \frac{\partial \phi_{\mathrm{wg}}^{(k)}}{\partial n} v_\beta \, \mathrm{d}\underline{s} = + \sum_{k=1}^{N_{\mathrm{modes}}} \mathrm{j}\beta_\mu^{(k)} \sqrt{Y_{\infty,\mu}^{(k)}} \left[a_\mu^{(k)} + b_\mu^{(k)} \right] \int_0^{b^{(k)}} h_{x,\mu} u_\beta(y, z_{\mathrm{wg}^{(k)}}) \mathrm{d}y $$

finally, it is possible to obtain

$$ \underline{\underline{B}}^{(k)} = \int_0^{b^{(k)}} h_{x,\mu} u_\beta(y, z_{\mathrm{wg}^{(k)}}) \mathrm{d}y $$

This equation must be satisfied for each k-th port.

To sum up, the system which must be solved in order to find the $\underline{x}$ vector of Galerkin method coefficients is

$$ \begin{aligned} \left({}^{(\underline{u})}\underline{\underline{K}} - k^2 \, {}^{(\underline{u})}\underline{\underline{M}} \right) \underline{x} &= \sum_{k=1}^{N_{\mathrm{ports}}} \underline{\underline{B}}^{(k)} \left(\underline{a}^{(k)} - w \underline{b}^{(k)} \right) \\ \underline{\underline{C}}^{(k)} \, \underline{x} &= \underline{\underline{D}}^{(k)} \left(\underline{a}^{(k)} + w \underline{b}^{(k)} \right) \\ \forall k = 1, 2, \ldots N_{\mathrm{ports}} & \end{aligned} \tag{3.42} $$

3.4.3 Determination of the scattering matrix by means of a reduced-order model

The final step for the formulation of the model of a E-plane or H-plane device is the determination of the scattering matrix of the device that defines the relationship between the scattered waves $\underline{b}$ and incident waves $\underline{a}$. Once the behavior of each device is known, the whole electromagnetic system can be modeled through the cascade of the corresponding scattering matrices.

The model must be valid in a wide range of frequencies; the way to obtain this is the evaluation of the solution of the system (3.42) in a small set of frequency points, collect the solutions and then apply an SVD decomposition in order to find a model with reduced order which can be used in a range of frequencies, instead of at a single frequency point. Considering for hypothesis that the following system is already processed, it is possible to modify these expressions in order to find the scattering matrix from known matrices.

$$\begin{aligned}\left({}^{(u)}\underline{\underline{\tilde{K}}} - k^2\underline{\underline{I}}\right)\underline{x} &= \sum_{k=1}^{N_{\text{ports}}} \underline{\underline{\tilde{B}}}^{(k)}\left(\underline{a}^{(k)} - w\underline{b}^{(k)}\right)\\ \underline{\underline{\tilde{C}}}^{(k)}\underline{x} &= \underline{\underline{\tilde{D}}}^{(k)}\left(\underline{a}^{(k)} + w\underline{b}^{(k)}\right)\\ \forall k = 1, 2, \ldots N_{\text{ports}}\end{aligned} \tag{3.43}$$

this system is slightly different from (3.42); as a matter of fact, the mass matrix is replaced with $\underline{\underline{I}}$, which is the identity matrix (of appropriate dimension). In fact, after the application of the SVD process, the basis functions are orthonormal.

From the second equation of (3.43), it is possible to find $\underline{b}^{(k)}$; so

$$\begin{aligned}\underline{b}^{(k)} &= w(\underline{\underline{\tilde{D}}}^{(k)})^{-1}\left[\underline{\underline{\tilde{C}}}^{(k)}\underline{x} - \underline{\underline{\tilde{D}}}^{(k)}\underline{a}^{(k)}\right] =\\ &= w(\underline{\underline{\tilde{D}}}^{(k)})^{-1}\underline{\underline{\tilde{C}}}^{(k)}\underline{x} - w\underline{\underline{I}}\,\underline{a}^{(k)}\end{aligned} \tag{3.44}$$

Now, the expression of $\underline{b}^{(k)}$ can be substituted in the first equation of (3.43), in order to find the unknown $\underline{x}$. So

$$\left({}^{(u)}\underline{\underline{\tilde{K}}} - k^2\underline{\underline{I}}\right)\underline{x} = \sum_{k=1}^{N_{\text{ports}}} \underline{\underline{\tilde{B}}}^{(k)}\underline{a}^{(k)} - \sum_{k=1}^{N_{\text{ports}}} \underline{\underline{\tilde{B}}}^{(k)}\underline{\underline{\tilde{D}}}^{(k)}\underline{\underline{\tilde{C}}}^{(k)}\underline{x} + \sum_{k=1}^{N_{\text{ports}}} \underline{\underline{\tilde{B}}}^{(k)}\underline{a}^{(k)}$$

because $w^2 = 1$, for both $w = \pm 1$ cases. So, by bringing each term which multiplies $\underline{x}$ at first term, it is possible to find

$$\left({}^{(u)}\underline{\underline{\tilde{K}}} - k^2\underline{\underline{I}} + \sum_{k=1}^{N_{\text{ports}}} \underline{\underline{\tilde{B}}}^{(k)}\underline{\underline{\tilde{D}}}^{(k)}\underline{\underline{\tilde{C}}}^{(k)}\right)\underline{x} = 2\sum_{k=1}^{N_{\text{ports}}} \underline{\underline{\tilde{B}}}^{(k)}\underline{a}^{(k)}$$

and by defining $\underline{\underline{\tilde{A}}}$ the matrix

$$\underline{\underline{\tilde{A}}} \triangleq {}^{(\underline{u})}\underline{\underline{\tilde{K}}} - k^2\underline{\underline{I}} + \sum_{k=1}^{N_{\text{ports}}} \underline{\underline{\tilde{B}}}^{(k)}\underline{\underline{\tilde{D}}}^{(k)}\underline{\underline{\tilde{C}}}^{(k)}$$

it is possible to find $\underline{x}$ as

$$\underline{x} = 2\sum_{k=1}^{N_{\text{ports}}} \underline{\underline{\tilde{A}}}^{-1}\underline{\underline{\tilde{B}}}^{(k)}\underline{a}^{(k)}$$

In order to evaluate $\underline{x}$ it is necessary to sum each contribution at each port. On the other hand, (3.44) is valid for a particular l-th port. Therefore, it is possible to write (3.44) as relative to the l-th port

$$\underline{b}^{(l)} = w(\underline{\underline{\tilde{D}}}^{(l)})^{-1}\underline{\underline{\tilde{C}}}^{(l)}\underline{x} - w\underline{\underline{I}}\,\underline{a}^{(l)}$$

where, by substituting $\underline{x}$, it is possible to find

$$\underline{b}^{(l)} = w(\underline{\underline{\tilde{D}}}^{(l)})^{-1}\underline{\underline{\tilde{C}}}^{(l)}\sum_{k=1}^{N_{\text{ports}}} 2\underline{\underline{\tilde{A}}}^{-1}\underline{\underline{\tilde{B}}}^{(k)}\underline{a}^{(k)} - w\underline{\underline{I}}\,\underline{a}^{(l)}$$

This expression has two kind of contributions: the one from the l-th port and the one from the other ports. So, this expression can be re-written emphasizing this fact

$$\underline{b}^{(l)} = \left[-w\underline{\underline{I}} + 2w(\underline{\underline{\tilde{D}}}^{(l)})^{-1}\underline{\underline{\tilde{C}}}^{(l)}\underline{\underline{\tilde{A}}}^{-1}\underline{\underline{\tilde{B}}}^{(l)}\right]\underline{a}^{(l)} + \\ + \sum_{\substack{k=1\\k\neq l}}^{N_{\text{ports}}} 2w(\underline{\underline{\tilde{D}}}^{(k)})^{-1}\underline{\underline{\tilde{C}}}^{(k)}\underline{\underline{\tilde{A}}}^{-1}\underline{\underline{\tilde{B}}}^{(k)}\underline{a}^{(k)}$$

From this expression, the determination of the scattering matrix between the l-th port and the i-th port is straightforward. In fact, the relationship between the l-th scattered wave and the l-th incident wave is

$$\underline{\underline{S}}^{(l,i)} = \begin{cases} w\left[2(\underline{\underline{\tilde{D}}}^{(i)})^{-1}\underline{\underline{\tilde{C}}}^{(i)}\underline{\underline{\tilde{A}}}^{-1}\underline{\underline{\tilde{B}}}^{(i)} - \underline{\underline{I}}\right], & \text{if } i = l \\ 2w(\underline{\underline{\tilde{D}}}^{(i)})^{-1}\underline{\underline{\tilde{C}}}^{(i)}\underline{\underline{\tilde{A}}}^{-1}\underline{\underline{\tilde{B}}}^{(i)}, & \text{if } i \neq l \end{cases}$$

therefore, it is possible to resume these cases in a single equation, using the Kronecker delta symbol

$$\underline{\underline{S}}^{(l,i)} = w\left[2(\underline{\underline{\tilde{D}}}^{(i)})^{-1}\underline{\underline{\tilde{C}}}^{(i)}\underline{\underline{\tilde{A}}}^{-1}\underline{\underline{\tilde{B}}}^{(i)} - \delta_{li}\underline{\underline{I}}\right]$$

CHAPTER 4

Analysis of devices with cylindrical symmetry

4.1 Introduction

In this chapter we address the problem of the computation of the scattering matrix of a two-port device with cylindrical symmetry, as the one sketched in Figure 4.1, consisting of two cylindrical-to-conical junction. The formulation is derived for devices filled with homogeneous permeability and permittivity. Indeed, this is the case of interest for microwave and millimeter wave devices aimed at satellite communications and scientific instrumentation. Just like in the previous chapter, the numerical method for the solution of the problem is based on a SEM scheme, considering the presence of edges by building basis functions which keep into account Meixner conditions. The main difference of this case with respect to the previous one is the type of symmetry of the structure; as a matter of fact, in this case the structure is invariant to the azimuthal angle φ, while in the previous case the invariance was with respect to a cartesian coordinate.

The first step of the procedure is the determination of all the electromagnetic field components as functions of E_φ and H_φ; these two components are both present in the formulation, and they are the ones which are expanded in order to formulate a Galerkin-based method. Then, boundary conditions are applied, and finally the numerical system which has as unknowns the vector of Galerkin coefficients is written.

4.2 Determination of electromagnetic field components

The formulation of the problem starts from Maxwell's equations, expressed in frequency domain;

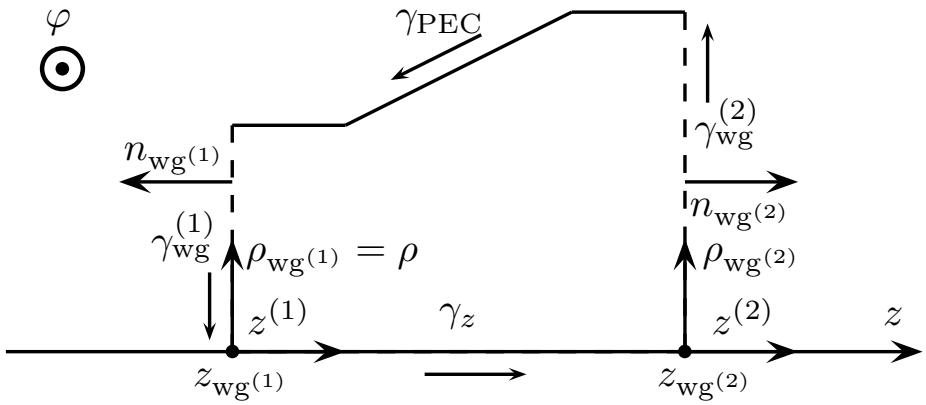

Figure 4.1: 2-D view of the connection of two circular waveguides through a conical section.

$$\begin{cases} \nabla \times \underline{E} = -\mathrm{j}\omega\mu\underline{H} \\ \nabla \times \underline{H} = \mathrm{j}\omega\epsilon\underline{E} \end{cases} \tag{4.1}$$

remembering that

$$\begin{aligned} k &= \omega\sqrt{\mu\epsilon} \\ Y &= \sqrt{\frac{\epsilon}{\mu}} = \frac{1}{Z} \end{aligned} \tag{4.2}$$

The first step for the solution of this problem is to express electric and magnetic fields components as functions of E_φ and H_φ, in order to solve the problem in φ first, and then to find all the other components.

Since this problem concerns the study of a structure with a circular transversal section with respect to z direction, it is necessary to write the curl operator in the cylindrical coordinate system, as follows

$$\nabla \times \underline{A} = \hat{\rho}\left(\frac{1}{\rho}\frac{\partial A_z}{\partial \varphi} - \frac{\partial A_\varphi}{\partial z}\right) + \hat{\varphi}\left(\frac{\partial A_\rho}{\partial z} - \frac{\partial A_z}{\partial \rho}\right) + \hat{\mathrm{z}}\frac{1}{\rho}\left(\frac{\partial(\rho A_\varphi)}{\partial \rho} - \frac{\partial A_\rho}{\partial \varphi}\right) \tag{4.3}$$

Using this last relation, it is necessary to write by components equations (4.1); the result is, for the first equation,

$$\begin{aligned} &\frac{1}{\rho}\frac{\partial E_z}{\partial \varphi} - \frac{\partial E_\varphi}{\partial z} = -\mathrm{j}\omega\mu H_\rho \\ &\frac{\partial E_\rho}{\partial z} - \frac{\partial E_z}{\partial \rho} = -\mathrm{j}\omega\mu H_\varphi \\ &\frac{1}{\rho}\left(\frac{\partial(\rho E_\varphi)}{\partial \rho} - \frac{\partial E_\rho}{\partial \varphi}\right) = -\mathrm{j}\omega\mu H_z \end{aligned}$$

while, for the second equation,

$$\frac{1}{\rho}\frac{\partial H_z}{\partial \varphi} - \frac{\partial H_\varphi}{\partial z} = \mathrm{j}\omega\epsilon E_\rho$$
$$\frac{\partial H_\rho}{\partial z} - \frac{\partial H_z}{\partial \rho} = \mathrm{j}\omega\epsilon E_\varphi$$
$$\frac{1}{\rho}\left(\frac{\partial(\rho H_\varphi)}{\partial \rho} - \frac{\partial H_\rho}{\partial \varphi}\right) = \mathrm{j}\omega\epsilon E_z$$

Recognized the invariance to φ, the dependance of the electromagnetic field on φ can be assumed to be

$$\mathrm{e}^{\mathrm{j}m\varphi}$$

so, it is possible to represent spectrally the dependence in φ by applying the spatial Fourier transform on the φ variable. In other words,

$$\frac{\mathrm{d}}{\mathrm{d}\varphi}\mathrm{e}^{\mathrm{j}m\varphi} = \mathrm{j}m\,\mathrm{e}^{\mathrm{j}m\varphi} \Longrightarrow \frac{\mathrm{d}}{\mathrm{d}\varphi} \longleftrightarrow \mathrm{j}m.$$

By performing this substitution on previous equations, it is possible to obtain

$$\frac{1}{\rho}\mathrm{j}mE_z - \frac{\partial E_\varphi}{\partial z} = -\mathrm{j}\omega\mu H_\rho \tag{4.4}$$
$$\frac{\partial E_\rho}{\partial z} - \frac{\partial E_z}{\partial \rho} = -\mathrm{j}\omega\mu H_\varphi \tag{4.5}$$
$$\frac{1}{\rho}\left(\frac{\partial(\rho E_\varphi)}{\partial \rho} - \mathrm{j}mE_\rho\right) = -\mathrm{j}\omega\mu H_z \tag{4.6}$$

and

$$\frac{1}{\rho}\mathrm{j}mH_z - \frac{\partial H_\varphi}{\partial z} = \mathrm{j}\omega\epsilon E_\rho \tag{4.7}$$
$$\frac{\partial H_\rho}{\partial z} - \frac{\partial H_z}{\partial \rho} = \mathrm{j}\omega\epsilon E_\varphi \tag{4.8}$$
$$\frac{1}{\rho}\left(\frac{\partial(\rho H_\varphi)}{\partial \rho} - \mathrm{j}mH_\rho\right) = \mathrm{j}\omega\epsilon E_z \tag{4.9}$$

The following step is the determination of the relationships between the φ components of the electromagnetic field and the other ones. From (4.9),

$$E_z = \frac{1}{\mathrm{j}\omega\epsilon}\frac{1}{\rho}\left(\frac{\partial(\rho H_\varphi)}{\partial \rho} - \mathrm{j}mH_\rho\right).$$

By substituting it in (4.4),

$$\frac{\mathrm{j}m}{\rho}\left\{\frac{1}{\mathrm{j}\omega\epsilon}\frac{1}{\rho}\left[\frac{\partial(\rho H_\varphi)}{\partial \rho} - \mathrm{j}mH_\rho\right]\right\} - \frac{\partial E_\varphi}{\partial z} = -\mathrm{j}\omega\mu H_\rho$$

then, it is necessary to re-arrange this formula and to simplify it as

$$-\mathrm{j}\omega\mu H_\rho = \frac{m}{\rho^2}\frac{1}{\omega\epsilon}\frac{\partial(\rho H_\varphi)}{\partial\rho} - \mathrm{j}\frac{m^2}{\rho^2\omega\epsilon}H_\rho - \frac{\partial E_\varphi}{\partial z}$$

i.e.

$$\frac{m}{\rho^2}\frac{1}{\omega\epsilon}\frac{\partial(\rho H_\varphi)}{\partial\rho} - \frac{\partial E_\varphi}{\partial z} = \frac{\mathrm{j}}{\omega\epsilon}\left(\frac{m^2}{\rho^2} - \omega^2\epsilon\mu\right)H_\rho$$

Now, considering the fact that

$$Yk = \sqrt{\frac{\epsilon}{\mu}}\omega\sqrt{\epsilon\mu} = \omega\epsilon$$

it is possible to write the H_ρ component as follows

$$\begin{aligned} H_\rho &= -\frac{\mathrm{j}\omega\epsilon}{\frac{m^2}{\rho^2} - k^2}\left(\frac{m}{\rho^2\omega\epsilon}\frac{\partial(\rho H_\varphi)}{\partial\rho} - \frac{\partial E_\varphi}{\partial z}\right) = \\ &= -\frac{\mathrm{j}}{m^2 - k^2\rho^2}\left(m\frac{\partial(\rho H_\varphi)}{\partial\rho} - kY\rho^2\frac{\partial E_\varphi}{\partial z}\right) \end{aligned} \tag{4.10}$$

Now, it is necessary to repeat the previous procedure, substituting (4.7) in (4.6),

$$E_\rho = \frac{1}{\mathrm{j}\omega\epsilon}\left(\frac{\mathrm{j}m}{\rho}H_z - \frac{\partial H_\varphi}{\partial z}\right)$$

in (4.6):

$$\frac{1}{\rho}\left\{\frac{\partial(\rho E_\varphi)}{\partial\rho} - \mathrm{j}m\left[\frac{1}{\mathrm{j}\omega\epsilon}\left(\frac{\mathrm{j}m}{\rho}H_z - \frac{\partial H_\varphi}{\partial z}\right)\right]\right\} = -\mathrm{j}\omega\mu H_z$$

Then, follow some re-organizations:

$$-\mathrm{j}\omega\mu H_z = \frac{1}{\rho}\frac{\partial(\rho E_\varphi)}{\partial\rho} - \frac{\mathrm{j}m}{\rho}\frac{1}{\mathrm{j}\omega\epsilon}\left(\frac{1}{\rho}\mathrm{j}mH_z - \frac{\partial H_\varphi}{\partial z}\right)$$

$$\omega\epsilon\rho\frac{\partial(\rho E_\varphi)}{\partial\rho} + \rho m\frac{\partial H_\varphi}{\partial z} = \mathrm{j}m^2H_z - \mathrm{j}\omega^2\mu\epsilon\rho^2H_z$$

so,

$$\mathrm{j}\left(m^2 - k^2\rho^2\right)H_z = \rho\omega\epsilon\frac{\partial(\rho E_\varphi)}{\partial\rho} + m\rho\frac{\partial H_\varphi}{\partial z}$$

then, finally,

$$H_z = -\frac{\mathrm{j}}{m^2 - k^2\rho^2}\left(kY\rho\frac{\partial(\rho E_\varphi)}{\partial\rho} + m\rho\frac{\partial H_\varphi}{\partial z}\right) \tag{4.11}$$

Every term of the right-hand side member of this equation is multiplied by ρ. This means that, for $\rho = 0$, the magnetic field component H_z equals zero. This result will be useful later.

Now, starting from a modified version of (4.6),

$$H_z = -\frac{1}{\mathrm{j}\omega\mu\rho}\left(\frac{\partial(\rho E_\varphi)}{\partial\rho} - \mathrm{j}mE_\rho\right)$$

and substituting it in (4.7), the result is

$$\frac{\mathrm{j}m}{\rho}\left[-\frac{1}{\mathrm{j}\omega\mu\rho}\left(\frac{\partial(\rho E_\varphi)}{\partial\rho} - \mathrm{j}mE_\rho\right)\right] - \frac{\partial H_\varphi}{\partial z} = \mathrm{j}\omega\epsilon E_\rho$$

then, it has to be manipulated:

$$-\frac{m}{\omega\mu}\frac{1}{\rho^2}\frac{\partial(\rho E_\varphi)}{\partial\rho} + \mathrm{j}\frac{m^2}{\omega\mu}\frac{1}{\rho^2}E_\rho - \frac{\partial H_\varphi}{\partial z} = \mathrm{j}\omega\epsilon E_\rho$$

so,

$$E_\rho\left(\mathrm{j}\omega\epsilon - \mathrm{j}\frac{m^2}{\omega\mu}\frac{1}{\rho^2}\right) = -\frac{m}{\omega\mu}\frac{1}{\rho^2}\frac{\partial(\rho E_\varphi)}{\partial\rho} - \frac{\partial H_\varphi}{\partial z}$$

$$-\frac{m}{\omega\mu}\frac{\partial(\rho E_\varphi)}{\partial\rho} - \rho^2\frac{\partial H_\varphi}{\partial z} = \rho^2\frac{\mathrm{j}}{\omega\mu}\left(\omega^2\epsilon\mu - \frac{m^2}{\rho^2}\right)E_\rho$$

so,

$$-m\frac{\partial(\rho E_\varphi)}{\partial\rho} - \rho^2 kZ\frac{\partial H_\varphi}{\partial z} = -\mathrm{j}\left(m^2 - k^2\rho^2\right)E_\rho$$

finally,

$$E_\rho = -\frac{\mathrm{j}}{m^2 - k^2\rho^2}\left(m\frac{\partial(\rho E_\varphi)}{\partial\rho} + kZ\rho^2\frac{\partial H_\varphi}{\partial z}\right) \tag{4.12}$$

Then, the last component E_z, can be calculated as follows. Starting from (4.4),

$$H_\rho = -\frac{1}{\mathrm{j}\omega\mu}\left(\frac{1}{\rho}\mathrm{j}mE_z - \frac{\partial E_\varphi}{\partial z}\right)$$

it has to be substituted in (4.9);

$$\frac{1}{\rho}\left\{\frac{\partial(\rho H_\varphi)}{\partial\rho} - \mathrm{j}m\left[-\frac{1}{\mathrm{j}\omega\mu}\left(\frac{1}{\rho}\mathrm{j}mE_z - \frac{\partial E_\varphi}{\partial z}\right)\right]\right\} = \mathrm{j}\omega\epsilon E_z$$

therefore,

$$\frac{1}{\rho}\frac{\partial(\rho H_\varphi)}{\partial\rho} + \mathrm{j}\frac{m^2}{\omega\mu}\frac{1}{\rho^2}E_z - \frac{m}{\omega\mu}\frac{1}{\rho}\frac{\partial E_\varphi}{\partial z} = \mathrm{j}\omega\epsilon E_z$$

so,

$$\frac{\mathrm{j}}{\omega\mu\rho^2}\left(m^2 - k^2\rho^2\right)E_z = -\frac{1}{\rho}\frac{\partial(\rho H_\varphi)}{\partial\rho} + \frac{m}{\omega\mu\rho}\frac{\partial E_\varphi}{\partial z}$$

and, finally,

$$E_z = -\frac{\mathrm{j}}{m^2 - k^2\rho^2}\left(m\rho\frac{\partial E_\varphi}{\partial z} - kZ\rho\frac{\partial(\rho H_\varphi)}{\partial\rho}\right) \tag{4.13}$$

Just like H_z, also E_z equals zero for $\rho = 0$ (i.e. in the z-axis).

Resume of electromagnetic field components

From the previous section it was possible to find four relationships between the derivatives of E_φ and H_φ, and all other components of the electromagnetic field. These results are summarized here.

$$E_\rho = -\frac{\mathrm{j}}{m^2 - k^2\rho^2}\left(m\frac{\partial(\rho E_\varphi)}{\partial\rho} + kZ\rho^2\frac{\partial H_\varphi}{\partial z}\right) \tag{4.14}$$

$$H_\rho = -\frac{\mathrm{j}}{m^2 - k^2\rho^2}\left(m\frac{\partial(\rho H_\varphi)}{\partial\rho} - kY\rho^2\frac{\partial E_\varphi}{\partial z}\right) \tag{4.15}$$

$$E_z = -\frac{\mathrm{j}}{m^2 - k^2\rho^2}\left(m\rho\frac{\partial E_\varphi}{\partial z} - kZ\rho\frac{\partial(\rho H_\varphi)}{\partial\rho}\right) \tag{4.16}$$

$$H_z = -\frac{\mathrm{j}}{m^2 - k^2\rho^2}\left(kY\rho\frac{\partial(\rho E_\varphi)}{\partial\rho} + m\rho\frac{\partial H_\varphi}{\partial z}\right) \tag{4.17}$$

4.2.1 Derivation of electromagnetic field components relationships

Although the two second-order equations in E_φ and H_φ only can be easily derived by inserting (4.14) - (4.17) in (4.5) - (4.8) respectively, it is convenient to shift differential operators from field components to test functions. To this end, there is a useful integral relation on vectors, proved in Appendix B.1.

$$\iint_\Sigma \left[\frac{\partial F_2}{\partial x} - \frac{\partial F_1}{\partial y}\right] v\,\mathrm{d}x\mathrm{d}y = -\iint_\Sigma \left[F_2\frac{\partial v}{\partial x} - F_1\frac{\partial v}{\partial y}\right]\mathrm{d}x\mathrm{d}y + \oint_\gamma (\underline{F}v)\cdot\mathrm{d}\underline{s} \tag{4.18}$$

The first step is to consider (4.5) and (4.8) and formulate them in weak form, by projecting them on two sets of test functions, $V^{(\mathrm{h})} = \left\{v_\beta^{(\mathrm{h})}\right\}$ and $V^{(\mathrm{e})} = \left\{v_\beta^{(\mathrm{e})}\right\}$ respectively. The projection operation involves the evaluation of integrals on the entire domain Σ, which is shown in Figure 4.1. Hence, (4.5) and (4.8) become

$$\iint_\Sigma \left[\frac{\partial E_\rho}{\partial z} - \frac{\partial E_z}{\partial\rho}\right] v_\beta^{(\mathrm{h})}\mathrm{d}\rho\mathrm{d}z = -\mathrm{j}\omega\mu\iint_\Sigma H_\varphi v_\beta^{(\mathrm{h})}\mathrm{d}\rho\mathrm{d}z,\ \forall v_\beta^{(\mathrm{h})} \in V^{(\mathrm{h})} \tag{4.19}$$

$$\iint_\Sigma \left[\frac{\partial H_\rho}{\partial z} - \frac{\partial H_z}{\partial\rho}\right] v_\beta^{(\mathrm{e})}\mathrm{d}\rho\mathrm{d}z = \mathrm{j}\omega\epsilon\iint_\Sigma E_\varphi v_\beta^{(\mathrm{e})}\mathrm{d}\rho\mathrm{d}z,\ \forall v_\beta^{(\mathrm{e})} \in V^{(\mathrm{e})} \tag{4.20}$$

Considering the following definitions,

$$\begin{cases} \underline{E}_\mathrm{t} \triangleq E_z\hat{\mathrm{z}} + E_\rho\hat{\rho} \\ \underline{H}_\mathrm{t} \triangleq H_z\hat{\mathrm{z}} + H_\rho\hat{\rho} \end{cases} \tag{4.21}$$

where $\underline{E}_\mathrm{t}$ and $\underline{H}_\mathrm{t}$ are field components transversal with respect to φ, the last two equations may be re-written applying (4.18) as follows

$$-\mathrm{j}kZ \iint_{\Sigma} H_{\varphi} v_{\beta}^{(\mathrm{h})} \mathrm{d}\rho\mathrm{d}z = -\iint_{\Sigma} \left[E_{\rho} \frac{\partial v_{\beta}^{(\mathrm{h})}}{\partial z} - E_{z} \frac{\partial v_{\beta}^{(\mathrm{h})}}{\partial \rho} \right] \mathrm{d}\rho\mathrm{d}z + \oint_{\gamma} \left[\underline{E}_{\mathrm{t}} v_{\beta}^{(\mathrm{h})} \right] \cdot \mathrm{d}\underline{s} \tag{4.22}$$

$$\mathrm{j}kY \iint_{\Sigma} E_{\varphi} v_{\beta}^{(\mathrm{e})} \mathrm{d}\rho\mathrm{d}z = -\iint_{\Sigma} \left[H_{\rho} \frac{\partial v_{\beta}^{(\mathrm{e})}}{\partial z} - H_{z} \frac{\partial v_{\beta}^{(\mathrm{e})}}{\partial \rho} \right] \mathrm{d}\rho\mathrm{d}z + \oint_{\gamma} \left[\underline{H}_{\mathrm{t}} v_{\beta}^{(\mathrm{e})} \right] \cdot \mathrm{d}\underline{s} \tag{4.23}$$

In the method of weighted residuals, the φ components of the electromagnetic field are written as series expansions, using two sets of functions, $\left\{ u_{\alpha}^{(\mathrm{e})} \right\}$ and $\left\{ u_{\alpha}^{(\mathrm{h})} \right\}$, as follows;

$$E_{\varphi} = \sum_{\alpha=0}^{\infty} c_{\alpha}^{(\mathrm{e})} u_{\alpha}^{(\mathrm{e})} \tag{4.24}$$

$$H_{\varphi} = \sum_{\alpha=0}^{\infty} c_{\alpha}^{(\mathrm{h})} u_{\alpha}^{(\mathrm{h})} \tag{4.25}$$

These two expansions now are substituted in (4.13) and (4.12), obtaining

$$E_{z} = -\frac{\mathrm{j}}{m^2 - k^2\rho^2} \left[m\rho \sum_{\alpha=0}^{\infty} c_{\alpha}^{(\mathrm{e})} \frac{\partial u_{\alpha}^{(\mathrm{e})}}{\partial z} - kZ\rho \sum_{\alpha=0}^{\infty} c_{\alpha}^{(\mathrm{h})} \frac{\partial (\rho u_{\alpha}^{(\mathrm{h})})}{\partial \rho} \right] \tag{4.26}$$

$$E_{\rho} = -\frac{\mathrm{j}}{m^2 - k^2\rho^2} \left[m \sum_{\alpha=0}^{\infty} c_{\alpha}^{(\mathrm{e})} \frac{\partial (\rho u_{\alpha}^{(\mathrm{e})})}{\partial \rho} + kZ\rho^2 \sum_{\alpha=0}^{\infty} c_{\alpha}^{(\mathrm{h})} \frac{\partial u_{\alpha}^{(\mathrm{h})}}{\partial z} \right] \tag{4.27}$$

Then, (4.22) can be re-written using the expansion for the φ components, and substituting (4.26) and (4.27):

$$\begin{aligned}
-\mathrm{j}kZ \sum_{\alpha=0}^{\infty} c_{\alpha}^{(\mathrm{h})} \iint_{\Sigma} u_{\alpha}^{(\mathrm{h})} v_{\beta}^{(\mathrm{h})} \mathrm{d}\rho\mathrm{d}z = {} & \sum_{\alpha=0}^{\infty} c_{\alpha}^{(\mathrm{e})} \iint_{\Sigma} \frac{\mathrm{j}m}{m^2 - k^2\rho^2} \frac{\partial (\rho u_{\alpha}^{(\mathrm{e})})}{\partial \rho} \frac{\partial v_{\beta}^{(\mathrm{h})}}{\partial z} \mathrm{d}\rho\mathrm{d}z + \\
& + \sum_{\alpha=0}^{\infty} c_{\alpha}^{(\mathrm{h})} \iint_{\Sigma} \frac{\mathrm{j}kZ\rho^2}{m^2 - k^2\rho^2} \frac{\partial u_{\alpha}^{(\mathrm{h})}}{\partial z} \frac{\partial v_{\beta}^{(\mathrm{h})}}{\partial z} \mathrm{d}\rho\mathrm{d}z + \\
& - \sum_{\alpha=0}^{\infty} c_{\alpha}^{(\mathrm{e})} \iint_{\Sigma} \frac{\mathrm{j}m\rho}{m^2 - k^2\rho^2} \frac{\partial u_{\alpha}^{(\mathrm{e})}}{\partial z} \frac{\partial v_{\beta}^{(\mathrm{h})}}{\partial \rho} \mathrm{d}\rho\mathrm{d}z + \\
& + \sum_{\alpha=0}^{\infty} c_{\alpha}^{(\mathrm{h})} \iint_{\Sigma} \frac{\mathrm{j}kZ\rho}{m^2 - k^2\rho^2} \frac{\partial (\rho u_{\alpha}^{(\mathrm{h})})}{\partial \rho} \frac{\partial v_{\beta}^{(\mathrm{h})}}{\partial \rho} \mathrm{d}\rho\mathrm{d}z + \\
& + \oint_{\gamma} \left[\underline{E}_{\mathrm{t}} v_{\beta}^{(\mathrm{h})} \right] \cdot \mathrm{d}\underline{s}
\end{aligned} \tag{4.28}$$

Re-organizing,

$$
\begin{aligned}
&-\mathrm{j}kZ\sum_{\alpha=0}^{\infty}c_{\alpha}^{(\mathrm{h})}\iint_{\Sigma}u_{\alpha}^{(\mathrm{h})}v_{\beta}^{(\mathrm{h})}\mathrm{d}\rho\mathrm{d}z=\\
&=\sum_{\alpha=0}^{\infty}c_{\alpha}^{(\mathrm{h})}\iint_{\Sigma}\left\{\frac{\mathrm{j}kZ}{m^2-k^2\rho^2}\rho\left[\rho\frac{\partial u_{\alpha}^{(\mathrm{h})}}{\partial z}\frac{\partial v_{\beta}^{(\mathrm{h})}}{\partial z}+\frac{\partial(\rho u_{\alpha}^{(\mathrm{h})})}{\partial\rho}\frac{\partial v_{\beta}^{(\mathrm{h})}}{\partial\rho}\right]\right\}\mathrm{d}\rho\mathrm{d}z+\\
&+\sum_{\alpha=0}^{\infty}c_{\alpha}^{(\mathrm{e})}\iint_{\Sigma}\left\{\frac{\mathrm{j}m}{m^2-k^2\rho^2}\left[\frac{\partial(\rho u_{\alpha}^{(\mathrm{e})})}{\mathrm{d}\rho}\frac{\partial v_{\beta}^{(\mathrm{h})}}{\partial z}-\rho\frac{\partial u_{\alpha}^{(\mathrm{e})}}{\partial z}\frac{\partial v_{\beta}^{(\mathrm{h})}}{\partial\rho}\right]\right\}\mathrm{d}\rho\mathrm{d}z+\\
&+\oint_{\gamma}\left[\underline{E}_{\mathrm{t}}v_{\beta}^{(\mathrm{h})}\right]\cdot\mathrm{d}\underline{s}
\end{aligned}
\tag{4.29}
$$

Now, the same procedure is repeated with equations (4.23), (4.10), (4.11); more in details:

$$
H_{\rho}=-\frac{\mathrm{j}}{m^2-k^2\rho^2}\left[m\sum_{\alpha=0}^{\infty}c_{\alpha}^{(\mathrm{h})}\frac{\partial(\rho u_{\alpha}^{(\mathrm{h})})}{\partial\rho}-kY\rho^2\sum_{\alpha=0}^{\infty}c_{\alpha}^{(\mathrm{e})}\frac{\partial u_{\alpha}^{(\mathrm{e})}}{\partial z}\right]
\tag{4.30}
$$

$$
H_{z}=-\frac{\mathrm{j}}{m^2-k^2\rho^2}\left[kY\rho\sum_{m=0}^{\infty}c_{\alpha}^{(\mathrm{e})}\frac{\partial(\rho u_{\alpha}^{(\mathrm{e})})}{\partial\rho}+m\rho\sum_{m=0}^{\infty}c_{\alpha}^{(\mathrm{h})}\frac{\partial u_{\alpha}^{(\mathrm{h})}}{\partial z}\right]
\tag{4.31}
$$

so, substituting these equations in (4.23), the result is

$$
\begin{aligned}
\mathrm{j}kY\sum_{\alpha=0}^{\infty}c_{\alpha}^{(\mathrm{e})}\iint_{\Sigma}u_{\alpha}^{(\mathrm{e})}v_{\beta}^{(\mathrm{e})}\mathrm{d}\rho\mathrm{d}z=&\sum_{\alpha=0}^{\infty}c_{\alpha}^{(\mathrm{h})}\iint_{\Sigma}\frac{\mathrm{j}m}{m^2-k^2\rho^2}\frac{\partial(\rho u_{\alpha}^{(\mathrm{h})})}{\partial\rho}\frac{\partial v_{\beta}^{(\mathrm{e})}}{\partial z}\mathrm{d}\rho\mathrm{d}z+\\
&-\sum_{\alpha=0}^{\infty}c_{\alpha}^{(\mathrm{e})}\iint_{\Sigma}\frac{\mathrm{j}kY\rho^2}{m^2-k^2\rho^2}\frac{\partial u_{\alpha}^{(\mathrm{e})}}{\partial z}\frac{\partial v_{\beta}^{(\mathrm{e})}}{\partial z}\mathrm{d}\rho\mathrm{d}z+\\
&-\sum_{\alpha=0}^{\infty}c_{\alpha}^{(\mathrm{e})}\iint_{\Sigma}\frac{\mathrm{j}kY\rho}{m^2-k^2\rho^2}\frac{\partial(\rho u_{\alpha}^{(\mathrm{e})})}{\partial\rho}\frac{\partial v_{\beta}^{(\mathrm{e})}}{\partial\rho}\mathrm{d}\rho\mathrm{d}z+\\
&-\sum_{\alpha=0}^{\infty}c_{\alpha}^{(\mathrm{h})}\iint_{\Sigma}\frac{\mathrm{j}m\rho}{m^2-k^2\rho^2}\frac{\partial u_{\alpha}^{(\mathrm{h})}}{\partial z}\frac{\partial v_{\beta}^{(\mathrm{e})}}{\partial\rho}\mathrm{d}\rho\mathrm{d}z+\\
&+\oint_{\gamma}\left[\underline{H}_{\mathrm{t}}v_{\beta}^{(\mathrm{e})}\right]\cdot\mathrm{d}\underline{s}
\end{aligned}
$$

Now, re-arraging,

$$
\begin{aligned}
&\mathrm{j}kY \sum_{\alpha=0}^{\infty} c_{\alpha}^{(\mathrm{e})} \iint_{\Sigma} u_{\alpha}^{(\mathrm{e})} v_{\beta}^{(\mathrm{e})} \mathrm{d}\rho \mathrm{d}z = \\
&= \sum_{\alpha=0}^{\infty} c_{\alpha}^{(\mathrm{h})} \iint_{\Sigma} \left\{ \frac{\mathrm{j}m}{m^2 - k^2\rho^2} \left[\frac{\partial(\rho u_{\alpha}^{(\mathrm{h})})}{\partial\rho} \frac{\partial v_{\beta}^{(\mathrm{e})}}{\partial z} - \rho \frac{\partial u_{\alpha}^{(\mathrm{h})}}{\partial z} \frac{\partial v_{\beta}^{(\mathrm{e})}}{\partial\rho} \right] \right\} \mathrm{d}\rho \mathrm{d}z + \\
&+ \sum_{\alpha=0}^{\infty} c_{\alpha}^{(\mathrm{e})} \iint_{\Sigma} \left\{ \frac{-\mathrm{j}kY}{m^2 - k^2\rho^2} \rho \left[\rho \frac{\partial u_{\alpha}^{(\mathrm{e})}}{\partial z} \frac{\partial v_{\beta}^{(\mathrm{e})}}{\partial z} + \frac{\partial(\rho u_{\alpha}^{(\mathrm{e})})}{\partial\rho} \frac{\partial v_{\beta}^{(\mathrm{e})}}{\partial\rho} \right] \right\} \mathrm{d}\rho \mathrm{d}z + \\
&+ \oint_{\gamma} \left[\underline{H}_{\mathrm{t}} v_{\beta}^{(\mathrm{e})} \right] \cdot \mathrm{d}\underline{s}
\end{aligned}
\tag{4.32}
$$

4.2.2 Application of boundary conditions

The next step is the exploitation of the boundary conditions in the evaluation of the line integrals appeared in (4.29) and (4.32). More in details, those integrals may be simplified, enforcing boundary conditions and keeping into account some previous considerations. With reference to Figure 4.1, the boundary conditions are related to both the metal walls and the continuity of the tangential fields at each waveguide port. By assuming that the metal walls are made of perfect electrical conductor (PEC), the relevant boundary condition is

$$
\hat{\mathrm{n}} \times \underline{E} = 0 \tag{4.33}
$$

This means that the E_{φ} component of the electric field must equal zero, because it is entirely tangential to the surface of the device. Moreover, this equation requires that, given $\hat{s}$ the unit vector used for the representation of the curvilinear abscissa, the transversal electric field with respect to the φ direction projected on the curve is zero. So, given (4.21), it is possible to observe that $\hat{s}$ has no components on φ direction. So, the two boundary conditions which come from the first equation are

$$
E_{\varphi} = 0 \tag{4.34}
$$

$$
\underline{E}_{\mathrm{t}} \cdot \hat{s} = 0 \tag{4.35}
$$

First of all, it may be necessary to review some informations about contour integrals. Given a parametric curve $\underline{s}(t)$ with $t \in [t_a, t_b]$ parameter, considering the integration of a vector field $\underline{F}$ over the curve $\underline{s}(t)$, it is possible to write

$$
\int_C \underline{F}(\underline{s}) \cdot \mathrm{d}\underline{s} = \int_{t_a}^{t_b} \underline{F}\left(\underline{s}(t)\right) \cdot \underline{s}'(t) \mathrm{d}t \tag{4.36}
$$

With reference to Figure 4.1, γ is a curve composed by the access lines, connecting the structure with the input waveguide, the PEC walls and the z-axis. In other words:

$$\gamma = \gamma_{\mathrm{PEC}} \bigcup \gamma_{\mathrm{wg}}^{(1)} \bigcup \gamma_{\mathrm{wg}}^{(2)} \bigcup \gamma_z$$

so, it is possible to separate by inspection the line integral in four contributions, which are: the two access lines (ports), the z-axis and the PEC contour. Hence, the line integral in (4.29) becomes

$$\begin{aligned}\oint_C \left(\underline{E}_{\mathrm{t}} v_\beta^{(\mathrm{h})}\right) \cdot \mathrm{d}\underline{s} = &\int_{\gamma_z} \left[\underline{E}_{\mathrm{t}}\left(\underline{s}(t)\right) v_\beta^{(\mathrm{h})}\left(\underline{s}(t)\right)\right] \cdot \underline{s}'(t)\mathrm{d}t + \\ &+ \int_{\gamma_{\mathrm{wg}}^{(2)}} \left[\underline{E}_{\mathrm{t}}\left(\underline{s}(t)\right) v_\beta^{(\mathrm{h})}\left(\underline{s}(t)\right)\right] \cdot \underline{s}'(t)\mathrm{d}t + \\ &+ \int_{\gamma_{\mathrm{wg}}^{(1)}} \left[\underline{E}_{\mathrm{t}}\left(\underline{s}(t)\right) v_\beta^{(\mathrm{h})}\left(\underline{s}(t)\right)\right] \cdot \underline{s}'(t)\mathrm{d}t + \\ &+ \int_{\gamma_{\mathrm{PEC}}} \left[\underline{E}_{\mathrm{t}}\left(\underline{s}(t)\right) v_\beta^{(\mathrm{h})}\left(\underline{s}(t)\right)\right] \cdot \underline{s}'(t)\mathrm{d}t\end{aligned}$$

As far as the line integral along the z-axis is concerned, it has to be noted that

$$\begin{aligned}\underline{E}_{\mathrm{t}} \cdot \underline{s}'(t) = \underline{E}_{\mathrm{t}} \cdot \hat{\mathrm{z}} = \\ = E_z\end{aligned}$$

Since $E_z = 0$ for $\rho = 0$ (see (4.16)), this contribution equals zero.

The line integral relative to the PEC contribution is zero because of the boundary condition (4.35), i.e.

$$\underline{E}_{\mathrm{t}} \cdot \mathrm{d}\underline{s} = 0.$$

Furthermore, the electromagnetic field has to be continue at each port. This means that, for each k-th port,

$$\int_{\gamma_{\mathrm{wg}}^{(k)}} \left[\underline{E}_{\mathrm{t}}\left(\underline{s}(t)\right) v_\beta^{(\mathrm{h})}\left(\underline{s}(t)\right)\right] \cdot \underline{s}'(t)\mathrm{d}t = \int_{\gamma_{\mathrm{wg}}^{(k)}} \left[\underline{E}_{\mathrm{t,wg}}\left(\underline{s}(t)\right) v_\beta^{(\mathrm{h})}\left(\underline{s}(t)\right)\right] \cdot \underline{s}'(t)\mathrm{d}t$$

This satisfies some of the continuity boundary condition at the input ports; in addition, it will be necessary to enforce continuity of the E_φ component too. In conclusion:

$$\begin{aligned}\oint_C \left(\underline{E}_{\mathrm{t}} v_\beta^{(\mathrm{h})}\right) \cdot \mathrm{d}\underline{s} = &\int_{\gamma_{\mathrm{wg}}^{(1)}} \left[\underline{E}_{\mathrm{t,wg}}\left(\underline{s}(t)\right) v_\beta^{(\mathrm{h})}\left(\underline{s}(t)\right)\right] \cdot \underline{s}'(t)\mathrm{d}t + \\ &+ \int_{\gamma_{\mathrm{wg}}^{(2)}} \left[\underline{E}_{\mathrm{t,wg}}\left(\underline{s}(t)\right) v_\beta^{(\mathrm{h})}\left(\underline{s}(t)\right)\right] \cdot \underline{s}'(t)\mathrm{d}t\end{aligned} \tag{4.37}$$

About (4.32), most of considerations remain the same. First of all,

$$\oint_C \left(\underline{H}_{\mathrm{t}} v_\beta^{(\mathrm{e})}\right) \cdot \mathrm{d}\underline{s} = \int_{\gamma_z} \left[\underline{H}_{\mathrm{t}}\left(\underline{s}(t)\right) v_\beta^{(\mathrm{e})}\left(\underline{s}(t)\right)\right] \cdot \underline{s}'(t)\mathrm{d}t + \\ + \int_{\gamma_{\mathrm{wg}}^{(2)}} \left[\underline{H}_{\mathrm{t}}\left(\underline{s}(t)\right) v_\beta^{(\mathrm{e})}\left(\underline{s}(t)\right)\right] \cdot \underline{s}'(t)\mathrm{d}t + \\ + \int_{\gamma_{\mathrm{wg}}^{(1)}} \left[\underline{H}_{\mathrm{t}}\left(\underline{s}(t)\right) v_\beta^{(\mathrm{e})}\left(\underline{s}(t)\right)\right] \cdot \underline{s}'(t)\mathrm{d}t + \\ + \int_{\gamma_{\mathrm{PEC}}} \left[\underline{H}_{\mathrm{t}}\left(\underline{s}(t)\right) v_\beta^{(\mathrm{e})}\left(\underline{s}(t)\right)\right] \cdot \underline{s}'(t)\mathrm{d}t$$

On the basis of (4.17), the z-axis contribution equals zero in this case too; furthermore, just like in the previous case, it is necessary to enforce the continuity condition on each port; Hence:

$$\int_{\gamma_{\mathrm{wg}}^{(k)}} \left[\underline{H}_{\mathrm{t}}\left(\underline{s}(t)\right) v_\beta^{(\mathrm{e})}\left(\underline{s}(t)\right)\right] \cdot \underline{s}'(t)\mathrm{d}t = \int_{\gamma_{\mathrm{wg}}^{(k)}} \left[\underline{H}_{\mathrm{t,wg}}\left(\underline{s}(t)\right) v_\beta^{(\mathrm{e})}\left(\underline{s}(t)\right)\right] \cdot \underline{s}'(t)\mathrm{d}t$$

H_φ continuity has to be enforced explicitly in this case too.
There is one last consideration, about the PEC contribution;

$$\int_{\gamma_{\mathrm{PEC}}} \left[\underline{H}_{\mathrm{t}}\left(\underline{s}(t)\right) v_\beta^{(\mathrm{e})}\left(\underline{s}(t)\right)\right] \cdot \underline{s}'(t)\mathrm{d}t$$

The PEC condition does not enforce the behavior of the transversal magnetic field to equal zero. On the other hand, in the integral there are also the test functions $v_\beta^{(\mathrm{e})}$. However, in the Galerkin version of the method of the weighted residuals method used in this thesis, the test functions $v_\beta^{(\mathrm{e})}$ coincide with the functions $u_\alpha^{(\mathrm{e})}$ used for the expansion of E_φ. Since the latter are defined in order to satisfy themselves the PEC conditions, the integral equals zero. In conclusion,

$$\oint_C \left(\underline{H}_{\mathrm{t}} v_\beta^{(\mathrm{e})}\left(\underline{s}(t)\right)\right) \cdot \mathrm{d}\underline{s} = \int_{\gamma_{\mathrm{wg}}^{(1)}} \left[\underline{H}_{\mathrm{t}}\left(\underline{s}(t)\right) v_\beta^{(\mathrm{e})}\left(\underline{s}(t)\right)\right] \cdot \underline{s}'(t)\mathrm{d}t + \\ + \int_{\gamma_{\mathrm{wg}}^{(2)}} \left[\underline{H}_{\mathrm{t}}\left(\underline{s}(t)\right) v_\beta^{(\mathrm{e})}\left(\underline{s}(t)\right)\right] \cdot \underline{s}'(t)\mathrm{d}t \tag{4.38}$$

From (4.37) and (4.38) it is possible to observe that all non-vanishing contributions to the electric and magnetic transversal fields circuitation integrals are the ones defined on the device ports. The latter can be either circular or conical waveguide ports. For circular waveguide ports, $\underline{s}'(t)$ is parallel to $\hat{\rho}$ and, hence,

$$\int_{\gamma_{\mathrm{wg}}^{(1)}} \left[\underline{E}_{\mathrm{t,wg}}\left(\underline{s}(t)\right) v_\beta^{(\mathrm{h})}\left(\underline{s}(t)\right)\right] \cdot \underline{s}'(t)\mathrm{d}t = -\int_0^{\rho_{\mathrm{wg}}^{(1)}} E_{\rho,\mathrm{wg}}(\rho, z_{\mathrm{wg}^{(1)}}) v_\beta^{(\mathrm{h})}(\rho, z_{\mathrm{wg}^{(1)}})\mathrm{d}\rho \tag{4.39}$$

$$\int_{\gamma_{\mathrm{wg}}^{(1)}} \left[\underline{H}_{\mathrm{t,wg}}\left(\underline{s}(t)\right) v_{\beta}^{(\mathrm{e})}\left(\underline{s}(t)\right)\right] \cdot \underline{s}'(t)\mathrm{d}t = -\int_{0}^{\rho_{\mathrm{wg}}^{(1)}} H_{\rho,\mathrm{wg}}(\rho, z_{\mathrm{wg}^{(1)}}) v_{\beta}^{(\mathrm{e})}(\rho, z_{\mathrm{wg}^{(1)}})\mathrm{d}\rho \tag{4.40}$$

$$\int_{\gamma_{\mathrm{wg}}^{(2)}} \left[\underline{E}_{\mathrm{t,wg}}\left(\underline{s}(t)\right) v_{\beta}^{(\mathrm{h})}\left(\underline{s}(t)\right)\right] \cdot \underline{s}'(t)\mathrm{d}t = \int_{0}^{\rho_{\mathrm{wg}}^{(2)}} E_{\rho,\mathrm{wg}}(\rho, z_{\mathrm{wg}^{(2)}}) v_{\beta}^{(\mathrm{h})}(\rho, z_{\mathrm{wg}^{(2)}})\mathrm{d}\rho \tag{4.41}$$

$$\int_{\gamma_{\mathrm{wg}}^{(2)}} \left[\underline{H}_{\mathrm{t,wg}}\left(\underline{s}(t)\right) v_{\beta}^{(\mathrm{e})}\left(\underline{s}(t)\right)\right] \cdot \underline{s}'(t)\mathrm{d}t = \int_{0}^{\rho_{\mathrm{wg}}^{(2)}} H_{\rho,\mathrm{wg}}(\rho, z_{\mathrm{wg}^{(2)}}) v_{\beta}^{(\mathrm{e})}(\rho, z_{\mathrm{wg}^{(2)}})\mathrm{d}\rho \tag{4.42}$$

4.2.3 Modal expansion of waveguide transversal fields

Now it is necessary to re-write $\underline{H}_{\mathrm{t,wg}}$ and $\underline{E}_{\mathrm{t,wg}}$ as functions of each incident wave $a_{\mu}^{(k)}$ relative to the μ-th mode and the k-th device port. It is possible to expand transversal fields of the waveguide as follows;

$$\begin{cases} \underline{E}_{\mathrm{t,wg}}^{(k)} = \sum_{\mu=0}^{\infty} V_{\mu}^{(k)}(z)\underline{e}_{\mu}^{(k)}(\underline{\rho}) \\ \underline{H}_{\mathrm{t,wg}}^{(k)} = \sum_{\mu=0}^{\infty} I_{\mu}^{(k)}(z)\underline{e}_{\mu}^{(k)}(\underline{\rho}) \end{cases} \tag{4.43}$$

Where $I_{\mu}^{(k)}(z)$ and $V_{\mu}^{(k)}(z)$ are respectively the modal current and the modal voltage for the k-th port of the device relative to the μ-th mode. Since these quantities satisfy modal transmission lines equations, it is possible to write

$$V_{\mu}^{(k)}(z) = V_{\mu}^{(k)+}\mathrm{e}^{-\mathrm{j}\beta_{\mu}^{(k)}z^{(k)}} + V_{\mu}^{(k)-}\mathrm{e}^{+\mathrm{j}\beta_{\mu}^{(k)}z^{(k)}}$$

Where each $z^{(k)}$ is the value of the z-coordinate considered, with respect to each local coordinate system, relative to each k-th port. Moreover, considering that power waves are defined as follows

$$a_{\mu}^{(k)} = \frac{V_{\mu}^{(k)+}}{\sqrt{Z_{\infty,\mu}^{(k)}}} \qquad b_{\mu}^{(k)} = \frac{V_{\mu}^{(k)-}}{\sqrt{Z_{\infty,\mu}^{(k)}}}$$

it is possible to write

$$V_{\mu}^{(k)}(z) = \sqrt{Z_{\infty,\mu}^{(k)}}a_{\mu}^{(k)}\mathrm{e}^{-\mathrm{j}\beta_{\mu}^{(k)}z^{(k)}} + \sqrt{Z_{\infty,\mu}^{(k)}}b_{\mu}^{(k)}\mathrm{e}^{+\mathrm{j}\beta_{\mu}^{(k)}z^{(k)}}$$

therefore, by substituting in (4.43), it is possible to obtain

$$\underline{E}_{\mathrm{t,wg}}^{(k)} = \sum_{\mu=0}^{\infty} \sqrt{Z_{\infty,\mu}^{(k)}} \left[a_{\mu}^{(k)}\mathrm{e}^{-\mathrm{j}\beta_{\mu}^{(k)}z^{(k)}} + b_{\mu}^{(k)}\mathrm{e}^{+\mathrm{j}\beta_{\mu}^{(k)}z^{(k)}}\right] \underline{e}_{\mu}^{(k)}(\underline{\rho}) \tag{4.44}$$

In order to find an expression for the transversal magnetic field, it is necessary to work on the total modal current.

$$I_\mu^{(k)}(z) = I_\mu^{(k)+}\mathrm{e}^{-\mathrm{j}\beta_\mu^{(k)}z^{(k)}} + I_\mu^{(k)-}\mathrm{e}^{+\mathrm{j}\beta_\mu^{(k)}z^{(k)}} = Y_{\infty,\mu}^{(k)}V_\mu^{(k)+}\mathrm{e}^{-\mathrm{j}\beta_\mu^{(k)}z^{(k)}} - Y_{\infty,\mu}^{(k)}V_\mu^{(k)-}\mathrm{e}^{+\mathrm{j}\beta_\mu^{(k)}z^{(k)}} =$$
$$= \sqrt{Y_{\infty,\mu}^{(k)}}\left[a_\mu^{(k)}\mathrm{e}^{-\mathrm{j}\beta_\mu^{(k)}z^{(k)}} - b_\mu^{(k)}\mathrm{e}^{+\mathrm{j}\beta_\mu^{(k)}z^{(k)}}\right]$$

so, finally,

$$\underline{H}_{\mathrm{t,wg}}^{(k)} = \sum_{\mu=0}^{\infty}\sqrt{Y_{\infty,\mu}^{(k)}}\left[a_\mu^{(k)}\mathrm{e}^{-\mathrm{j}\beta_\mu^{(k)}z^{(k)}} - b_\mu^{(k)}\mathrm{e}^{+\mathrm{j}\beta_\mu^{(k)}z^{(k)}}\right]\underline{h}_\mu^{(k)}(\underline{\rho}) \tag{4.45}$$

Equations (4.44) and (4.45) are useful because they have informations about both ρ and φ field components in the waveguide; so, it is possible to re-write the integrals as follows:

$$\int_0^{\rho_{\mathrm{wg}}^{(k)}} E_{\rho,\mathrm{wg}}(\rho, z_{\mathrm{wg}^{(k)}})v_\beta^{(\mathrm{h})}(\rho, z_{\mathrm{wg}^{(k)}})\mathrm{d}\rho =$$
$$= \sum_{\mu=0}^{\infty}\sqrt{Z_{\infty,\mu}^{(k)}}\left[a_\mu^{(k)} + b_\mu^{(k)}\right]\int_0^{\rho_{\mathrm{wg}}^{(k)}} e_{\rho,\mu}^{(k)}(\rho)v_\beta^{(\mathrm{h})}(\rho, z_{\mathrm{wg}^{(k)}})\mathrm{d}\rho \tag{4.46}$$

Using the same procedure, it is possible to find the following relationship

$$\int_0^{\rho_{\mathrm{wg}}^{(k)}} H_{\rho,\mathrm{wg}}(\rho, z_{\mathrm{wg}^{(k)}})v_\beta^{(\mathrm{e})}(\rho, z_{\mathrm{wg}^{(k)}})\mathrm{d}\rho =$$
$$= \sum_{\mu=0}^{\infty}\sqrt{Y_{\infty,\mu}^{(k)}}\left[a_\mu^{(k)} - b_\mu^{(k)}\right]\int_0^{\rho_{\mathrm{wg}}^{(k)}} h_{\rho,\mu}^{(k)}(\rho)v_\beta^{(\mathrm{e})}(\rho, z_{\mathrm{wg}^{(k)}})\mathrm{d}\rho \tag{4.47}$$

The dependance on $z^{(k)}$ disappeared because, since each system is local, $z^{(k)} = 0,\ \forall k$; as a matter of fact, each port is in the origin of its own local coordinate system.

4.2.4 Continuity of φ components

In order to guarantee the continuity of the electromagnetic field at the interface between the input waveguides and the device, it is necessary to enforce the continuity of E_φ and H_φ components too. In other words, it is necessary to satisfy

$$\begin{cases} E_\varphi = E_{\varphi,\mathrm{wg}}^{(k)} \\ H_\varphi = H_{\varphi,\mathrm{wg}}^{(k)} \end{cases}$$

Starting from the φ component of the electric field, as known from (4.24), it may be expanded as

$$E_\varphi = \sum_{\alpha=0}^{\infty} c_\alpha^{(\mathrm{e})} u_\alpha^{(\mathrm{e})}$$

So, the continuity condition for E_φ may be written in weak form, projecting both left-hand and right-hand sides of the equation on a set of test functions. In order to reduce the complexity of the system, as test functions it is possible to choose waveguide modal function φ components, $e_{\varphi,q}$, where q is the modal index for the 1-dimensional projection. So, since these functions, for a fixed φ angle, are only functions of ρ, it is possible to write, for input circular waveguides:

$$\int_0^{\rho_{\mathrm{wg}}^{(k)}} E_\varphi(\rho, z_{\mathrm{wg}^{(k)}}) e_{\varphi,\nu}^{(k)}(\rho)\mathrm{d}\rho = \int_0^{\rho_{\mathrm{wg}}^{(k)}} E_{\varphi,\mathrm{wg}}^{(k)}(\rho, z_{\mathrm{wg}^{(k)}}) e_{\varphi,\nu}^{(k)}(\rho)\mathrm{d}\rho$$

which can be re-written, expanding the right-hand side member in the modal basis, as

$$\begin{aligned} &\sum_{\alpha=0}^{\infty} c_\alpha^{(\mathrm{e})} \int_0^{\rho_{\mathrm{wg}}^{(k)}} u_\alpha^{(\mathrm{e})}(\rho, z_{\mathrm{wg}^{(k)}}) e_{\varphi,\nu}^{(k)}(\rho)\mathrm{d}\rho = \\ &= \sum_{\mu=0}^{\infty} \sqrt{Z_{\infty,\mu}^{(k)}} \left[a_\mu^{(k)} + b_\mu^{(k)}\right] \int_0^{\rho_{\mathrm{wg}}^{(k)}} e_{\varphi,\mu}^{(k)}(\rho) e_{\varphi,\nu}^{(k)}(\rho)\mathrm{d}\rho \end{aligned} \tag{4.48}$$

The same procedure should be repeated about H_φ. Recalling (4.25),

$$H_\varphi = \sum_{\alpha=0}^{\infty} c_\alpha^{(\mathrm{h})} u_\alpha^{(\mathrm{h})}$$

it is possible to find, for H_φ the following relationship, using $h_{\varphi,\nu}$ as test functions,

$$\begin{aligned} &\sum_{\alpha=0}^{\infty} c_\alpha^{(\mathrm{h})} \int_0^{\rho_{\mathrm{wg}}^{(k)}} u_\alpha^{(\mathrm{h})}(\rho, z_{\mathrm{wg}^{(k)}}) h_{\varphi,\nu}^{(k)}(\rho)\mathrm{d}\rho \\ &= \sum_{\mu=0}^{\infty} \sqrt{Y_{\infty,\mu}^{(k)}} \left[a_\mu^{(k)} - b_\mu^{(k)}\right] \int_0^{\rho_{\mathrm{wg}}^{(k)}} h_{\varphi,\mu}^{(k)}(\rho) h_{\varphi,\nu}^{(k)}(\rho)\mathrm{d}\rho \end{aligned} \tag{4.49}$$

4.3 Evaluation of expansion and test functions

The objective of this section is the determination of the expansion and test functions for the φ components of the electric and magnetic fields in each patch. These functions must comply with boundary conditions (4.34) and (4.35), recalled here.

$$\begin{cases} E_\varphi = 0 \\ \underline{E}_{\mathrm{t}} \cdot \hat{s} = 0 \end{cases} \tag{4.50}$$

The first step is the definition of a non-specialized orthogonal basis for each sub-domain, mapped in a canonical 2-dimensional domain, which is the $[-1, 1]^2$ square.

Then, these functions are weighted with Meixner functions, in order to take into account the presence of edges. It is necessary to start from these weighted functions and apply to them PEC boundary conditions, in order to find more specialized functions. Finally, they must be orthonormalized and "glued", finding global basis functions (basis functions for the whole domain) $u_\alpha^{(\mathrm{e,h})}$, which were used in the theoretical formulation of the problem. This subsection is focused on the enforcing of boundary conditions, so on the determination of linear systems which must be solved in order to find basis functions which satisfy PEC boundary conditions.

In the most general case, there is a unique set of vector basis functions, $\left\{f_{\alpha'}^{(\mathrm{e},i)}\right\}$ and $\left\{f_{\alpha''}^{(\mathrm{h},i)}\right\}$, which are electric and magnetic components respectively. α' and α'' are indexes of this vector; the former one is relative to electric components, while the latter one is relative to magnetic components. Therefore, electric and magnetic φ components can be expanded as follows:

$$\begin{cases} E_\varphi(\underline{\rho}) = \displaystyle\sum_{\alpha'=0}^{N_\mathrm{e}} y_{\alpha'}^{(\mathrm{e})}\ f_{\alpha'}^{(\mathrm{e},i)}(\underline{\rho}) \\ H_\varphi(\underline{\rho}) = \displaystyle\sum_{\alpha''=0}^{N_\mathrm{h}} y_{\alpha''}^{(\mathrm{h})}\ f_{\alpha''}^{(\mathrm{h},i)}(\underline{\rho}) \end{cases} \qquad \forall \underline{\rho} \in \mathcal{D}^{(i)} \tag{4.51}$$

where $\underline{\rho} = (z, \rho)$, is the transversal cylindrical coordinate, with respect to the invariance coordinate φ.

$E_\varphi = 0$ boundary condition

It is possible to start from the first PEC boundary condition, which is $E_\varphi = 0$. This condition can be satisfied in weak form, by testing it on a set of functions v_q. For each j-th parametric curve $\gamma_j^{(i)} \in \gamma_{\mathrm{PEC}}^{(i)}$, relative to the i-th patch,

$$\langle E_\varphi, v_q \rangle|_{\gamma_j^{(i)}} = 0$$

this can be written in integral form

$$\begin{aligned} \int_{\gamma_j^{(i)}} E_\varphi v_q \mathrm{d}\gamma &= \sum_{\alpha'} y_{\alpha'}^{(\mathrm{e})} \int_{\gamma_j^{(i)}} f_{\alpha'}^{(\mathrm{e},i)} v_q \mathrm{d}\gamma \\ &= \sum_{\alpha'} y_{\alpha'}^{(\mathrm{e})} L_{q\alpha'}^{(\mathrm{e},i)} = 0 \end{aligned} \tag{4.52}$$

It is important to remark that the integral is a line integral, where the $\gamma_j^{(i)}$ line represents each j-th PEC side belonging to $\mathcal{D}^{(i)}$.

$\underline{E}_\mathrm{t} \cdot \hat{s} = 0$ boundary condition

Considering the reference system in Figure 4.2, $\hat{s}$ is 90° degrees rotated with respect to $\hat{\nu}$. Considering ϑ the angle of the normal of the surface evaluated starting from the z-axis to the y-axis,

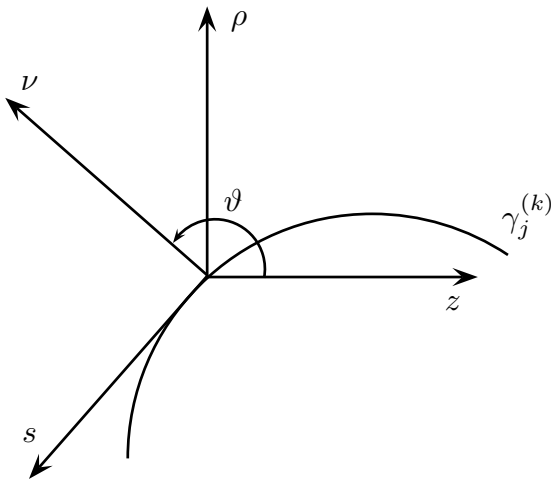

Figure 4.2: Reference system for the PEC boundary condition

$$\hat{\nu} = \hat{\mathrm{z}}\cos\vartheta + \hat{\rho}\sin\vartheta$$

so, for the previous consideration,

$$\begin{aligned}\hat{s} &= \hat{\mathrm{z}}\cos\left(\vartheta + \frac{\pi}{2}\right) + \hat{\rho}\cos\left(\vartheta + \frac{\pi}{2}\right) = \\ &= -\hat{\mathrm{z}}\sin\vartheta + \hat{\rho}\cos\vartheta\end{aligned} \tag{4.53}$$

Since $\underline{E}_{\mathrm{t}}$ is trasversal to φ,

$$\underline{E}_{\mathrm{t}} = E_z\hat{\mathrm{z}} + E_\rho\hat{\rho}$$

therefore,

$$\underline{E}_{\mathrm{t}} \cdot \hat{s} = -E_z\sin\vartheta + E_\rho\cos\vartheta \tag{4.54}$$

E_z and E_ρ are known from (4.13) and (4.12) respectively, so they are recalled and then substituted in (4.54).

$$\begin{aligned}E_\rho &= -\frac{\mathrm{j}}{m^2 - k^2\rho^2}\left(m\frac{\partial(\rho E_\varphi)}{\partial\rho} + kZ\rho^2\frac{\partial H_\varphi}{\partial z}\right) \\ E_z &= -\frac{\mathrm{j}}{m^2 - k^2\rho^2}\left(m\rho\frac{\partial E_\varphi}{\partial z} - kZ\rho\frac{\partial(\rho H_\varphi)}{\partial\rho}\right)\end{aligned}$$

so

$$\begin{aligned}\underline{E}_{\mathrm{t}} \cdot \hat{s} = &-\frac{\mathrm{j}}{m^2 - k^2\rho^2}\left(kZ\rho\frac{\partial(\rho H_\varphi)}{\partial\rho} - m\rho\frac{\partial E_\varphi}{\partial z}\right)\sin\vartheta + \\ &-\frac{\mathrm{j}}{m^2 - k^2\rho^2}\left(m\frac{\partial(\rho E_\varphi)}{\partial\rho} + kZ\rho^2\frac{\partial H_\varphi}{\partial z}\right)\cos\vartheta\end{aligned}$$

by re-arranging this equation, it is possible to identify two contributions;

$$\underline{E}_{\mathrm{t}} \cdot \hat{\mathrm{s}} = -\frac{\mathrm{j}}{m^2 - k^2\rho^2}\left[kZ\rho\left(\frac{\partial(\rho H_\varphi)}{\partial\rho}\sin\vartheta + \rho\frac{\partial H_\varphi}{\partial z}\cos\vartheta\right) + \right. \\ \left. + m\left(\frac{\partial(\rho E_\varphi)}{\partial\rho}\cos\vartheta - \rho\frac{\partial E_\varphi}{\partial z}\sin\vartheta\right)\right] \tag{4.55}$$

At this point, the second term can be expanded, obtaining

$$-\rho\frac{\partial E_\varphi}{\partial z}\sin\vartheta + \rho\frac{\partial E_\varphi}{\partial\rho}\cos\vartheta + E_\varphi\cos\vartheta = \\ = \rho\left(-\frac{\partial E_\varphi}{\partial z}\sin\vartheta + \frac{\partial E_\varphi}{\partial\rho}\cos\vartheta\right) + E_\varphi\cos\vartheta$$

The term inside the parentheses equals the directional derivative of E_φ along s. In fact, it is known that

$$\frac{\partial E_\varphi}{\partial s} = \hat{s}\cdot\left(\nabla_{\mathrm{t}}^{(\varphi)}E_\varphi\right)$$

where $\nabla_{\mathrm{t}}^{(\varphi)}$ is the gradient in cylindrical coordinates, transversal with respect to the φ variable. It may be written as

$$\nabla_{\mathrm{t}}^{(\varphi)} = \hat{\rho}\frac{\partial}{\partial\rho} + \hat{\mathrm{z}}\frac{\partial}{\partial z}$$

So, recalling $\hat{s}$ from (4.53),

$$\hat{s}\cdot\left(\nabla_{\mathrm{t}}^{(\varphi)}E_\varphi\right) = -\sin\vartheta\frac{\partial E_\varphi}{\partial z} + \cos\vartheta\frac{\partial E_\varphi}{\partial\rho}$$

just like in the second term. Therefore, the right-hand side of (4.55) can be re-written as:

$$\rho\frac{\partial E_\varphi}{\partial s} + E_\varphi\cos\vartheta$$

In the previous subsection, E_φ was enforced to equal zero in the entire PEC plane. This means that the derivatives evaluated on the PEC plane in tangential directions with respect to it, must equal zero, because the field is identically zero. Therefore,

$$E_\varphi = 0\ \forall s\in\gamma_j^{(i)} \Longrightarrow \frac{\partial E_\varphi}{\partial s} = 0\ \forall s\in\gamma_j^{(i)}$$

This means that the second term is vanishing. Therefore, the condition which has to be satisfied is just

$$\underline{E}_{\mathrm{t}}\cdot\hat{s} = 0 \Longrightarrow -\frac{\mathrm{j}}{m^2 - k^2\rho^2}\left[kZ\rho\left(\frac{\partial(\rho H_\varphi)}{\partial\rho}\sin\vartheta + \rho\frac{\partial H_\varphi}{\partial z}\cos\vartheta\right)\right] = 0$$

So, it is necessary to request that the expression inside inner parentheses equals zero; therefore,

$$H_\varphi \sin\vartheta + \rho\frac{\partial H_\varphi}{\partial \rho}\sin\vartheta + \rho\frac{\partial H_\varphi}{\partial z}\cos\vartheta = \\ = H_\varphi \sin\vartheta + \rho\frac{\partial H_\varphi}{\partial \nu} = 0 \tag{4.56}$$

In fact, considering the definition of directional derivative:

$$\frac{\partial H_\varphi}{\partial \nu} = \hat{\rho}\frac{\partial H_\varphi}{\partial \rho}\sin\vartheta + \hat{\mathrm{z}}\frac{\partial H_\varphi}{\partial z}\cos\vartheta$$

it is possible to prove that:

$$\frac{\partial H_\varphi}{\partial \nu} = (\nabla_{\mathrm{t}} H_\varphi)\cdot\hat{\nu}$$

this proves (4.56).

This is a boundary condition which enforces the value of a linear combination of a field component and its normal derivative with respect to the PEC surface; therefore, it is a Robin condition.

It is remarkable the fact that this boundary condition has no dependance on frequency; as a matter of fact, this result is not trivial, because in previous steps there was a relationship between E_φ, H_φ, and k. Moreover, functions $f_{\alpha''}^{(\mathrm{e},i)}(\underline{\rho})$ and $f_{\alpha''}^{(\mathrm{h},i)}(\underline{\rho})$ are not coupled, because boundary conditions enforce the behavior of electric or magnetic fields E_φ and H_φ but not of their combinations.

In order to enforce (4.56), it is possible to formulate it in weak form;

$$\langle \underline{E}_{\mathrm{t}}\cdot\hat{s}, v_q\rangle = \int_{\gamma_j^{(i)}} \underline{E}_{\mathrm{t}}\cdot\hat{s}\, v_q \,\mathrm{d}\gamma = \\ = \int_{\gamma_j^{(i)}} \left(H_\varphi\sin\vartheta + \rho\frac{\partial H_\varphi}{\partial\nu}\right) v_q\,\mathrm{d}\gamma = 0 \tag{4.57}$$

Expanding with $f_{\alpha''}^{(\mathrm{h},i)}(\underline{\rho})$ functions, it is possible to find the following integral formulation

$$\sum_{\alpha''} y_{\alpha''}^{(\mathrm{h})} \int_{\gamma_j^{(i)}} \left[f_{\alpha''}^{(\mathrm{h},i)}\sin\vartheta + \rho\frac{\partial}{\partial\nu}\, f_{\alpha''}^{(\mathrm{h},i)}\right] v_q\,\mathrm{d}\gamma = \\ = \sum_{\alpha''} L_{q\alpha''}^{(\mathrm{h},i)} y_{\alpha''}^{(\mathrm{h})}$$

where

$$L_{q\alpha''}^{(\mathrm{h},i)} = \int_{\gamma_j^{(i)}} \left[f_{\alpha''}^{(\mathrm{h},i)}\sin\vartheta + \rho\frac{\partial}{\partial\nu}\, f_{\alpha''}^{(\mathrm{h},i)}\right] v_q\,\mathrm{d}\gamma = \\ = \int_{\gamma_j^{(i)}} \left[f_{\alpha''}^{(\mathrm{h},i)}\sin\vartheta + \rho\left(\frac{\partial}{\partial z}\, f_{\alpha''}^{(\mathrm{h},i)}\cos\vartheta + \frac{\partial}{\partial\rho}\, f_{\alpha''}^{(\mathrm{h},i)}\sin\vartheta\right)\right] v_q\mathrm{d}\gamma \tag{4.58}$$

4.4 Determination of the linear system

Given equations (4.29) and (4.32), they have to be re-written in order to take into account simplified expressions of contour integrals (4.46) and (4.47), and to expand derivatives of $(\rho\, u_\alpha^{(\mathrm{e,h})})$; therefore, it is possible to write

$$
\begin{aligned}
&-\mathrm{j}kZ\sum_{\alpha=0}^{\infty} c_\alpha^{(\mathrm{h})} \iint_\Sigma u_\alpha^{(\mathrm{h})} v_\beta^{(\mathrm{h})} \mathrm{d}\rho\mathrm{d}z = \\
&= \sum_{\alpha=0}^{\infty} c_\alpha^{(\mathrm{h})} \iint_\Sigma \left\{ \frac{\mathrm{j}kZ}{m^2-k^2\rho^2}\rho \left[\rho \frac{\partial u_\alpha^{(\mathrm{h})}}{\partial z}\frac{\partial v_\beta^{(\mathrm{h})}}{\partial z} + \rho \frac{\partial u_\alpha^{(\mathrm{h})}}{\partial \rho}\frac{\partial v_\beta^{(\mathrm{h})}}{\partial \rho} + u_\alpha^{(\mathrm{h})}\frac{\partial v_\beta^{(\mathrm{h})}}{\partial \rho} \right] \right\} \mathrm{d}\rho\mathrm{d}z + \\
&+ \sum_{\alpha=0}^{\infty} c_\alpha^{(\mathrm{e})} \iint_\Sigma \left\{ \frac{\mathrm{j}m}{m^2-k^2\rho^2} \left[\rho \frac{\partial u_\alpha^{(\mathrm{e})}}{\mathrm{d}\rho}\frac{\partial v_\beta^{(\mathrm{h})}}{\partial z} + u_\alpha^{(\mathrm{e})}\frac{\partial v_\beta^{(\mathrm{h})}}{\partial z} - \rho \frac{\partial u_\alpha^{(\mathrm{e})}}{\partial z}\frac{\partial v_\beta^{(\mathrm{h})}}{\partial \rho} \right] \right\} \mathrm{d}\rho\mathrm{d}z + \\
&+ \sum_{\mu=0}^{\infty} \sqrt{Z_{\infty,\mu}^{(2)}} \left[a_\mu^{(2)} + b_\mu^{(2)} \right] \int_0^{\rho_{\mathrm{wg}}^{(2)}} e_{\rho,\mu}^{(2)}(\rho) v_\beta^{(\mathrm{h})}(\rho, z_{\mathrm{wg}^{(2)}}) \mathrm{d}\rho + \\
&- \sum_{\mu=0}^{\infty} \sqrt{Z_{\infty,\mu}^{(1)}} \left[a_\mu^{(1)} + b_\mu^{(1)} \right] \int_0^{\rho_{\mathrm{wg}}^{(1)}} e_{\rho,\mu}^{(1)}(\rho) v_\beta^{(\mathrm{h})}(\rho, z_{\mathrm{wg}^{(1)}}) \mathrm{d}\rho
\end{aligned}
\tag{4.59}
$$

$$
\begin{aligned}
&\mathrm{j}kY\sum_{\alpha=0}^{\infty} c_\alpha^{(\mathrm{e})} \iint_\Sigma u_\alpha^{(\mathrm{e})} v_\beta^{(\mathrm{e})} \mathrm{d}\rho\mathrm{d}z = \\
&= \sum_{\alpha=0}^{\infty} c_\alpha^{(\mathrm{h})} \iint_\Sigma \left\{ \frac{\mathrm{j}m}{m^2-k^2\rho^2} \left[\rho \frac{\partial u_\alpha^{(\mathrm{h})}}{\partial \rho}\frac{\partial v_\beta^{(\mathrm{e})}}{\partial z} + u_\alpha^{(\mathrm{h})}\frac{\partial v_\beta^{(\mathrm{e})}}{\partial z} - \rho \frac{\partial u_\alpha^{(\mathrm{h})}}{\partial z}\frac{\partial v_\beta^{(\mathrm{e})}}{\partial \rho} \right] \right\} \mathrm{d}\rho\mathrm{d}z + \\
&- \sum_{\alpha=0}^{\infty} c_\alpha^{(\mathrm{e})} \iint_\Sigma \left\{ \frac{\mathrm{j}kY}{m^2-k^2\rho^2}\rho \left[\rho \frac{\partial u_\alpha^{(\mathrm{e})}}{\partial z}\frac{\partial v_\beta^{(\mathrm{e})}}{\partial z} + \rho \frac{\partial u_\alpha^{(\mathrm{e})}}{\partial \rho}\frac{\partial v_\beta^{(\mathrm{e})}}{\partial \rho} + u_\alpha^{(\mathrm{e})}\frac{\partial v_\beta^{(\mathrm{e})}}{\partial \rho} \right] \right\} \mathrm{d}\rho\mathrm{d}z + \\
&+ \sum_{\mu=0}^{\infty} \sqrt{Y_{\infty,\mu}^{(2)}} \left[a_\mu^{(2)} - b_\mu^{(2)} \right] \int_0^{\rho_{\mathrm{wg}}^{(2)}} h_{\rho,\mu}^{(2)}(\rho) v_\beta^{(\mathrm{e})}(\rho, z_{\mathrm{wg}^{(2)}}) \mathrm{d}\rho + \\
&- \sum_{\mu=0}^{\infty} \sqrt{Y_{\infty,\mu}^{(1)}} \left[a_\mu^{(1)} - b_\mu^{(1)} \right] \int_0^{\rho_{\mathrm{wg}}^{(1)}} h_{\rho,\mu}^{(1)}(\rho) v_\beta^{(\mathrm{e})}(\rho, z_{\mathrm{wg}^{(1)}}) \mathrm{d}\rho
\end{aligned}
\tag{4.60}
$$

Up to this point every equation was written in terms of series. Actually, it is not necessary to evaluate a sum of infinite terms in order to calculate these expressions, because just few contributions are significative. Therefore, it is possible to write approximated expressions for (4.59), (4.60), and for boundary conditions (4.48) and (4.49) considering just few terms. Moreover, they can be written as a combination of inner products instead of integrals.

$$
\begin{aligned}
&\mathrm{j}kZ \sum_{\alpha=0}^{N_{\mathrm{fun}}} c_\alpha^{(\mathrm{h})} \left\{ \left\langle u_\alpha^{(\mathrm{h})}, v_\beta^{(\mathrm{h})} \right\rangle + \left\langle \frac{\rho^2}{m^2-k^2\rho^2} \frac{\partial}{\partial z} u_\alpha^{(\mathrm{h})}, \frac{\partial}{\partial z} v_\beta^{(\mathrm{h})} \right\rangle + \right. \\
&\qquad \left. + \left\langle \frac{\rho^2}{m^2-k^2\rho^2} \frac{\partial}{\partial \rho} u_\alpha^{(\mathrm{h})}, \frac{\partial}{\partial \rho} v_\beta^{(\mathrm{h})} \right\rangle + \left\langle \frac{\rho}{m^2-k^2\rho^2} u_\alpha^{(\mathrm{h})}, \frac{\partial}{\partial \rho} v_\beta^{(\mathrm{h})} \right\rangle \right\} + \\
&+\mathrm{j}m \sum_{\alpha=0}^{N_{\mathrm{fun}}} c_\alpha^{(\mathrm{e})} \left\{ \left\langle \frac{\rho}{m^2-k^2\rho^2} \frac{\partial}{\partial \rho} u_\alpha^{(\mathrm{e})}, \frac{\partial}{\partial z} v_\beta^{(\mathrm{h})} \right\rangle + \left\langle \frac{1}{m^2-k^2\rho^2} u_\alpha^{(\mathrm{e})}, \frac{\partial}{\partial z} v_\beta^{(\mathrm{h})} \right\rangle + \right. \\
&\qquad \left. - \left\langle \frac{\rho}{m^2-k^2\rho^2} \frac{\partial}{\partial z} u_\alpha^{(\mathrm{e})}, \frac{\partial}{\partial \rho} v_\beta^{(\mathrm{h})} \right\rangle \right\} = \\
&\qquad = \sum_{\mu=0}^{N_{\mathrm{modes}}} \sqrt{Z_{\infty,\mu}^{(1)}} \left[a_\mu^{(1)} + b_\mu^{(1)} \right] \left\langle e_{\rho,\mu}^{(1)}, v_\beta^{(\mathrm{h})} \right\rangle \Big|_{\gamma_{\mathrm{wg}}^{(1)}} \\
&\qquad - \sum_{\mu=0}^{N_{\mathrm{modes}}} \sqrt{Z_{\infty,\mu}^{(2)}} \left[a_\mu^{(2)} + b_\mu^{(2)} \right] \left\langle e_{\rho,\mu}^{(2)}, v_\beta^{(\mathrm{h})} \right\rangle \Big|_{\gamma_{\mathrm{wg}}^{(2)}}
\end{aligned}
\tag{4.61}
$$

$$
\begin{aligned}
&\mathrm{j}kY \sum_{\alpha=0}^{N_{\mathrm{fun}}} c_\alpha^{(\mathrm{e})} \left\{ \left\langle u_\alpha^{(\mathrm{e})}, v_\beta^{(\mathrm{e})} \right\rangle + \left\langle \frac{\rho^2}{m^2-k^2\rho^2} \frac{\partial}{\partial z} u_\alpha^{(\mathrm{e})}, \frac{\partial}{\partial z} v_\beta^{(\mathrm{e})} \right\rangle + \right. \\
&\qquad \left. + \left\langle \frac{\rho^2}{m^2-k^2\rho^2} \frac{\partial}{\partial \rho} u_\alpha^{(\mathrm{e})}, \frac{\partial}{\partial \rho} v_\beta^{(\mathrm{e})} \right\rangle + \left\langle \frac{\rho}{m^2-k^2\rho^2} u_\alpha^{(\mathrm{e})}, \frac{\partial}{\partial \rho} v_\beta^{(\mathrm{e})} \right\rangle \right\} + \\
&+\mathrm{j}m \sum_{\alpha=0}^{N_{\mathrm{fun}}} c_\alpha^{(\mathrm{h})} \left\{ \left\langle \frac{\rho}{m^2-k^2\rho^2} \frac{\partial}{\partial z} u_\alpha^{(\mathrm{h})}, \frac{\partial}{\partial \rho} v_\beta^{(\mathrm{e})} \right\rangle \right\} \\
&\qquad - \left\langle \frac{\rho}{m^2-k^2\rho^2} \frac{\partial}{\partial \rho} u_\alpha^{(\mathrm{h})}, \frac{\partial}{\partial z} v_\beta^{(\mathrm{e})} \right\rangle - \left\langle \frac{1}{m^2-k^2\rho^2} u_\alpha^{(\mathrm{h})}, \frac{\partial}{\partial z} v_\beta^{(\mathrm{e})} \right\rangle = \\
&\qquad + \sum_{\mu=0}^{N_{\mathrm{modes}}} \sqrt{Y_{\infty,\mu}^{(2)}} \left[a_\mu^{(2)} - b_\mu^{(2)} \right] \left\langle h_{\rho,\mu}^{(2)}, v_\beta^{(\mathrm{e})} \right\rangle \Big|_{\gamma_{\mathrm{wg}}^{(2)}} \\
&\qquad - \sum_{\mu=0}^{N_{\mathrm{modes}}} \sqrt{Y_{\infty,\mu}^{(1)}} \left[a_\mu^{(1)} - b_\mu^{(1)} \right] \left\langle h_{\rho,\mu}^{(1)}, v_\beta^{(\mathrm{e})} \right\rangle \Big|_{\gamma_{\mathrm{wg}}^{(1)}}
\end{aligned}
\tag{4.62}
$$

These equations have to be coupled with continuity conditions from (4.48) and (4.49), obtaining the following extra equations:

$$
\begin{aligned}
&\sum_{\alpha=0}^{N_{\mathrm{fun}}} c_\alpha^{(\mathrm{e})} \left\langle u_\alpha^{(\mathrm{e})} e_{\varphi,\nu}^{(k)} \right\rangle \Big|_{\gamma_{\mathrm{wg}}^{(k)}} = \sum_{\mu=0}^{N_{\mathrm{modes}}} \sqrt{Z_{\infty,\mu}^{(\mu)}} \left[a_\mu^{(k)} + b_\mu^{(k)} \right] \left\langle e_{\varphi,\mu}^{(k)} e_{\varphi,\nu}^{(k)} \right\rangle \Big|_{\gamma_{\mathrm{wg}}^{(k)}}, \\
&\qquad \nu = 0, 1, ..., N_{\mathrm{modes}}
\end{aligned}
\tag{4.63}
$$

$$\sum_{\alpha=0}^{N_{\text{fun}}} c_{\alpha}^{(\text{h})} \left\langle u_{\alpha}^{(\text{h})} h_{\varphi,\nu}^{(i)} \right\rangle \Big|_{\gamma_{\text{wg}}^{(k)}} = \sum_{\mu=0}^{N_{\text{modes}}} \sqrt{Y_{\infty,\mu}^{(k)}} \left[a_{\mu}^{(k)} - b_{\mu}^{(k)} \right] \left\langle h_{\varphi,\mu}^{(k)} h_{\varphi,\nu}^{(k)} \right\rangle \Big|_{\gamma_{\text{wg}}^{(k)}},$$
$$\nu = 0, 1, ..., N_{\text{modes}} \tag{4.64}$$

Where $k = 1, 2$, in 2-port devices case.

It is possible to re-arrange equations (4.61) and (4.62) in order to obtain a linear system. Actually, these two equations must be satisfied $\forall v_{\beta}^{(\text{e/h})} \in V^{(\text{e/h})}$; therefore, there are two systems of integral equations. This must be coupled with another system, in order to enforce continuity boundary conditions for both E_{φ} and H_{φ}.

To sum up, it is necessary to write a system in this form;

$$\begin{cases} \underline{\underline{A}}^{(\text{e,e})} \underline{c}^{(\text{e})} + \underline{\underline{A}}^{(\text{e,h})} \underline{c}^{(\text{h})} = \sum_{k=1}^{2} (-1)^k \, \underline{\underline{B}}^{(\text{e},k)} \underline{a}^{(k)} - \sum_{k=1}^{2} (-1)^k \, \underline{\underline{B}}^{(\text{e},k)} \underline{b}^{(k)} \\ \underline{\underline{A}}^{(\text{h,e})} \underline{c}^{(\text{e})} + \underline{\underline{A}}^{(\text{h,h})} \underline{c}^{(\text{h})} = \sum_{k=1}^{2} (-1)^{k+1} \, \underline{\underline{B}}^{(\text{h},k)} \underline{a}^{(k)} + \sum_{k=1}^{2} (-1)^{k+1} \, \underline{\underline{B}}^{(\text{h},k)} \underline{b}^{(k)} \end{cases}$$

$$\begin{cases} \underline{\underline{C}}^{(\text{e},k)} \underline{c}^{(\text{e})} = \underline{\underline{D}}^{(\text{e},k)} \underline{a}^{(k)} + \underline{\underline{D}}^{(\text{e},k)} \underline{b}^{(k)} \\ \underline{\underline{C}}^{(\text{h},k)} \underline{c}^{(\text{h})} = \underline{\underline{D}}^{(\text{h},k)} \underline{a}^{(k)} - \underline{\underline{D}}^{(\text{h},k)} \underline{b}^{(k)} \end{cases} \quad \forall k \in \{1, 2\}$$

The unknown of the system is the vector $\underline{c}$ of coefficients for field expansions (4.24) - (4.25).

APPENDIX A

Appendix of Chapter 2

A.1 Resume of Bessel functions main properties

It may be useful to recall some important properties of Bessel functions; this subsection is mainly focused on $\mathrm{J}_n(x)$, where x often in the text is $k\rho$. The power series representation of $\mathrm{J}_n(x)$ is

$$\mathrm{J}_n(x) = \sum_{m=0}^{\infty} \frac{(-1)^m}{m!(n+m)!} \left(\frac{x}{2}\right)^{n+2m}$$

This expression leads to the following formula

$$\mathrm{J}_n(-x) = (-1)^n \, \mathrm{J}_n(x)$$

If $x \sim 0$, it is possible to approximate the expression with

$$\mathrm{J}_n(x) \sim \frac{1}{n!} \left(\frac{x}{2}\right)^n$$

If $x \to \infty$, there is an asymptotic expression

$$\mathrm{J}_n(x) \sim \sqrt{\frac{2}{\pi x}} \cos\left(x - \frac{\pi}{4} - n\frac{\pi}{2}\right)$$

Now in order to use a simpler notation, every following relation will be represented using a generic function $Z_n(x)$; Z_n may be J_n (n-th order Bessel function of first kind), Y_n (Bessel function of second kind), $\mathrm{H}_n^{(1,2)}$ (Hankel functions of first or second kind).

In order to find recursive relations, there are two important expressions

$$\frac{\mathrm{d}}{\mathrm{d}x} \left[x^n Z_n(x)\right] = x^n Z_{n-1}(x)$$

$$\frac{\mathrm{d}}{\mathrm{d}x} \left[x^{-n} Z_n(x)\right] = -x^{-n} Z_{n+1}(x)$$

These two equations are useful to integrate Bessel functions multiplied by their argument. From these expressions it is possible to obtain the **recursive relations**

$$x\frac{\mathrm{d}}{\mathrm{d}x}Z_n(x) = nZ_n(x) - xZ_{n+1}(x) = -nZ_n(x) + xZ_{n-1}(x)$$

$$2\frac{\mathrm{d}}{\mathrm{d}x}Z_n(x) = Z_{n-1}(x) - Z_{n+1}(x)$$

$$2nZ_n(x) = x\left[Z_{n-1}(x) + Z_{n+1}(x)\right]$$

Using the theory of Laurent expansions it is possible to obtain the following integral relation; starting from

$$\mathrm{e}^{\frac{1}{2}x\left(t-\frac{1}{t}\right)} = \sum_{n=-\infty}^{+\infty} \mathrm{J}_n(x)t^n$$

it is possible to prove that

$$\begin{aligned}\mathrm{J}_n(x) &= \frac{1}{2\pi}\int_{-\pi}^{+\pi} \mathrm{e}^{-\mathrm{j}n\vartheta+\mathrm{j}x\sin\vartheta}\mathrm{d}\vartheta = \\ &= \frac{1}{\pi}\int_0^{\pi} \cos\left(n\vartheta - x\sin\vartheta\right)\mathrm{d}\vartheta\end{aligned}$$

Other important formulae are the integral ones; the first one is the Lommel's integral formula

$$\int_0^x Z_n(kx)Z_n(lx)x\mathrm{d}x = \frac{x}{k^2-l^2}\left[kZ_n(lx)Z_{n+1}(kx) - lZ_n(kx)Z_{n+1}(lx)\right]$$

and the following relation

$$\int_0^x Z_n^2(kx)x\mathrm{d}x = \frac{x^2}{2}\left[\frac{\mathrm{d}}{\mathrm{d}x}Z_n(x) + \left(1-\frac{n^2}{k^2x^2}\right)Z_n^2(kx)\right]$$

A.1.1 Resume of spherical Bessel functions properties

In this subsection we will show some properties of spherical Bessel and Hankel functions, in order to be able to manage them. Spherical Bessel and Hankel functions are solutions of spherical Bessel equation, but they are strictly related with Bessel and Hankel functions. In fact,

$$\begin{aligned}\mathrm{j}_n(x) &= \sqrt{\frac{\pi}{2x}}\mathrm{J}_{n+\frac{1}{2}}(x) \\ \mathrm{y}_n(x) &= \sqrt{\frac{\pi}{2x}}\mathrm{Y}_{n+\frac{1}{2}}(x)\end{aligned} \tag{A.1}$$

Between spherical Bessel and Hankel functions there is the same relationship of cylindrical Bessel and Hankel functions;

$$\begin{aligned} \mathrm{h}_n^{(1)}(x) &= \mathrm{j}_n(x) + \mathrm{jy}_n(x) \\ \mathrm{h}_n^{(2)}(x) &= \mathrm{j}_n(x) - \mathrm{jy}_n(x) \end{aligned} \tag{A.2}$$

Since these functions are so related with Bessel functions, almost every property of cylindrical Bessel or Hankel functions is a property of spherical Bessel or Hankel functions too.

A.2 Unwrap functions

In this appendix is included the MATLAB® code of unwrap functions for both TM and TE modes of a circular waveguide.

Approximation of $\angle H_m^{(1,2)}(x)$

```
function phi=f_Eval_Hphiapprox(z,m)
% function phi=f_Eval_Hphiapprox(z,m)
%
% This function extimates the phase of MATLAB function besselh(nu,1,z,1),
% which implements the Hankel function of first kind. This function keeps
% into account the exp(jz), since it is already inside besselh().
%
% For case m=0, it is used the -pi/4 constant. For m>0, it is used the
% asymptotic expansion after the first zero of the Bessel function of
% second kind Y. These functions are an implementation of formulae from
% Abramowitz-Stegun (more in details, (9.2.29), without considering as
% previously written the term in "x", already into besselh()).
%
% Input parameters
%
% z : variable in which Hankel function is evaluated
%
% m : azimuthal index (order of Hankel function)
%
% Outputs
%
% phi : approximation of the phase of Hankel function
%

if m==0
    phi=-pi/4*ones(1,length(z));
else
    phi=-pi/2*ones(1,length(z))-z;
    yz=m+0.9315768*m^(1/3)+0.260351*m^(-1/3)+0.01198/m-0.0060*m^(-5/3)-0.001*m↩
        ^(-7/3); % 2nd kind Bessel function 1st zero approximation
    ind=find(z>yz);
    mu=4*m^2;
    phi(ind)=-(m/2+0.25)*pi+(mu-1)./(8*z(ind))+... % Phase approximation for H_m↩
        ^{(1)} (Abramowitz-Stegun, 9.2.29).
        (mu-1)*(mu-25)./(6*(4*z(ind)).^3)+(mu-1)*(mu^2-114*mu+1073)./(5*(4*z(ind)↩
            ).^5)+...
        (mu-1)*(5*mu^3-1535*mu^2+54703*mu-375733)./(14*(4*z(ind)).^7);
end
```

Unwrap function for cylindrical waveguide TM modes

```
function phi=f_Eval_CylRTPSTM(kt,rext,m,mode)
% function phi=f_Eval_CylRTPSTM(kt,rext,m,mode)
%
% This function evaluates the Round Trip Phase Shift, divided by 2 pi, for
```

```
% TM modes of an empty waveguide with circular transversal section. This
% function is based on the use of f_Eval_Hphiapprox, which approximates the
% phase of the Hankel function of first kind. In this function it is
% necessary to keep into account the presence of the exp(x).
%
% Input parameters
%
% kt : value of kt, in order to perform the estimation ;
%
% rext : radius of the transversal section of the waveguide
%
% m : azimuthal index
%
% mode : radial index n
%
% Outputs
%
% phi : approximated RTPS
%

phi=(1+mode)*ones(1,length(kt));

ind=find(kt~=0);
if ~isempty(ind)
    thetaext=f_Eval_Hphiapprox(kt(ind)*rext,m);
    h1ext=besselh(m,1,kt(ind)*rext,1);
    h2ext=conj(h1ext);
    phi(ind)=0.5-(2*angle(h1ext.*exp(-j*thetaext))+...
        +2*kt(ind)*rext...
        +2*thetaext)/(2*pi)+mode;
end % if ~isempty(ind)
```

Approximation of the phase of the derivative of $H_m^{(1,2)}(x)$

```
function phi=f_Eval_HDerphiapprox(z,m)
% function phi=f_Eval_HDerphiapprox(z,m)
%
% This function extimates the phase of the derivative of MATLAB function
% besselh(nu,1,z,1), which implements the Hankel function of first kind.
% This function keeps into account the exp(jz), since it is already inside
% besselh().
%
% For case m=0, it is used the -pi/4 constant. For m>0, it is used the
% asymptotic expansion after the first zero of the Bessel function of
% second kind Y. These functions are an implementation of formulae from
% Abramowitz-Stegun (more in details, (9.2.31), without considering as
% previously written the term in "x", already into besselh()).
%
% Input parameters
%
% z : variable in which Hankel function is evaluated
%
% m : azimuthal index (order of Hankel function)
%
% Outputs
%
% phi : approximation of the phase of Hankel function
%

if m==0
    a=0.75;
    phi=pi/2-a+sqrt(a^2+z.^2)-z;
else
    phi=pi/2*ones(1,length(z))-z;
    jpz=m+0.8086165*m^(1/3)+0.07249*m^(-1/3)-0.05097/m+0.094*m^(-5/3);
    ind=find(z>jpz);
    mu=4*m^2;
    phi(ind)=-(m/2-0.25)*pi+(mu+3)./(8*z(ind))+...
```

```
        (mu^2+46*mu-63)./(6*(4*z(ind)).^3)+...
        (mu^3+185*mu^2-2053*mu+1899)./(5*(4*z(ind)).^5);
end
```

Unwrap function for cylindrical waveguide TE modes

```
function phi=f_Eval_CylRTPSTE(kt,rext,m,mode)
% function phi=f_Eval_CylRTPSTE(kt,rext,m,mode)
%
% This function evaluates the Round Trip Phase Shift, divided by 2 pi, for
% TE modes of an empty waveguide with circular transversal section. This
% function is based on the use of f_Eval_HDerphiapprox, which approximates
% the phase of the Hankel function of first kind. In this function it is
% necessary to keep into account the presence of the exp(x).
%
% Input parameters
%
% kt : value of kt, in order to perform the estimation ;
%
% rext : radius of the transversal section of the waveguide
%
% m : azimuthal index
%
% mode : radial index n
%
% Outputs
%
% phi : approximated RTPS
%

phi=(1+mode)*ones(1,length(kt));
ind=find(kt~=0);
if ~isempty(ind)
    thetaext=f_Eval_HDerphiapprox(kt(ind)*rext,m);
    h1ext=besselh([m;m+1],1,kt(ind)*rext,1);
    if length(ind)>1
        h1extD=-h1ext(:,2)+m./(kt(ind)*rext).'.*h1ext(:,1);
        phi(ind)=.5-(2*angle(h1extD.'.*exp(-j*thetaext))+...
            +2*kt(ind)*rext...
            +2*thetaext)/(2*pi)+mode;
    else %if length(ind)>1
        h1extD=-h1ext(2)+m./(kt(ind)*rext).'.*h1ext(1);
        h2extD=conj(h1extD);
        phi(ind)=0.5-(2*angle(h1extD.'.*exp(-j*thetaext))+...
            +2*kt(ind)*rext...
            +2*thetaext)/(2*pi)+mode;

    end %if length(ind)>1
end %if ~isempty(ind)
```

A.3 Resume of associated Legendre functions properties

Just like Bessel functions or trigonometric functions, also associated Legendre functions satisfy several relationships. First of all, a recurrence relation, which may be used for instance in spectral methods

$$(n-m+1)\,\mathrm{P}_{n+1}^{m}(x) = (2n+1)x\mathrm{P}_{n}^{m}(x) - (n+m)\mathrm{P}_{n-1}^{m}(x) \tag{A.3}$$

Another useful relationship is:

$$\left(1-x^2\right)\frac{\mathrm{d}}{\mathrm{d}x}\mathrm{P}_n^m(x) = (n+m)\mathrm{P}_{n-1}^m(x) - nx\mathrm{P}_n^m(x) \tag{A.4}$$

this permits to represent the "Legendre operator" in (2.6) and (2.7) if necessary.

Another useful property, for the evaluation of associated Legendre function derivative using associated Legendre functions of different order, is the following one;

$$\left(x^2-1\right)\frac{\mathrm{d}\mathrm{P}_p^m(x)}{\mathrm{d}x} = (p+m)\,(p-m+1)\,\sqrt{x^2-1}\,\mathrm{P}_p^{m-1}(x) \tag{A.5}$$

Finally, some important values, useful for instance to enforce boundary conditions, are

$$\mathrm{P}_n^m(1) = \begin{cases} 1, & \text{if } m = 0, \\ 0, & \text{if } m \neq 0. \end{cases} \tag{A.6}$$

$$\mathrm{P}_n^m(1) = \begin{cases} (-1)^n, & \text{if } m = 0, \\ 0, & \text{if } m \neq 0. \end{cases} \tag{A.7}$$

A.4 Properties of Gegenbauer polynomials

Solutions of equation (2.12) are Gegenbauer Polynomials[1] $G(x) = \mathrm{C}_\kappa^{(\lambda)}(x)$. Gegenbauer equation was found starting from associated Legendre function, so using m instead of λ as a parameter for identifying the solution we are interested in. However, it is possible to relate associated Legendre functions and Gegenbauer polynomials using the following formulae;

$$\begin{aligned} \mathrm{P}_n^m(x) &= \mathrm{k}_1\left(1-x^2\right)^{\frac{m}{2}}\mathrm{C}_{n-m}^{\left(m+\frac{1}{2}\right)}(x) \\ \mathrm{C}_\kappa^{(\lambda)}(x) &= \mathrm{k}_2\left(1-x^2\right)^{-\frac{\left(\lambda-\frac{1}{2}\right)}{2}}\mathrm{P}_{\kappa+\lambda-\frac{1}{2}}^{\lambda-\frac{1}{2}}(x) \end{aligned} \tag{A.8}$$

where $\mathrm{k}_{1,2}$ are two constants. The first equation shows how a Legendre function of order m and degree n is related with the Gegenbauer polynomial using n and m to identify it (it is simply (2.11) equation). The second equation is the inverse of the first one, so it relates a Gegenbauer polynomial with an associated Legendre function using κ and λ as parameters. From these two equations it is possible to deduce some relations between Gegenbauer and associated Legendre polynomials parameters;

$$\begin{aligned} m &= \lambda - \frac{1}{2} \\ \kappa &= n - m \end{aligned} \tag{A.9}$$

Gegenbauer polynomials have several useful properties. The first interesting formula gives the value of Gegenbauer polynomials in $x = 1$;

[1] also known as ultraspherical polynomials

$$\mathrm{C}_{\kappa}^{(\lambda)}(x) = \binom{\kappa + 2\lambda - 1}{\kappa} \tag{A.10}$$

this property may be useful to implement a boundary condition for $x = 1$. In order to work on $x = -1$, there is the following relationship;

$$\mathrm{C}_{\kappa}^{(\lambda)}(-x) = (-1)^{\kappa}\mathrm{C}_{\kappa}^{(\lambda)}(x) \tag{A.11}$$

Another useful property is the one which may be used to evaluate the derivative of a Gegenbauer polynomial, which is

$$\frac{\mathrm{d}}{\mathrm{d}x}\mathrm{C}_{\kappa}^{(\lambda)}(-x) = 2\lambda\mathrm{C}_{\kappa-1}^{(\lambda+1)}(x) \tag{A.12}$$

there is another relationship between derivatives of Gegenbauer polynomials;

$$\begin{aligned} \frac{\mathrm{d}}{\mathrm{d}x}\left[\mathrm{C}_{\kappa+1}^{(\lambda)}(x) - \mathrm{C}_{\kappa-1}^{(\lambda)}(x)\right] &= 2(\kappa+\lambda)\mathrm{C}_{\kappa}^{(\lambda)}(x) \\ &= 2\lambda\left[\mathrm{C}_{\kappa}^{(\lambda+1)}(x) - \mathrm{C}_{\kappa-2}^{(\lambda+1)}(x)\right] \\ &\kappa \geq 1, \mathrm{C}_{-1}^{(\lambda)}(x) = 0 \end{aligned} \tag{A.13}$$

The last differential equation shown is the actual Gegenbauer equation, which is connected to the equation in $G(x)$

$$\left(1 - x^2\right)\frac{\mathrm{d}^2}{\mathrm{d}x^2}\mathrm{C}_{\kappa}^{(\lambda)}(x) - (2\lambda+1)\frac{\mathrm{d}}{\mathrm{d}x}\mathrm{C}_{\kappa}^{(\lambda)}(x) + \kappa(\kappa+2\lambda)\mathrm{C}_{\kappa}^{(\lambda)}(x) \tag{A.14}$$

Finally, a fundamental property is the recurrence relationship between Gegenbauer polynomials, which may be used for many purposes:

$$\kappa\mathrm{C}_{\kappa}^{(\lambda)}(x) = 2(\kappa+\lambda-1)x\mathrm{C}_{\kappa-1}^{(\lambda)}(x) - (\kappa+2\lambda-2)\mathrm{C}_{\kappa-2}^{(\lambda)}(x), \quad \kappa \geq 2 \tag{A.15}$$

where

$$\begin{aligned} \mathrm{C}_{0}^{(\lambda)}(x) &= 1 \\ \mathrm{C}_{1}^{(\lambda)}(x) &= 2\lambda x \end{aligned} \tag{A.16}$$

In this study λ will equal $n\frac{\pi}{2}$, where n is an odd integer number. κ may be either integer or non-integer, depending on the considered calculations. Most of the time Gegenbauer polynomials will be used as expansion or test functions, not as solutions of Gegenbauer equations, so κ will be an integer number and so it will be renamed as n, for coherence with previous cases.

A.5 Chebyshev polynomials

In order to implement numerical methods based on Chebyshev polynomials of first kind $\mathrm{T}_n(x)$ (which will be named simply "Chebyshev polynomials"), it may be useful to introduce their most significative relationships.

Chebyshev polynomials can be generated using the following trigonometric definition

$$\mathrm{T}_n(\cos\vartheta) = \cos(n\vartheta) \tag{A.17}$$

where

$$x = \cos\vartheta$$

so

$$\mathrm{T}_n(x) = \cos(n \arccos\vartheta) \tag{A.18}$$

Moreover, there is a recurrence relationship for the computation of Chebyshev polynomials. Given

$$\mathrm{T}_0(x) = 1 \quad \mathrm{T}_1(x) = x$$

it is possible to compute all other Chebyshev polynomials as

$$\mathrm{T}_{n+1}(x) = 2x\mathrm{T}_n(x) - \mathrm{T}_{n-1}(x) \tag{A.19}$$

About remarkable values, it may be shown that

$$\mathrm{T}_n(1) = 1 \tag{A.20}$$

Furthermore, Chebyshev polynomials of even order are even functions, of odd order are odd functions.

$$\mathrm{T}_n(-x) = (-1)^n\mathrm{T}_n(x) \tag{A.21}$$

so, for the $x = -1$,

$$\mathrm{T}_n(-1) = (-1)^n \tag{A.22}$$

Finally, there is a differential relationship between Chebyshev polynomials of first and second kind $\mathrm{U}_n(x)$

$$\frac{\mathrm{d}}{\mathrm{d}x}\mathrm{T}_n(x) = n\mathrm{U}_{n-1}(x), \quad n = 1, 2... \tag{A.23}$$

There are recurrence relationships for Chebyshev polynomials of the second kind too; considering that

$$\mathrm{U}_0(x) = 1 \quad \mathrm{U}_1(x) = 2x$$

it may be proved that

$$\mathrm{U}_{n+1}(x) = 2x\mathrm{U}_n(x) - \mathrm{U}_{n-1}(x) \tag{A.24}$$

Finally, about the boundary values of Chebyshev polynomials of second kind

$$\mathrm{U}_n(1) = n + 1 \tag{A.25}$$

$$\mathrm{U}_n(-1) = (-1)^n \mathrm{U}_n(x) = (-1)^n (n+1) \tag{A.26}$$

Those formulae can be used together in order to find the boundary value of the derivative of Chebyshev polynomials. In fact,

$$\frac{\mathrm{d}}{\mathrm{d}x}\mathrm{T}_n(x)\bigg|_{x=-1} = n\mathrm{U}_{n-1}(-1) = n^2(-1)^{n-1} \tag{A.27}$$

A.6 Interval mapping

Orthogonal polynomials are solutions of differential equations with singularities which are located in $x = \pm 1$. Therefore, the interval $\xi \in [-1; 1]$ is called **canonical interval** . On the other hand, for this study the interesting interval is usually $x \in [x_0, 1]$.

Numerical methods belonging to both pseudospectral and spectral families are easier to apply to differential equations (with appropriate boundary conditions) defined in ξ interval; therefore, the equation has to be re-written using ξ instead of x as independent variable. To sum up, the procedure is:

1. find the mapping function from ξ interval $[-1, 1]$ to x interval $[x_0, 1]$;
2. re-write the differential equation in ξ variable;
3. solve it by applying a numerical method;
4. represent the solution in the natural interval x.

The mapping function may be basically any function which maps $x = x_0$ and $x = x_1$ points in $\xi = -1$ and $\xi = +1$ points respectively. The first idea is to use a linear transformation:

$$x = J_1\xi + J_0 \tag{A.28}$$

so, considering two points x_0 and x_1, where x_1 will be mapped in $+1$ at the end of the calculations,

$$\begin{cases} x_0 = -a + b \\ x_1 = a + b \end{cases}$$

from which:

$$\begin{aligned} x_1 + x_0 &= 2b \\ \Longrightarrow b = J_0 &= \frac{x_1 + x_0}{2} \end{aligned} \tag{A.29}$$

$$\begin{aligned} x_1 - x_0 &= 2a \\ \Longrightarrow a = J_1 &= \frac{x_1 - x_0}{2} \end{aligned} \tag{A.30}$$

Now it is possible to substitute x with (A.28). The last problem is the representation of the derivatives.

$$\begin{aligned} \frac{\mathrm{d}G(x)}{\mathrm{d}x} &= \frac{\mathrm{d}G(\xi)}{\mathrm{d}\xi}\frac{\mathrm{d}\xi}{\mathrm{d}x} = \frac{\mathrm{d}G(\xi)}{\mathrm{d}\xi}\left(\frac{\mathrm{d}x}{\mathrm{d}\xi}\right)^{-1} = \\ &= \frac{1}{J_1}\frac{\mathrm{d}G(\xi)}{\mathrm{d}\xi} \end{aligned} \tag{A.31}$$

$$\begin{aligned} \frac{\mathrm{d}^2G(x)}{\mathrm{d}x^2} &= \frac{\mathrm{d}}{\mathrm{d}x}\left[\frac{\mathrm{d}G(x)}{\mathrm{d}x}\right] = \frac{\mathrm{d}}{\mathrm{d}x}\left[\frac{1}{J_1}\frac{\mathrm{d}G(\xi)}{\mathrm{d}\xi}\right] = \\ &= \frac{1}{J_1^2}\frac{\mathrm{d}^2G(\xi)}{\mathrm{d}\xi^2} \end{aligned} \tag{A.32}$$

APPENDIX B

Appendix of Chapters 3 and 4

B.1 A vector integral theorem

Here is reported the proof of the integral vector theorem used in Subsection 4.2.1 for the application of Galerkin method. Given a vector field $\underline{F}$ defined as

$$\underline{F} = F_1\hat{\mathrm{x}} + F_2\hat{\mathrm{y}}$$

and a set of test functions $\{v_i\}$, where $F_1, F_2, v_i \in \mathrm{C}^{(1)}(\Sigma)$, Σ is an open domain, $\Sigma \subset \mathbb{R}^2$, where $\partial\Sigma$ is defined as a simple, piece-wise regular closed arch γ, counterclockwise,

$$\iint_{\Sigma}\left[\frac{\partial F_2}{\partial x} - \frac{\partial F_1}{\partial y}\right] v\,\mathrm{d}x\mathrm{d}y = -\iint_{\Sigma}\left[F_2\frac{\partial v}{\partial x} - F_1\frac{\partial v}{\partial y}\right]\mathrm{d}x\mathrm{d}y + \oint_{\gamma}(\underline{F}v)\cdot\mathrm{d}\underline{s} \tag{B.1}$$

Proof

Given $\underline{F}$ a vector field and v a scalar function, there is the following vector relationship;

$$\nabla_{\mathrm{t}} \times (\underline{F}v) = (\nabla_{\mathrm{t}} v) \times \underline{F} + (\nabla_{\mathrm{t}} \times \underline{F})\, v \tag{B.2}$$

Another useful relationship is the scalar Stokes theorem;

$$\iint_{\Sigma}[\nabla \times \underline{F}]\cdot\hat{\mathrm{z}}\,\mathrm{d}\Sigma = \oint_{\gamma}\underline{F}\cdot\mathrm{d}\underline{s} \tag{B.3}$$

It is possible to re-write the integrand as follows;

$$\nabla \times \underline{F} = -\hat{\mathrm{x}}\frac{\partial F_2}{\partial x} + \hat{\mathrm{y}}\frac{\partial F_1}{\partial z} + \hat{\mathrm{z}}\left(\frac{\partial F_2}{\partial x} - \frac{\partial F_1}{\partial y}\right)$$

then, considering the "$\hat{\mathrm{z}}\cdot$" operation, the equation becomes

$$\iint_{\Sigma} \left[\frac{\partial F_2}{\partial x} - \frac{\partial F_1}{\partial y} \right] \mathrm{d}x\mathrm{d}y = \oint_{\gamma} \underline{F} \cdot \mathrm{d}\underline{s} \tag{B.4}$$

So, by substituting (B.4) in (B.2),

$$\oint_{\gamma} (\underline{F}v) \cdot \mathrm{d}\underline{s} = \iint_{\Sigma} [\nabla \times (\underline{F}v)] \cdot \hat{\mathrm{z}}\, \mathrm{d}\Sigma =$$
$$= \iint_{\Sigma} [(\nabla_{\mathrm{t}} v) \times \underline{F}] \cdot \hat{\mathrm{z}}\, \mathrm{d}\Sigma + \iint_{\Sigma} [\nabla_{\mathrm{t}} \times \underline{F}]\, v\, \mathrm{d}\Sigma$$

then,

$$\iint_{\Sigma} [\nabla_{\mathrm{t}} \times \underline{F}]\, v\, \mathrm{d}\Sigma = - \iint_{\Sigma} [(\nabla_{\mathrm{t}} v) \times \underline{F}] \cdot \hat{\mathrm{z}}\, \mathrm{d}\Sigma + \oint_{\gamma} (\underline{F}v) \cdot \mathrm{d}\underline{s}$$

Now, integrands belonging to the first and to the second integrals can be re-written by components; considering the second one,

$$(\nabla_{\mathrm{t}} v) \times \underline{F} = \hat{\mathrm{z}} \cdot \left[\left(\frac{\partial v}{\partial x} \hat{\mathrm{x}} + \frac{\partial v}{\partial y} \hat{\mathrm{y}} \right) \times (F_1 \hat{\mathrm{x}} + F_2 \hat{\mathrm{y}}) \right] =$$
$$= F_2 \frac{\partial v}{\partial x} - F_1 \frac{\partial v}{\partial y}$$

therefore, by substituting this expression (and the previous one) in the last integral expression, it is possible to find (B.1).

B.2 Computation of a line integral

In this section are shown steps necessary to reach results shown in Subsection 4.2.2.

$$\int_{t_{a_{\mathrm{wg}(1)}}}^{t_{b_{\mathrm{wg}(1)}}} \left[\underline{E}_{\mathrm{t,wg}} (\underline{s}(t))\, v_{\beta}^{(\mathrm{h})} (\underline{s}(t)) \right] \cdot \underline{s}'(t) \mathrm{d}t$$

As it is possible to see from Figure 4.1, the integral relative to the port (1) must be done starting from the upper point $(\rho_{\mathrm{wg}(1)}, 0)$, ending to the lower point $(0, 0)$ (considering the (ρ, z) plane). Furthermore, the piece of curve $\underline{s}(t)$ which connects these two points is a piece of a straight line. So, it is possible to write

$$\underline{s}(t) = -\hat{\rho}\gamma(t)$$

where $\gamma(t)$ is the equation of a straight line in t which satisfies

$$\begin{cases} \underline{s}(t_{a_{\mathrm{wg}(1)}}) = -\hat{\rho}\gamma(t_{a_{\mathrm{wg}(1)}}) = \hat{\rho}\, \rho_{\mathrm{wg}(1)} \\ \underline{s}(t_{b_{\mathrm{wg}(1)}}) = -\hat{\rho}\gamma(t_{b_{\mathrm{wg}(1)}}) = \hat{\rho}\, 0 = 0 \end{cases}$$

so

$$\begin{cases} \gamma(t_{a_{\mathrm{wg}^{(1)}}}) = -\rho_{\mathrm{wg}^{(1)}} \\ \gamma(t_{b_{\mathrm{wg}^{(1)}}}) = 0 \end{cases}$$

The straight line which satisfies previous equations can be calculated as follows

$$\frac{\gamma(t) - (-\rho_{\mathrm{wg}^{(1)}})}{0 - (-\rho_{\mathrm{wg}^{(1)}})} = \frac{t - t_{a_{\mathrm{wg}^{(1)}}}}{t_{b_{\mathrm{wg}^{(1)}}} - t_{a_{\mathrm{wg}^{(1)}}}}$$

so

$$\gamma(t) = \frac{\rho_{\mathrm{wg}^{(1)}}}{t_{b_{\mathrm{wg}^{(1)}}} - t_{a_{\mathrm{wg}^{(1)}}}}(t - t_{a_{\mathrm{wg}^{(1)}}}) - \rho_{\mathrm{wg}^{(1)}}$$

This is the most general choice for $\gamma(t)$. The smartest choice implies the use of canonical integral bounds.

$$\begin{cases} t_{a_{\mathrm{wg}^{(1)}}} = 0 \\ t_{b_{\mathrm{wg}^{(1)}}} = 1 \end{cases}$$

so, the parametric curve becomes

$$\gamma(t) = \rho_{\mathrm{wg}^{(1)}} t - \rho_{\mathrm{wg}^{(1)}}$$

And

$$\underline{s}(t) = -\hat{\rho}\left[\rho_{\mathrm{wg}^{(1)}} t - \rho_{\mathrm{wg}^{(1)}}\right] \Longrightarrow \mathrm{d}\underline{s}(t) = -\hat{\rho}\rho_{\mathrm{wg}^{(1)}}\mathrm{d}t$$

Finally, keeping into account all these considerations, the integral becomes

$$\begin{aligned} &\int_{t_{a_{\mathrm{wg}^{(1)}}}}^{t_{b_{\mathrm{wg}^{(1)}}}} \left[\underline{E}_{\mathrm{t,wg}}\left(\underline{s}(t)\right) v_{\beta}^{(\mathrm{h})}\left(\underline{s}(t)\right)\right] \cdot \underline{s}'(t)\mathrm{d}t \\ &= \int_{0}^{1} \left[\underline{E}_{\mathrm{t,wg}}\left(-\hat{\rho}\left(\rho_{\mathrm{wg}^{(1)}} t - \rho_{\mathrm{wg}^{(1)}}\right)\right) v_{\beta}^{(\mathrm{h})}\left(-\hat{\rho}\left(\rho_{\mathrm{wg}^{(1)}} t - \rho_{\mathrm{wg}^{(1)}}\right)\right)\right] \cdot \left[-\hat{\rho}\rho_{\mathrm{wg}^{(1)}}\right] \mathrm{d}t = \\ &= -\int_{0}^{1} \left[E_{\rho,\mathrm{wg}}\left(-\hat{\rho}\left(\rho_{\mathrm{wg}^{(1)}} t - \rho_{\mathrm{wg}^{(1)}}\right)\right) v_{\beta}^{(\mathrm{h})}\left(-\hat{\rho}\left(\rho_{\mathrm{wg}^{(1)}} t - \rho_{\mathrm{wg}^{(1)}}\right)\right)\right] \rho_{\mathrm{wg}^{(1)}}\mathrm{d}t \end{aligned}$$

Now, it is possible to proceed, defining the following change of variable;

$$\tau = \rho_{\mathrm{wg}^{(1)}} t - \rho_{\mathrm{wg}^{(1)}} \Longrightarrow \mathrm{d}\tau = -\rho_{\mathrm{wg}^{(1)}}$$

so, for $t = 1$, $\tau = 0$, and for $t = 0$, $\tau = -\rho_{\mathrm{wg}^{(1)}}$. Moreover,

$$\mathrm{d}t = \frac{1}{\rho_{\mathrm{wg}^{(1)}}}\mathrm{d}\tau$$

so

$$= -\int_{-\rho_{\mathrm{wg}^{(1)}}}^{0} \left[E_{\rho,\mathrm{wg}}\left(-\hat{\rho}\tau\right) v_{\beta}^{(\mathrm{h})}\left(-\hat{\rho}\tau\right)\right] \mathrm{d}\tau$$

Finally, with a last change of variable, $\rho = -\tau$, which implies $\mathrm{d}\tau = -\mathrm{d}\rho$, it is obtained

$$\int_{t_{a_{\mathrm{wg}^{(1)}}}}^{t_{b_{\mathrm{wg}^{(1)}}}} \left[\underline{E}_{\mathrm{t,wg}}\left(\underline{s}(t)\right) v_{\beta}^{(\mathrm{h})}\left(\underline{s}(t)\right)\right] \cdot \underline{s}'(t)\mathrm{d}t = -\int_{0}^{\rho_{\mathrm{wg}^{(1)}}} E_{\rho,\mathrm{wg}}(\rho, z_{\mathrm{wg}^{(1)}}) v_{\beta}^{(\mathrm{h})}(\rho, z_{\mathrm{wg}^{(1)}})\mathrm{d}\rho$$

B.3 Determination of modal eigenfunctions for the circular waveguide

Usually, the generating functions Φ_{mn} and Ψ_{mn} of the modal eigenfunctions for TM and TE modes, are provided for linear polarization:

$$\Phi_{mn} = A_{mn}\,\mathrm{J}_m(k'_{\mathrm{t},i}\rho) \begin{matrix}\cos\\ \sin\end{matrix} m\varphi$$

$$\Psi_{mn} = B_{mn}\,\mathrm{J}_m(k''_{\mathrm{t},i}\rho) \begin{matrix}\cos\\ \sin\end{matrix} m\varphi$$

In Chapter 4 circularly polarized fields have been considered, since the dependance on the azimuthal coordinate φ is assumed to be $\mathrm{e}^{+\mathrm{j}m\varphi}$. Therefore, in this case,

$$\begin{aligned}\Phi_{mn} &= A_{mn}\,\mathrm{J}_m(k'_{\mathrm{t},i}\rho)\,\mathrm{e}^{+\mathrm{j}m\varphi}\\ \Psi_{mn} &= B_{mn}\,\mathrm{J}_m(k''_{\mathrm{t},i}\rho)\,\mathrm{e}^{+\mathrm{j}m\varphi}\end{aligned} \tag{B.5}$$

The objective of this section is to calculate A_{mn} and B_{mn}, in this case.

Starting with Φ_{mn}, given a the radius of the transversal section of the waveguide,

$$\begin{aligned}\langle\Phi_i, \Phi_j\rangle &= \int_0^{2\pi}\int_0^a \Phi_i\Phi_j^*\rho\mathrm{d}\rho\mathrm{d}\varphi = \delta_{ij}\int_0^{2\pi}\int_0^a A_{mn}^2\mathrm{J}_m^2(k'_{\mathrm{t},i}\rho)\mathrm{e}^{+\mathrm{j}m\varphi}\mathrm{e}^{-\mathrm{j}m\varphi}\rho\mathrm{d}\rho\mathrm{d}\varphi\\ &= A_{mn}^2\delta_{ij}\int_0^{2\pi}\mathrm{d}\varphi\int_0^a \rho\mathrm{J}_m^2(k'_{\mathrm{t},i}\rho)\mathrm{d}\rho = 2\pi\delta_{ij}A_{mn}^2\int_0^a \rho\mathrm{J}_m^2(k'_{\mathrm{t},i}\rho)\mathrm{d}\rho\end{aligned}$$

where i and j are multiple indexes, of type (m, n).

Recalling the following integral formula relative to Bessel functions,

$$\int_0^x Z_n^2(kx)x\mathrm{d}x = \frac{x^2}{2}\left[\frac{\mathrm{d}}{\mathrm{d}x}Z_n(x) + \left(1 - \frac{n^2}{k^2x^2}\right)Z_n^2(kx)\right]$$

one contribution goes to zero (in fact, $\mathrm{J}_m(k'_{\mathrm{t},i}a) = 0$, since $k'_{\mathrm{t},i} = \frac{\chi_{mn}}{a}$, where χ_{mn} is the n-th zero of the m-order Bessel function of first kind), this integral is known in closed form, and the result is

$$\langle\Phi_i, \Phi_j\rangle = \pi A_{mn}^2 a^2\left[\mathrm{J}_{m+1}(k'_{\mathrm{t},i}a)\right]^2$$

therefore,

$$A_{mn} = \frac{1}{\sqrt{\pi}} \frac{1}{a\,\mathrm{J}_{m+1}(k'_{\mathrm{t},i}a)} \tag{B.6}$$

It is possible to repeat the same procedure on Ψ_{mn}, and the result is, considering again Lommel's formula (where one integral vanishes, since $k''_{\mathrm{t},i} = \frac{\chi'_{mn}}{a}$, where χ'_{mn} is the n-th zero of the first derivative of the m-order Bessel function of first kind), obtaining

$$B_{mn} = \frac{1}{\sqrt{\pi}} \frac{\chi'_{mn}}{\sqrt{\chi'^2_{mn} - m^2}} \frac{1}{a\,\mathrm{J}_m(k''_{\mathrm{t},i}a)} \tag{B.7}$$

So

$$\begin{aligned} \Phi_{mn} &= \frac{1}{\sqrt{\pi}} \frac{\mathrm{J}_m(k'_{\mathrm{t},i}\rho)}{a\,\mathrm{J}_{m+1}(k'_{\mathrm{t},i}a)} \mathrm{e}^{+\mathrm{j}m\varphi} \\ \Psi_{mn} &= \frac{1}{\sqrt{\pi}} \frac{\chi'_{mn}}{\sqrt{\chi'^2_{mn} - m^2}} \frac{\mathrm{J}_m(k''_{\mathrm{t},i}\rho)}{a\,\mathrm{J}_m(k''_{\mathrm{t},i}a)} \mathrm{e}^{+\mathrm{j}m\varphi} \end{aligned} \tag{B.8}$$

The objective is to evaluate $\underline{e}'_i(\underline{\rho})$, $\underline{h}'_i(\underline{\rho})$, $\underline{h}''_i(\underline{\rho})$, $\underline{e}''_i(\underline{\rho})$. There are some relationships between eigenfunctions, which are recalled here

$$\begin{aligned} \underline{e}'_i(\underline{\rho}) &= -\frac{\nabla_{\mathrm{t}}\Phi_i(\underline{\rho})}{k'_{\mathrm{t},i}} \\ \underline{h}''_i(\underline{\rho}) &= -\frac{\nabla_{\mathrm{t}}\Psi_i(\underline{\rho})}{k''_{\mathrm{t},i}} \end{aligned} \tag{B.9}$$

and some impedance conditions between modal eigenfunctions

$$\begin{aligned} \underline{h}'_i(\underline{\rho}) &= \hat{\mathrm{z}} \times \underline{e}'_i(\underline{\rho}) \\ \underline{e}''_i(\underline{\rho}) &= \underline{h}''(\underline{\rho}) \times \hat{\mathrm{z}} \end{aligned} \tag{B.10}$$

Finally, the gradient in cylindrical coordinates equals

$$\nabla_{\mathrm{t}} f = \frac{\partial f}{\partial \rho}\hat{\rho} + \frac{1}{\rho}\frac{\partial f}{\partial \varphi}\hat{\varphi} \tag{B.11}$$

TM modes

$$\begin{aligned} \underline{e}'_i(\underline{\rho}) &= -\frac{1}{k'_{\mathrm{t},i}} \left[\frac{1}{\sqrt{\pi}} k'_{\mathrm{t},i} \frac{\mathrm{J}'_m(k'_{\mathrm{t},i}\rho)}{a\,\mathrm{J}_{m+1}(k'_{\mathrm{t},i}a)} \mathrm{e}^{+\mathrm{j}m\varphi}, \quad \frac{1}{\rho}\frac{\mathrm{j}m}{\sqrt{\pi}} \frac{\mathrm{J}_m(k'_{\mathrm{t},i}\rho)}{a\,\mathrm{J}_{m+1}(k'_{\mathrm{t},i}a)} \mathrm{e}^{+\mathrm{j}m\varphi} \right] = \\ &= \left[-\frac{1}{\sqrt{\pi}} \frac{\mathrm{J}'_m(k'_{\mathrm{t},i}\rho)}{a\mathrm{J}_{m+1}(k'_{\mathrm{t},i}a)} \mathrm{e}^{+\mathrm{j}m\varphi}, \quad \frac{-\mathrm{j}m}{\sqrt{\pi}k'_{\mathrm{t},i}a} \frac{\mathrm{J}_m(k'_{\mathrm{t},i}\rho)}{\rho\,\mathrm{J}_{m+1}(k'_{\mathrm{t},i}a)} \mathrm{e}^{+\mathrm{j}m\varphi} \right] \end{aligned} \tag{B.12}$$

so,

$$\underline{h}'_i = \hat{\mathrm{z}} \times \underline{e}'_i = \hat{\rho}\left(-e'_\varphi\right) - \hat{\varphi}\left(-e'_\rho\right)$$

so, finally,

$$\begin{cases} h'_\rho = -e'_\varphi \\ h'_\varphi = e'_\rho \end{cases} \tag{B.13}$$

TE modes

$$\begin{aligned} \underline{h}''_i(\underline{\rho}) &= -\frac{1}{k''_{\mathrm{t},i}} \left[\frac{k''_{\mathrm{t},i}}{\sqrt{\pi}} \frac{\chi'_{mn}}{\sqrt{\chi'^2_{mn} - m^2}} \frac{\mathrm{J}'_m(k''_{\mathrm{t},i}\rho)}{a\,\mathrm{J}_m(k''_{\mathrm{t},i}a)} \mathrm{e}^{+\mathrm{j}m\varphi}, \quad \frac{1}{\rho} \frac{\mathrm{j}m}{\sqrt{\pi}} \frac{\chi'_{mn}}{\sqrt{\chi'^2_{mn} - m^2}} \frac{\mathrm{J}_m(k''_{\mathrm{t},i}\rho)}{a\,\mathrm{J}_m(k''_{\mathrm{t},i}a)} \mathrm{e}^{+\mathrm{j}m\varphi} \right] = \\ &= \left[-\frac{k''_{\mathrm{t},i}}{\sqrt{\pi}} \frac{1}{\sqrt{(k''_{\mathrm{t},i}a)^2 - m^2}} \frac{\mathrm{J}'_m(k''_{\mathrm{t},i}\rho)}{\mathrm{J}_m(k''_{\mathrm{t},i}a)} \mathrm{e}^{+\mathrm{j}m\varphi}, \quad \frac{-\mathrm{j}m}{\sqrt{\pi}} \frac{1}{\sqrt{(k''_{\mathrm{t},i}a)^2 - m^2}} \frac{\mathrm{J}_m(k''_{\mathrm{t},i}\rho)}{\rho\,\mathrm{J}_m(k''_{\mathrm{t},i}a)} \mathrm{e}^{+\mathrm{j}m\varphi} \right] \end{aligned} \tag{B.14}$$

Then, since

$$\underline{h}''_i = \begin{bmatrix} h''_\rho, & h''_\varphi, & 0 \end{bmatrix}$$

so,

$$\underline{e}''_i = \underline{h}''_i \times \hat{\mathrm{z}} = \hat{\rho}\left(h''_\varphi\right) - \hat{\varphi}\left(-h''_\rho\right)$$

so, finally,

$$\begin{cases} e''_\rho = h''_\varphi \\ e''_\varphi = -h''_\rho \end{cases} \tag{B.15}$$

B.3.1 Derivatives of modal eigenfunctions

It may be interesting to evaluate the expression of the derivatives of modal eigenfunctions with respect to ρ; in fact, along φ, the derivative operation of each one of the eigenfunctions is trivial.

Derivatives of TM eigenfunctions

The first component which can be derived along ρ is e'_ρ.

$$\begin{aligned} \frac{\partial e'_\rho}{\partial \rho} &= -\frac{1}{a\sqrt{\pi}\mathrm{J}_{m+1}(k'_{\mathrm{t},i}a)} \frac{\partial}{\partial \rho} \mathrm{J}'_m(k'_{\mathrm{t},i}\rho) = \\ &= -\frac{k'_{\mathrm{t},i}}{a\sqrt{\pi}\mathrm{J}_{m+1}(k'_{\mathrm{t},i}a)} \mathrm{J}''_m(k'_{\mathrm{t},i}\rho) \end{aligned}$$

It is possible to find an expression of $\mathrm{J}''_m(k'_{\mathrm{t},i}\rho)$ using the following trick; recalling the Bessel equation from [1],

$$x^2\mathrm{J}''_m(x) + x\mathrm{J}'_m(x) + (x^2 - m^2)\mathrm{J}_m(x) = 0$$

this can be re-written isolating the second derivative with respect to the whole argument at the left-hand member of the equation, obtaining

$$\mathrm{J}''_m(x) = -\frac{1}{x} J'_m(x) - \left(1 - \frac{m^2}{x^2}\right) J_m(x)$$

where $x = k'_{\mathrm{t},i}\rho$; "prime" and "second" apexes indicate the first and the second derivative with respect to the whole argument x respectively. This can be applied to the previous calculation, obtaining

$$\frac{\partial e'_\rho}{\partial \rho} = -\frac{k'_{\mathrm{t},i}}{a\sqrt{\pi}\mathrm{J}_{m+1}(k'_{\mathrm{t},i}a)} \left[-\frac{1}{k'_{\mathrm{t},i}\rho}\mathrm{J}'_m(k'_{\mathrm{t},i}\rho) - \left(1 - \frac{m^2}{k'^2_{\mathrm{t},i}\rho^2}\right)\mathrm{J}_m(k'_{\mathrm{t},i}\rho)\right]$$

This procedure can be applied to other components, when necessary. The following component which has to be differentiated is e'_φ, as follows

$$\frac{\partial e'_\varphi}{\partial \rho} = \frac{\mathrm{j}m}{\sqrt{\pi}k'_{\mathrm{t},i}a\mathrm{J}_{m+1}(k'_{\mathrm{t},i}a)} \left[-\frac{1}{\rho^2}\mathrm{J}_m(k'_{\mathrm{t},i}\rho) + k'_{\mathrm{t},i}\frac{\mathrm{J}'_m(k'_{\mathrm{t},i}\rho)}{\rho}\right]$$

Then, conditions (B.13) can be applied to derivatives too, since the derivation operator is linear.

Derivatives of TE eigenfunctions

Using the same derivation procedure, it is possible to obtain

$$\frac{\partial e''_\varphi}{\partial \rho} = \frac{k''_{\mathrm{t},i}}{\sqrt{\pi}\sqrt{(k''_{\mathrm{t},i}\rho)^2 - m^2}\mathrm{J}_m(k''_{\mathrm{t},i}a)} k''_{\mathrm{t},i} \left[-\frac{1}{k''_{\mathrm{t},i}a}\mathrm{J}'_m(k''_{\mathrm{t},i}\rho) - \left(1 - \frac{m^2}{k''^2_{\mathrm{t},i}\rho^2}\right)\mathrm{J}_m(k''_{\mathrm{t},i}\rho)\right]$$

$$\frac{\partial h''_\varphi}{\partial \rho} = \frac{\mathrm{j}m}{\sqrt{\pi}\sqrt{(k''_{\mathrm{t},i}a)^2 - m^2}\mathrm{J}_m(k''_{\mathrm{t},i}a)} \left[-\frac{1}{\rho^2}\mathrm{J}_m(k''_{\mathrm{t},i}\rho) + \frac{1}{\rho}k''_{\mathrm{t},i}\mathrm{J}'_m(k''_{\mathrm{t},i}\rho)\right]$$

Where, for the determination of remaining components, it is possible to use (B.15) relationships.

Resume of circular waveguide mode functions

Considering the $\mathrm{e}^{+\mathrm{j}m\varphi}$ polarization, modal eigenfunctions are, for TM modes:

$$\begin{aligned}
e'_\rho &= -\frac{1}{\sqrt{\pi}} \frac{\mathrm{J}'_m(k'_{\mathrm{t},i}\rho)}{a\mathrm{J}_{m+1}(k'_{\mathrm{t},i}a)} \mathrm{e}^{+\mathrm{j}m\varphi} \\
e'_\varphi &= \frac{-\mathrm{j}m}{\sqrt{\pi}k'_{\mathrm{t},i}a} \frac{\mathrm{J}_m(k'_{\mathrm{t},i}\rho)}{\rho\,\mathrm{J}_{m+1}(k'_{\mathrm{t},i}a)} \mathrm{e}^{+\mathrm{j}m\varphi} \\
h'_\rho &= \frac{\mathrm{j}m}{\sqrt{\pi}k'_{\mathrm{t},i}a} \frac{\mathrm{J}_m(k'_{\mathrm{t},i}\rho)}{\rho\,\mathrm{J}_{m+1}(k'_{\mathrm{t},i}a)} \mathrm{e}^{+\mathrm{j}m\varphi} \\
h'_\varphi &= -\frac{1}{\sqrt{\pi}} \frac{\mathrm{J}'_m(k'_{\mathrm{t},i}\rho)}{a\mathrm{J}_{m+1}(k'_{\mathrm{t},i}a)} \mathrm{e}^{+\mathrm{j}m\varphi}
\end{aligned}$$

and, for TE modes:

$$
\begin{aligned}
e''_{\rho} &= \frac{-\mathrm{j}m}{\sqrt{\pi}} \frac{1}{\sqrt{(k''_{\mathrm{t},i}a)^2 - m^2}} \frac{\mathrm{J}_m(k''_{\mathrm{t},i}\rho)}{\rho\,\mathrm{J}_m(k''_{\mathrm{t},i}a)} \mathrm{e}^{+\mathrm{j}m\varphi} \\
e''_{\varphi} &= \frac{k''_{\mathrm{t},i}}{\sqrt{\pi}} \frac{1}{\sqrt{(k''_{\mathrm{t},i}a)^2 - m^2}} \frac{\mathrm{J}'_m(k''_{\mathrm{t},i}\rho)}{\mathrm{J}_m(k''_{\mathrm{t},i}a)} \mathrm{e}^{+\mathrm{j}m\varphi} \\
h''_{\rho} &= -\frac{k''_{\mathrm{t},i}}{\sqrt{\pi}} \frac{1}{\sqrt{(k''_{\mathrm{t},i}a)^2 - m^2}} \frac{\mathrm{J}'_m(k''_{\mathrm{t},i}\rho)}{\mathrm{J}_m(k''_{\mathrm{t},i}a)} \mathrm{e}^{+\mathrm{j}m\varphi} \\
h''_{\varphi} &= \frac{-\mathrm{j}m}{\sqrt{\pi}} \frac{1}{\sqrt{(k''_{\mathrm{t},i}a)^2 - m^2}} \frac{\mathrm{J}_m(k''_{\mathrm{t},i}\rho)}{\rho\,\mathrm{J}_m(k''_{\mathrm{t},i}a)} \mathrm{e}^{+\mathrm{j}m\varphi}
\end{aligned}
$$

These formulas can be re-written, considering the $\mathrm{e}^{-\mathrm{j}m\varphi}$ polarization, as follows; for TM modes:

$$
\begin{aligned}
e'_{\rho} &= -\frac{1}{\sqrt{\pi}} \frac{\mathrm{J}'_m(k'_{\mathrm{t},i}\rho)}{a\mathrm{J}_{m+1}(k'_{\mathrm{t},i}a)} \mathrm{e}^{-\mathrm{j}m\varphi} \\
e'_{\varphi} &= \frac{\mathrm{j}m}{\sqrt{\pi}k'_{\mathrm{t},i}a} \frac{\mathrm{J}_m(k'_{\mathrm{t},i}\rho)}{\rho\,\mathrm{J}_{m+1}(k'_{\mathrm{t},i}a)} \mathrm{e}^{-\mathrm{j}m\varphi} \\
h'_{\rho} &= -\frac{\mathrm{j}m}{\sqrt{\pi}k'_{\mathrm{t},i}a} \frac{\mathrm{J}_m(k'_{\mathrm{t},i}\rho)}{\rho\,\mathrm{J}_{m+1}(k'_{\mathrm{t},i}a)} \mathrm{e}^{-\mathrm{j}m\varphi} \\
h'_{\varphi} &= -\frac{1}{\sqrt{\pi}} \frac{\mathrm{J}'_m(k'_{\mathrm{t},i}\rho)}{a\mathrm{J}_{m+1}(k'_{\mathrm{t},i}a)} \mathrm{e}^{-\mathrm{j}m\varphi}
\end{aligned}
$$

and, for TE modes:

$$
\begin{aligned}
e''_{\rho} &= \frac{\mathrm{j}m}{\sqrt{\pi}} \frac{1}{\sqrt{(k''_{\mathrm{t},i}a)^2 - m^2}} \frac{\mathrm{J}_m(k''_{\mathrm{t},i}\rho)}{\rho\,\mathrm{J}_m(k''_{\mathrm{t},i}a)} \mathrm{e}^{-\mathrm{j}m\varphi} \\
e''_{\varphi} &= \frac{k''_{\mathrm{t},i}}{\sqrt{\pi}} \frac{1}{\sqrt{(k''_{\mathrm{t},i}a)^2 - m^2}} \frac{\mathrm{J}'_m(k''_{\mathrm{t},i}\rho)}{\mathrm{J}_m(k''_{\mathrm{t},i}a)} \mathrm{e}^{-\mathrm{j}m\varphi} \\
h''_{\rho} &= -\frac{k''_{\mathrm{t},i}}{\sqrt{\pi}} \frac{1}{\sqrt{(k''_{\mathrm{t},i}a)^2 - m^2}} \frac{\mathrm{J}'_m(k''_{\mathrm{t},i}\rho)}{\mathrm{J}_m(k''_{\mathrm{t},i}a)} \mathrm{e}^{-\mathrm{j}m\varphi} \\
h''_{\varphi} &= \frac{\mathrm{j}m}{\sqrt{\pi}} \frac{1}{\sqrt{(k''_{\mathrm{t},i}a)^2 - m^2}} \frac{\mathrm{J}_m(k''_{\mathrm{t},i}\rho)}{\rho\,\mathrm{J}_m(k''_{\mathrm{t},i}a)} \mathrm{e}^{-\mathrm{j}m\varphi}
\end{aligned}
$$

B.4 Verification of boundary conditions

In Section 4.3 we found the boundary condition (4.56) for the H_φ component of the electromagnetic field, which must be satisfied in every PEC surface of the structure.

This condition is here recalled

$$H_\varphi \sin\vartheta + \rho\frac{\partial H_\varphi}{\partial \rho}\sin\vartheta + \rho\frac{\partial H_\varphi}{\partial z}\cos\vartheta = \\ = H_\varphi \sin\vartheta + \rho\frac{\partial H_\varphi}{\partial \nu} = 0$$

Since this condition is applicable to each cylindrical structure, it is possible to verify its validity on a circular waveguide, using as H_φ the mode functions of the circular waveguide. Indeed, they are solutions of Maxwell equations in the cylindrical domain, therefore they must satisfy this condition.

About the condition $E_\varphi = 0$, the verification is trivial; in fact, it is implicit in the definition of modal eigenfunctions. Recalling from the previous section the expressions of modal eigenfunctions, it is necessary to verify

$$h_\varphi \sin\vartheta + \rho\frac{\partial h_\varphi}{\partial \nu} = 0$$

By considering the fact that this verification is performed on the waveguide boundary, i.e. for $\vartheta = 90°$ and $\rho = a$, the expression becomes

$$h_\varphi + \rho\frac{\partial h_\varphi}{\partial \rho} = 0$$

where h_φ can be either the TE mode or the TM mode eigenfunction. The two cases will be verified separately.

B.4.1 TM case

The expression which must be verified is

$$h'_\varphi + \rho\frac{\partial h'_\varphi}{\partial \rho} = 0$$

Considering the expression found in the previous section, remembering that

$$k'_{\mathrm{t},i} = \frac{\chi_{mn}}{a}$$

where χ_{mn} is the n-th zero of the Bessel function of first kind and m-th order, it is necessary to recall the expressions of h'_φ and of its derivative, calculated in the previous section, considering that it must be evaluated on $\rho = a$, $\mathrm{J}_m(\chi_{mn}) = 0$. So:

$$h'_\varphi = -\frac{1}{\sqrt{\pi}}\frac{\mathrm{J}'_m(k'_{\mathrm{t},i}\rho)}{a\mathrm{J}_{m+1}(k'_{\mathrm{t},i}a)}\mathrm{e}^{+\mathrm{j}m\varphi}$$

applying (B.13) to the derivative of e'_ρ with respect to ρ evaluated in the previous section, it is possible to find:

$$\frac{\partial h'_\varphi}{\partial \rho} = \frac{\partial e'_\rho}{\partial \rho} = -\frac{k'_{\mathrm{t},i}}{a\sqrt{\pi}\mathrm{J}_{m+1}(k'_{\mathrm{t},i}a)}\left[-\frac{1}{k'_{\mathrm{t},i}\rho}\mathrm{J}'_m(k'_{\mathrm{t},i}\rho) - \left(1 - \frac{m^2}{k'^2_{\mathrm{t},i}\rho^2}\right)\mathrm{J}_m(k'_{\mathrm{t},i}\rho)\right]$$

By combining these two equations, evaluated in $\rho = a$, it is possible to find:

$$-\frac{1}{\sqrt{\pi}}\frac{\mathrm{J}'_m(k'_{\mathrm{t},i}a)}{a\mathrm{J}_{m+1}(k'_{\mathrm{t},i}a)}\mathrm{e}^{+\mathrm{j}m\varphi} + a\frac{k'_{\mathrm{t},i}}{a\sqrt{\pi}\mathrm{J}_{m+1}(k'_{\mathrm{t},i}a)}\frac{1}{k'_{\mathrm{t},i}a}\mathrm{J}'_m(k'_{\mathrm{t},i}a) = 0$$

So, the boundary condition is verified for TM mode functions of the circular waveguide.

B.4.2 TE case

For the TE case, it is necessary to verify the validity of

$$h''_\varphi + \rho\frac{\partial h''_\varphi}{\partial \rho} = 0$$

From the previous section, it is known that

$$h''_\varphi = \frac{-\mathrm{j}m}{\sqrt{\pi}}\frac{1}{\sqrt{(k''_{\mathrm{t},i}a)^2 - m^2}}\frac{\mathrm{J}_m(k''_{\mathrm{t},i}\rho)}{\rho\,\mathrm{J}_m(k''_{\mathrm{t},i}a)}\mathrm{e}^{+\mathrm{j}m\varphi}$$

and

$$\frac{\partial h''_\varphi}{\partial \rho} = -\frac{\mathrm{j}m}{\sqrt{\pi}\sqrt{(k''_{\mathrm{t},i}a)^2 - m^2}\mathrm{J}_m(k''_{\mathrm{t},i}a)}\left[-\frac{1}{\rho^2}\mathrm{J}_m(k''_{\mathrm{t},i}\rho) + \frac{1}{\rho}k''_{\mathrm{t},i}\mathrm{J}'_m(k''_{\mathrm{t},i}\rho)\right]$$

Remembering that

$$k''_{\mathrm{t},i} = \frac{\chi'_{mn}}{a}$$

where χ'_{mn} is the n-th zero of the first derivative of the Bessel function of first kind and m-th order, evaluating in $\rho = a$ all these expressions, it is possible to find

$$\frac{-\mathrm{j}m}{\sqrt{\pi}}\frac{1}{\sqrt{(k''_{\mathrm{t},i}a)^2 - m^2}}\frac{\mathrm{J}_m(k''_{\mathrm{t},i}a)}{a\,\mathrm{J}_m(k''_{\mathrm{t},i}a)} + a\frac{-\mathrm{j}m}{\sqrt{\pi}\sqrt{(k''_{\mathrm{t},i}a)^2 - m^2}\mathrm{J}_m(k''_{\mathrm{t},i}a)}\left(-\frac{1}{a^2}\mathrm{J}_m(k''_{\mathrm{t},i}a)\right) = 0$$

Therefore, this condition is satisfied also for TE waveguide modes.

B.5 Coefficients for the Galerkin system of cylindrical junctions

From (4.61), (4.62), (4.63), (4.64), it is possible to obtain by inspection every coefficient of the system.

$$A^{(\mathrm{e,e})}_{\beta\alpha} = \mathrm{j}kY \left\{ \left\langle u^{(\mathrm{e})}_{\alpha}, v^{(\mathrm{e})}_{\beta} \right\rangle + \left\langle \frac{\rho^2}{m^2 - k^2\rho^2} \frac{\partial}{\partial z} u^{(\mathrm{e})}_{\alpha}, \frac{\partial}{\partial z} v^{(\mathrm{e})}_{\beta} \right\rangle + \right.$$
$$\left. + \left\langle \frac{\rho^2}{m^2 - k^2\rho^2} \frac{\partial}{\partial \rho} u^{(\mathrm{e})}_{\alpha}, \frac{\partial}{\partial \rho} v^{(\mathrm{e})}_{\beta} \right\rangle + \left\langle \frac{\rho}{m^2 - k^2\rho^2} u^{(\mathrm{e})}_{\alpha}, \frac{\partial}{\partial \rho} v^{(\mathrm{e})}_{\beta} \right\rangle \right\} \quad \text{(B.16)}$$

$$A^{(\mathrm{e,h})}_{\beta\alpha} = \mathrm{j}m \left\{ \left\langle \frac{\rho}{m^2 - k^2\rho^2} \frac{\partial}{\partial z} u^{(\mathrm{h})}_{\alpha}, \frac{\partial}{\partial \rho} v^{(\mathrm{e})}_{\beta} \right\rangle \right\}$$
$$- \left\langle \frac{\rho}{m^2 - k^2\rho^2} \frac{\partial}{\partial \rho} u^{(\mathrm{h})}_{\alpha}, \frac{\partial}{\partial z} v^{(\mathrm{e})}_{\beta} \right\rangle - \left\langle \frac{1}{m^2 - k^2\rho^2} u^{(\mathrm{h})}_{\alpha}, \frac{\partial}{\partial z} v^{(\mathrm{e})}_{\beta} \right\rangle \quad \text{(B.17)}$$

$$A^{(\mathrm{h,e})}_{\beta\alpha} = \mathrm{j}m \left\{ \left\langle \frac{\rho}{m^2 - k^2\rho^2} \frac{\partial}{\partial \rho} u^{(\mathrm{e})}_{\alpha}, \frac{\partial}{\partial z} v^{(\mathrm{h})}_{\beta} \right\rangle + \left\langle \frac{1}{m^2 - k^2\rho^2} u^{(\mathrm{e})}_{\alpha}, \frac{\partial}{\partial z} v^{(\mathrm{h})}_{\beta} \right\rangle + \right.$$
$$\left. - \left\langle \frac{\rho}{m^2 - k^2\rho^2} \frac{\partial}{\partial z} u^{(\mathrm{e})}_{\alpha}, \frac{\partial}{\partial \rho} v^{(\mathrm{h})}_{\beta} \right\rangle \right\} \quad \text{(B.18)}$$

$$A^{(\mathrm{h,h})}_{\beta\alpha} = \mathrm{j}kZ \left\{ \left\langle u^{(\mathrm{h})}_{\alpha}, v^{(\mathrm{h})}_{\beta} \right\rangle + \left\langle \frac{\rho^2}{m^2 - k^2\rho^2} \frac{\partial}{\partial z} u^{(\mathrm{h})}_{\alpha}, \frac{\partial}{\partial z} v^{(\mathrm{h})}_{\beta} \right\rangle + \right.$$
$$\left. + \left\langle \frac{\rho^2}{m^2 - k^2\rho^2} \frac{\partial}{\partial \rho} u^{(\mathrm{h})}_{\alpha}, \frac{\partial}{\partial \rho} v^{(\mathrm{h})}_{\beta} \right\rangle + \left\langle \frac{\rho}{m^2 - k^2\rho^2} u^{(\mathrm{h})}_{\alpha}, \frac{\partial}{\partial \rho} v^{(\mathrm{h})}_{\beta} \right\rangle \right\} \quad \text{(B.19)}$$

$$B^{(\mathrm{e},k)}_{\beta\mu} = \sqrt{Y^{(k)}_{\infty,\mu}} \left\langle h^{(k)}_{\rho,\mu}, v^{(\mathrm{e})}_{\beta} \right\rangle \Big|_{\gamma_{\mathrm{wg}^{(k)}}} \quad \text{(B.20)}$$

$$B^{(\mathrm{h},k)}_{\beta\mu} = \sqrt{Z^{(k)}_{\infty,\mu}} \left\langle e^{(k)}_{\rho,\mu}, v^{(\mathrm{h})}_{\beta} \right\rangle \Big|_{\gamma_{\mathrm{wg}^{(k)}}} \quad \text{(B.21)}$$

$$C^{(\mathrm{e},k)}_{\nu\alpha} = \left\langle u^{(\mathrm{e})}_{\alpha} e^{(k)}_{\varphi,\nu} \right\rangle \Big|_{\gamma_{\mathrm{wg}^{(k)}}} \quad \text{(B.22)}$$

$$C^{(\mathrm{h},k)}_{\nu\alpha} = \left\langle u^{(\mathrm{h})}_{\alpha} h^{(k)}_{\varphi,\nu} \right\rangle \Big|_{\gamma_{\mathrm{wg}^{(k)}}} \quad \text{(B.23)}$$

$$D^{(\mathrm{e},k)}_{\nu\mu} = \sqrt{Z^{(k)}_{\infty,\mu}} \left\langle e^{(k)}_{\varphi,\mu} e^{(k)}_{\varphi,\nu} \right\rangle \Big|_{\gamma^{(k)}_{\mathrm{wg}}} \quad \text{(B.24)}$$

$$D^{(\mathrm{h},k)}_{\nu\mu} = \sqrt{Y^{(k)}_{\infty,\mu}} \left\langle h^{(k)}_{\varphi,\mu} h^{(k)}_{\varphi,\nu} \right\rangle \Big|_{\gamma^{(k)}_{\mathrm{wg}}} \quad \text{(B.25)}$$

Bibliography

[1] Abramowitz M. , Stegun I. A. , *Handbook of mathematical functions*, Dover Publications, New York, 1964.

[2] Barozzi G. C. , *Matematica per l'ingegneria dell'informazione*, Zanichelli editore, Bologna, 2004.

[3] Bhattacharyya A. K. , Goyette G. , *A Novel Horn RadiatorWith High Aperture Efficiency and Low Cross-Polarization and Applications in Arrays and Multibeam Reflector Antennas*, *IEEE Trans. on Antennas and Propagation*, vol. 52, no. 11, pp 2850-2859, November 2004.

[4] Boyd J. P. , *Chebyshev and Fourier Spectral Methods*, Dover Publications, Mineola (NY), 2000.

[5] Canavero F. , Montrosset I. , Orta R. , *Linee di trasmissione*, Levrotto e Bella, Torino, 1990.

[6] Collin R. E. , *Foundations for Microwave Engineering*, IEEE Press, John Wiley & Sons, Hoboken, New Jersey, 2001.

[7] Dennery P. , Krzywicki A. , *Mathematics for physicists*, Dover Publications, Mineola, New York, 1996.

[8] Felsen L. B. , Marcuvitz N. , *Radiation and scattering of waves*, Prentice-Hall, Englewood Cliffs, NJ, 1972.

[9] Gottlieb D. , Orszag S. A. , *Numerical analysis of spectral methods: theory and applications*, Capital City Press, Montpeller, Vermont, 1977.

[10] Jones D. S. , *The theory of Electromagnetism*, Pergamon Press, Oxford, 1964.

[11] Kreyzig E. , *Advanced engineering mathematics*, John Wiley & Sons, Hoboken, Singapore, 2006.

[12] Marcuvitz N. , *Waveguide handbook*, McGraw-Hill, New York, 1951.

[13] Orefice M. , *Note di Antenne*, 2002.

[14] Orta R. , *Teoria delle Linee di Trasmissione*, 1999.

[15] Pelosi G., Coccili R., Selleri S. , *Quick Finite Elements for Electromagnetic Waves*, Artech House, Norwood, MA, 1998.

[16] Peverini O. A., Addamo G., Virone G., Tascone R., Orta R. , *A Spectral-Element Method for the Analysis of 2-D Waveguide Devices With Sharp Edges and Irregular Shapes*, *IEEE Trans. Microw. Theory Tech.*, vol. 59, no. 7, pp 1685-1695, July 2011.

[17] Rainville E. D. , *Special Functions*, The Macmillan Company, New York, 1960.

[18] Rao S. K. , *Design and Analysis of Multiple-Beam Reflector Antennas*, *IEEE Antennas and Propagation Magazine*, vol. 41, No. 4, August 1999.

[19] Chan K. K. , Rao S. K. , *Design of High Efficiency Circular Horn Feeds for Multibeam Reflector Applications*, *IEEE transactions on Antennas and Propagation*, vol. 56, No. 1, January 2008.

[20] Rao S. K. et al. , *Development of a 45 GHz Multiple-Beam Antenna for Military Satellite Communications*, *IEEE Antennas and Propagation Magazine*, vol. 43, No. 10, October 1995.

[21] Szegö G. , *Orthogonal Polynomials*, American Mathematical Society, Providence, Rhode Island, 1939.

[22] Tang K.T. , *Mathematical Methods for Engineers and Scientists 2*, Springer-Verlag, Berlin Heidelberg, 2007.

[23] Van Bladel J. , *Singular Electromagnetic Fields*, Clarendon Press, Oxford, 1991

[24] Weideman J. A. C. , Reddy S. C. , *A MATLAB Differentiation Matrix Suite*, ACM Transactions on Mathematical Software, Vol 26, No. 4, December 2000.

[25] Zhang S. , Jin J. , *Computation of special functions*, John Wiley & Sons, 1996.

[26] Zappelli L. , *On the Definition of the Generalized Scattering Matrix of a Lossless Radial Line*, *IEEE transactions on microwave theory and techniques*, vol. 52, No. 6, June 2004.